UNIVERSIDADE ESTADUAL PAULISTA
"JÚLIO DE MESQUITA FILHO"
Câmpus de São José do Rio Preto

ANA CAROLINA NAZARÉ

Preparação e Avaliação de Diidroxibenzoatos de Alquila contra *Xanthomonas citri* subsp. *citri* e no controle do Cancro Cítrico

São José do Rio Preto
2019

ANA CAROLINA NAZARÉ

Preparação e Avaliação de Diidroxibenzoatos de Alquila contra *Xanthomonas citri* subsp. *citri* e no controle do Cancro Cítrico

Tese apresentada como parte dos requisitos para obtenção do título de Doutora em Química, junto ao Programa de Pós-Graduação em Química, do Instituto de Biociências, Letras e Ciências Exatas da Universidade Estadual Paulista "Júlio de Mesquita Filho", Câmpus de São José do Rio Preto.

Financiadora: FAPESP – Processo 2015/08089-6

Orientador: Prof. Dr. Luis Octávio Regasini
Coorientador: Prof. Dr. Henrique Ferreira e
Prof. Dr. José Belasque Jr.

São José do Rio Preto
2019

N335p

Nazaré, Ana Carolina

Preparação e Avaliação de Diidroxibenzoatos de Alquila contra Xanthomonas citri subsp. citri e no controle do Cancro Cítrico / Ana Carolina Nazaré. -- São José do Rio Preto, 2019

185 p. : il., tabs.

Tese (doutorado) - Universidade Estadual Paulista (Unesp), Instituto de Biociências Letras e Ciências Exatas, São José do Rio Preto

Orientador: Luis Octávio Regasini

Coorientador: Henrique Ferreira

1. fitobacterioses. 2. compostos fenólicos. 3. ésteres alquílicos. 4. Xanthomonas. 5. doenças citrícolas. I. Título.

Sistema de geração automática de fichas catalográficas da Unesp. Biblioteca do Instituto de Biociências Letras e Ciências Exatas, São José do Rio Preto. Dados fornecidos pelo autor(a).

Essa ficha não pode ser modificada.

ANA CAROLINA NAZARÉ

Preparação e Avaliação de Diidroxibenzoatos de Alquila contra *Xanthomonas citri* subsp. *citri* e no controle do Cancro Cítrico

Tese apresentada como parte dos requisitos para obtenção do título de Doutora em Química, junto ao Programa de Pós-Graduação em Química, do Instituto de Biociências, Letras e Ciências Exatas da Universidade Estadual Paulista "Júlio de Mesquita Filho", Câmpus de São José do Rio Preto.

Financiadora: FAPESP – Processo 2015/08089-6

Comissão Examinadora

Prof. Dr. Luis Octávio Regasini
UNESP – São José do Rio Preto
Orientador

Profa. Dra. Rosana Marta Kolb
UNESP – Assis

Prof. Dr. Carlos Henrique Gomes Martins
UFU – Uberlândia

Profa. Dra. Vera Aparecida de Oliveira Tiera
UNESP – São José do Rio Preto

Dra. Janaina de Cássia Orlandi Sardi
UNICAMP – Piracicaba

São José do Rio Preto
19 de julho de 2019

Dedico este trabalho à minha família,
em especial meus pais **Elaine Borsari Nazaré** e **Nilton Nazaré**,
ao meu irmão **Eduardo Nazaré**
e ao meu companheiro de vida **Maicon Segalla Petrônio**.

AGRADECIMENTOS

Aos meus pais que se dedicaram e trabalharam muito para que eu pudesse estudar. Obrigada pelo esforço diário, pela educação que me proporcionaram não só no âmbito do conhecimento intelectual, mas também no quesito pessoal. Obrigada pelo apoio em minhas decisões e por me mostrarem que sou capaz.

À minha família, muito obrigada pelo carinho, afeto, amor, respeito e por entenderem que nem sempre posso estar presente fisicamente.

Ao meu companheiro de vida Maicon Segalla Petrônio, obrigada pela parceria, atenção, dedicação, carinho, amor, respeito, cumplicidade e pelas conversas sobre tudo, por me compreender tão bem e por me apoiar em todas as minhas decisões e indecisões. Você é parte fundamental nas minhas escolhas!

Ao meu orientador Prof. Dr. Luis Octávio Regasini pela oportunidade oferecida, por confiar em minha capacidade, por disponibilizar de seu tempo e laboratório para que eu pudesse desenvolver este trabalho, obrigada por todos os ensinamentos e puxões de orelha, obrigada pelo comprometimento ao longo destes anos de meu doutoramento. Obrigada por sempre me desafiar e por me fazer enxergar novas possibilidades! Agradeço por poder participar de um grupo tão colaborativo que me fez crescer pessoal e intelectualmente.

Aos professores Dr. Henrique Ferreira e Dr. José Belasque Jr. pela coorientação neste trabalho. Meus sinceros agradecimentos ao Prof. Dr. Henrique Ferreira por ceder seu laboratório, pela confiança, por sua disponibilidade, atenção, por sua paciência e educação, obrigada por me ensinar muito além da microbiologia.

Aos professores, Dr. Dirk-Jan Scheffers, Dra. Eleni Gomes, Dra. Paula Rahal, Dra. Rosana Marta Kolb, Dr. Osmar Malaspina, Dr. Eduardo Alves de Almeida e seus alunos Dra. Aleksandra Zielinska, Me. Diego A. Monteiro, Dra. Marilia de Freitas Calmon Saiki, Me. Graciele Fernanda de Souza Pinto, Me. Adna Suelen Dorigo, Dra. Annelise de Souza Rosa-Fontana e Dr. Danilo Grünig Humberto da Silva pela colaboração, atenção e pela ajuda na realização de alguns dos ensaios/análises contidos neste trabalho.

Aos amigos de jornada acadêmica Me. Carlos Roberto Polaquini, Me. Mariana Bastos dos Santos, Me. Daiane Bertolin Anselmo, Caroline Sprengel Lima, Me. Thaíse Borges, Me. Beatriz Carvalho Marques, Me. Gabriela Miranda Ayusso, Me. Mayara Aparecida Rocha Garcia, Me. Laíza Araujo e Me. Guilherme Silva Torrezan, obrigada

aos que embarcaram nas minhas aventuras empreendedoras, por encararem os desafios lado a lado, por compartilhar conhecimento, por me apoiarem, pela convivência sempre tão alegre mesmo nos dias mais cansativos, pela amizade, barzinhos, baladinhas, comilanças e pelas risadas que não foram poucas.

Ao grupo de Rio Claro Me. Lúcia Bonci Cavalca, Me. Caio Zamuner, Me. Kenny Umino Sato, Me. Camila Malvessi, Me. Guilherme Dilarri, Dra. Luana Morão, Dr. Luiz Leonardo Saldanha, por me acolherem e me ensinarem com paciência a rotina de um laboratório de microbiologia, vencer o medo da autoclave foi difícil! Obrigada pelo carinho, atenção, cafés e cervejinhas.

Aos grandes amigos que a vida me deu, obrigada pela admiração, atenção, carinho e por todos os bons momentos de risada e descontração.

Ao Dr. Fábio Rogério de Moraes, técnico responsável do Centro Multiusuário de Inovação Biomolecular, do Instituto de Biociências, Letras e Ciências Exatas, da UNESP, Câmpus São José do Rio Preto, pelas análises de Ressonância Nuclear Magnética nos equipamentos Bruker Avance III 9,397 T (400 MHz) e 14,095 T (600 MHz). À Dra. Lucinéia Vizzotto Marconcini pelo treinamento fornecido para a utilização do espectrômetro Bruker Fourier (300 MHz) do Laboratório-II de Ressonância Magnética Nuclear, Instituto de Química, da UNESP, Câmpus Araraquara.

Aos funcionários do Instituto de Biociências, Letras e Ciências Exatas, André Luis Domingues, João L. A. de Toledo Netto, Eliane Cristina Gonçalves do Nascimento Alíria Sena, Alex Antônio do Santos e todos que de alguma forma me ajudaram nesta caminhada.

À Fundação de Amparo à Pesquisa do Estado de São Paulo (FAPESP), pela bolsa concedida (2015/08089-6) para a realização do presente trabalho.

À Comissão Examinadora, pela disponibilidade e aceite em tornar esse trabalho mais completo.

RESUMO

O cancro cítrico afeta variedades citrícolas de importância econômica mundial, sendo causado pela *Xanthomonas citri* subsp. *citri*. (Xcc), uma bactéria Gram-negativa. O controle do cancro cítrico é realizado por meio do manejo integrado com aplicações de substâncias cúpricas, plantio de cultivares menos suscetíveis, uso de quebra-ventos e controle da larva minadora de citros. No entanto, o uso excessivo de cobre pode ocasionar acúmulo no solo e afetar negativamente o crescimento radicular de plantas cítricas, e consequentemente a absorção de nutrientes. Por esta razão, a busca por substâncias anti-Xcc seguras ao meio ambiente e eficientes é de crucial importância. Neste trabalho utilizamos o planejamento de substâncias sintéticas anti-Xcc. Sendo assim, foram sintetizados 36 diidroxibenzoatos de alquila (DHB), dentre os quais, 14 apresentaram atividade anti-Xcc. Dentre estes, três ésteres com os menores valores de CIM e com sete carbonos na cadeia lateral (heptila) foram selecionados, **4** (52 µM), **16** (80 µM) e **28** (88 µM). O ensaio de curva de crescimento de Xcc demonstrou que os DHB selecionados promoveram atraso na fase exponencial, prolongando o tempo para Xcc atingir a fase estacionária. O efeito dos DHB **4**, **16** e **28** sobre a permeabilidade da membrana de Xcc foi comparado ao controle nisina, sendo o derivado DHB **28** mais efetivo (93,8%), do que **16** (41,3%) e **4** (13,9%). Os dados do ensaio de inibição da atividade GTPásica sugerem que os ésteres **4**, **16** e **28** podem promover alterações nos protofilamentos, levando à despolimerização da proteína mutante sensível à temperatura de filamento Z (FtsZ) e assim impedindo a divisão celular bacteriana. A viabilidade de aplicação dos DHB **4**, **16** e **28** foi comprovada por meio de ensaios de citotoxicidade, sendo os valores CI_{50} superiores a 100 µM contra as células eucarióticas testadas. As células de Xcc perderam a capacidade de colonizar o hospedeiro após tratamento com as substâncias **4**, **16** e **28** a ½ CIM e CIM, inibindo o aparecimento de sintomas de cancro cítrico nas folhas de laranja doce (*Citrus sinensis*). Os DHB **4**, **16** e **28** foram avaliados quanto a capacidade protetora de plantas jovens de laranja doce e a incidência de sintomas diminuiu 33,3 % (**4**), 15,3 % (**16**) e 28,6 % (**28**), valores próximos ao oxicloreto de cobre (26,7 %). Os ésteres mantiveram comportamento similar ao oxicloreto de cobre em relação a severidade dos sintomas de cancro cítrico. A fitotoxicidade dos três DHB foi avaliada em ensaio com *Lactuca sativa*, causando menor interferência no crescimento das plântulas quando comparados com o

oxicloreto de cobre presente nas formulações a base de cobre utilizadas nas lavouras citrícolas. Os ésteres não causaram alterações nos parâmetros fotossintéticos, tais como a taxa de transpiração, condutância estomática, assimilação máxima, rendimento quântico efetivo de conversão fotoquímica do PSII, coeficiente de extinção fotoquímica do PSII e coeficiente de extinção não fotoquímica do PSII em plantas jovens de *C. sinensis*. Na avaliação da toxicidade contra abelhas sem ferrão (*Scaptotrigona postica*), os ésteres **4**, **16** e **28** provocaram mortalidade similar ao oxicloreto de cobre.

Palavras-chave: cancro cítrico, compostos fenólicos, fitobacteriose, ésteres de alquila

ABSTRACT

Citrus cancer affects citrus varieties of worldwide economic importance, being caused by *Xanthomonas citri* subsp. *citri.* (Xcc), a Gram-negative bacterium. The control of citrus canker is accomplished through integrated management with applications of cupric substances, planting of less susceptible cultivars, use of windbreaks and control of citrus-mining larva. However, excessive use of copper can cause soil accumulation and negatively affect root growth of citrus plants, and consequently nutrient absorption. For this reason, the search for environmentally safe and efficient anti-Xcc substances is of crucial importance. In this paper we use the planning of anti-Xcc synthetic substances. Thus, 36 alkyl dihydroxybenzoates (DHB) were synthesized, which showed anti-Xcc activity. Among them, three esters with the lowest MIC values and seven carbons in the side chain (heptyl) were selected, **4** (52 µM), **16** (80 µM) and **28** (88 µM). The Xcc growth curve assay showed that the selected DHB promoted exponential phase delay, extending the time for Xcc to reach the stationary phase. The effect of DHB **4**, **16** and **28** on Xcc membrane permeability was compared to nisin control, with DHB **28** being the most effective derivative (93.8%) than **16** (41.3%) and **4** (13, 9%). Data from the GTPase inhibition assay suggest that esters **4**, **16** and **28** may promote changes in protofilaments, leading to depolymerization of the Filamentous temperature sensitive protein Z (FtsZ) and thus preventing bacterial cell division. The viability of application of DHB **4**, **16** and **28** was confirmed by cytotoxicity assays, with IC_{50} values greater than 100 µM against eukaryotic cells tested. Xcc cells lost the ability to colonize the host after treatment with coumpounds **4**, **16** and **28** at ½ MIC and MIC, inhibiting the appearance of symptoms of citrus canker on sweet orange leaves (*Citrus sinensis*). DHB **4**, **16** and **28** were evaluated for the protective capacity of sweet orange young plants and the incidence of symptoms decreased by 33.3% (**4**), 15.3% (**16**) and 28.6% (**28**) to copper oxychloride (26.7%). The esters maintained copper oxychloride-like behavior with respect to the severity of citrus canker symptoms. The phytotoxicity of the three DHB was evaluated in a *Lactuca sativa* assay, causing less interference in seedling growth when compared to copper oxychloride present in the copper base formulations used in citrus crops. The esters did not cause changes in photosynthetic parameters, such as transpiration rate, stomatal conductance, maximum assimilation, PSII photochemical conversion effective quantum yield, PSII photochemical extinction coefficient and PSII non-

photochemical extinction coefficient in young *C. sinensis*. In the evaluation of toxicity against stingless bees (*Scaptotrigona postica*), esters **4**, **16** and **28** caused similar mortality to copper oxychloride.

Keywords: citric canker, phenolic compounds, phytobacteriosis, alkyl esters

LISTA DE FIGURAS

Capítulo 1

Capítulo 2

Appendix A – Supplementary Materials

Capítulo 3

LISTA DE ESQUEMAS

LISTA DE TABELAS

Capítulo 2

LISTA DE ABREVIATURAS E SÍMBOLOS

µg – microgramas

µL – microlitros

µM – micromolar

ACHN – human renal adenocarcinoma cell line

C18 – octadecylsilane

$CDCl_3$ – deuterated chloroform

CEIS – Centro de Estudos de Insetos Sociais

CFM – Concentração Fungicida Mínima

CIM – Concentração Inibitória Mínima

CLAE – cromatografia líquida de alta eficiência

COOH – carboxila

CS – Copper Sulfate

d – doublet

DA – dihydroxybenzoic acid

dd – doublet of doublet

DHB – diidroxibenzoatos de áquila

DMSO – dimethylsulfoxide

DMSO d_6 – deuterated dimethylsulfoxide

EFSA – European Food Safety Authority

EzrA – septation ring formation regulator

FAO – Food and Agriculture Organization

FCAV – Faculdade de Ciências Agrárias e Veterinária

FEA – Faculdade de Economia Administração e Contabilidade

FtsA – Filamentous temperature sensitive protein A

FtsZ – Filamentous temperature sensitive protein Z

Fundecitrus – Fundo de Defesa da Citricultura

g – gramas

GDF – guanosina-5’-difosfato

GFP – green fluorescente protein

GTP – guanosina-5’-trifosfato

GTPase – guanosina-5’- trifosfatase

HaCaT – human keratinocyte cell line

HepG2 – human liver cancer cell line

HP – Hewlett-Packard Company

HPLC – High-Performance Liquid Chromatography

Huh-7.5 – human hepatoma cell line

Hz – Hertz

IAN – 3-indolacetonitrila

IBGE – Instituto Brasileiro de Geografia e Estatística

IC_{50} – Inhibitory concentration

Lafep – Laboratório de Anatomia e Fisiologia Ecológica de Plantas

LAQ – Laboratório de Antibióticos e Quimioterápicos

LECA – Laboratório de Ecotoxicologia e Conservação de Abelhas

LEGO – Laboratório de Estudos Genômicos

LGB – Laboratório de Genética de Bactérias

MBC – Minimum Bactericidal Concentration

mg – miligramas

MIC – Minimum Inhibitory Concentration

MinC – cell division inhibitor C

MinD – ATP bindin protein MinD

mL – mililitros

MRC-5 – human lung fibroblast cell line

MTT – 3-(4,5-dimetil-2-tiazolil)-2,5-difenil – tetrazólio brometo

NC –negative control

NMR – Nuclear Magnetic Resonance

NYG – Nitrogen Yeast Glicerol

OD – Optical Density

OECD – Organisation for Economic Co-operation and Development

OH – hidroxila

PC – positive control

PEP – phosphoenol pyruvate

Pi – fosfato inorgânico

PI – propidium iodide

REMA – Resazurin Microtiter Assay

s – singlet

SAA – Secretaria da Agricultura e Abastecimento

SepF – cell division protein SepF

SMR – Sistema de Mitigação de Risco

SOPP – ortofenilfenato de sódio

TA – triidroxibenzoato de alquila

TLC – thin layer chromatography

UE – União Europeia

USDA – United States Department of Agriculture

USP – Universidade de São Paulo

VC – vehicle control

VERO – monkey kidney epithelial cell line

Xcc – *Xanthomonas citri* subsp. *citri*

ZapA – Z ring associate protein A

ZipA – Z interacting protein A

SUMÁRIO

Capítulo 1: Considerações gerais

Capítulo 2: Desing of Antibacterial Agents: Alkyl Dihydroxybenzoates against *Xanthomonas citri* subsp. *citri*

Capítulo 3: Heptyl dihydroxybenzoates as an alternative to copper to prevent citrus canker

Capítulo 1

1. CONSIDERAÇÕES INICIAIS

A cultura de laranja é destaque no setor citrícola, tanto em volume de produção quanto aos benefícios econômicos. A estimativa da safra de laranja 2019/20 é de 388,89 milhões de caixas (40,8 kg) no cinturão citrícola de São Paulo e Triângulo Mineiro, com o total de 173,973 milhões de árvores produtivas, dados de março de 2019. Avaliando a produtividade por hectare, tem-se a estimativa de 1051 caixas por hectar na safra de 2019/20, representando um aumento de 295 caixas em relação a safra anterior de 2018/19 (Fundecitrus, 2019). Neste sentido, o setor citrícola gera um PIB de US$ 6,5 bilhões de dólares (Neves & Trombin, 2017).

Contudo, doenças e pragas acometem as lavouras de citros, diminuindo a produção e causando problemas fitossanitários, sendo necessário o manejo adequado para o controle e desinfecção dos pomares. Assim, o objetivo desta tese foi o estudo de substâncias com atividade antibacteriana contra *Xantomonas citri* subsp. *citri* (Xcc), uma bactéria causadora de uma doença endêmica, o cancro cítrico.

Esta tese está distribuída em quatro capítulos (1-4). O **Capítulo 1** se constituiu por uma breve introdução seguida de uma revisão de literatura pontuando a importância da citricultura e os prejuízos causados pelo cancro cítrico no Brasil e suas medidas de controle. Neste capítulo foram destacadas a divisão celular bacteriana e substâncias capazes de inibir o crescimento bacteriano por meio de danos ou perturbações causadas à Xcc. Por fim, foi salientada a atividade antimicrobiana dos diidroxibenzoatos de alquila (DHB) contra outras espécies bacterianas.

No **Capítulo 2** foram descritas a preparação, purificação e identificação de 36 diidroxibenzoatos de alquila, seguidas da determinação de pureza e hidrofobicidade destes ésteres. Foram avaliadas a atividade anti-Xcc dos 36 DHB, e posteriormente selecionou-se três substâncias com menores valores de concentração inibitória mínima (CIM). Os ésteres **4**, **16** e **28** foram selecionados e avaliados quanto a alterações no padrão da curva de crescimento de Xcc, na permeabilidade de membrana de Xcc e inibição sobre a atividade GTPásica de FtsZ, uma proteína envolvida na divisão celular. A toxicidade dos ésteres selecionados foi avaliada contra linhagens celulares de queratinócitos não tumorigênicos (HaCaT) CLS 300493, hepatoma humano (Huh-7.5) ATCC® PTA-8561, células pulmonares humanas de

linhagem normal (MRC-5) ATCC CCL-171, células renais de macaco de linhagem normal (VERO) ATCC® CCL81 e células renais carcinogênicas humanas (ACHN) ATCC® CRL1611. Os resultados foram publicados no periódico International Journal of Molecular Sciences (IJMS) em outubro de 2018.

O **Capitulo 3** é a sequência de estudos dos ésteres selecionados, quanto a capacidade de interferir na patogenicidade de Xcc, sob ação protetora de plantas jovens de laranja doce (*Citrus sinensis*), avaliando a incidência e a severidade do cancro cítrico. O potencial fitotóxico dos DHB **4**, **16** e **28** foi avaliado contra o desenvolvimento inicial de alface (*Lactuca sativa*) e na interferência nos parâmetros fotossintéticos de plantas jovens de *C. sinensis*. Por fim, foi estudada a toxicidade das substâncias **4**, **16** e **28** contra abelhas sem ferrão (*Scaptotrigona postica*).

No **Capitulo 4** foram compiladas as considerações finais discutindo os resultados dos capítulos 2 e 3. Finalizando com uma conclusão geral.

2. INTRODUÇÃO E REVISÃO DE LITERATURA

O cancro cítrico é causado pela bactéria *Xanthomonas citri* subsp. *citri* (Xcc) (Stall & Seymour, 1983; Gottwald et al., 2002). Xcc acomete as principais variedades de citros de importância comercial, causando lesões necróticas de aspecto marrom eruptivo em folhas, frutos e ramos (Behlau & Belasque Jr., 2014). Xcc provoca a desfolha e queda prematura de frutos, provocando a depreciação da qualidade dos frutos, e consequentemente, tornando o seu comércio inviável (Bitancourt, 1957; Gottwald et al., 2002; Behlau & Belasque Jr., 2014).

O estado de São Paulo detém cerca de 75% da produção nacional de laranja (Neves et al., 2010; IBGE, 2018). A legislação para controle do cancro cítrico em São Paulo até 2016 determinava a erradicação das plantas sintomáticas e realização de inspeções frequentes, junto a pulverização de substâncias cúpricas (Massari & Belasque Jr., 2006; Behlau et al., 2016). No início de 2017, o estado de São Paulo por meio da publicação da Resolução SAA 10, definiu o Sistema de Mitigação de Risco (SMR) como medida oficial de controle (São Paulo, 2017).

As regiões endêmicas do cancro cítrico trabalham com estratégias de manejo integrado, utilizando medidas de controle como: a) pulverizações com substâncias cúpricas, b) utilização de quebra-ventos (com espécies de casuarinas, grevíleas,

pinus, eucaliptos e corymbia); c) controle do inseto minador de citros e d) emprego de cultivares resistentes à Xcc (Behlau & Belasque Jr., 2014). O manejo integrado reduz as perdas de produção, mas não elimina a bactéria do pomar, tornando o comércio de exportação de frutas impróprio em áreas de quarentena (Choi et al., 2017).

Li e Wang (2014) estudaram a atividade anti-Xcc de aminoácidos e derivados indólicos (Li & Wang, 2014). Gholami e colaboradores avaliaram o potencial anti-Xcc de antibióticos como ampicilina, penicilina, cloranfenicol, estreptomicina e canamicina (Gholami et al., 2018). Porém a utilização de antibióticos em larga escala, dispersos no ambiente vem sendo bastante contestada. Como alternativa ecologicamente sustentável foram descritas recentemente a capacidade inibitória de extratos de fungos filamentosos da Antártica contra Xcc (Vieira et al., 2018).

O nosso grupo de pesquisa tem a premissa de buscar alternativas com menor impacto ambiental, e para tanto, estuda a atividade de substâncias com esqueletos carbônicos baseados em produtos naturais. Em 2013, Silva e colaboradores demonstraram a atividade anti-Xcc de uma série de galatos de alquila (3,4,5-triidroxibenzoato de alquila) os quais inibiram o crescimento de Xcc e reduziram sua patogenicidade em *Citrus limonia* (Silva et al., 2013). Posteriormente, o mecanismo de ação destes galatos foi elucidado, evidenciando sua ação sobre a membrana em combinação com a inibição da proteína FtsZ (Król et al., 2015; Kopacz et al., 2018). Visando avaliar a segurança dessas substâncias foram realizadas investigações citotóxicas, genotóxicas e mutagênicas (Silva et al., 2017). Recentemente foi avaliada a atividade anti-Xcc de galatos de alquila monoacetilados. Com a inserção do grupo acetila ocorreu aumento na lipofilicidade, conferindo maior potência para os galatos de alquila monoacetilados quando comparados aos galatos de alquila não esterificados (Savietto et al., 2018).

A similaridade estrutural entre os galatos e diidroxibenzoatos somada a atividade antimicrobiana dos diidroxibenzoatos contra outras espécies bacterianas, sugeriu uma potencial atividade contra Xcc, bem como potencial atividade inibitória da proteína FtsZ, justificando o investimento químico e biológico nesta classe de ésteres (Nihei, Nihei & Kubo, 2003; Merkl et al., 2010; Alves et al, 2013; Soares et al., 2014; Medina-Alarcón et al, 2017).

Na presente tese foram estudados 36 diidroxibenzoatos de alquila, variando o tamanho das cadeias alquílicas laterais para observar o efeito da lipofilicidade.

Adicionalmente, foram observadas diferentes posições das hidroxilas, visando encontrar substâncias mais potentes anti-Xcc e no controle do cancro cítrico.

2.1. Importância da citricultura

A citricultura brasileira ascendeu na década de 60 com a forte geada na Flórida (EUA). A partir da década de 80, a cultura de laranja passou a ser a quinta mais produzida no país (FAO, 2015). Desde então, o Brasil se destaca como um dos maiores produtores de laranja, seguido pela China, União Europeia, Estados Unidos e México (Fares et al., 2017).

Além do suco concentrado e congelado de laranja e do suco de laranja não-concentrado, os subprodutos do processo industrial, incluindo óleos essenciais das cascas de laranjas, essências aquosas e oleosas, terpenos cítricos (limoneno), farelo de polpa cítrica, polpa congelada e álcool obtido da fermentação das laranjas, também podem ser comercializados (Neves et al., 2010; CitrusBr, 2016).

O cinturão citrícola de São Paulo e Triângulo Mineiro possui aproximadamente 450 mil hectares, gerando por volta de 200 mil empregos diretos e indiretos. Segundo Neves e Trombim (2017), a geração de empregos deste setor tem relação direta com os índices de qualidade de vida destes municípios (Neves & Trombim, 2017).

2.2. Surgimento do cancro cítrico e seu prejuízo para a citricultura

Nos últimos cem anos, surgiram muitas doenças com impacto na cultura citrícola, tais como: leprose (1933), tristeza (1937), cancro cítrico (1957), pinta preta (1980), clorose variegada dos citros (1987), morte súbita dos citros (2001), e greening/HLB (2004) (Sanches et al., 2014). Dentre estas doenças, o cancro cítrico reduz a produtividade dos pomares, devido a desfolha das plantas e queda prematura dos frutos. O aparecimento dos sintomas causa a depreciação, inviabilizando o comércio de frutos *in natura* (Bitancourt, 1957; Gottwald et al., 2001, 2002; Behlau et al., 2007, 2008; Behlau & Belasque, 2014; Lanza et al., 2018).

O cancro cítrico causa impacto econômico mundial devido à restrição do acesso ao mercado da União Europeia (UE). Apesar da ausência de evidência documentada para a introdução de frutas com lesões de cancro (Gottwald et al., 2009), a UE considera a importação de frutos infectados e até mesmo frutas expostas ao

patógeno como um risco inaceitável (EFSA, 2013; Painel da EFSA sobre Fitossanidade, 2014).

O cancro cítrico causa lesões em toda a parte aérea, principalmente nos tecidos jovens, que são mais suscetíveis à bactéria, que penetra via estômatos ou ferimentos mecânicos. As lesões atingem de 2 a 12 mm de diâmetro, sendo eruptivas, levemente salientes e de coloração palha ou pardacenta, que vão se tornando de aspecto corticoso, e algumas vezes circundado por um halo amarelo (Rosetti, 2001; Duan et al., 2018).

Nas folhas (**Figura 1**), os sintomas aparecem de 4 a 7 dias após a infecção (Vernieri et al., 2003). As lesões são salientes nas faces adaxial e abaxial, com manchas claras que exibem um centro necrosado, duro e lignificado (Schubert et al., 2001; Gottwald et al., 2002; Brunning & Gabriel, 2003). Nos frutos, as lesões são de aspecto pardo, salientes e algumas vezes ocorre um halo amarelo que circunda as lesões (Rosetti, 2001; Feichtenberger et al., 2005; Amorim; Rezende & Bergamin Filho, 2011). Em estágio avançado, parecem crostas escuras com fissuras, às vezes concêntricas, com pequenas ou grandes crateras, por onde exsuda a bactéria. Nos ramos, os sintomas ocorrem como lesões salientes de cor parda como aqueles apresentados em folhas e frutos.

Além dos sintomas citados, o cancro cítrico, quando bem estabelecido no hospedeiro, provoca redução da área foliar, diminuindo a capacidade fotossintética, e indução da produção de etileno, prejudicando a qualidade dos frutos remanescentes e causando a seca de novos ramos (Brown, 2001; Francis et al., 2009; Dewdney & Graham, 2012).

Figura 1 – Sintomas de cancro cítrico: manchas eruptivas amarelas em folhas de *Citrus sinensis*

Fonte: Laboratório de Genética de Bactérias

O cancro cítrico inicia-se a partir de uma planta doente com lesões ativas, e a disseminação da bactéria para as plantas vizinhas ocorre principalmente pela ação de chuva acompanhada de ventos, ou pelo trânsito de pessoas e maquinário nos pomares (Stall; Seymour, 1983; Leite Jr., 1990; Bock et al., 2005).

2.3. Estratégias de controle do cancro cítrico

A disseminação de fitobacterioses representa um risco para a citricultura, pois além de comprometer a produtividade dos pomares, exige investimentos em prevenção e controle, impactando diretamente na rentabilidade do citricultor (Sanches et al., 2014).

A prática realizada no Brasil, e em outros países é a pulverização de pomares com produtos à base de cobre, que são capazes de reduzir a população bacteriana na superfície foliar, mas o seu uso a longo prazo pode induzir resistência e acúmulo no solo (Belasque Jr. et al., 2009; Behlau et al., 2010; Hasabi et al., 2014).

Em áreas endêmicas a doença é controlada pelo manejo integrado com: a) pulverizações preventivas com bactericidas a base de cobre; b) o uso de quebra-ventos; c) o controle da larva minadora dos citros e d) plantio de variedades menos suscetíveis ao cancro cítrico (Scapin et al., 2015; Graham et al., 2016, Behlau et al., 2017). Contudo, nas áreas com baixa incidência de infecção, as medidas de controle empregadas são: exclusão e erradicação (Gottwald et al., 2001). A estratégia de erradicação foi empregada em São Paulo por quase 60 anos, sofrendo inúmeras modificações na legislação. Em 1987, o critério de erradicação foi modificado, sendo estabelecida a eliminação de plantas doentes e das demais plantas no raio de 50 metros (Brasil, 1987). Em 1995, alterou-se para a eliminação de plantas doentes em uma área circundante de 30 metros (Brasil, 1995).

Bergamin Filho e Amorim (1999) observaram o aumento do cancro cítrico entre os anos de 1996 a 1999, tendo em 1999 o critério de erradicação modificado, no qual: a) talhões com incidência superior a 0,5% de plantas contaminadas deveriam ser completamente eliminados e b) talhões com incidência de até 0,5% de plantas contaminadas deveriam ser eliminadas as plantas sintomáticas e as demais contidas no raio de 30 metros (Bergamin Filho et al., 2000).

Levantamentos realizados no estado São Paulo pelo Fundecitrus mostraram que a erradicação do cancro cítrico baseado na incidência de plantas doentes, de julho

de 1999 a junho de 2009 manteve a doença controlada, com baixa incidência de plantas doentes. Em 2009, a legislação foi alterada, sendo o critério para controle de cancro cítrico no estado de São Paulo baseado na erradicação de plantas em um raio de 30 metros a partir da planta doente, independentemente da incidência da infecção no talhão (Belasque Jr. et al., 2010).

Em 2012, a citricultura paulista enfrentou o maior nível de disseminação do cancro cítrico desde 2000 (Behlau et al., 2016). Diante desse histórico, o uso de substâncias cúpricas tornou-se essencial, juntamente com a realização de inspeções periódicas (Behlau & Belasque Jr., 2014).

A partir de novembro de 2013 foi preconizado pela Secretaria da Agricultura (Resolução SAA – 147) a não obrigatoriedade da erradicação de plantas que estivessem num raio de 30 metros da planta doente. No entanto, adotou-se a eliminação de plantas contaminadas e pulverização com substâncias cúpricas dentro do raio de 30 metros (São Paulo, 2013). Com a utilização de protocolos mais maleáveis na eliminação de plantas contaminadas, houve um crescimento significativo na ocorrência do cancro cítrico no parque citrícola paulista (Behlau & Belasque, 2014; Behlau et al., 2016), sendo o emprego do manejo da doença indispensável a partir de 2017.

Em 2017, São Paulo foi oficializado como área sob Sistema de Mitigação de Risco (SMR). A Secretaria de Agricultura e Abastecimento publicou a Resolução SAA nº 10 que delimita todo o território paulista como área de controle do cancro cítrico. O Sistema de Mitigação de Risco é uma medida fitossanitária que objetiva: reduzir o potencial de inóculo, e permitir o trânsito e exportação de frutos cítricos oriundos de áreas com ocorrência de cancro cítrico (São Paulo, 2017). No início de 2018, o Ministério da Agricultura, Pecuária e Abastecimento (MAPA) publicou uma nova legislação que regulamenta o controle do cancro cítrico no país, e estabeleceu por meio da Instrução Normativa nº 21, quatro cenários: i) Área sem ocorrência; ii) Área Livre da Praga; iii) Área sob Erradicação ou Supressão e; iv) Área sob Sistema de Mitigação de Risco (SMR) (Brasil, 2018).

2.4. *Xanthomonas citri* subsp. *citri*

Pertencente ao gênero *Xanthomonas,* o agente etiológico do cancro cítrico foi isolado primeiramente pela pesquisadora Clara Henriette Hasse, em 1915, e

classificado como *Pseudomonas citri*. A partir de então, teve sua classificação alterada por mais algumas vezes, sendo em 1949 reclassificada como *Xanthomonas citri*, por Dowson (Khan & Hingorani, 1970), e novamente reclassificada como *Xanthomonas axonopodis* pv. *citri* por Vauterin (Vauterin et al., 1995; Hartung et al., 1996). Em 2006, a bactéria teve sua classificação mais uma vez alterada para *Xanthomonas citri* subsp. *citri* (Schaad et al., 2006).

Xcc apresenta morfologia de bastonete com 1,5 a 2,0 µm de comprimento e 0,5 a 0,7 µm de largura, sendo uma bactéria Gram-negativa, aeróbica, não fixadora de nitrogênio, uniflagelada polar, não forma esporos e não é exigente nutricionalmente (Galli, 1980; Bedendo, 1995). Raramente é encontrada livre no solo, sendo altamente adaptada ao crescimento endofítico (Swings & Civerolo, 1993).

Essa bactéria pode formar colônias amarelas e mucoides na maioria dos meios de cultura, devido à produção de xantomonadina (pigmento importante na proteção contra raios ultravioleta) e de goma xantana (exopolissacarídeo que auxilia na dispersão e sobrevivência do patógeno), respectivamente. Suas colônias são visíveis após 2 a 3 dias de incubação a 28 ºC (Meyer & Bogdanove, 2009).

A Xcc pode sobreviver por meses em material vegetal em decomposição e se disseminar facilmente. Entretanto, para que a infecção ocorra no hospedeiro, a bactéria deve entrar em contato com ferimentos no tecido da planta ou através dos estômatos, acessando o interior das folhas (Gottwald, Graham & Schubert, 2002; Gonçalves-Zuliani et al., 2016). A colonização ocorre no mesofilo foliar levando ao aparecimento de sintomas previamente descritos no **item 2.2**, p.31.

2.5. Divisão celular bacteriana

O processo de divisão bacteriana envolve a invaginação da membrana em conjunto com a parede celular subsequente à formação do septo divisional na região mediana da célula, causando a separação dos cromossomos duplicados. Após a septação e término do processo de divisão, o peptidoglicano do septo bacteriano é hidrolisado, permitindo a separação definitiva das células-filhas (Migocki et al., 2002; Errington; Daniel & Scheffers, 2003; Vicente et al., 2006; Lutkenhaus, 2007).

A divisão celular de procariotos possui proteínas específicas, sendo assim considerado um alvo promissor no desenvolvimento de antibacterianos (Hogan et al., 2018). O divisomo é um complexo macromolecular que controla a divisão bacteriana,

iniciada a partir da polimerização da proteína FtsZ (*Filamentous temperature-sensitive protein Z*). Essa proteína é um homólogo distante da tubulina de eucariotos (Goehring & Gueiros Filho, 2005; Li & Ma, 2015; Panda et al., 2016). A proteína FtsZ é constituída por duas subunidades globulares separadas por uma hélice alfa central, formando um filamento polarizado (Mukherjee & Lutkenhaus, 1994). Além da subunidade globular, há a região *C*-terminal, que possui estrutura aleatória (Durvale, 2013). Esta proteína é responsável pela organização de uma estrutura polimérica e anelar, denominada anel Z, o qual se situa internamente à membrana citoplasmática, na posição mediana da célula, sendo o local em que será iniciada a divisão celular.

Fatores diversos controlam o processo de septação bacteriana, estimulando ou inibindo a formação do anel Z (Lutkenhaus, 2007). Há sistemas que protegem os cromossomos contra guilhotinamento o qual poderia ocosionar o fechamento prematuro do anel Z sobre a massa cromossômica ainda não completamente segregada (Wu & Errington, 2004; Bernhardt & de Boer, 2005).

O anel Z mostra-se como uma estrutura altamente conservada entre os procariotos, atuando como força-motriz para a constrição e divisão celular (Huang et al., 2007). Dessa forma, inibidores do divisomo podem atuar como antibacterianos de amplo espectro de ação (Lock & Harry, 2008).

A proteína FtsZ possui atividade GTPásica, sendo capaz de hidrolisar guanosina trifosfato (GTP) em guanosina difosfato (GDP) e fosfato inorgânico (Pi). A ligação de FtsZ com GTP produz subunidades GTP−FtsZ que irão compor os protofilamentos retilíneos e estáveis, que iniciam o processo de anelação (Chen et al., 2005; Schoenemann & Margolin, 2017). A hidrólise de GTP induz alterações conformacionais no sítio de ligação com o nucleotídeo, alterando a volta T7, responsável por interações cabeça-cauda entre os monômeros, culminando na dissociação dos protofilamentos e despolimerização (Weiss, 2004). As substâncias capazes de reduzir ou aumentar a atividade GTPásica de FtsZ promovem alterações nos protofilamentos, impedindo a divisão celular bacteriana.

A inibição da formação do anel Z, por meio da ligação à proteína FtsZ, constitui-se em uma estratégia para o desenvolvimento de agentes antibacterianos de interesse agrícola de elevada patenteabilidade (Hong & Xie, 2013, Stokes et al., 2013).

2.6. Substâncias anti-*Xanthomonas*

As substâncias cúpricas são amplamente utilizadas no controle de fitobacterioses (Leite Jr. & Mohan, 1990; Gottwald et al., 2002; Sales Jr. et al., 2005; Scapin et al., 2015; Graham et al., 2016, Canteros et al., 2017). A aplicação de produtos a base de cobre na lavoura protege o tecido vegetal da infecção e reduz a população bacteriana na superfície foliar. Esta proteção foliar ocorre por ação mecânica, formando uma película temporária, necessitando de reaplicações (Behlau et al., 2010). O cátion cobre não possui atividade curativa ou sistêmica (Lamichhane et al., 2018).

A ação preventiva com frequentes aplicações e dose de cátion cobre ajustada importantes para obtenção do controle adequado do cancro cítrico (Gottwald et al., 2002, Stein et al., 2007, Behlau et al., 2010), mas a exposição repetida e prolongada pode induzir resistência bacteriana (Behlau et al., 2013; Richard et al., 2017).

Na Argentina, existem relatos da ocorrência de resistência ao cátion cobre em linhagens de Xcc obtidas de viveiros que receberam aplicações sucessivas de substâncias cúpricas (Canteros, 1999). Richard e colaboradores (2017) descreveram resistência ao cátion cobre em linhagens de Xcc na França.

Considerando que o cátion cobre diminui a infecção pelo efeito de contato com a bactéria na superfície foliar, a eficiência de programas de aplicações de produtos a base de cobre pode ser prejudicada pela lixiviação causada por chuvas e pelo vento (Behlau et al., 2010; Graham et al., 2010).

Altos níveis de cobre podem reduzir a fertilidade do solo e causar estresse nas plantas, diminuindo o rendimento das culturas (Dumestre et al., 1999). Aplicações excessivas de formulações a base de cobre, altas temperaturas e tempo seco podem causar fitotoxicidade (Behlau et al., 2017).

Controles alternativos contra Xcc têm sido recentemente estudados. Li e Wang (2014) descreveram a redução de biofilme de Xcc por meio do aminoácido D-leucina e do derivado indólico 3-indoliacetonitrila, com diminuições do número de lesões de cancro cítrico e aumenta a sensibilidade bacteriana ao cobre. Gholami e colaboradores (2018) estudaram a atividade anti-Xcc de enzimas proteolíticas como: proteinase K, tripsina, pepsina, papainase e catalase. No ensaio de digestão enzimática, a proteinase K, tripsina e pepsina inibiram a atividade bacteriana. Os antibióticos penicilina G, ampicilina, cloranfenicol, tetraciclina, estreptomicina, e

ciprofloxacina (**Figura 2**) foram avaliados contra Xcc, obtendo-se valores de concentração inibitória mínima (CIM) na faixa de 0,0015 a 16 µg mL^{-1}, sendo a penicilina G a mais potente (Gholami et al., 2018).

Figura 2. Antibióticos avaliados contra *Xanthomonas citri* subsp. *citri* e seus valores de concentração inibitória mínima (CIM)

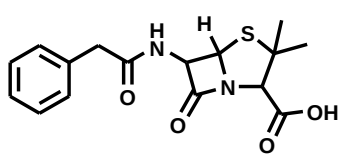

penicilina G, CIM 0,015 µg mL^{-1}

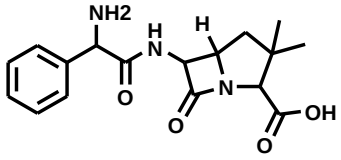

ampicilina, CIM 0,15 µg mL^{-1}

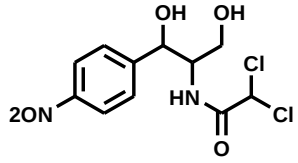

clorafenicol, CIM 0,06 µg mL^{-1}

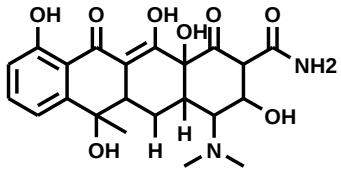

tetraciclina, CIM 0,06 µg mL^{-1}

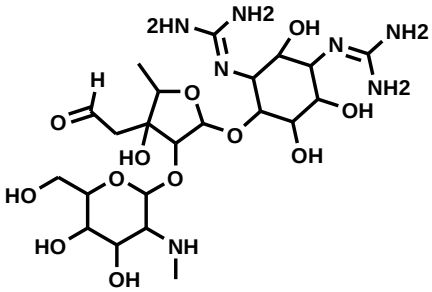

estreptomicina, CIM 16 µg mL^{-1}

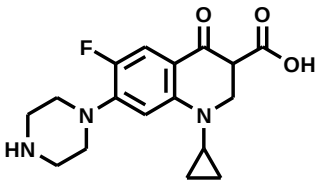

ciprofloxacina, CIM 0,15 µg mL^{-1}

Fonte: autora

Redondo e colaboradores avaliaram a eficácia dos tratamentos bactericidas atualmente aprovados (NaCl, $CuSO_4$, NaClO, ortofenilfenato de sódio [SOPP], Aquazix® [mistura de peróxido de hidrogênio com prata] e Zixvirox® [mistura de peróxido de hidrogênio com ácido peracético] para a desinfecção de Xcc em frutas no *packing house* (Davey & O 'Toole, 2000; Monier & Lindow, 2003; Danhorn & Fuqua, 2007, Redondo et al., 2015). Os autores concluíram que os bactericidas reduziram a formação de biofilmes de modo dose-dependente, o que foi observado anteriormente para o cloreto de sódio, conhecido por induzir a formação de biofilme de *Escherichia coli* (Karatan & Watnick, 2009).

2.7. Diidroxibenzoatos de alquila e sua atividade antimicrobiana

Os DHB são substâncias fenólicas provenientes da biossíntese do acetato ou do ácido chiquímico. São caracterizados por uma carboxila (COOH) e duas hidroxilas

(OH), as quais conferem propriedades antioxidantes e anti-inflamatórias (Bravo, 1998; Simões et al., 2003).

Os DHB apresentam atividade antimicrobiana, incluindo ação contra bactérias Gram-positivas, Gram-negativas e fungos, incluindo: *Escherichia coli*, *Bacillus cereus*, *Listeria monocytogenes*, *Fusarium culmorum* e *Saccharomyces cerevisiae*. Dentre os DHB, destacam-se protocatecuato de butila (**26**), protocatecuato de nonila (**30**) e gentisato de butila (**14**) (**Figura 3**), os quais inibiram o crescimento bacteriano e fúngico com valores de concentração inibitória mínima (CIM) compreendidos entre 1,25 a 2,50 mM (Nihei, Nihei & Kubo, 2003, 2004; Merkl et al., 2010).

Figura 3. Diidroxibenzoatos de alquila com atividade antimicrobiana: gentisato de butila (**14**) e protocatecuatos de butila (**26**), hexila (**27**), heptila (**28**), octila (**29**), nonila (**30**), decila (**31**) e dodecila (**32**).

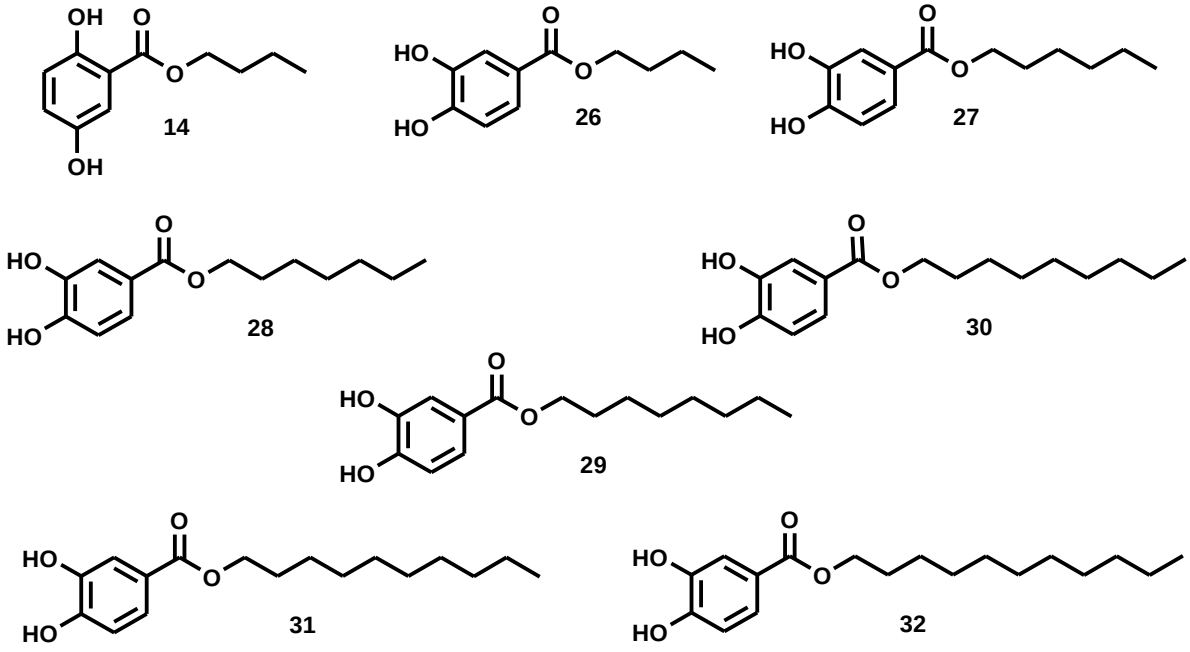

Fonte: autora

Alves e colaboradores demonstraram a atividade antimicrobiana dos ácidos *p*-hidroxibenzóico, β-resorcílico, protocatecuico, gálico, vanílico e siríngico (**Figura 4**, p. 40) contra isolados clínicos de bactérias Gram-negativas como: *E. coli*, *Proteus mirabilis*, *Morganella morganni*, *Pasteurella multocida* e *Neisseria gonorrhoeae* (Alves et al., 2013). Os ácidos com maior atividade antibacteriana foram o ácido β-resorcílico e o ácido protocatecuico, destacando-se a atividade dos ácidos β-resorcílico, vanílico

e siríngico (CIM 0,5 mg mL^{-1}) e *p*-cumárico (CIM 1,0 mg mL^{-1}) contra *Staphylococcus aureus* resistente a meticilina (MRSA). Os autores sugeriram que a presença da carboxila (COOH) e dois grupos hidroxila (OH) *para* ou *orto* posicionados no anel benzênico foram importantes para a atividade anti-MRSA.

Figura 4. Ácidos avaliados contra isolados clínicos de bactérias Gram-negativas

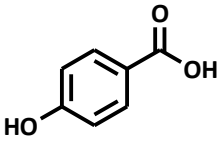

ácido p-hidroxibenzoico

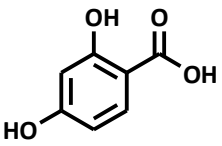

ácido β-resorcílico

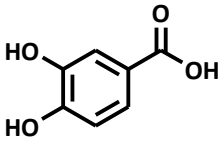

ácido protocatecuico

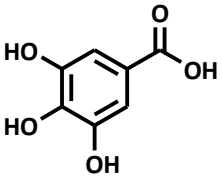

ácido gálico

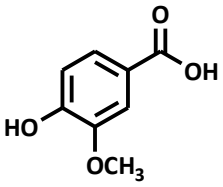

ácido vanílico

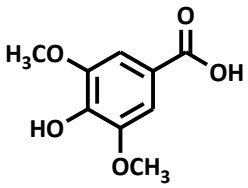

ácido siríngico

Fonte: autora

Soares e colaboradores descreveram a atividade antidermatofítica de DHB, os quais inibiram o crescimento de *Trichophyton rubrum* e *T. mentagrophytes* (**Figura 3**, p. 39). Dentre esses, destacou-se o protocatecuato de heptila (**28**), que apresentou valores de concentração fungicida mínima (CFM) inferiores a 4,0 µg mL^{-1}, atuando sinergicamente com o fluconazol, um fármaco antifúngico (Soares et al., 2014).

Recentemente foram avaliadas as atividades antifúngicas dos protocatecuatos de hexila (**27**), heptila (**28**), octila (**29**), nonila (**30**), decila (**31**) e dodecila (**32**) (**Figura 3**, p. 39), os quais demonstraram potencial inibitório no crescimento de *Paracoccidioides brasiliensis* e *Paracoccidioides lutzii*, com valores de CIM entre 0,24 e 0,97 µg mL^{-1}. A citotoxicidade destas substâncias foi avaliada usando o revelador de sulforrodamina B a 0,4% contra linhagem celular MRC-5 (fibroblasto de pulmão humano). Os protocatecuatos avaliados demonstraram elevadas viabilidades celulares, destacando o hexila (**27**), nonila (**30**) e dodecila (**32**) (**Figura 3**, p. 39) com menor toxicidade à MRC-5 (Medina-Alarcón et al, 2017).

Com o problema da ineficiente diminuição da população bacteriana de Xcc descrita no **item 2.1**, p. 31 e os esforços na procura de alternativas eficazes (**item 2.6**, p. 37), este trabalho se faz relevante na busca de substâncias úteis ao controle do cancro cítrico. Silva e colaboradores indicaram a ação anti-Xcc de galatos de alquila

(3,4,5-triidroxibenzoatos de alquila), destacando-se o galato de heptila (**Figura 5**). Este galato foi capaz de inibir o crescimento de Xcc, em modelos *in vitro* e *in planta* (Silva et al., 2013). Os estudos de mecanismos de ação antibacteriana dos galatos envolvem a ação sobre a membrana e perturbação de FtsZ (Król et al., 2015).

Figura 5. Estrutura do galato de heptila, um 3,4,5-triidroxibenzoato de alquila (TA) com atividade anti-Xcc e inibição da proteína FtsZ

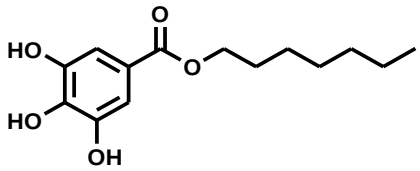

Fonte: autora

A similaridade estrutural entre os TA (**Figura 5**) e os DHB (**14, 26–32**) (**Figuras 3**, p. 39) sugere que estes últimos possuem potencial atividade contra Xcc, bem como potencial atividade inibitória de FtsZ, justificando o investimento químico e biológico nesta classe de ésteres.

3. OBJETIVO GERAL

O objetivo geral desse estudo foi investigar a atividade anti-Xcc e anti-cancro cítrico de diidroxibenzoatos de alquila, bem como avaliar sua toxicidade.

3.1. Objetivos específicos

A) Sintetizar 36 DHB, sendo 12 β-resorcilatos (**Série I**), 12 gentisatos (**Série II**) e 12 protocatecuatos (**Série III**), por meio da reação de esterificação de Fischer;

B) Determinar a hidrofobicidade dos DHB por meio do coeficiente de partição octanol-água (log$P_{o/a}$) utilizando CLAE-DAD;

C) Avaliar a susceptibilidade de *Xanthomonas citri* subsp. *citri* aos DHB, por meio do ensaio de microdiluição em caldo utilizando resazurina como revelador de viabilidade celular (Resazurin Microtiter Assay - REMA);

D) Avaliar os efeitos de DHB selecionados sobre a curva de crescimento de Xcc;

E) Avaliar o efeito de DHB selecionados sobre a permeabilidade da membrana de Xcc;

F) Avaliar o efeito inibitório sobre a divisão celular de DHB selecionados utilizando o método de inibição da atividade GTPásica de FtsZ;

G) Avaliar a atividade tóxica dos DHB contra células eucarióticas utilizando metodologia de MTT;

H) Avaliar a patogenicidade de Xcc após o tratamento com DHB selecionados em folhas de *Citrus sinensis* (laranja doce do tipo 'pera');

I) Avaliar *in planta* os DHB selecionados utilizando ensaio de indução de cancro cítrico em C*itrus sinensis* (laranja doce do tipo 'pera');

J) Avaliar a toxicidade de DHB selecionados contra o crescimento inicial de *Lactuca sativa* (alface);

K) Avaliar a toxicidade de DHB selecionados contra *Citrus sinensis*, avaliando os parâmetros fotossintéticos;

L) Avaliar a toxicidade de DHB selecionados contra *Scaptotrigona postica* (abelhas sem ferrão).

4. REFERÊNCIAS

ALVES, M. J. et al. Antimicrobial activity of phenolic compounds identified in wild mushroons, SAR analysis and docking studies. **Journal of Applied Microbiology**, v. 115, n. 2, p. 346–357, 2013.

AMORIM, L.; REZENDE, J. A. M.; BERGAMIN FILHO, A. **Manual de Fitopatologia.** 4. ed. Agronômica Ceres, 1. 704 p., 2011.

BEDENDO, I. P. OÍDIOS. In: BERGAMIN FILHO, A.; KIMATI, H.; AMORIM, L. **Manual de fitopatologia**, 3. ed. São Paulo: Ceres, 1, 866–871, 1995.

BEHLAU, F. et al. Characterization of a unique copper resistance gene cluster in *Xanthomonas campestris* pv. *campestris* isolated in Trinidad, West Indies. **European Journal of Plant Pathology**, v. 147, n. 3, p. 671–681, 2016.

BEHLAU, F. et al. Copper sprays and windbreaks for control of citrus canker on young orange trees in southern Brazil. **Crop Protection**, v. 27, n. 3-5, p. 807–813, 2008.

BEHLAU, F. et al. Effect of frequency of copper applications on control of citrus canker and the yield of young bearing sweet orange trees. **Crop Protection**, v. 29, n. 3, p. 300–305, 2010.

BEHLAU, F. et al. Evidence for acquisition of copper resistance genes from different sources in citrus-associated xanthomonads. **Phytopathology**, v. 103, n. 5, p. 409–418, 2013.

BEHLAU, F. et al. Incidência e severidade de cancro cítrico em laranja 'Pêra Rio' sob condições de controle químico e proteção com quebra-vento. **Fitopatologia Brasileira**, v. 32, n. 4, p. 311–317, 2007.

BEHLAU, F. et al. Soluble and insoluble copper formulations and metallic copper rate for control of citrus canker on sweet orange trees. **Crop Protection**, v. 94, p. 185-191, 2017.

BEHLAU, F.; BELASQUE JR., J. **Cancro cítrico: a doença e seu controle**. 1 ed. Araraquara, SP: Fundecitrus, 94 p., 2014.

BEHLAU, F.; FONSECA, A. E.; BELASQUE JR., J. A comprehensive analysis of the Asiatic citrus canker eradication programme in São Paulo state, Brazil, from 1999 to 2009. **Plant Pathology**, v. 65, n. 8, p. 1390–1399, 2016.

BELASQUE JR, J. et al. Prováveis consequências do abrandamento da metodologia de erradicação do cancro cítrico no Estado de São Paulo. **Tropical Plant Pathology**, v. 35, n. 5, p. 314–317, 2010.

BELASQUE JR., J.; FERNANDES, N. G.; MASSARI, C. A. O sucesso da campanha de erradicação do cancro cítrico no Estado de São Paulo, Brasil. **Summa Phytopathologica**, v. 35, n. 2, p. 91, 2009.

BERGAMIN FILHO, A., AMORIN, L., LARANJEIRA, F.F., GOTTWALD, T.R. 2000. Epidemiology of citrus canker in Brazil with and without the Asian citrus leaf miner. **International Citrus Canker Research Workshop**. Fort Pierce, Division of Plant Industry, Florida Department of Agriculture and Consumer Services. p. 24-25, 2000.

BERNHARDT, T. G.; DE BOER, P. A. SlmA, a nucleoid-associated, FtsZ binding protein required for blocking septal ring assembly over Chromosomes in *E. coli*. **Molecular Cell**, v. 18, n. 5, p. 555–564, 2005.

BITANCOURT, A. A. **O cancro cítrico.** O Biológico, São Paulo, v. 23, n. 6, p. 101–111, 1957.

BOCK, C. H.; PARKER, P. E.; GOTTWALD, T. R. Effect of simulated wind-driven rain on duration and distance of dispersal of *Xanthomonas axonopodis* pv. *citri* from canker-infected citrus trees. **Plant Disease**, v. 89, n. 1, p. 71–80, 2005.

BRASIL. **Instrução Normativa nº 21**, de 25 de abril de 2018. Institui, em todo o território nacional, os critérios e procedimentos para o estabelecimento e manutenção do status fitossanitário relativo à praga denominada Cancro Cítrico (*Xanthomonas citri* subsp. *citri*) Diário Oficial da União. 11 de maio 2018. Seção 1.

BRASIL. Ministério da Agricultura, do Abastecimento e da Reforma Agrária – Secretaria de Defesa Agropecuária. **Portaria 282**. Diário Oficial da União, Brasília, 21476–21478, 1987.

BRASIL. Ministério da Agricultura, do Abastecimento e da Reforma Agrária – Secretaria de Defesa Agropecuária. **Portaria 62**. Diário Oficial da União, Brasília, 3970–3972, 1995.

BRAVO, L. Polyphenols: chemistry, dietary sources, metabolism and nutrition significance. **Nutrition Reviews**, v. 56, n. 11, p. 317–333, 1998.

BROWN, K. Florida fights to stop citrus canker. **Science**, v. 292, n. 5525, p. 2275–2278, 2001.

BRUNNING, A. M.; GABRIEL, D. W. *Xanthomonas citri*: breaking the surface. **Molecular Plant Pathology**, v. 4, p. 141-157, 2003.

CANTEROS, B. I. Copper resistance in *Xanthomonas campestris* pv. *citri*. In: **Plant pathogenic bacteria Proceedings of the International Society of Bacteriology Centre for Advanced Study in Botany**, 455–459. Edited by A. Mahadevan. Chennai, India: University of Madras, 1999.

CANTEROS, B. I., GOCHEZ, A. M., MOSCHINI, R. C. Management of citrus canker in Argentina, a success story. **Plant Pathology**, v. 33, n. 5, p. 441–449, 2017.

CHEN, Y. et al. A rapid fluorescence assay for FtsZ assembly indicates cooperative assembly with a dimer nucleus. **Biophysical Journal**, v. 88, n. 1, p. 505–514, 2005.

CHOI, J. et al. Selection of small synthetic antimicrobial peptides inhibiting *Xanthomonas citri* subsp. *citri* causing citrus canker. **The Plant Pathology Journal**, v. 33, n. 1, p. 87−94, 2017.

CitrusBR. Disponível em <http://www.citrusbr.com/economia/?ec=07> acesso em 18 de outubro de 2016.

DANHORN, T.; FUQUA, C. Biofilm formation by plant-associated bacteria. **Annual Reviews Microbiology**, v. 61, p. 401–422, 2007.

DAVEY, M. E.; O'TOOLE, G. A. Microbial biofilms: from ecology to molecular genetics. **Microbiology and Molecular Biology Reviews**,v. 64, n. 4, 847–867, 2000.

DEWDNEY, M. M.; GRAHAM, J. H. Florida Citrus Pest Management Guide: Citrus Canker. **University of Florida**, p. 182–186, 2012.

DUAN, S. et al. Functional characterization of the citrus canker susceptibility gene *CsLOB1*. **Molecular Plant Pathology,** v. 19, n. 8, p. 1908−1916, 2018.

DUMESTRE, A. et al. Copper speciation and microbial activity in long-term contaminated soils. **Archives of Environmental Contamination and Toxicology**, v. 36, n. 2, p. 124–131, 1999.

DURVALE, M. C. **Estudo genético da interação entre as proteínas FtsZ e SpoIIE em *Bacillus subtilis***, 2013. 66 f. Dissertação (Mestrado em Bioquímica) – Instituto de Química, Universidade de São Paulo, São Paulo, 2013.

EFSA Panel on Plant Health. Scientific opinion on the risk to plant health of *Xanthomonas citri* pv*. citri and Xanthomonas citri* pv*. aurantifolii* for the EU territory. EFSA J. 12, 3556e3734, 2014.

EFSA. Event Report: Technical Meeting with USDA APHIS on Citrus Canker- Video-conference, Parma 20 March 2013. EFSA Supporting Publication, pp. 1e13. EN-477, 2013.

ERRINGTON, J.; DANIEL, R. A., SCHEFFERS, D. J. Cytokinesis in Bacteria **Microbiology and Molecular Biolology Reviews**, v. 67, n. 1, p. 52–65, 2003.

FAO, Food and Agriculture Organization of the United Nation Statistics Division. Statistic Database. 2015. Disponível em <http://faostat3.fao.org/home/E> acesso em 28 de junho de 2018.

FARES, A. et al. Potential climate change impacts on citrus water requirement across major producing areas in the world. **Journal of Water and Climate Change**, v. 8, n. 4, p. 576−592, 2017.

FEICHTENBERGER, E. et al. Doenças dos Citros (*Citrus* spp.). In: Kimati H. et al. **Manual de Fitopatologia: doenças das plantas cultivadas**, 4 ed. Editora Agronômica Ceres, 2, p. 239, 2005.

FRANCIS, M. I. et al. Soil application of imidacloprid and related SAR-inducing compounds produces effective and persistent control of citrus canker. **European Journal Plant Pathology**, v. 124, p. 283–292, 2009.

FUNDECITRUS, Sumário Executivo: Estimativa de Safra de laranja 2019/2020 do cinturão citrícola de São Paulo e Triângulo/Sudoeste Mineiro. Disponível em : <https://www.fundecitrus.com.br/pdf/pes_relatorios/2019_05_10_Sum%C3%A1rio_Executivo_da_Estimativa_da_Safra_de_Laranja_2019-2020.pdf>. Acessado em: 10 de maio de 2019.

GALLI, F. **Manual de fitopatologia: doenças das plantas cultivadas**. São Paulo, Ceres, 2, 587 p., 1980.

GHOLAMI, D. et al. Comparison of antibiotics and bacteriocins antibacterial activity on *Xanthomonas citri* subsp. *citri*. **Iranian Journal of Fisheries Sciences**, v. 17, n. 1, p. 162-178, 2018.

GOEHRING, N. W.; GUEIROS-FILHO F. Premature targeting of a cell division protein to midcell allows dissection of divisome assembly in *Escherichia coli.* **Genes Development**, v. 19, n. 1, p. 127–137, 2005.

GONÇALVES-ZULIANI, A. M. O. et al. Reaction of detached leaves from different varieties of sweet orange to inoculation with *Xanthomonas citri* subsp. *citri*. **Summa Phytopathologica**, v. 42, n. 2, p. 125−133, 2016

GOTTWALD, T. et al. The epidemiological significance of post-pakinghouse survival of *Xanthomonas citri* subsp. *citri* for dissemination of Asiatic citris canker via infect fruit. **Crop Protection**, v. 28, p. 508-524, 2009.

GOTTWALD, T. R. et al. Geo-referenced spatiotemporal analysis of the urban citrus canker epidemic in Florida. **Phytopathology**, v. 92, n. 4, p. 361–377, 2002.

GOTTWALD, T. R. et. al. The citrus canker epidemic in Florida: the scientific basis of regulatory eradication policy for an invasive species. **Phytopathology**, v. 91, n. 1, p. 30–34, 2001.

GOTTWALD, T. R.; GRAHAM, J. H.; SCHUBERT, T. S. Citrus canker: the pathogen and its impact. **Plant Health Progress**, v. 10, p. 32, 2002.

GRAHAM, J. H., BROOKS, C., YONCE, H. D. Importance of early season copper sprays for protection of Hamlin orange fruit against citrus canker infection and premature fruit drop. **Proceedings Florida State Horticultural Society**, v. 129, p. 74–78, 2016.

GRAHAM, J. H.; DEWDNEY, M. M.; MYERS, M. E. Streptomycin and copper formulations for control of citrus canker on grapefruit. **Proceedings of the Florida State Horticultural Society**, v. 123, p. 92–98, 2010.

HARTUNG, W. et al. Abscisic acid in soils: what is its function and which factors and mechanismis influence its concentration? **Pant and Soil**, v. 184, p. 105–110, 1996.

HASABI, V. et al. *In vitro* and *in vivo* Antibacterial activity of some Organic and Inorganic Salts Against Asiatic Citrus Canker Agent *Xanthomonas citri* subsp. c*itri.* **Turkish Journal of Agriculture – Food Science and Technology**, v. 2, n. 6, p. 296–300, 2014.

HONG, W.; XIE, J. Progress of FtsZ inhibitors as novel antibiotics leads. **Critical Reviews in Eukaryotic Gene Expression**, v. 23, n. 4, p.327–338, 2013.

HUANG, Q. et al. FtsZ: A Novel Target for Tuberculosis Drug Discovery. **Current Topics in Medicinal Chemistry**, v. 7, n. 5, p. 527–543, 2007.

Instituto Brasileiro de Geografia e Estatística (IBGE) Levantamento Sistemático da Produção Agrícola – LSPA Disponível em <https://sidra.ibge.gov.br/home/ispa/brasil> acesso em 01 de agosto de 2018.

KARATAN, E. & WATNICK, P. Signals, regulatory networks, and materials that build and break bacterial biofilms. **Microbiology and Molecular Biology Reviews**, v. 73, n. 2, p. 310-347, 2009.

KHAN I. D.; HINGORANI M. K. Strain studies in *Xanthomonas citri* (Hasse) Dowson. **Journal of Horticultural Science**, v. 45, n. 1, p. 15–17, 1970.

KOPACZ, M. M. et al. Purification and characterization of FtsZ from the citrus canker pathogen *Xanthomonas citri* subsp. *citri*. **MicrobiologyOpen**, p. e00706, 2018.

KRÓL, E. et al. Antibacterial activity of alkyl gallates is a combination of direct targeting of FtsZ and permeabilization of bacterial membranes. **Frontiers in Microbiology**, v. 6, p. 1-12, 2015.

LAMICHHANE, J. R. et al. Thirteen decades of antimicrobial copper compounds applied in agriculture. **Agronomy for Sustainable Development**, v. 38, n.28, 2018.

LANZA, F. E. et al. Characteristics of citrus canker lesions associated with premature drop of sweet orange fruit. **Phytopathology**, p. PHYTO-04-18-0114-R, 2018.

LEITE JR., R. P. **Cancro cítrico: prevenção e controle no Paraná**. Londrina: Fundação Instituto Agronômico do Paraná, 1990.

LEITE JR., R. P.; MOHAM, S. K. Integrated management of the citrus bacterial canker disease caused by *Xanthomonas campestris* pv. *citri* in the State of Paraná, Brazil. **Crop Protection**, v. 9, n. 1, p. 3–7, 1990.

LI, J.; WANG, N. Foliar application of biofilm formation-inhibiting compounds enhances control of citrus canker caused by *Xanthomonas citri* subsp. *citri*. **Phytopatology**, v. 104, n. 2, p. 134–42, 2014.

LI, X.; MA, S. Advances in the discovery of novel antimicrobials targeting the assembly of bacterial cell division protein FtsZ. **European Journal of Medicinal Chemistry**, v. 95, p. 1−15, 2015.

LOCK, R. L.; HARRY, E. J. Cell-division inhibitors: new insights for future antibiotics. **Nature Reviews Drug Discovery**, v. 7, n. 4, p. 324 –338, 2008.

LUTKENHAUS, J. Assembly Dynamics of the Bacterial MinCDE System and Spatial Regulation of the Z Ring. **Annual Reviews Biochemistry**, v. 76, p. 539–562, 2007.

MASSARI, C. A.; BELASQUE JR., J. A campanha de erradicação do cancro cítrico no Estado de São Paulo - Situação atual e contaminação em viveiros. **Laranja**, v. 27, p. 41–55, 2006.

MEDINA-ALARCÓN, K. P. et al. Alkyl Protocatechuate Loaded Nanostructured Lipid Systems as a Treatment Strategy for *Paracoccidioides brasiliensis* and *Paracoccidioides litizii In Vitro.* **Frontiers in Microbiology** v.12, n. 8, p. 1048, 2017.

MERKL, R. et al. Antimicrobial and Antioxidant Properties of Phenolic Acids Alkyl Esters, **Czech Journal of Food Sciences**., v. 28, n. 4, p. 275-279, 2010.

MEYER, D. F., BOGDANOVE, A. J. Genomics-driven advances in *Xanthomonas* biology. In: Jackson, R.W. (Ed.). **Plant pathogenic bacteria: genomics and molecular biology**. Norfolk, UK: Caister Academic Press. p. 147-1161, 2009.

MIGOCKI, M. D. et al. The Min system is not required for precise placement of the midcell Z ring in *Bacillus subtilis*. Eur. Mol. Biol. Org. Rep., v. 3, p. 1163–1167, 2002.

MONIER, J. M.; LINDOW, S. E. Differential survival of solitary and aggregated bacterial cells promotes aggregate formation on leaf surfaces. **Proceedings of the National Academy of Sciences**, v. 100, n. 26, p. 15977–15982, 2003.

MUKHERJEE, A., LUTKENHAUS, J. Guanine nucleotide-dependent assembly of FtsZ into filaments. **Journal Bacteriology**, v. 176, n. 9, p. 2754–2758, 1994.

NEVES, M. F. & TROBIM, V. G. **Anuário da Citricultura** 1ªEd. SP, CitrusBr, 2017.

NEVES, M. F. et al. Análisis del Sector Sucroenergético Brasileiro Bajo um Enfoque de Planificación Estratégica. **Agroalimentaria** (Caracas), v. 17, p. 29–45, 2011.

NEVES, M. F. et al. **O Retrato da Citricultura Brasileira**. Elaborado por: MARKESTRAT (Centro de Pesquisa e Projetos em Marketing e Estratégia). Coordenador: Marcos Fava Neves. Ribeirão Preto, SP, 2010.

NIHEI, K., NIHEI A. & KUBO I. Rational Design of Antimicrobial Agents: Antifungal Activity of Alk(en)yl Dihydroxybenzoates and Dihydroxyphenyl Alkanoates. **Bioorganic & Medicinal Chemistry Letters**, v. 13, n. 22, p. 3993–3996, 2003.

PANDA, D. et al. Identification of agents targeting FtsZ assembly. **Future Medicinal Chemistry**, v. 8, n. 10, p. 1111−1132, 2016.

REDONDO, C. et al. Influence of selected bactericides on biofilm formation and viability of *Xanthomonas citri* subsp. *citri*. **Crop Protection**, v. 78, p. 204–213, 2015.

RICHARD, D. et al. Complete Genome Sequences of Six Copper-Resistant *Xanthomonas citri* pv. *citri* Strains Causing Asiatic Citrus Canker, Obtained Using Long-Read Technology. **Genome Announcements**, v. 5, n. 12, p. e00010-17, 2017.

ROSETTI V. V. **Manual ilustrado de doenças dos citros**. Piracicaba: Esalq – Fundecitrus, 207p., 2001.

SALES, JR., R. et al. Efeito de kasugamicina e oxicloreto de cobre no controle da mancha aquosa do meloeiro. **Fitopatologia Brasileira**, v. 30, p. 295–298, 2005.

SANCHES, A. L. R. et al. Análise Econômica da Prevenção e Controle do Cancro Cítrico no Estado de São Paulo. **Revista de Economia e Sociologia Rural**, v. 52, n. 3, p. 549–566, 2014.

SÃO PAULO (ESTADO). **Resolução da Secretaria de Agricultura e Abastecimento (SAA) nº 10**, de 20 de fevereiro de 2017. Disponível em: <https://www.defesa.agricultura.sp.gov.br/legislacoes/resolucao-saa-10-de-20-02-2017,1093.html> Acessado em 15 de setembro de 2017.

SÃO PAULO (ESTADO). **Resolução da Secretaria de Agricultura e Abastecimento (SAA) nº 147**, de 31 de outubro de 2013. Diário Oficial do Estado de São Paulo, 1ºde novembro de 2013, Seção 1. p. 50, 2013.

SAVIETTO, A.; et al. Antibacterial activity of monoacetylated alkyl gallates against *Xanthomonas citri* subsp. *citri*. **Archives Microbiology**, v. 200, n. 6, p. 929–937, 2018.

SCAPIN, M. S. et al. Tree-row-volume-based sprays of copper bactericide for control of citrus canker. **Crop Protection**, v. 77, p. 119–126, 2015.

SCHAAD, N. W. et al. Emended classification of Xanthomonad patogens on citrus. **Systematic and Applied Microbiology**, v. 29, n. 8, p. 690–695, 2006.

SCHOENEMANN, K. M.; MARGOLIN, W. Bacterial division: FtsZ treadmills to build a beautiful wall. **Current Biology**, v. 27, n. 8, p. R301−R303, 2017.

SCHUBERT, T. S. et al. Meeting the challenge of Eradicating Citrus Canker in Florida-Again. **Plant Disease**, v. 85, n. 4, p. 340–356, 2001.

SILVA, I. C. et al. Antibacterial Activity of Alkyl Gallates against *Xanthomonas citri* subsp. *citri*. **Journal Bacteriolology**, v. 195, n. 1, p. 85, 2013.

SILVA, I. C. et al. Evaluation of cytotoxic, apoptotic, mutagenic, and chemopreventive activities of semi-synthetic esters of gallic acid. **Food and Chemical Toxicology**, v. 105, p. 300−307, 2017.

SIMÕES, C. M. O et al. **Farmacognosia: da planta ao medicamento**. 5ed.Florianópolis/Porto Alegre: Editora da UFSC/Editora da UFRGS, v. 1, p. 467-497, 2003

SOARES, L. A. et al. Anti-*Trichophyton* Activity of Protocatechuates and Their Synergism with Fluconazol. **Evidence-Based Complementary and Alternative Medicine**, 2014.

STALL, R. E.; SEYMOUR, C. P. Canker, a threat to citrus in the gulf-coast states. **Plant Disease**, v. 67, p. 581–585, 1983.

STEIN, B. et al. Citrus leaf miner control and copper fungicides sprays for management of citrus canker on lemon in Tucuman, Argentina. **Proceedings Florida State Horticultural Society**, v. 120, p. 127-131, 2007.

STOKES, N. R. et al. An Improved Small-Molecule Inhibitor of FtsZ with Superior *In Vitro* Potency, Drug-Like Properties, and *In Vivo* Efficacy. **Antimicrobial Agents and Chemotherapy**, v. 57, n. 1, p. 317–325, 2013.

SWINGS, J. G.; CIVEROLO, E. L. ***Xanthomonas***. London: Chapman & Hall, 1993. 399 p.

USDA, United States Department of Agriculture. Citrus: World Markets and Trade Foreign Agricultural Service/USDA Office of Global Analysis (2018). Disponível em <https://apps.fas.usda.gov/psdonline/circulars/citrus.pdf> acesso em 01 de agosto de 2018.

VAUTERIN, L. et al. Reclassification of *Xanthomonas* **International Journal of Systematic Bacteriology**, v. 45, n. 3, p. 472–489, 1995.

VERNIERI, C. J.; GOTTWALD T. R.; PRUVOST O. Disease development and symptom expression of *Xanthomonas axonopodi* pv. *citri* in various plant citrus tissues. **Phytopatology**, v. 93, p. 832–843, 2003.

VICENTE, M. et al. Septum Enlightenment: Assembly of Bacterial Division Proteins. **Journal Bacteriology**, v. 188, n. 1, p. 19–27, 2006.

VIEIRA, G. et al. Terrestrial and marine Antarctic fungi extracts active against *Xanthomonas citri* subsp. *citri*. **Letters in Applied Microbiology**, v. 67, n. 1, p. 64−71, 2018.

WEISS, D. S. Bacterial cell division and the septal ring. **Molecular Microbiology**, v. 54, n. 3, p. 588–597, 2004.

WU, L. J.; ERRINGTON, J. Coordination of cell division and chromosome segregation by a nucleoid occlusion protein in *Bacillus subtilis.* **Cell**, v. 117, n. 7, p. 915–925, 2004.

Capítulo 2

Capítulo 2: Artigo – "Design of Antibacterial Agents: Alkyl Dihydroxybenzoates against *Xanthomonas citri* subsp. *citri*"

Artigo publicado na revista International Journal of Molecular Sciences em outubro de 2018.

International Journal of *Molecular Sciences*

MDPI

Article

Design of Antibacterial Agents: Alkyl Dihydroxybenzoates against *Xanthomonas citri* subsp. *citri*

Ana Carolina Nazaré [1,*], Carlos Roberto Polaquini [1], Lúcia Bonci Cavalca [2,3], Daiane Bertholin Anselmo [1], Marilia de Freitas Calmon Saiki [4], Diego Alves Monteiro [4], Aleksandra Zielinska [3], Paula Rahal [4], Eleni Gomes [4], Dirk-Jan Scheffers [3], Henrique Ferreira [2] and Luis Octavio Regasini [1,*]

1 Department of Chemistry and Environmental Sciences, Institute of Biosciences, Humanities and Exact Sciences, São Paulo State University, São José do Rio Preto, SP 15054-000, Brazil; carlos_polaquini@hotmail.com (C.R.P.); daiane_bertholin@hotmail.com (D.B.A.)

2 Department of Biochemistry and Microbiology, Biosciences Institute, São Paulo State University, Rio Claro, SP 13506-900, Brazil; l.bonci@hotmail.com (L.B.C.); henrique.ferreira@unesp.br (H.F.)

3 Department of Molecular Microbiology, Groningen Biomolecular Sciences and Biotechnology Institute, University of Groningen, 9747 AG Groningen, The Netherlands; a.u.zielinska@rug.nl (A.Z.); d.j.scheffers@rug.nl (D.-J.S.)

4 Department of Biology, Institute of Biosciences, Humanities and Exact Sciences, São Paulo State University, IBILCE, São José do Rio Preto, SP 15054-000, Brazil; macal131@gmail.com (M.d.F.C.S.); diego8monteiro@hotmail.com (D.A.M.); prahal@ibilce.unesp.br (P.R.); eleni@ibilce.unesp.br (E.G.)

* Correspondence: acarolnazare@gmail.com (A.C.N.); luis.regasini@unesp.br (L.O.R.); Tel.: +55-17-3221-2362 (L.O.R.)

Received: 24 August 2018; Accepted: 1 October 2018; Published: 6 October 2018

check for updates

Design of Antibacterial Agents: Alkyl Dihydroxybenzoates against *Xanthomonas citri* subsp. *citri*

Ana Carolina Nazaré [1,*], Carlos Roberto Polaquini [1], Lúcia Bonci Cavalca [2,3], Daiane Bertholin Anselmo [1], Marilia de Freitas Calmon Saiki [4], Diego Alves Monteiro [4], Aleksandra Zielinska [3], Paula Rahal [4], Eleni Gomes [4], Dirk-Jan Scheffers [3], Henrique Ferreira [2] and Luis Octavio Regasini [1,*]

[1] Department of Chemistry and Environmental Sciences, Institute of Biosciences, Humanities and Exact Sciences, São Paulo State University, São José do Rio Preto, SP, 15054-000, Brazil; carlos_polaquini@hotmail.com (C. R. P.); daiane_bertholin@hotmail.com (D. B. A.)

[2] Department of Biochemistry and Microbiology, Biosciences Institute, São Paulo State University, Rio Claro, SP, 13506-900, Brazil; l.bonci@hotmail.com (L. B. C.); henrique.ferreira@unesp.br (H. F.)

[3] Department of Molecular Microbiology, Groningen Biomolecular Sciences and Biotechnology Institute, University of Groningen, Groningen, 9747 AG. The Netherlands; a.u.zielinska@rug.nl (A. Z.); d.j.scheffers@rug.nl (D. J. S.); l.bonci@hotmail.com (L. B. C.)

[4] Department of Biology, Institute of Biosciences, Humanities and Exact Sciences, São Paulo State University, IBILCE, São José do Rio Preto, SP, 15054-000, Brazil; macal131@gmail.com (M. d. F. C. S.); diego8monteiro@hotmail.com (D. A. M.); prahal@ibilce.unesp.br (P. R.); eleni@ibilce.unesp.br (E.G.)

*****Correspondence: acarolnazare@gmail.com (A. C. N.); luis.regasini@unesp.br (L. O. R.); Tel.: +55-17-3221-2362 (L. O. R.)

ABSTRACT

Xanthomonas citri subsp. *citri* (Xcc) causes citrus canker, affecting sweet orange-producing areas around the world. The current chemical treatment available for this disease is based on cupric compounds. For this reason, the objective of this study was to design antibacterial agents. In order to do this, we analyzed the anti-Xcc activity of 36 alkyl dihydroxybenzoates and we found 14 active compounds. Among them, three esters with the lowest minimum inhibitory concentration values were selected; compounds **4** (52 µM), **16** (80 µM) and **28** (88 µM). Our study demonstrated that alkyl dihydroxybenzoates cause a delay in the exponential phase. The permeability capacity of alkyl dihydroxybenzoates in a quarter of MIC was compared to nisin (positive control). Compound **28** was the most effective (93.8), compared to compound **16** (41.3) and compound **4** (13.9) by percentage values. Finally, all three compounds showed inhibition of FtsZ GTPase activity, and promoted changes in protofilaments, leading to depolymerization, which prevents bacterial cell division. In conclusion, heptyl dihydroxybenzoates (compounds **4**, **16** and **28**) are promising anti-Xcc agents which may serve as an alternative for the control of citrus canker.

Keywords: citrus canker; antimicrobial; plant disease; membrane disruption; phenolic acids

1. INTRODUCTION

Citrus canker is caused by *Xanthomonas citri* subsp. *citri* (Xcc), which is responsible for a severe form of the disease (Asian citrus canker) [1–3]. Typical symptoms of this plant disease are brownish eruptive lesions on their aerial parts, which may be surrounded by chlorotic halos. Bacteria infect leaves, stems, and fruit, which leads to defoliation, twig dieback and early fruit drop. As a consequence, the disease brings significant economic losses to the citrus sector [3–6].

These phytopathogens enter the plant through stomata and injuries caused during crop management or by the citrus leaf miner (*Phyllocnistis citrella).* They colonize the intercellular space in the apoplast and break down the leaf epidermis as a result of cell hyperplasia [6]. Rainfall, wind and movement of infected seedlings moving are the causes for this bacterial dissemination [7]. Under current legislation, the state of São Paulo in Brazil was has been declared a Risk Mitigation System (RMS) area [8]. This is a control that aims to reduce citrus canker inoculum potential.

The chemical control of citrus canker is carried out with copper-based antibacterials [9–11]. Copper applications reduce the intensity of the disease and the number of inoculations into the plant, because bacterial survival is reduced [10–16]. Although copper sprays reduce crop loss and help to control citrus canker, they may also negatively affect the environment [17]. Copper may accumulate in the soil, and can cause adverse effects on root growth and on nutrient uptake by citrus trees [18–22]. In addition, the emergence of copper-resistant bacterial strains is a reality. [23,24].

Phenolic compounds have been evaluated as an alternative to current citrus canker treatment. In our previous studies, potent antibacterial activities of a homologous series of alkyl gallates (3,4,5-trihydroxybenzoates) [25] were described. The antibacterial mechanism of these compounds involves action on the membrane and they promote cell death by a combination of mechanisms: FtsZ inhibition, membrane permeability, and possibly another activity [26]. In order to improve the anti-Xcc activity of alkyl gallates, four monoacetylated gallates were synthesized and tested against Xcc [27]. As expected, the insertion of the acetyl group on the alkyl gallates conferred an increase of lipophilicity on these compounds, and made them more potent than the pattern phenolic compounds [25,27]. Altogether, these data suggest that modifications in hydroxyl groups may result in increased anti-Xcc potency.

Therefore, our research group has investigated dihydroxybenzoic acids and their alkyl esters as antimicrobials against Gram-positive and Gram-negative bacteria and yeasts [28–30]. Besides their antimicrobial activity, we selected these compounds in order to investigate the relevance of the number and position of the hydroxyls to anti-Xcc activity. According to Nihei, Nihei and Kubo, in order to elicit activity as the hydrophilic 'head' portion, two hydroxyl groups are essential [29].

In our continuing search for anti-Xcc agents from phenolic natural products-based compounds, we synthesized three series of alkyl esters from β-resorcilic, gentisic and protocatechuic acids. The anti-Xcc activity of these esters was evaluated against X. *citri* subsp. *citri* strain 306 (IBSBF 1594) to derive preliminary structure-activity relationships. The three most active compounds (**4**, **16** and **28**) were investigated regarding their toxicity against eukaryotic cell lines and their effects on the growth of Xcc. In addition, their ability to act on membrane and cell division by inhibition of the GTPase activity of FtsZ were carried out.

2. RESULTS

2.1. Synthesis, Purification and Identification of Alkyl Dihydroxybenzoates

The new antibacterial agents were synthesized in three different series with 12 alkyl dihydroxybenzoates each: series I (**1**–**12**), series II (**13**–**24**) and series III (**25**–**36**). Each series had carboxylic acids as precursors; they were the 2,4 dihydroxybenzoic (or β-resorcilic) acid (I), the 2,5 dihydroxybenzoic (or gentisic) acid (II) and the 3,4 dihydroxybenzoic (or protocatechuic) acid (III). Different purification methods were used in order to obtain the pure compounds; low temperature hexane washes, hexane and acetone crystallization techniques, and normal phase column chromatography. The purity degree analysis was carried out with high-performance liquid chromatography (HPLC), and was measured by integrating the peaks of the chromatograms. The values varied from 76.5% to 99.9% (**Table 1**, p. 62), thus validating our methodologies for purifying and obtaining the compounds. The alkyl dihydroxybenzoates structures were determined by ^{1}H and ^{13}C NMR analyses. Spectra and chromatograms are presented as supplementary material.

2.2. Partition Coefficient Study

The partition coefficients were measured by HPLC method according to OECD 117 – Guidelines for the Testing of Chemicals [31] to all compounds. The log Po/w values of the alkyl dihydroxybenzoates and carboxyl acids were ranged from 0.8 to 7.0 (**Table 1**, p. 62).

2.3. Determination of MIC and MBC against Xanthomonas citri subsp. citri Assay

The antibacterial potential of carboxylic acids and their esters were compared to copper oxychloride (a commercial active often used to combat citrus canker). Minimal inhibitory concentration (MIC) values were determined by REMA assay, which measures cellular respiratory activity.

We assayed the carboxylic acids (2,4 dihydroxybenzoic acid, 2,5 dihydroxybenzoic acid and 3,4 dihydroxybenzoic acid) which demonstrated they were inactive since they did not inhibit Xcc growth (MIC > 100 μg mL^{-1}). However, 14 esters showed potential anti-Xcc activity, with MIC values lower than 100 μg mL^{-1} (**2**–**4**, **11**, **15**, **16**, **22**–**24**, **27**–**30** and **36**).

The minimal bactericidal concentration (MBC) was determined by observing the bacterial growth in Petri dishes transferred from the REMA plates. We observed bactericidal action for compounds **11**, **22**–**24**, **31** and **36** at 100 μg mL^{-1}, compounds **2**, **3**, **15**, **27**–**30** at 50 μg mL^{-1} and compounds **4** and **16** at 25 μg mL^{-1}.

2.4. Cytotoxicity Assay

The cytotoxicity of the three most potent compounds (**4**, **16** and **28**) was evaluated using the MTT test. This test is based on the reduction of 3-(4,5-dimethyl-2-thiazolyl)-2,5-diphenyl-2-tetrazole bromide by viable cells, with formation of violet insoluble formazan crystals. Five cell lines were used in order to evaluate the cytotoxic effect of the compounds as a whole.

Thus, it can be seen in **Table 2**, p. 63 that compounds **4**, **16** and **28** had low cytotoxic potential because they showed IC_{50} values above 100 μM for MRC-5 (human lung fibroblast cell line), VERO (monkey kidney epithelial cell line) and ACHN (human renal adenocarcinoma cell line). In contrast, HaCaT (human keratinocyte cell line) and Huh-7.5 (human hepatoma cell line) were more sensitive to selected compounds, with

IC_{50} values in the range of 70 µM, with the exception of compound **16** (20.60 µM) for Huh-7.5. The kanamycin (control) and copper oxychloride showed IC_{50} values above 200 µM and 200 µg mL^{-1}, respectively.

2.5. Growth Curve

According to the growth curves of the positive control (PC) and vehicle control (DMSO), it was observed that Xcc reaches the maximum growth phase in a period of 15 h. The growth rates of Xcc under the effects of dihydroxybenzoic acids (DA) **4**, **16** and **28** were measured at concentrations equivalent to MIC and ½ MIC. The early growth inhibition (lag phase), which happens in the first hours of contact (period of the first cellular divisions) can be a dynamic process. The lag phase delay was observed in the three compounds tested, and it showed that the higher the concentration, the higher the death rate. This can be explained because the compounds have bacteriostatic action; that is, as the time passes, the cells become able to recover and restart doubling. Another important finding is that the lag phase consists in the cell adaptation to the new medium conditions and the bacterial population is smaller in relation to the exponential phase facilitates the action of the compounds in the first hours (**Figure 1**, p. 64) [31]. Observing the exposure of Xcc to compounds **4**, **16** and **28** it can be seen that there was a delay in the exponential phase, prolonging the time taken for the bacteria to reach the stationary phase.

When we evaluated the concentration-response behavior of the compounds, we obtained a decrease in the curves with the concentration of the ½ MIC. Compared to the PC and DMSO, it was more evident in the MIC curve, which showed that for all three compounds, the higher the concentration, the greater the influence on Xcc.

2.6. Cellular Membrane Permeability of Xcc Using the Live/Dead Kit

Membrane integrity was measured by using the commercial assay Live/Dead BacLight® bacterial viability kit (Invitrogen, Carlsbad, CA, USA). We observed cells with intact membrane in fluorescent blue (SYTO 9) and cells with disturbance or affected membrane integrity in red or pink (propidium iodide). The data analyses were plotted as the percentage of cells permeated by propidium iodide (**Figure 2**, p. 65).

The nisin was used as a positive control for causing pores in the membrane [26]. When we observed the permeability capacity of alkyl dihydroxybenzoates in ¼

MIC and compared these to nisin (79.47%), we noticed that compound **28** was the most effective, because its permeation ability reached 93.8%, while for compound **16** it was 41.3%, and for compound **4**, 13.9%.

Permeation percentages were obtained by fluorescence optical microscopy (**Figure 3**, p. 66). Compound **28** showed high permeability, evidencing the entry of propidium iodide (PI) into cells. This behavior is similar to that of the positive control (nisin). For this reason, the target of compound **28** is membrane - related.

2.7. Inhibition Assays of GTPase Activity

The cell division process is mediated by the formation of the Z ring, coordinated by GTP hydrolysis activity of FtsZ [33–35]. Because of this, we evaluated the inhibition of GTPase activity of purified FtsZ from Xcc, incubated with compounds **4**, **16** and **28** using the continuous substrate regeneration assay [36].

When evaluating the behavior of compounds **4**, **16** and **28**, we could see decay in the GTPase activity of FtsZ. These data suggest that all three compounds promoted changes in protofilaments, leading to depolymerization, which reduces bacterial cell division.

2.8. Figures, Tables and Schems

Table 1. Antibacterial activities against *Xanthomonas citri* subsp. *citri*, purity and log $P_{o/w}$ of dihydroxybenzoates **1**–**36.**

	Entry	R	Purity	log $P_{o/w}$	MIC μg mL^{-1} (MIC in μM)	MBC μg mL^{-1}
	2,4 DHB acid	H	85.7	2.6	>100 (>648)	>100
	1	CH_2CH_3	87.6	2.8	>100 (>548)	>100
	2	$(CH_2)_3CH_3$	85.6	3.9	39.8 (189)	50
	3	$(CH_2)_5CH_3$	81.7	5.0	20.0 (84)	50
	4	$(CH_2)_6CH_3$	83.8	5.1	13.2 (52)	25
Series I 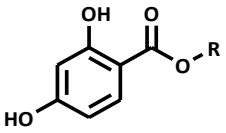	**5**	$(CH_2)_7CH_3$	79.6	6.1	>100 (>375)	>100
	6	$(CH_2)_8CH_3$	99.0	6.2	>100 (>356)	>100
	7	$(CH_2)_9CH_3$	99.5	6.9	>100 (>340)	>100
	8	$(CH_2)_{11}CH_3$	>99.9	7.0	>100 (>310)	>100
	9		93.2	2.6	>100 (>510)	>100
	10		>99.9	2.2	>100 (>450)	>100
	11		>99.9	4.0	40.5 (171)	100
	2,5 DHB acid	H	97.3	2.8	>100 (>648)	>100
	13	CH_2CH_3	98.3	2.4	>100 (>549)	>100
	14	$(CH_2)_3CH_3$	82.0	3.4	>100 (>475)	>100
	15	$(CH_2)_5CH_3$	80.1	4.5	33.5 (140)	50
	16	$(CH_2)_6CH_3$	99.3	5.0	20.2 (80)	25
Series II 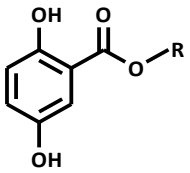	**17**	$(CH_2)_7CH_3$	79.8	5.2	>100 (>375)	>100
	18	$(CH_2)_8CH_3$	>99.9	5.7	>100 (>357)	>100
	19	$(CH_2)_9CH_3$	76.5	6.3	>100 (>340)	>100
	20	$(CH_2)_{11}CH_3$	>99.9	6.8	>100 (>310)	>100
	21		>99.9	2.2	>100 (>510)	>100
	22		>99.9	3.0	83.5 (375)	100
	23		>99.9	3.5	90.4 (382)	100
	24		>99.9	3.1	59.7 (231)	100
	3,4 DHB acid	H	99.6	0.8	>100 (>648)	>100
	25	CH_2CH_3	99.1	1.7	>100 (>549)	>100
	26	$(CH_2)_3CH_3$	99.1	2.6	>100 (>475)	>100
	27	$(CH_2)_5CH_3$	99.1	3.7	44.4 (186)	50
	28	$(CH_2)_6CH_3$	98.5	4.3	22.2 (88)	50
	29	$(CH_2)_7CH_3$	98.5	4.9	31.2 (117)	50
Series III 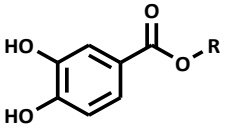	**30**	$(CH_2)_8CH_3$	97.9	5.5	26.7 (95)	50
	31	$(CH_2)_9CH_3$	91.3	6.0	>100 (>340)	100
	32	$(CH_2)_{11}CH_3$	>99.9	6.9	>100 (>310)	>100
	33		>99.9	1.4	>100 (>510)	>100
	34		>99.9	2.2	>100 (>450)	>100
	35		>99.9	2.7	>100 (>423)	>100
	36	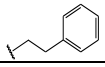	>99.9	2.4	89.1 (345)	100
	copper oxychloride				43.1	-
	Kanamycin				19.9 (40)	-

MIC—minimal inhibitory concentration; MBC—minimal bactericidal concentration.

Table 2. IC_{50} value of compounds **4**, **16** and **28** in μM against cell lines.

Compounds	HaCaT	Huh-7,5	MRC-5	VERO	ACHN
4	64.86 ± 8.91 [a]	70.63 ± 5.52 [a]	127.45 ± 4.59 [b,c,h]	111.4 ± 8.34 [c,f,h]	152.9 ± 7.07 [d]
16	69.81 ± 4.87 [a]	20.60 ± 0.23 [e]	144.8 ± 6.29 [b,d]	93.55 ± 1.93 [f]	140.35 ± 7.56 [b,d]
28	74.02 ± 11.74 [a,g]	64.84 ± 14.91 [a]	128.7 ± 2.12 [b,c,h]	92.31 ± 9.34 [f,g]	114.05 ± 9.97 [g]
Kanamycin	>200 [i]	>200 [i]	>200 [i]	>200 [i]	>200 [i]
copper oxychloride	>200 [i]	>200 [i]	>200 [i]	>200 [i]	>200 [i]

Different letters indicate statistical significance $p < 0.05$ in Tukey's multiple comparisons test.

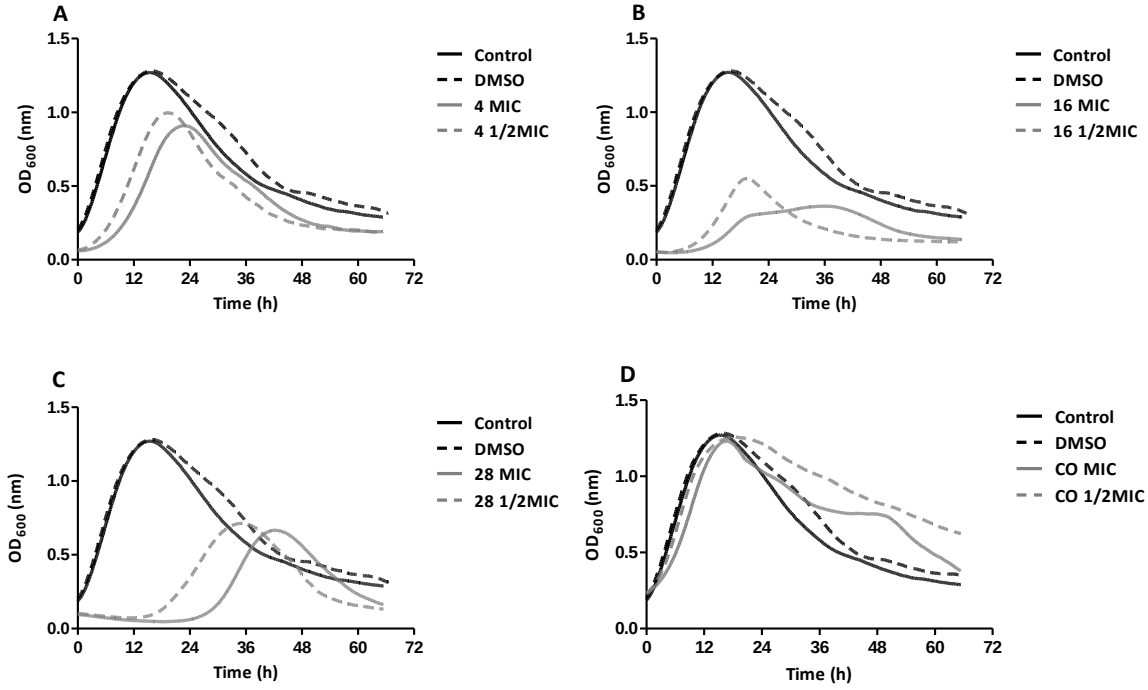

Figure 1. Growth curve profiles of *Xanthomonas citri* subsp. *citri* with treatments in MIC and ½ MIC values of alkyl dihydroxybenzoates for 72 h. **A** Compound **4**, **B** compound **16**, **C** compound **28**, and **D** copper oxychloride (CO) in comparison to control (untreated) and DMSO (vehicle control).

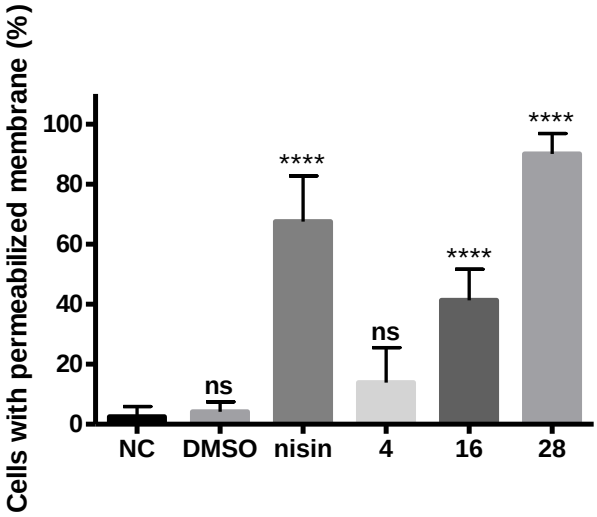

Figure 2. Cellular permeability evaluation in the presence of alkyl dihydroxybenzoates (**** $p < 0.0001$, ANOVA with Dunnett's post-test), ns = not significant.

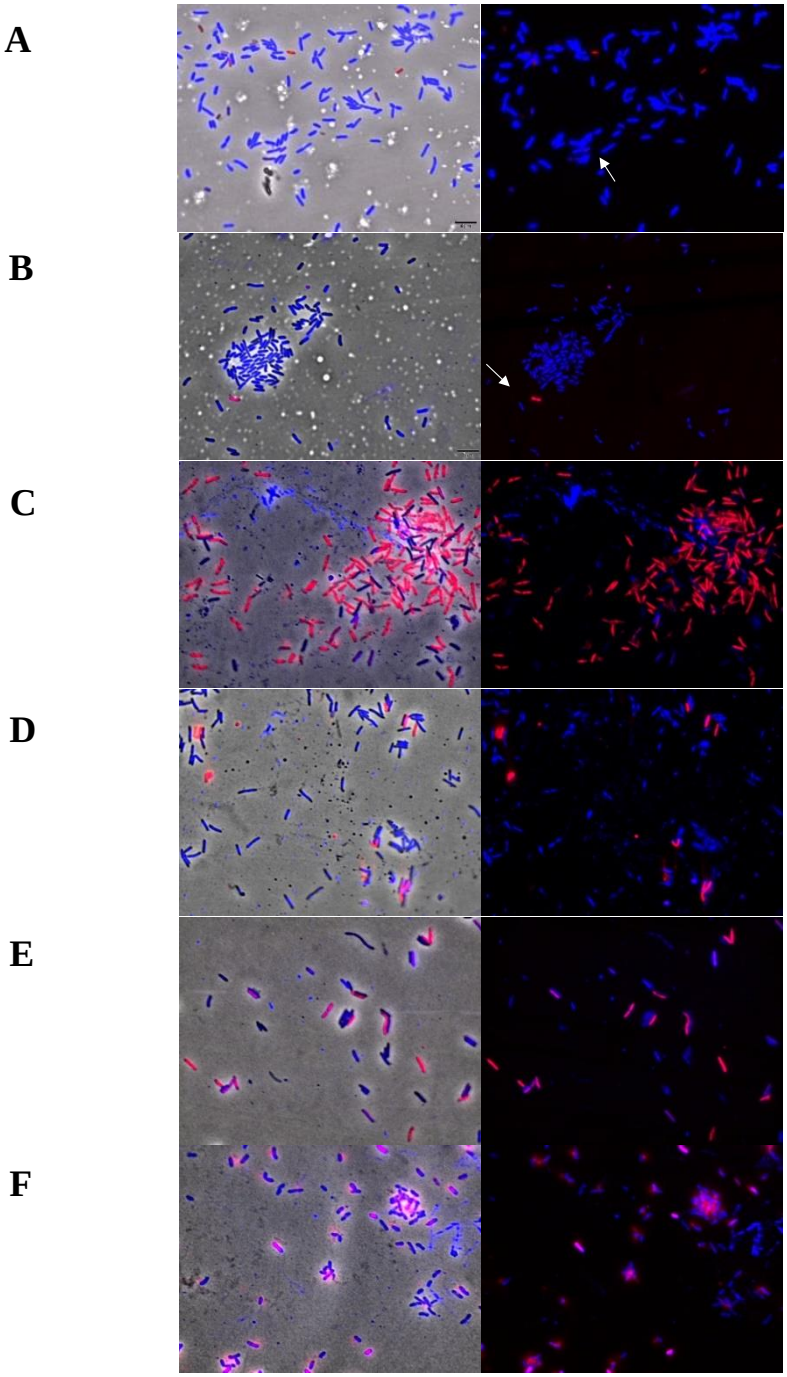

Figure 3. Optical microscopy of fluorescence images at ¼ MIC of alkyl dihydroxybenzoates for 15 min. (**A**) Negative control (untreated), (**B**) vehicle control (DMSO), (**C**) positive control (nisin), (**D**) compound **4**, (**E**) compound **16,** and (**F**) compound **28**.

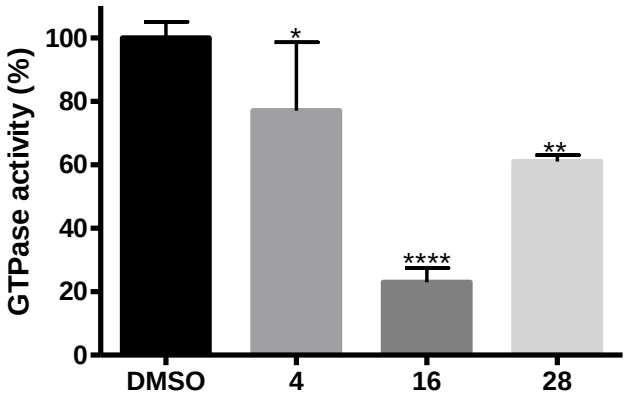

Figure 4. Inhibition of GTPase activity of alkyl dihydroxybenzoates in MIC value (*p<0.04, ** p < 0.001, **** p < 0.0001, ANOVA with Dunnett's post-test).

3. DISCUSSION

Xanthomonas is one of the most important genera among the phytopathogens. It causes diseases in economically important cultivars such as rice, beans, tomatoes, oranges, peppers, passion fruit, grapes and others [5].

In this study, we have focused our work on Xcc, which is the main cause of citrus canker. The chemical control of citrus canker is mainly through application of cupric compounds, but the emergence of copper-resistant strains has encouraged research into new compounds [37–39]. Recently, other effective compounds against Xcc have been reported, such as bismerthiazol [40] and 3-indolylacetonitrile [41], which are promising agents against citrus canker.

The 2,4 DHB, 2,5 DHB and 3,4 DHB acids were inactive (MIC > 100 μg mL^{-1}). Then, we evaluated three ester homologous series containing ethyl, butyl, hexyl, octyl, decyl and dodecyl dihydroxybenzoates. In general, hexyl and octyl dihydroxybenzoates displayed potent activity against Xcc. Thus, we decided to evaluate heptyl and nonyl esters. Heptyl dihydroxybenzoates **4**, **16** and **28** exhibited the lowest MIC values. Subsequently the branched, cyclic and aromatic esters were evaluated to analyze the hypothetical effects of stereoelectronic parameters on the anti-Xcc effect. However, clear conclusions about the relationship between structure and activity were not established. Copper oxychloride showed anti-Xcc activity, with the MIC value of 43.1 μg mL^{-1}.

In our previous study, we described the anti-Xcc activity of alkyl gallates (alkyl 3,4,5-trihydroxybenzoates). In order to investigate the relevance of number and position of hydroxyl groups on anti-Xcc activity, alkyl dihydroxybenzoates were evaluated. Heptyl dihydroxybenzoates (**4**—52 μM, **16**—80 μM and **28**—88 μM) were more active than heptyl gallate (MIC = 116 μM) [25]. This set of data indicated that reduction in the number of hydroxyls increased anti-Xcc activity. Comparisons among MIC values of compounds **4**, **16** and **28** suggested the hydroxyls at positions 2 and 4 (compound **4**) increased anti-Xcc activity when compared to positions 2 and 5 (compound **16**), as well as 3 and 4 (compound **28**).

This was corroborated using other data regarding the dihydroxybenzoic acids (DA) and their esters that had antimicrobial activity described, against Gram-positive and Gram-negative bacteria [42–48] and yeasts [29]. Some DAs, such as 2,3; 2,4; 2,5;

2,6 and 3,4 show activity against *Campylobacter jejuni*, *Escherichia coli*, *Listeria monocytogenes* and *Salmonella enterica* [30].

Merkl and collaborators studied the antimicrobial activity of the phenolic acids and their alkyl esters, against *E. coli*, *Bacillus cereus*, *L. monocytogenes*, *Saccharomyces cerevisiae* and *Fusarium culmorum* and reported significant differences between values of MIC of acids and their esters. In general, butyl esters were twice as potent as their acids. In addition to this, the authors associated the increase of antibacterial activity with the size of the side alkyl chain [28].

With the increase of the alkyl chain, a considerable decrease in solubility occurs in aqueous medium (culture medium). This favors the formation of micelles, which are not able to cross bacterial cells. The amphiphilic character of the alkyl dihydroxybenzoates allows the micellar formation due to the hydrophilicity of the hydroxyl groups on the phenolic ring, and the long carbonic chain is highly hydrophobic [49].

The compound with the highest lipophilicity was the dodecyl 2,4 dihydroxybenzoate (**8**), and the compound with the lowest lipophilicity was the 3,4 dihydroxybenzoic acid (**3,4-DHB acid**). As the side chain increased, the lipophilicity of these compounds increased; that is, the interaction of the compounds with the C18 column was more intense, culminating in longer retention times, being slightly different for the branched and cyclic compounds. Compound **4** has two hydroxyls at the 2,4 (meta) positions, compound **16** has two hydroxyls at the 2.5 (para), and compound **28** has another two at the 3,4 (ortho) positions. The log $P_{o/w}$ values of 5.1 (compound **4**), 5.0 (compound **16**) and 4.3 (compound **28**) obtained through the partition coefficient are relatively close, with compound **4** being more lipophilic.

Branched compounds **9** (2.6), **21** (2.2) and **33** (1.4) presented smaller than their isomers **2** (3.9), **14** (3.4) and **26** (2.6). This is due to the fact that branching reduces the size of the molecule, decreasing the surface area and making it difficult to solvate in the non-polar phase [50], similar to cyclic compounds.

In this work, we demonstrated that heptyl dihydroxybenzoates had no cytotoxicity. Our results corroborate those of Medina-Alarcón and colleagues (2017), who reported that protocatechuates did not show cytotoxicity in MRC-5 and HepG2 cell lines [51].

When we observed the growth curves treated with the compounds, we noticed a delay in the exponential phase, which prolonged the time taken for the bacterium to

reach the stationary phase. This delay is more evident when increasing the concentration of the compounds; the greater the concentration, the greater the influence on Xcc. The ester interactions with Xcc showed different curves, which is an interesting fact, since the esters have the same side carbonic chain size. Therefore, this made us consider the influence of hydroxyl positions on kinetics growth. Concerning the growth curve, it was observed that, compared to the PC and the DMSO, Xcc bacterial growth suffered a delay of approximately 18 h to reach the stationary phase. However, when comparing the compounds, **16** demonstrated a greater inhibition of bacterial growth, decreasing the height of the curve significantly; that is, with a lower optical density. Therefore, it can be inferred that its action on Xcc is greater than the action of compound **4**. The profile of compound **28** showed increased bacterial growth delay of 20 to 30 h, and even beyond this time it continued to inhibit the growth of Xcc more effectively than compound **4**, but with less killing capacity than compound **16** (**Figure 1**, p. 64).

When we evaluated copper oxychloride, we found an MIC value of 43.1 μg mL^{-1} to potential anti-Xcc activity on cell lines tested that did not demonstrate cytotoxicity. On the growth curves treated with the copper oxychloride, we noticed that the curve pattern did not change and the copper oxychloride was inactive under the conditions tested. Behlau and colleagues (2017), described copper oxychloride as an insoluble copper formulation (ICuF) (syn. fixed copper), and being the most studied and commonly used form of copper for the control of citrus canker [12,17], this could explain the low activity of copper oxychloride in our trials.

The minimal bactericidal concentration was determined by observing the bacterial growth in Petri dishes transferred from the REMA plates. We obtained bactericidal action in compounds **11**, **22**–**24**, **31** and **36** at the concentration of 100 μg mL^{-1}, in compounds **2**, **3**, **15**, **27**–**30** at the concentration of 50 μg mL^{-1} and in compounds **4** and **16** at the concentration of 25 μg mL^{-1}.

Finally, we investigated the alkyl dihydroxybenzoates for interference in the modulation of FtsZ cell-mediated Xcc cell division [52]. FtsZ is strongly related to α/β-tubulin in three-dimensional structure [53], the possession of GTPase activity [35,54] and the ability to polymerize in a nucleotide-dependent manner in vitro [34,55]. The continuous substrate regeneration assay was performed to characterize GTPase activity similar to bacterial self-assembling tubulin, FtsZ [56]. The compounds **4**, **16** and **28** showed decay in the GTPase activity of FtsZ. These data suggest that all three

compounds promoted changes in protofilaments, leading to depolymerization, which prevents bacterial cell division.

All compounds affected membrane integrity (**Figure 2**, p.65), but only compound **28** showed high permeability similar to nisin. Therefore, similar to alkyl gallates [26], compounds **4**, **16** and **28** possibly promote cell death by some combination of the FtsZ inhibition and membrane permeabilization mechanisms.

In summary, three series of alkyl dihydroxybenzoates were designed and synthesized as part of our ongoing search for anti-Xcc agents based on natural phenolic compounds. The heptyl dihydroxybenzoates (compounds **4**, **16** and **28**) displayed potent anti-Xcc activity. Furthermore, due to preliminary low toxicity against eukaryotic cells, as well as the ability to act on membrane and cell division, these compounds are promising agents against citrus canker.

4. METHODS

4.1. Synthesis of Alkyl Dihydroxybenzoates

The esters of dihydroxybenzoic acids were prepared by Fischer's Esterification (Scheme 1) methodology with modifications [25,57]. 6 mmol of carboxylic acids were dissolved in 18 mmol of alkyl alcohols (ethanol, 1-butanol, 1-hexanol, 1-heptanol, 1-octanol, 1-nonanol, 1-decanol, 1-dodecanol, 2-propanol, cyclopentanol, cyclohexanol and 2-phenylethanol) under constant magnetic stirring. After complete dissolution, catalytic amounts of sulfuric acid (1–3 drops) were added. The reactions were maintained at temperatures close to boiling point for the respective alcohols and were conducted for a period of 1–3 days. The progress of the reaction was checked by thin layer chromatography (TLC) [7:3 *n*-hexane: ethyl acetate]. After the conversion, the residue was partitioned 3 times with ethyl acetate. Later, it was washed with distilled water (3 times) and 1 mol L^{-1} sodium bicarbonate solution (3 times). The organic phase was dried using a rotary evaporator. The crude products were purified with a low temperature hexane washes, crystallized with hexane or acetone and over normal phase column chromatography (silica gel 0.06–0.20 mm, ACROS Organics, New Jersey, USA). All compounds were identified with the use of NMR spectra on a Bruker Avance III 14.1 T, Bruker Avance III 9.4 T and Bruker Fourier 7.1 T spectrometer, using deuterated chloroform ($CDCl_3$) or deuterated dimethylsulfoxide (DMSO-d_6) as solvents. Compounds were analyzed by HPLC for determination of their purity.

Scheme 1. Preparation of alkyl dihydroxybenzoates by Fischer's Esterification.

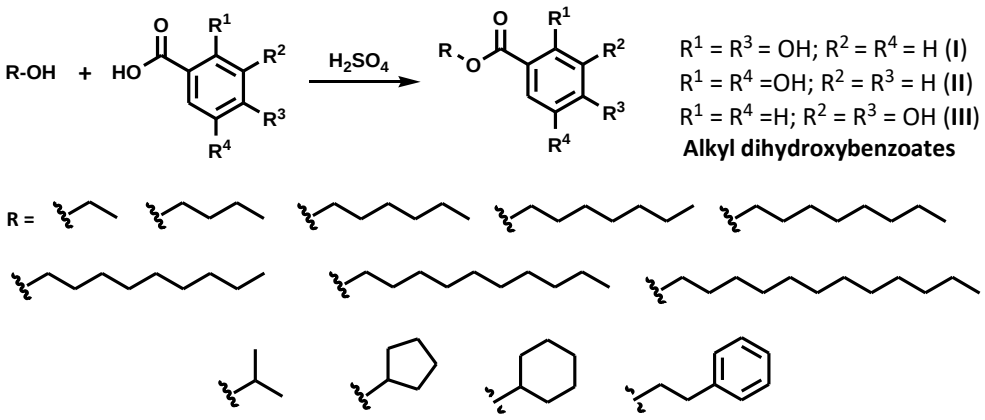

Series **I** (2,4 dihydroxybenzoic acid), **II** (2,5 dihydroxybenzoic acid), **III** (3,4 dihydroxybenzoic acid).

4.2. Partition Coefficient Determination Log $P_{o/w}$ by HPLC

The log $P_{o/w}$ were determined using the HPLC procedure according to OECD Guidelines for the Testing of Chemicals [32,59] on a system equipped with a binary pump, automatic sampler column (Agilent® Technologies, Santa Clara, CA, USA, model 1220 Infinity), and photodiode array system Zorbax Eclipse Plus C-18 column (4.6 × 250 mm, 5 µm, Agilent® Technologies, Santa Clara, CA, USA). The analyses were performed with the use of an isocratic flow in methanol: water (3:1) at 1.0 mL min^{-1}. We injected 20.0 µL and analyses were performed at 254 nm. We used as reference compounds thiourea, phenol, acetophenone, benzoic acid, benzene, toluene, biphenyl, fluoranthene and triphenylamine in order to construct the curve log K × log $P_{o/w}$. The lipophilicity of alkyl dihydroxybenzoates was determined from their retention times and interpolation in linearity curve log K × log $P_{o/w}$. We performed the analyses in duplicate.

4.3. Determination of MIC and MBC against *Xanthomonas citri* subsp*. citri* Assay

The antibacterial activity of alkyl dihydroxybenzoates and the determination of minimum inhibition concentration (MIC) were performed by the fluorimetric method Resazurin Microtiter Assay (REMA) with some modifications [25,59]. An overnight culture of *X. citri* subsp. *citri* strain 306 (IBSBF 1594) [60] was grown in 20 mL in Nitrogen Yeast Glycerol (NYG) at 29 °C in constant agitation of 180–200 rpm. After 12 h, the Xcc inoculum was dispersed in NYG medium and distributed into a 96 well microtiter plate to a final volume of 100 µL per well (10^5 CFU per well). Stock solutions

of tested compounds at 10 mg mL^{-1} were prepared in dimethyl sulfoxide (DMSO) and dispersed in NYG medium to obtain DMSO 1% and the final compound concentration range of 0.78–100 µg mL^{-1}. The negative control was constituted of 100 µL culture medium. In addition, the copper oxychloride was tested as a comparison to alkyl dihydroxybenzoates and kanamycin (20 µg mL^{-1}), which was used as a control antibiotic. The plate was subsequently incubated at 29 °C for 12 h, and 15 µg mL^{-1} freshly prepared resazurin solution in water was added to each well, and the plate was incubated for 2 h. The fluorescence was determined on a Synergy H1 (BioTek, Winooski, VT, USA) microplate reader using the excitation and emission filters at wavelengths of 530 and 590 nm respectively. After the REMA assay, the minimum bactericidal concentration (MBC) assay was performed using a 96-pin stainless steel plate replicator, accurately transferring the wells from the REMA plate to Petri dishes Petri dishes were incubated in oven B.O.D. at 29 °C for 24 to 48 h [61]. The experiments were performed in triplicate.

4.4. Determination of Cytotoxicity

The cytotoxicity of compounds **4**, **16**, **28** and copper oxychloride was determined by MTT assay [62]. The cell lines used were HaCaT (human keratinocyte cell line—CLS 300493), Huh-7.5 (human hepatoma cell line—ATCC® PTA-8561), MRC-5 (human lung fibroblast cell line—ATCC CCL-171), VERO (monkey kidney epithelial cell line—ATCC® CCL81) and ACHN (human renal adenocarcinoma cell line—ATCC® CRL1611). The cells were cultured in appropriate medium recommended by the American Type Culture Collection.

The assay was performed with the concentration of 10^4 cells for both cell lines, distributed in 96-well plates and incubated at 37 °C in a 5% CO_2 controlled atmosphere oven for 24 h. After the incubation period, the cells were treated with the compounds with a range of 1.56–200 µmol L^{-1} and incubated for 24 h. The supernatant was removed, then 100 µL of 3-(4,5-dimethyl-2-thiazolyl)-2,5-diphenyl-2*H*-tetrazolium (MTT) salt at 1 mg mL^{-1} diluted in DMEM medium (Gibco Life Technologies, Gaithersburg, MD, USA) was added and incubated for 30 min. Subsequently, the MTT was removed, then 100 µL of DMSO under agitation for 5 min at 60 rpm was added. The plates were read at 570 nm in a FLUOstar Omega/BMG LABTECH plate reader, Offenburg, BW, DE. We carried out the experiments in triplicate and three independent events for statistical analysis (GraphPad Software, San Diego, CA, USA). The MTT

assay is based on the tetrazolium salt (yellow-colored) reduction to formazan (purple-colored) by metabolically active cells [63].

4.5. Growth Curve

An isolated colony of *Xanthomonas citri* subsp. *citri* was inoculated in NYG medium for 12 h at 29 °C. After this, the optical density (OD 600 nm) was measured and adjusted to ~0.1. Positive controls (cells and culture medium) and cells with treatments of compounds **4**, **16** and **28** were then prepared in MIC and ½ MIC values. Optical density reading was measured on a Synergy H1-BioTek plate reader every 30 min for 72 h. The growth curves were plotted with GraphPad Prism software. At the same time, the degradation assay was performed, solubilizing the compounds in DMSO, which were later incorporated in NYG medium. Later, we scanned the compounds to measure the absorbance values from 210 to 700 nm, and the maximum lambda value of each compound was selected after scanning. After that, punctual readings were carried out every 30 min for 72 h.

4.6. Cellular Membrane Permeability of Xcc Using the Live/Dead Kit

Phase contrast microscopy was used to observe changes in cell shape and signs of cell division alteration using an objective lens with a magnification of 100×. To evaluate the Xcc cells' membrane integrity, the BacLight® kit was used. Mixtures of SYTO 9 dyes and propidium iodide (PI). SYTO 9 (blue) can stain nucleic acids in general—with intact or damaged membranes. On the other hand, PI (red) penetrates only the bacteria with damaged membranes, causing overlap in the fluorescence of SYTO 9. Therefore, using a mixture of the dyes, the bacteria with disturbed cell membranes are stained in fluorescent red and the intact cell membranes are stained in fluorescent blue. The Xcc cells at density of 10^6 cells mL^{-1} were submitted to 15 min treatments with compounds **4**, **16** and **28** at ¼ MIC values. Cellular immobilization was performed on slides containing 1% agarose gel in 0.85% saline buffer. The slides were prepared with 1.0 mL of the agarose solution, which was dispersed in optical microscopy slides and on each slide another slide was placed so that the gel continued like a thin film and was of homogeneous height. The slides were dried at room temperature for approximately 20 min and opened at the time of use, when 10 µL of the cell suspension was deposited in the center and covered with the cover slip. The cells were visualized using the Olympus BX-61 optical microscope equipped with

OrcaFlash 2.8 monochrome camera (Hamamatsu, Shizuoka, Japan). Cell Sensation software v11 (Olympus) was used to document and analyze the images.

4.7. Inhibition Assays of GTPase Activity

The evaluation of the inhibition of GTPase activity was measured by the characterization of the FtsZ from Xcc [36,57]. This methodology is known as continuous assay of substrate regeneration and consists of the hydrolysis of guanosine triphosphate (GTP) in guanosine diphosphate (GDP) and inorganic phosphate. The GTP is regenerated by the enzyme pyruvate kinase which, in turn, converts the phosphoenol pyruvate (PEP) to pyruvate. The pyruvate produced by this reaction is reduced to lactate by lactate dehydrogenase, using NADH [64].

Reagent stocks were dispersed in Tris 50 buffer (1:1 tris:KCl at pH 7.9). We also prepared two mixtures: Mixture 1—magnesium chloride ($MgCl_2$), pyruvate kinase/lactate dehydrogenase, phosphoenol-pyruvate, NADH and GTP, adding or not the test compounds to MIC values; and mixture 2—Xcc-FtsZ. The assay was performed in a 96-well plate, 75 µL of mixture 1 was pipetted into a well and incubated for 5 min at 30 °C; then 75 µL of mixture 2 was added and the readings started. A Biotek Synergy MX plate reader was used. The readings were performed every 5 s, at the wavelength of 340 nm at 30 °C, under constant stirring.

The total volume of 150 µL presented the following concentrations: 5 mM $MgCl_2$; pyruvate kinase/lactate dehydrogenase 20 U mL^{-1}; 2 mM phosphoenol-pyruvate; 1 mM NADH; 400 µM GTP; Xcc-FtsZ 5 µM.

4.8. Statistical Analysis

All assays were performed in triplicate. The data were analyzed using one-way analysis of variance (ANOVA) followed by Tukey's test for Table 2, and Dunnett's test for Figures 2 and 4. The data analyses were plotted with GraphPad Prism version 5.0 (GraphPad, San Diego, CA, USA).

Supplementary Materials: Supplementary materials can be found at Appendix A.

Author Contributions: L. O. R., H. F., D. J. S., E. G. and P. R. conceived and designed the experiments; A. C. N., C. R. P., L. B. C., D. B. A., M. d. F. C. S., D. A. M. and A. Z. performed the experiments; all authors contributed to data analysis.

Funding: This research was funded by Coordination for the Improvement of Higher Education Personnel (CAPES), Brazilian Council for Scientific and Technological Development (CNPq) (Grants 471129/2013-5 and 306251/2016-7), the São Paulo Research Foundation (FAPESP) (Grants 2013/50367-8, 2014/18330-0, 2015/50162-2 and 2017/50216-0) and "Biobased Economy" from the Netherlands Organisation for Scientific research (NWO, 729.004.005) to D. J. S.

Acknowledgments: A.C.N. thanks FAPESP for research fellowship (2015/08089-6), C.R.P. thanks the *National Institute of Science and Genomics Technology for Citrus Improvement (Citrus-INCT) research fellowship (Grants* FAPESP 2014/50880-0 and 465440/2014-2). The authors gratefully acknowledge the Center for Biomolecular Innovation (Grants FAPESP 2009/53989-4).

Conflicts of Interest: The authors declare no conflict of interest.

5. REFERENCES

1. Schaad, N.W.; Postnikova, E.; Lacy, G.H.; Sechler, A.; Agarkova, I.; Stromberg, P.E.; Stromberg, V.K.; Vidaver, A.K. Reclassification of *Xanthomonas campestris* pv. *citri* (ex Hasse 1915) dye 1978 forms, A.; B/C/D, and E as, *X*. *smithii* subsp. *citri* (ex Hasse) sp. nov. nom. rev. comb. nov., *X. fuscans* subsp. *aurantifolii* (ex Gabriel 1989) sp. nov. nom. rev. comb. nov., and, *X*. *alfalfae* subsp. *citrumelo* (ex Riker and Jones) Gabriel et al., 1989 sp. nov.nom. rev. comb. nov.; *X. campestris* pv. malvacearum (ex smith 1901) dye1978 as, *X*. *smithii* subsp. *smithii* nov. comb. nov. nom. nov.; *X. campestris* pv. alfalfae (ex Riker and Jones, 1935) dye 1978 as, *X*. *alfalfae* subsp. *alfalfa* ex Riker et al., 1935) sp. nov. nom. rev.; and "var. fuscans" of, *X*. *campestris* pv. phaseoli (ex Smith, 1987) dye 1978 as, *X*. *fuscans* subsp. *fuscans* sp2005. nov. *Syst. Appl. Microbiol.* **2005**, *28*, 494–518.
2. Schaad, N.W.; Postnikova, E.; Lacy, G.; Sechler, A.; Agarkova, I.V.; Stromberg, P.E.; Stromberg, V.K.; Vidaver, A.M. Emended classification of xanthomonad pathogens on citrus. *Syst. Appl. Microbiol.* **2006**, *29*, 690–695.
3. Gottwald, T.R.; Graham, J.H.; Schubert, T.S. Citrus canker: The pathogen and its impact. *Plant Health Prog.* **2002**, *10*, 32.
4. Dalla Pria, M.; Christiano, R.C.; Furtado, E.L.; Amorim, L.; Bergamin Filho, A. Effect of temperature and leaf wetness duration on infection of sweet oranges by Asiatic citrus canker. *Plant Pathol.* **2006**, *55*, 657–663.
5. Graham, J.H.; Gottwald, T.R.; Cubero, J.; Achor, D.S. *Xanthomonas axonopodis pv. citri*: Factors affecting successful eradication of citrus canker. Mol. *Plant Pathol.* **2004**, *5*, 1–15.
6. Brunings, A.M.; Gabriel, D.W. *Xanthomonas citri*: Breaking the surface. Mol. *Plant Pathol.* **2003**, *4*, 141–157.

7. Bock, C.H.; Parker, P.E.; Gottwald, T.R. Effect of simulated winddriven rain on duration and distance of dispersal of *Xanthomonas axonopodis* pv. citri from canker-infected citrus trees. *Plant Dis.* **2005**, *89*, 71–80.
8. São Paulo (Estado). *Resolução da Secretaria de Agricultura e Abastecimento (SAA) No 10*; Diário Oficial do Estado de São Paulo: São Paulo, Brazil, 2017.
9. Kuhara, S. Present epidemic status and control of the citrus canker disease (*Xanthomonas citri* (Hasse) Dowson) in Japan. *Rev. Plant Prot. Res.* **1978**, *11*, 132–142.
10. Stall, R.E.; Miller, J.W.; Marco, G.M.; Canteros, B.I. Timing of sprays to control cancrosis of grapefruit in Argentina. *Proc. Int. Soc. Citric.* **1982**, *1*, 414–417.
11. Leite, R.P., Jr.; Mohan, S.K. Integrated management of the citrus bacterial canker disease caused by *Xanthomonas campestris* pv. citri in the State of Paraná, Brazil. *Crop Protect.* **1990**, *9*, 3–7.
12. Behlau, F.; Amorim, L.; Belasque, J., Jr.; Bergamin Filho, A.; Leite, R.P., Jr.; Graham, J.H.; Gottwald, T.R. Annual and polyetic progression of citrus canker on trees protected with copper sprays. *Plant Pathol.* **2010**, *59*, 1031–1036.
13. Graham, J.H. Varietal susceptibility to citrus canker: Observations from southern Brazil. *Citrus Ind.* **2001**, *82*, 15–17.
14. Schubert, T.S.; Rizvi, S.A.; Sun, X.; Gottwald, T.R.; Graham, J.H.; Dixon, W.N. Meeting the challenge of eradication citrus canker in Florida—Again. *Plant Dis.* **2001**, *85*, 340–356.
15. Leite, R.P., Jr.; Mohan, S.K.; Pereira, A.L.; Campacci, C.A. Controle integrado de cancro cítrico—Efeito da resistência genética e da aplicação de bactericidas. *Fitopatol. Brás.* **1987**, *12*, 257–263.
16. Stall, R.E.; Miller, J.W.; Marco, G.M.; Canteros, B.I. Population dynamics of Xanthomonas citri causing cancrosis of citrus in Argentina. *Proc. Fla. State Hort. Soc.* **1980**, *93*, 10–14.
17. Behlau, F.; Scandelai, L.H.M.; da Silva, G.J., Jr.; Lanza, F.E. Soluble and insoluble copper formulations and metallic copper rate for control of citrus canker on sweet orange trees. *Crop Prot.* **2017**, *94*, 185–191.
18. Cornu, J.Y.; Huguenot, D.; Jézéquel, K.; Lollier, M.; Lebeau, T. Bioremediation of copper-contaminated soils by bacteria. *World J. Microbiol. Biotechnol.* **2017**, *33*, 26.
19. Brunetto, G.; de Melo, G.W.; Terzano, R.; Del Buono, D.; Astolfi, S.; Tomasi, N.; Pii, Y.; Mimmo, T.; Cesco, S. Copper accumulation in vineyard soils: Rhizosphere processes and agronomic practices to limit its toxicity. *Chemosphere* **2016**, *162*, 293–307.
20. Fones, H.; Preston, G.M. The impact of transition metals on bacterial plant disease. *FEMS Microbiol. Rev.* **2013**, *37*, 495–519.
21. Fan, J.; He, Z.; Ma, L.Q.; Stoffella, P.J. Accumulation and availability of copper in citrus grove soils as affected by fungicide application. *J. Soil. Sediment.* **2011**, *11*, 639–648.
22. Alva, A.K.; Graham, J.H.; Anderson, C.A. Soil pH and copper effects on young ‘Hamlin’ orange trees. *Soil Sci. Soc. Am. J.* **1995**, *59*, 481–487.

23. Behlau, F.; Canteros, B.I.; Minsavage, G.V.; Jones, J.B.; Graham, J.H. Molecular characterization of copper resistance genes from *Xanthomonas citri* subsp. citri and *Xanthomonas alfafae* subsp. citrumelonis. *Appl. Environ. Microbiol.* **2011**, *77*, 4089–4096.

24. Canteros, B.I. Copper resistance in *Xanthomonas campestris* pv. citri. In Proceedings of the 9th International Conference Centre for Advanced Study in Botany Plant Pathogenic Bacteria, Chennai, India, 21–23 December 1999; pp. 455–459.

25. Silva, I.C.; Regasini, L.O.; Petronio, M.S.; Silva, D.H.; Bolzani, V.D.; Belasque, J.; Sacramento, L.V.; Ferreira, H. Antibacterial activity of alkyl gallates against *Xanthomonas citri* subsp. citri. *J. Bacteriol.* **2013**, *195*, 85–94.

26. Król, E.; de Sousa Borges, A.; da Silva, I.; Polaquini, C.R.; Regasini, L.O.; Ferreira, H.; Scheffers, D.J. Antibacterial activity of alkyl gallates is a combination of direct targeting of FtsZ and permeabilization of bacterial membranes. *Front Microbiol.* **2015**, *6*, 1–12.

27. Savietto, A.; Polaquini, C.R.; Kopacz, M.; Scheffers, D.J.; Marques, B.C.; Regasini, L.O.; Ferreira, H. Antibacterial activity of monoacetylated alkyl gallates against *Xanthomonas citri* subsp. *citri*. *Arch. Microbiol.* **2018**, *200*, 929–937.

28. Merkl, R.; Hradkova, I.; Filip, V.; Smi Drkal, J. Antimicrobial and Antioxidant Properties of Phenolic Acids Alkyl Esters. *Czech J. Food* **2010**, *28*, 275–279.

29. Nihei, K.; Nihei, A.; Kubo, I. Rational Design of Antimicrobial Agents: Antifungal Activity of Alk(en)yl Dihydroxybenzoates and Dihydroxyphenyl Alkanoates. *Biol. Med. Chem. Lett.* **2003**, *13*, 3993–3996.

30. Friedman, M.; Henika, P.R.; Mandrell, R.E. Antibacterial Activities of Phenolic Benzaldehydes and Benzoic Acids against Campylobacter jejuni, Escherichia coli, Listeria monocytogenes, and *Salmonella enterica*. *J. Food Prot.* **2003**, *10*, 1811–1821.

31. Chatterjee, T.; Chatterjee, B.K.; Majumdar, D.; Chakrabarti, P. Antibacterial effect of silver nanoparticles and the modeling of bacterial growth kinetics using a modified Gompertz model. *Biochim Biophys Acta* **2015**, *2*, 299–306.

32. OECD. *Test No. 117: Partition Coefficient (N-Octanol/Water), HPLC Method*; OECD Publishing: Paris, France, 2004.

33. Chen, Y.; Erickson, H.P. Rapid in vitro Assmbly Dynamics and Subunit Turnover of FtsZ Dementrated by Fluorescence Resonance Energy Tranfer. *J. Biol. Chem.* **2005**, *280*, 22549–22554.

34. Mukherjee, A.; Lutkenhaus, J. Guanine Nucleotide-Dependent Assembly of FtsZ INTO Filaments. *J. Bacteriol.* **1994**, *176*, 2754–2758.

35. de Boer, P.A.; Crossley, R.E. & Rothfield, L.I. Roles of MinC and MinD in the Site-Specific Septation Block Mediated by The MinCDE System of *Escherichia coli*. *J. Bacteriol.* **1992**, *174*, 63–70.

36. Kopacz, M.M.; Lorenzoni, A.S.; Polaquini, C.R.; Regasini, L.O.; Scheffers, D.J. Purification and characterization of FtsZ from the citrus canker pathogen *Xanthomonas citri* subsp. *citri*. *Microbiol. Open* **2018**, *5*, e00706.

37. Martins, P.M.M.; Merfa, M.V.; Takita, M.A.; de Souza, A.A. Persistence in Phytogenic Bacteria: Do Know Enough? *Front. Microniol.* **2018**, *9*, 1–14.

38. Gochez, A.M.; Huguet-Tapia, J.C.; Minsavage, G.V.; Shantaraj, D.; Jalan, N.; Strauß, A.; Lahaye, T.; Wang, N.; Canteros, B.I.; Jones, J.B.; Potnis, N. Pacbio sequencing of copper-tolerant *Xanthomonas citri* reveals presence of a chimeric plasmid structure and provides insights into reassortment and shuffling of transcription activator-like effectors among, *X*. *citri* strains. *BMC Genom.* **2018**, *19*, 16.

39. Richard, D.; Tribot, N.; Boyer, C.; Terville, M.; Boyer, K.; Javegny, S.; Roux-Cuvelier, M.; Pruvost, O.; Moreau, A.; Chabirand, A.; Vernière, C. First report of copper-resistant Xanthomonas citri pv. citri pathotype a causing Asiatic citrus canker in Réunion, France. *Plant Dis.* **2017**, *101*, 503.

40. Yu, X.; Armstrong, C.M.; Zhou, M.; Duan, Y. Bismerthiazol Inhibits *Xanthomonas citri* subsp. *citri* Growth and Induces Differential Expression of Citrus Defense-Related Genes. *Phytopathology* **2016**, *7*, 693–701.

41. Li, J.; Wang, N. Foliar application of biofilm formation-inhibiting compounds enhances control of citrus canker caused by *Xanthomonas citri* subsp. *citri*. *Phytopathology* **2014**, *104*, 134–142.

42. Bisignano, C.; Filocamo, A.; La Camera, E.; Zummo, S.; Fera, M.T.; Mandalari, G. Antibacterial activities of almond skins on *cagA*-positive and-negative clinical isolates of *Helicobacter pylori. BMC Microbiol*. **2013**, *13*, 103.

43. Mandalari, G.; Bisignano, C.; D'Arrigo, M.; Ginestra, G.; Arena, A.; Tomaino, A.; Wickham, M.S. Antimicrobial potential of polyphenols extracted from almond skins. *Lett. Appl. Microbiol.* **2010**, *51*, 83–89.

44. Ayaraman, P.; Sakharkar, M.K.; Lim, C.S.; Tang, T.H.; Sakharkar, K.R. Activity and interactions of antibiotic and phytochemical combinations against *Pseudomonas aeruginosa in vitro*. *Int. J. Biol. Sci.* **2010**, *6*, 556–568.

45. Kuete, V.; Nana, F.; Ngameni, B.; Mbaveng, A.T.; Keumedjio, F.; Ngadjui, B.T. Antimicrobial activity of the crude extract, fractions and compounds from stem bark of *Ficus ovate* (Moraceae). *J. Ethnopharmacol.* **2009**, *124*, 556–561.

46. Chao, C.Y.; Yin, M.C. Antibacterial effects of roselle calyx extracts and protocatechuic acid in ground beef and apple juice. *Foodborne Pathog. Dis.* **2009**, *6*, 201–206.

47. Liu, W.; Hsu, C.; Yin, M. In Vitro Anti-Helicobacter pylori Activity of Diallyl Sulphides and Protocatechuic Acid. *Phytother. Res.* **2008**, *22*, 53–57.

48. Liu, K.; Tsao, S.; Yin, M. In vitro Antibacterial Activity of Roselle Calyx and Protocatechuic Acid Acids. *Phytother. Res.* **2005**, *19*, 942–945.

49. Wermuth, C.G. *The Pratice of Medicinal Chemistry*; London Academic Press: London, UK, 2008; Volume 3, pp. 273–287.

50. Bahmani, A.; Saaidpour, S.; Rostami, A. A Simple, Robust and Efficient Computational Method for n-Octanol/Water Partition Coefficients of Substituted Aromatic Drugs. *Sci. Rep.* **2017**, *7*, 5760.

51. Medina-Alarcón, K.P.; Singulani, J.L.; Voltan, A.R.; Sardi, J.C.; Petrônio, M.S.; Santos, M.B.; Polaquini, C.R.; Regasini, L.O.; Bolzani, V.S.; da Silva, D.H.; Chorilli,

M. Alkyl Protocatechuate Loaded Nanostructured Lipid Systems as a Treatment Strategy for *Paracoccidioides brasiliensis* and *Paracoc cidioides litizii*. *In Vitro Front. Microbiol.* **2017**, *8*, 1048.

52. Lutkenhaus, J.; Addinall, S.G. Bacterial cell division and the Z ring. *Annu. Rev. Biochem*. **1997**, *66*, 93–116.
53. Löwe, J.; Amos, L.A. Crystal structure of the bacterial cell-division protein FtsZ. *Nature* **1998**, *8*, 391.
54. RayChaudhuri, D.; Park, J.T. Escherichia coli cell-division gene ftsZ encodes a novel GTP-binding protein. *Nature* **1992**, *17*, 359–392.
55. Erickson, H.P.; Stoffler, D. Protofilaments and rings, two conformations of the tubulin family conserved from bacterial FtsZ to alpha/beta and gamma tubulin. *J. Cell Biol.* **1996**, *135*, 5–8.
56. Margalit, D.N.; Romberg, L.; Mets, R.B.; Hebert, A.M.; Mitchison, T.J.; Kirschner, M.W.; RayChaudhuri, D. Targeting Cell Division: Small-Molecule Inhibitors of FtsZ GTPase Perturb Cytokinetic Ring Assembly and Induce Bacterial Lethality. *Proc. Natl. Acad. Sci. USA 2004, 101, 11821–11826.*
57. Zeraik, M.L.; Petrônio, M.S.; Coelho, D.; Regasini, L.O.; Silva, D.H.; da Fonseca, L.M.; Machado, S.A.; Bolzani, V.S.; Ximenes, V.F. Improvement of Pro-Oxidant Capacity of Protocatechuic Acid by Esterification. *PLoS ONE*. **2014**, *9*, e110277.
58. Polaquini, C.R.; Torrezan, G.S.; Santos, V.R.; Nazaré, A.C.; Campos, D.L.; Almeida, L.A.; Silva, I.C.; Ferreira, H.; Pavan, F.R.; Duque, C.; Regasini, L.O. Antibacterial and Antitubercular Activities of Cinnamylideneacetophenones. *Molecules* **2017**, *22*, 1685.
59. Palomino, J.C.; Martin, A.; Camacho, M.; Guerra, H.; Swings, J.; Portaels, F. Resazurin microtiter assay plate: Simple and inexpensive method for detection of drug resistence in Mycobacterium tuberculosis. *Antimicrob. Agents Chemother.* **2002**, *46*, 8.
60. da Silva, A.R.; Ferro, J.A.; Reinach, F.C.; Farah, C.S.; Furlan, L.R.; Quaggio, R.B.; Monteiro-Vitorello, C.B.; Van Sluys, M.A.; Almeida, N.A.; Alves, L.M.; et al. Comparison of the genomes of two Xanthomonas pathogens with differing host specificities. *Nature* **2002**, *417*, 459.
61. Morão, L.G.; Polaquini, C.R.; Santos, M.B.; Regasini, L.O.; Ferreira, H. Atividade anti-*Xanthomonas citri* subsp *citri* de hibridos moleculares curcumina-cinamaldeido: Uma alternativa para a citricultura. *Ciencia & Tecnologia* **2016**, *8*, 1–2.
62. Mosman, T. Rapid colorimetric assay for cellular growth and survival: Application to proliferation and cytotoxicity assays. *J. Immunol. Methods* **1983**, *65*, 55–63.
63. Berridge, M.V.; Herst, P.M.; Tan, A.S. Tetrazolium dyes as tools in cell biology: New insights into their cellular reduction. *Biotechnol. Annu. Rev.* **2005**, *11*, 127–52.
64. Ingerman, E.; Nunnari, J. A Continuous, Regenerative Coupled GTPase Assay for Dynamin-Related Proteins. *Methods Enzymol.* **2005**, *404*, 611–619.

Appendix A – Supplementary Materials

1. SPECTROSCOPY DATA ANALYSES

The purity of compounds was measured on HPLC-PAD equipment, the analysis were performed for calculations of partition coefficient, using MeOH:H_2O (3:1) as isocratic mobile phase. The NMR spectra were recorded on a Bruker Avance III 14.1 T (600 MHz), Bruker Avance III 9.4 T (400 MHz) and Bruker Fourier 7.1 T (300 MHz) spectrometers, using $CDCl_3$ or DMSO-d_6 as solvent. The chemical shifts (δ) and coupling constants (J) were expressed in ppm and Hz, respectively. Multiplicities were reported as singlet (s), doublet (d), doublet of doublet (dd), triplet (t), quartet (q), and septet (sp).

1.1. ethyl 2,4 dihydroxybenzoate (**1**)

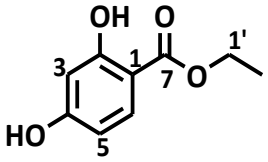

Pale yellow solid

Yield: 20 %

Purity: 87.6 %

^{1}H NMR (400 MHz, $CDCl_3$) δ_H in ppm (multiplicity; *J* in Hz): 11.09 (s, 2-OH), 7.77 (d, 8.8, H-6), 6.42 (d, 2.4, H-3), 6.39 (dd, 8.8 and 2.4, H-5), 5.92 (s; 4-OH), 4.39 (q, 7.2, H-1'), 1.42 (t, 7.2, H-2')

^{13}C NMR (100 MHz, $CDCl_3$) δ_C in ppm: 170.0 (C-7), 163.6 (C-4), 162.0 (C-2), 131.9 (C-3), 107.8 (C-5), 106.1 (C-1), 103.1 (C-6), 61.1 (C-1'), 14.2 (C-2')

1.2. butyl 2,4 dihydroxybenzoate (**2**)

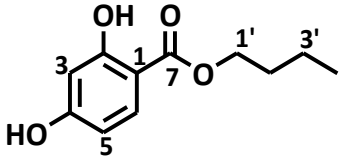

White crystal

Yield: 98 %

Purity: 85.6 %

^{1}H NMR(400 MHz, $CDCl_3$) δ_H in ppm (multiplicity; *J* in Hz): 11.09 (s, 2-OH), 7.76 (d, 8.4, H-6), 6.42 (d, 2.4, H-3), 6.39 (dd, 8.4 and 2.4, H-5), 5.93 (s, 4-OH), 4.34 (t, 6.4, H-1'), 1.81–1.73 (H-2'), 1.54–1.45 (H-3'), 1.00 (t, 7.6, H-4')

^{13}C NMR (100 MHz, $CDCl_3$) δ_C in ppm:170.1 (C-7), 163.6 (C-4), 162.0 (C-2), 131.9 (C-3), 107.8 (C-5), 106.1 (C-1), 103.1 (C-6), 64.9 (C-1'), 30.6 (C-2'), 19.2 (C-3'), 13.7 (C-4')

1.3. hexyl 2,4 dihydroxybenzoate (**3**)

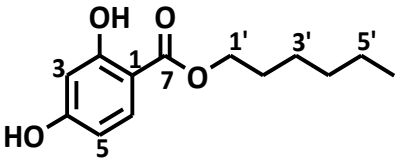

White crystal

Yield: 92 %

Purity: 81.7 %

^{1}H NMR (400 MHz, $CDCl_3$) δ_H in ppm (multiplicity; *J* in Hz): 11.08 (s, 2-OH), 7.76 (d, 8.8, H-6), 6.42 (d, 2.4, H-3), 6.39 (dd, 8.8 and 2.4, H-5), 5.83 (s, 4-OH), 4.33 (t, 6.8, H-1'), 1.80–1.76 (H-2'), 1.47–1.36 (H-3'−H-5'), 0.93 (t, 6.8, H-6')

^{13}C NMR (100 MHz, $CDCl_3$) δ_C in ppm: 170.1 (C-7), 163.7 (C-4), 162.0 (C-2), 131.9 (C-3), 107.7 (C-5), 106.1 (C-1), 103.1 (C-6), 65.2 (C-1'), 31.4, 28.6, 25.6, and 22.5 (C-2'−C-5'), 14.0 (C-6')

1.4. heptyl 2,4 dihydroxybenzoate (**4**)

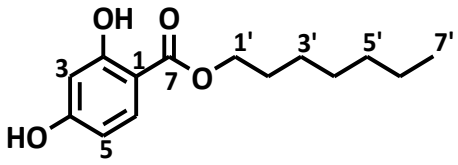

White crystal

Yield: 82 %

Purity: 83.8 %

^{1}H NMR (600 MHz, $CDCl_3$) δ_H in ppm (multiplicity; *J* in Hz): 11.09 (s, 2-OH), 7.76 (d, 9.0, H-6), 6.42 (d, 2.4, H-3), 6.40 (dd, 9.0 and 2.4, H-5), 5.90 (s, 4-OH), 4.32 (t, 6.7, H-1'), 1.80–1.76 (H-2'), 1.47–1.27 (H-3'−H-6'), 0.91 (t, 6.9, CH_3)

^{13}C NMR (150 MHz, $CDCl_3$) δ_C in ppm: 170.1 (C-7), 163.7 (C-4), 161.9 (C-2), 131.9 (C-3), 107.7 (C-5), 106.1 (C-1), 103.1 (C-6), 65.2 (C-1'), 31.7, 28.9, 28.6, 25.9, and 22.6 (C-2'−C-6'), 14.1 (C-7')

1.5. octyl 2,4 dihydroxybenzoate (**5**)

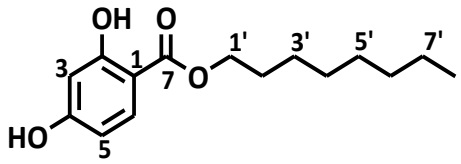

White crystal

Yield: 82 %

Purity: 79.6 %

^{1}H NMR (400 MHz, $CDCl_3$) δ_H in ppm (multiplicity; *J* in Hz): 7.74 (d, 8.4, H-6), 6.40–6.37 (H-3 and H-5), 4.31 (t, 6.4, H-1'), 1.80–1.73 (H-2'), 1.46–1.30 (H-3'–H-7'), 0.91 (t, 6.4, H-8')

^{13}C NMR (100 MHz, $CDCl_3$) δ_C in ppm: 170.7 (C-7), 163.6 (C-4), 162.2 (C-2), 131.9 (C-3), 107.9 (C-5), 106.0 (C-1), 103.1 (C-6), 65.2 (C-1'), 31.8, 29.2, 29.1, 28.6, 26.0, and 22.6 (C-2'−C-7'), 14.1 (H-8')

1.6. nonyl 2,4 dihydroxybenzoate (**6**)

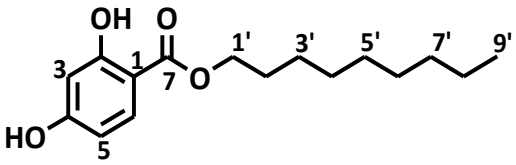

White crystal

Yield: 98 %

Purity: 99.0 %

^{1}H NMR (600 MHz, $CDCl_3$) δ_H in ppm (multiplicity; *J* in Hz): 11.08 (s, 2-OH), 7.76 (d, 8.8, H-6), 6.42 (d, 2.4, H-3), 6.39 (dd, 8.8 and 2.4, H-5), 5.83 (s, 4-OH), 4.35 (t, 6.7, H-1'), 1.81–1.76 (H-2'), 1.47–1.29 (H-3'–H-8'), 0.90 (t, 6.8, H-9')

^{13}C NMR (100 MHz, $CDCl_3$) δ_C in ppm: 170.1 (C-7), 163.6 (C-4), 162.0 (C-2), 131.9 (C-3), 107.8 (C-5), 106.1 (C-1), 103.1 (C-6), 65.2 (C-1'), 31.9, 29.5, 29.2, 28.6, 26.0, and 22.7 (C-2'−C-8'), 14.1 (C-9')

1.7. decyl 2,4 dihydroxybenzoate (**7**)

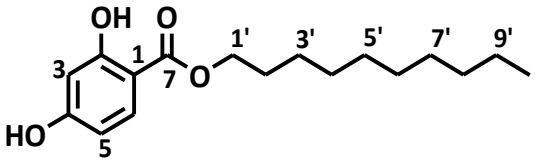

Pale yellow solid

Yield: 95 %

Purity: 99.5 %

^{1}H NMR (400 MHz, $CDCl_3$) δ_H in ppm (multiplicity; *J* in Hz): 11.08 (s, 2-OH), 7.76 (d, 8.4 Hz, H-6), 6.42 (d, 2.4, H-3), 6.39 (dd, 8.4 and 2.4, H-5), 5.65 (s, 4-OH), 4.33 (t, 6.4, H-1'), 1.81–1.74 (H-2'), 1.47–1.29 (H-3'–H-9'), 0.90 (t, 6.8, H-10')

^{13}C NMR (100 MHz, $CDCl_3$) δ_C in ppm: 170.1 (C-7), 163.6 (C-4), 162.0 (C-2), 131.9 (C-3), 107.8 (C-5), 106.1 (C-1), 103.1 (C-6), 65.3 (C-1'), 31.9, 29.5, 29.3, 29.2, 28.6, 26.0, and 22.7 (C-2'−C-9'), 14.1 (C-10')

1.8. dodecyl 2,4 dihydroxybenzoate (**8**)

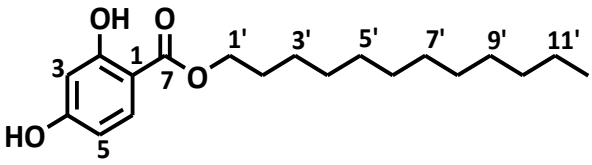

White crystal

Yield: 99 %

Purity: > 99.9 %

^{1}H NMR (300 MHz, $CDCl_3$) δ_H in ppm (multiplicity; *J* in Hz): 11.07 (s, 2-OH), 7.75 (d, 8.4, H-6), 6.41 (d, 2.1, H-3) 6.38 (dd, 8.4 and 2.1, H-5), 5.68 (s, 4-OH), 4.31 (t, 6.6, H-1'), 1.81–1.72 (H-2'), 1.43–1.27 (H-3'–H-11'), 0.89 (t, 6.6, H-12')

^{13}C NMR (100 MHz, $CDCl_3$) δ_C in ppm: 170.1 (C-7), 163.7 (C-4), 162.0 (C-2), 131.8 (C-3), 107.8 (C-5), 106.1 (C-1), 103.1 (C-6), 65.2 (C-1'), 31.9, 29.7, 29.6, 29.5, 29.4, 29.3, 29.2, 28.6, 26.0, and 22.7 (C-2'−C-11'), 14.1 (C-12')

1.9. isopropyl 2,4 dihydroxybenzoate (**9**)

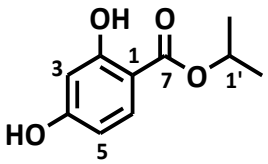

Brown oil

Yield: 68 %

Purity: 93.2 %

^{1}H NMR (600 MHz, $CDCl_3$) δ_H in ppm (multiplicity; *J* in Hz): 11.21 (s, 2-OH), 7.75 (d, 9.0, H-6), 6.42 (d, 2.4, H-3), 6.39 (dd, 9.0 and 2.4, H-5), 5.27 (sp, 6.6, H-1'), 1.39 (d, 6.6, H-2')

^{13}C NMR (150 MHz, $CDCl_3$) δ_C in ppm: 169.7 (C-7), 163.6 (C-4), 162.0 (C-2), 131.9 (C-3), 107.8 (C-5), 106.3 (C-1), 103.0 (C-6), 68.9 (C-1'), 21.9 (C-2')

1.10. cyclopentyl 2,4 dihydroxybenzoate (**10**)

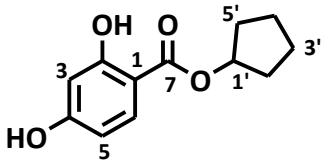

White crystal

Yield: 40 %

Purity: > 99.9 %

^{1}H NMR (600 MHz, $CDCl_3$) δ_H in ppm (multiplicity; *J* in Hz): 11.17 (s, 2-OH), 7.72 (d, 8.4, H-6), 6.41 (d, 2.4, H-3), 6.38 (dd, 8.4 and 2.4, H-5), 5.44– 5.41 (H-1'), 2.03–1.59 (H-2'–H-5')

^{13}C NMR (150 MHz, $CDCl_3$) δ_C in ppm: 169.5 (C-7), 163.7 (C-4), 161.9 (C-2), 131.9 (C-3), 107.7 (C-5), 106.5 (C-1), 103.1 (C-6), 73.5 (C-1'), 31.6 (C-2' and C-5'), 23.6 (C-3' and C-4')

1.11. cyclohexyl 2,4 dihydroxybenzoate (**11**)

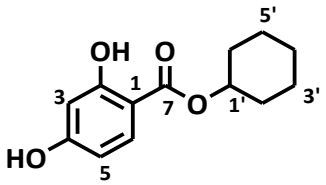

Brown oil

Yield: 92 %

Purity: > 99.9%

^{1}H NMR (600 MHz, $CDCl_3$) δ_H in ppm (multiplicity; *J* in Hz): 11.18 (s, 2-OH), 7.78 (d, 8.4, H-6), 6.42 (d, 2.4, H-3), 6.39 (dd, 8.4 and 2.4, H-5), 5.83 (s, 4-OH), 5.07– 5.02 (H-1'), 1.97–1.34 (H-2'−H-6')

^{13}C NMR (150 MHz, $CDCl_3$) δ_C in ppm: 169.5 (C-7), 163.7 (C-4), 161.9 (C-2), 131.9 (C-3), 107.7 (C-5), 106.5 (C-1), 103.1 (C-6), 73.5 (C-1'), 31.6 (C-2' and C-6'), 25.4 (C-4'), 23.6 (C-3' and C-5')

1.13. ethyl 2,5 dihydroxybenzoate (**13**)

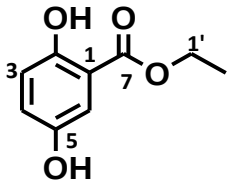

Pale yellow crystal

Yield: 32 %

Purity: 98.3 %

^{1}H NMR (400 MHz, $CDCl_3$) δ_H in ppm (multiplicity; *J* in Hz): 10.44 (s, 2-OH), 7.32 (d, 3.2, H-6), 7.03 (dd, 8.8 and 3.2, H-4), 6.89 (d, 8.8, H-3), 4.41 (q, 7.2, H-1'), 1.42 (t, 7.2, H-2')

^{13}C NMR (100 MHz, $CDCl_3$) δ_C in ppm: 169.8 (C-7), 155.8 (C-2), 147.7 (C-5), 123.9 (C-4), 118.5 (C-3), 114.8 (C-6), 112.4 (C-1), 61.5 (C-1'), 14.2 (C-2')

1.14. butyl 2,5 dihydroxybenzoate (**14**)

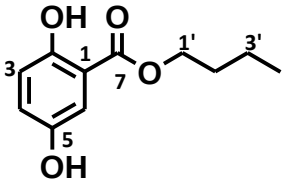

Pale yellow crystal

Yield: 87 %

Purity: 82.0 %

^{1}H NMR (400 MHz, $CDCl_3$) δ_H in ppm (multiplicity; *J* in Hz): 10.44 (s, 2-OH), 7.31 (d, 2.8, H-6), 7.03 (dd, 8.8 and 2.8, H-4), 6.90 (d, 8.8, H-3), 4.90 (s; 5-OH), 4.36 (t, 6.8, H-1'), 1.81−1.74 (H-2'), 1.54−1.45 (H-3'), 1.01 (t, 7.2, H-4')

^{13}C NMR (100 MHz, $CDCl_3$) δ_C in ppm: 169.8 (C-7), 155.9 (C-2), 147.7 (C-5), 123.9 (C-4), 118.5 (C-3), 114.7 (C-6), 112.5 (C-1), 65.3 (C-1'), 30.6 (C-2'), 19.2 (C-3'), 13.7 (C-4')

1.15. hexyl 2,5 dihydroxybenzoate (**15**)

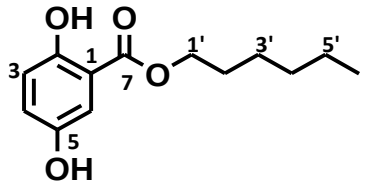

Pale yellow oil

Yield: 67 %

Purity: 80.1 %

^{1}H NMR (400 MHz, $CDCl_3$) δ_H in ppm (multiplicity; *J* in Hz): 10.44 (s, 2-OH), 7.31 (d, 3.2, H-6), 7.03 (dd, 9.2 and 3.2, H-4), 6.89 (d, 9.2, H-3), 4.35 (t, 6.8, H-1'), 1.83−1.75 (H-2'), 1.48−1.36 (H-3'–H-5'), 0.93 (t, 6.8, H-6')

^{13}C NMR (100 MHz, $CDCl_3$) δ_C in ppm: 169.8 (C-7), 155.9 (C-2), 147.7 (C-5), 123.9 (C-4), 118.5 (C-3), 114.7 (C-6), 112.5 (C-1), 65.6 (C-1'), 31.4, 28.5, 25.6, and 22.5 (C-2'–C-5'), 14.0 (C-6')

1.16. heptyl 2,5 dihydroxybenzoate (**16**)

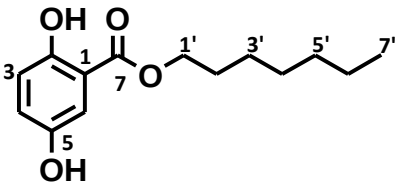

Pale yellow crystal

Yield: 40 %

Purity: 99.3 %

^{1}H NMR (600 MHz, $CDCl_3$) δ_H in ppm (multiplicity; *J* in Hz): 10.45 (s, 2-OH), 7.31 (d, 3.0, H-6), 7.03 (dd, 9.0 and 3.0, H-4), 6.90 (d, 9.0, H-3), 4.35 (t, 6.7, H-1'), 1.81–1.77 (H-2'), 1.48–1.27 (H-3'–H-6'), 0.92 (t, 6.9, H-7')

^{13}C NMR (150 MHz, $CDCl_3$) δ_C in ppm: 169.8 (C-7), 155.9 (C-2), 147.6 (C-5), 123.9 (C-4), 118.5 (C-3), 114.7 (C-6), 112.5 (C-1), 65.6 (C-1'), 31.7, 28.9, 28.6, 25.9, and 22.6 (C-2'–C6'), 14.1 (C-7')

1.17. octyl 2,5 dihydroxybenzoate (**17**)

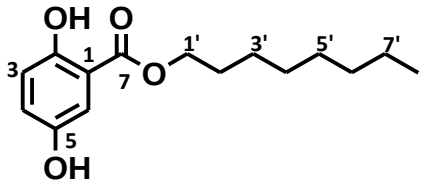

Pale yellow crystal

Yield: 95 %

Purity: 79.8 %

^{1}H NMR (400 MHz, $CDCl_3$) δ_H in ppm (multiplicity; *J* in Hz): 10.45 (s, 2-OH), 7.31 (d, 3.2, H-6), 7.03 (dd, 9.2 and 3.2, H-4), 6.90 (d, 9.2, H-3), 4.35 (t, 6.8, H-1'), 1.82−1.75 (H-2'), 1.49−1.31 (H-3'–H-7'), 0.91 (t, 6.8, H-8')

^{13}C NMR (100 MHz, $CDCl_3$) δ_C in ppm: 169.8 (C-7), 155.9 (C-2), 147.7 (C-5), 123.9 (C-4), 118.5 (C-3), 114.8 (C-6), 112.5 (C-1), 65.7 (C-1'), 31.8, 29.2, 29.1, 28.5, 26.0, and 22.6 (C-2'–C7'), 14.1 (C-8')

1.18. nonyl 2,5 dihydroxybenzoate (**18**)

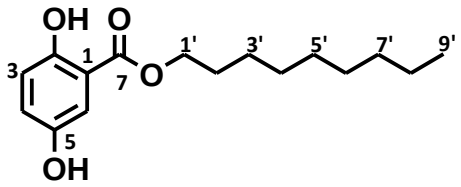

Pale yellow crystal

Yield: 99 %

Purity: > 99.9 %

^{1}H NMR (600 MHz, $CDCl_3$) δ_H in ppm (multiplicity; *J* in Hz): 10.46 (s, 2-OH), 7.31 (d, 3.0, H-6), 7.03 (dd, 9.0 and 3.0, H-4), 6.90 (d, 9.0, H-3), 4.35 (t, 6.7, H-1'), 1.81–1.76 (H-2'), 1.47–1.29 (H-3'–H-8'), 0.90 (t, 6.8, H-9')

^{13}C NMR (150 MHz, $CDCl_3$) δ_C in ppm: 169.9 (C-7), 155.8 (C-2), 147.7 (C-5), 123.9 (C-4), 118.5 (C-3), 114.7 (C-6), 112.5 (C-1), 65.7 (C-1'), 31.9, 29.5, 29.3, 28.5, 26.0, and 22.7 (C-2'–C-8'), 14.1 (C-9')

1.19. decyl 2,5 dihydroxybenzoate (**19**)

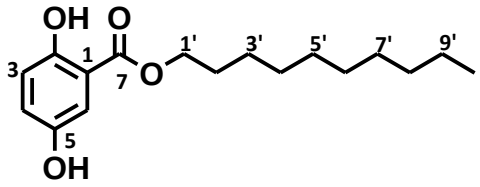

Pale yellow crystal

Yield: 70 %

Purity: 76.5 %

^{1}H NMR (400 MHz, $CDCl_3$) δ_H in ppm (multiplicity; *J* in Hz): 10.44 (s, 2-OH), 7.31 (d, 3.2, H-6), 7.02 (dd, 9.2 and 3.2, H-4), 6.90 (d, 9.2, H-3), 4.84 (s, 5-OH), 4.35 (t, 6.4, H-1'), 1.82−1.75 (H-2'), 1.47−1.30 (H-3'–H-9'), 0.90 (t, 6.8, H-10')

^{13}C NMR (100 MHz, $CDCl_3$) δ_C in ppm: 169.8 (C-7), 155.9 (C-2), 147.7 (C-5), 123.9 (C-4), 118.5 (C-3), 114.8 (C-6), 112.5 (C-1), 65.6 (C-1'), 31.9, 29.6, 29.5, 29.3, 29.2, 28.5, 26.0, and 22.7 (C-2'–C-9'), 14.1 (C-10')

1.20. dodecyl 2,5 dihydroxybenzoate (**20**)

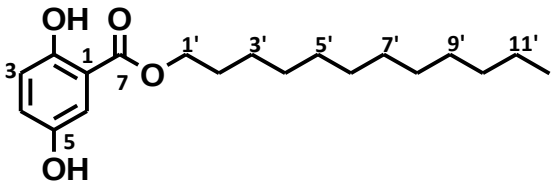

Pale yellow crystal

Yield: 99 %

Purity: > 99.9 %

^{1}H NMR (300 MHz, $CDCl_3$) δ_H in ppm (multiplicity; *J* in Hz): 10.43 (s, 2-OH), 7.30 (d, 3.3, H-6), 7.02 (dd, 8.7 and 3.3, H-4), 6.89 (d, 8.7, H-3), 4.34 (t, 6.6, H-1'), 1.82−1.73 (H-2'), 1.42−1.27 (H-3'–H-11'), 0.89 (t, 6.3, H-12')

^{13}C NMR (100 MHz, $CDCl_3$) δ_C in ppm: 169.8 (C-7), 155.9 (C-2), 147.7 (C-5), 123.9 (C-4), 118.5 (C-3), 114.7 (C-6), 112.5 (C-1), 65.6 (C-1'), 31.9, 29.7, 29.6, 29.5, 29.3, 29.2, 28.6, 26.0, and 22.7 (C-2'–C-11'), 14.1 (C-12')

1.21. isopropyl 2,5 dihydroxybenzoate (**21**)

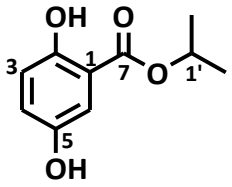

Pale yellow solid

Yield: 80 %

Purity: > 99.9 %

^{1}H NMR (400 MHz, $CDCl_3$) δ_H in ppm (multiplicity; *J* in Hz): 10.51 (s, 2-OH), 7.31 (d, 3.2, H-6), 7.02 (dd, 9.2 and 3.2, H-4), 6.89 (d, 9.2, H-3), 5.29 (sp, 6.4, H-1'), 1.40 (d, 6.4, H-2')

^{13}C NMR (150 MHz, $CDCl_3$) δ_C in ppm: 169.3 (C-7), 155.9 (C-2), 147.6 (C-5), 123.8 (C-4), 118.4 (C-3), 114.8 (C-6), 112.8 (C-1), 69.4 (C-1'), 21.8 (C-2')

1.22. cyclopentyl 2,5 dihydroxybenzoate (**22**)

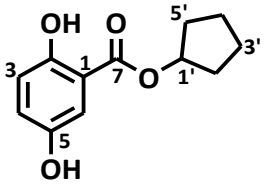

White solid

Yield: 75 %

Purity: > 99.9 %

^{1}H NMR (300 MHz, $CDCl_3$) δ_H in ppm (multiplicity; *J* in Hz): 10.50 (s, 2-OH), 7.27 (d, 3.0, H-6), 7.00 (dd, 9.0 and 3.0, H-4), 6.88 (d, 9.0, H-3), 5.45–5.41 (H-1'), 4.76 (s, 5-OH), 1.97–1.67 (H-2'–H-5')

^{13}C NMR (150 MHz, $CDCl_3$) δ_C in ppm: 169.5 (C-7), 155.9 (C-2), 147.5 (C-5), 123.7 (C-4), 118.4 (C-3), 114.8 (C-6), 112.8 (C-1), 78.6 (C-1'), 32.7 (C-2' and C-5'), 23.8 (C-3' and C-4')

1.23. cyclohexyl 2,5 dihydroxybenzoate (**23**)

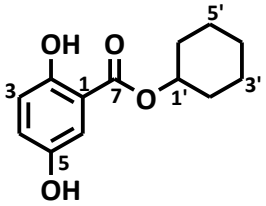

Pale yellow solid

Yield: 75 %

Purity: > 99.9 %

^{1}H NMR (300 MHz, $CDCl_3$) δ_H in ppm (multiplicity; *J* in Hz): 10.51 (s, 2-OH), 7.32 (d, 3.0, H-6), 7.01 (dd, 9.0 and 3.0, H-4), 6.88 (d, 9.0, H-3), 5.10–5.02 (H-1'), 1.93–1.26 (H-2'–H-6')

^{13}C NMR (150 MHz, $CDCl_3$) δ_C in ppm: 169.2 (C-7), 155.9 (C-2), 147.6 (C-5), 123.8 (C-4), 118.4 (C-3), 114.8 (C-6), 112.9 (C-1), 74.0 (C-1'), 31.5 (C-2' and C-6'), 25.3 (C-3' and C-5'), 23.5 (C-4')

1.24. phenylethyl 2,5 dihydroxybenzoate (**24**)

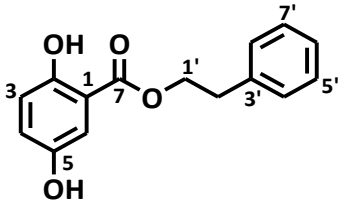

Pale yellow oil

Yield: 7 %

Purity: > 99.9 %

^{1}H NMR (400 MHz, $CDCl_3$) δ_H in ppm (multiplicity; *J* in Hz): 10.33 (s, 2-OH), 7.38−7.28 (H-4'−H-8'), 7.26 (d, 3.2, H-6), 7.02 (dd, 8.8 and 3.2, H-4), 6.90 (d, 8.8, H-3), 4.69 (s, 5-OH), 4.55 (t, 6.8, H-1'), 3.12 (t, 6.8, H-2')

^{13}C NMR (150 MHz, $CDCl_3$) δ_C in ppm: 169.6 (C-7), 156.0 (C-2), 147.6 (C-5), 137. 4 (C-3'), 128,9 (C-5' and C-7'), 128.7 (C-4' and C-8'), 126.8 (C-6'), 124.1 (C-4), 118.5 (C-3), 114.7 (C-6), 112.2 (C-1), 65.9 (C-1'), 35,0 (C-2')

1.25. ethyl 3,4 dihydroxybenzoate (**25**)

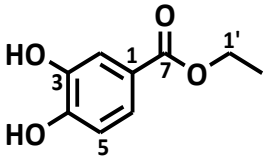

Pale yellow solid

Yield: 90 %

Purity: 99.1 %

^{1}H NMR (400 MHz, DMSO-*d*$_6$) δ_H in ppm (multiplicity; *J* in Hz): 7.35 (d, 2.4, H-2), 7.31 (dd, 8.4 and 2.4, H-6), 6.80 (d, 8.4, H-5), 4.31 (q, 7.2, H-1'), 1.27 (t, 7.2, H-2')

^{13}C NMR (100 MHz, DMSO-*d*$_6$) δ_C in ppm: 166.2 (C-7), 150.8 (C-4), 145.5 (C-3), 122.2 (C-6), 121.2 (C-1), 116.7 (C-5), 115.7 (C-2), 60.5 (C-1'), 14.7 (C-2')

1.26. butyl 3,4 dihydroxybenzoate (**26**)

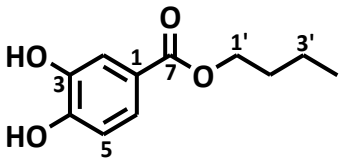

Pale yellow solid

Yield: 98 %

Purity: 99.1 %

^{1}H NMR (400 MHz, $CDCl_3$) δ_H in ppm (multiplicity; *J* in Hz): 7.67 (H-2), 7.58 (dd, 8.4 and 1.6, H-6), 6.93 (d, 8.4, H-5), 4.31 (t, 6.8, H-1'), 1.79−172 (H-2'), 1.53−1.44 (H-3'), 0.99 (t, 5.4, H-4')

^{13}C NMR (100 MHz, $CDCl_3$) δ_C in ppm: 167.1 (C-7), 148.9 (C-4), 143.1 (C-3), 123.7 (C-6), 122.7 (C-1), 116.6 (C-5), 114.8 (C-2), 65.0 (C-1'), 30.7 (C-2'), 19.3 (C-3'), 13.8 (C-4')

1.27. hexyl 3,4 dihydroxybenzoate (**27**)

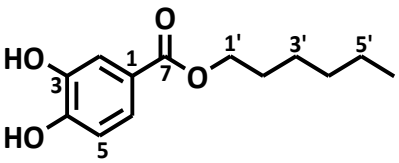

Pale yellow crystal

Yield: 87 %

Purity: 99.1 %

^{1}H NMR (400 MHz, DMSO-*d*$_6$) δ_H in ppm (multiplicity; *J* in Hz): 7.35 (d, 2.4, H-2), 7.31 (dd, 2.4 and 8.0, H-5), 6.81 (d, 8.0, H-6), 4.18 (t, 6.4, H-1'), 1.70−1.63 (H-2'), 1.39–1.30 (H-3'–H-5'), 0.87 (t, 7.2, H-6')

^{13}C NMR (100 MHz, DMSO-*d*$_6$) δ_C in ppm: 166.2 (C-7), 150.9 (C-4), 145.5 (C-3), 122.2 (C-6), 121.1 (C-1), 116.6 (C-5), 115.7 (C-2), 64.4 (C-1'), 31.4, 28.7, 25.6, and 22.5 (C-2'–C-5'), 14.4 (C-6')

1.28. heptyl 3,4 dihydroxybenzoate (**28**)

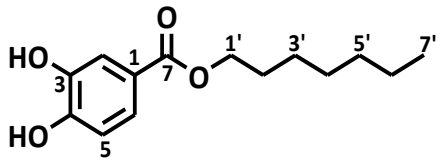

White crystal

Yield: 96 %

Purity: 98.5 %

^{1}H NMR (600 MHz, DMSO-*d*$_6$) δ_H in ppm (multiplicity; *J* in Hz): 9.80 (s, 4-OH), 9.39 (s, 3-OH), 7.35 (d, 1.8, H-2), 7.31 (dd, 8.4 and 1.8, H-6), 6.81 (d, 8.4, H-5), 4.17 (t, 6.5, H-1'), 1.68–1.63, (H-2'), 1.38–1.26 (H-3'−H-6'), 0.86 (t, 6.9, H-7')

^{13}C NMR (150 MHz, DMSO-*d*$_6$) δ_C in ppm: 166.2 (C-7), 150.8 (C-4), 145.5 (C-3), 122.2 (C-6), 121.2 (C-1), 116.6 (C-5), 115.8 (C-2), 64.5 (C-1'), 31.7, 28.8, 28.7, 26.0, and 22.5 (C-2'–C-6'), 14.4 (C-7')

1.29. octyl 3,4 dihydroxybenzoate (**29**)

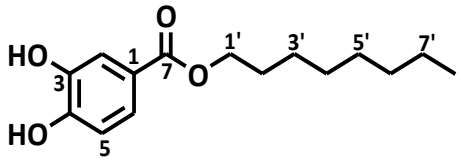

White crystal

Yield: 76 %

Purity: 98.5 %

^{1}H NMR (400 MHz, $CDCl_3$) δ_H in ppm (multiplicity; *J* in Hz): 7.70 (d, 2.0, H-2), 7.58 (dd, 8.4 and 2.0, H-6), 6.93 (d, 8.4, H-5), 4.30 (t, 6.8, H-1'), 1.80−1.73 (H-2'), 1.48–1.30 (H-3'–H-7'), 0.90 (t, 6.8, H-8')

^{13}C NMR (100 MHz, $CDCl_3$) δ_C in ppm: 167.3 (C-7), 148.9 (C-4), 143.2 (C-3), 123.7 (C-6), 122.6 (C-1), 116.7 (C-5), 114.8 (C-2), 65.4 (C-1'), 31.8, 29.2, 29.1, 28.7, 26.0, and 22.6 (C-2'–C-7'), 14.1 (C-8')

1.30. nonyl 3,4 dihydroxybenzoate (**30**)

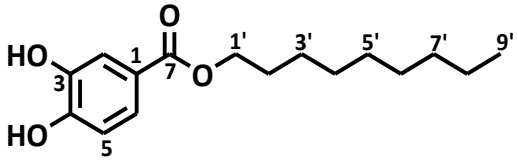

White solid

Yield: 98 %

Purity: 97.9 %

^{1}H NMR (300 MHz, $CDCl_3$) δ_H in ppm (multiplicity; *J* in Hz): 7.67 (d, 2.1, H-2), 7.58 (dd, 8.4 and 2.1, H-6), 6.92 (d, 8.4, H-5), 6.42 (s, 4-OH), 6.15 (s, 3-OH), 4.29 (t, 6.7, H-1'), 1.78–1.71 (H-2'), 1.44–1.28 (H-3'–H-8'), 0.89 (t, 6.7, H-9')

^{13}C NMR (150 MHz, DMSO-d_6) δ_C in ppm: 166.2 (C-7), 150.8 (C-4), 145.5 (C-3), 122.2 (C-6), 121.2 (C-1), 116.6 (C-5), 115.7 (C-2), 64.5 (C-1'), 31.7, 29.4, 29.2, 29.1, 28.7, 26.0, and 22.6 (C-2'–C-8'), 14.1 (C-9')

1.31. decyl 3,4 dihydroxybenzoate (**31**)

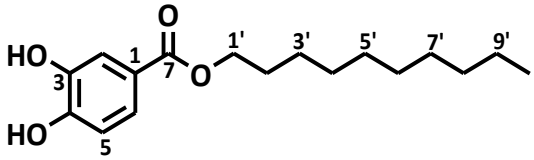

White solid

Yield: 95 %

Purity: 91.3 %

^{1}H NMR (400 MHz, $CDCl_3$) δ_H in ppm (multiplicity; *J* in Hz): 7.68–7.67 (H-2), 7.59 (dd, 8.4 and 1.6, H-6), 6.93 (d, 8.4, H-5), 4.30 (t, 6.8, H-1'), 1.80−1.73 (H-2'), 1.48–1.29 (H-3'–H-9'), 0.90 (t, 6.8, H-10')

^{13}C NMR (100 MHz, $CDCl_3$) δ_C in ppm: 166.9 (C-7), 148.8 (C-4), 143.1 (C-3), 123.7 (C-6), 121.5 (C-1), 116.6 (C-5), 114.8 (C-2), 65.3 (C-1'), 31.9, 29.5, 29.3, 28.7, 26.0, and 22.7 (C-2'–C-9'), 14.1 (C-10')

1.32. dodecyl 3,4 dihydroxybenzoate (**32**)

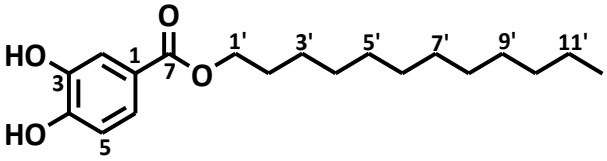

White solid

Yield: 82 %

Purity: > 99.9 %

^{1}H NMR (300 MHz, $CDCl_3$) δ_H in ppm (multiplicity; *J* in Hz): 9.78 (s, 4-OH), 9.36 (s, 3-OH), 7.34 (d, 2.1, H-2), 7.29 (dd, 8.1 and 2.1, H-6), 6.79 (d, 8.1, H-5), 4.16 (t, 6.3, H-1'), 1.67−1.60 (H-2'), 1.38−1.23 (H-3'–H-11'), 0.84 (t, 6.3, H-12')

^{13}C NMR (100 MHz, $CDCl_3$) δ_C in ppm: 166.5 (C-7), 152.9 (C-4), 148.6 (C-3), 123.5 (C-6), 123.2 (C-1), 112.0 (C-5), 110.2 (C-2), 65.0 (C-1'), 31.9, 29.7, 29.6, 29.5, 29.3, 29.2, 28.8, 26.1, and 22.7 (C-2'–C-11'), 14.1 (C-12')

1.33. isopropyl 3,4 dihydroxybenzoate (**33**)

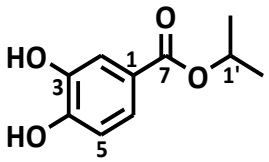

White solid

Yield: 56 %

Purity: > 99.9 %

^{1}H NMR (300 MHz, DMSO-d_6) δ_H in ppm (multiplicity; *J* in Hz): 9.75 (s, 4-OH), 9.34 (s, 3-OH), 7.34 (d, 2.1, H-2), 7.28 (dd, 8.4 and 2.1, H-6), 6.79 (d, 8.4, H-5), 5.04 (h, 6.3, H-1'), 1.26 (d, 6.3, H-2')

^{13}C NMR (150 MHz, DMSO-d_6) δ_C in ppm: 165.6 (C-7), 150.7 (C-4), 145.5 (C-3), 122.1 (C-6), 121.6 (C-1), 116.6 (C-5), 115.7 (C-2), 67.7 (C-1') 22.2 (C-2')

1.34. cyclopentyl 3,4 dihydroxybenzoate (**34**)

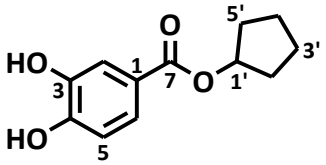

White solid

Yield: 68 %

Purity: > 99.9 %

^{1}H NMR (300 MHz, DMSO-d_6) δ_H in ppm (multiplicity; *J* in Hz): 9.75 (s, 4-OH), 9.34 (s, 3-OH), 7.32 (d, 2.1, H-2), 7.27 (dd, 8.1 and 2.1, H-6), 6.78 (d, 8.1, H-5), 5.23–5.20 (H-1'), 1.89–1.59 (H-2'–H-5')

^{13}C NMR (150 MHz, DMSO-d_6) δ_C in ppm: 165.9 (C-7), 150.7 (C-4), 145.4 (C-3), 122.1 (C-6), 121.6 (C-1), 116.6 (C-5), 115.7 (C-2), 76.9 (C-1'), 32.8 (C-2' and C-5'), 23.8 (C-3' and C-4')

1.35. cyclohexyl 3,4 dihydroxybenzoate (**35**)

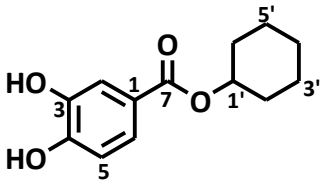

White crystal

Yield: 74 %

Purity: > 99.9 %

^{1}H NMR (600 MHz, DMSO-*d*$_6$) δ_H in ppm (multiplicity; *J* in Hz): 7.36 (d, 1.8, H-2), 7.31 (dd, 8.4 and 1.8, H-6), 6.80 (d, 8.4, H-5), 4.86–4.82 (H-1'), 1.52–1.30 (H-2'–H-6')

^{13}C NMR (150 MHz, DMSO-*d*$_6$) δ_C in ppm: 165.5 (C-7), 150.7 (C-4), 145.5 (C-3), 122.2 (C-6), 121.6 (C-1), 116.7 (C-5), 115.7 (C-2), 72.1 (C-1'), 31.6 (C-2' and C-6'), 25.4 (C-4'), 23.5 (C-3' and C-5')

1.36. phenylethyl 3,4 dihydroxybenzoate (**36**)

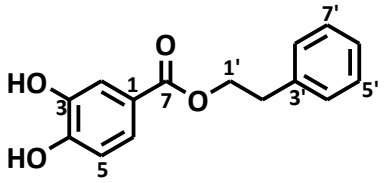

White crystal

Yield: 21 %

Purity: > 99.9 %

^{1}H NMR (300 MHz, DMSO-*d*$_6$) δ_H in ppm (multiplicity; *J* in Hz): 7.32–7.18 (H-2, H-6 and H-4'–H-8'), 6.78 (d, 8.4, H-5), 4.37 (t, 6.6, H-1'), 2.98 (t, 6.6 Hz, H-2')

^{13}C NMR (150 MHz, DMSO-*d*$_6$) δ_C in ppm: 166.1 (C-7), 150.9 (C-4), 145.5 (C-3), 138.7 (C-3'), 129.4 (C-5' and C-7'), 128.8 (C-4' and C-8'), 126.8 (C-6'), 122.2 (C-6), 121.0 (C-1), 116.7 (C-5), 115.7 (C-2), 65.2 (C-1'), 35.0 (C-2').

Figure S1. I) ^{1}H NMR spectrum of compound **1** (400 MHz – $CDCl_3$)

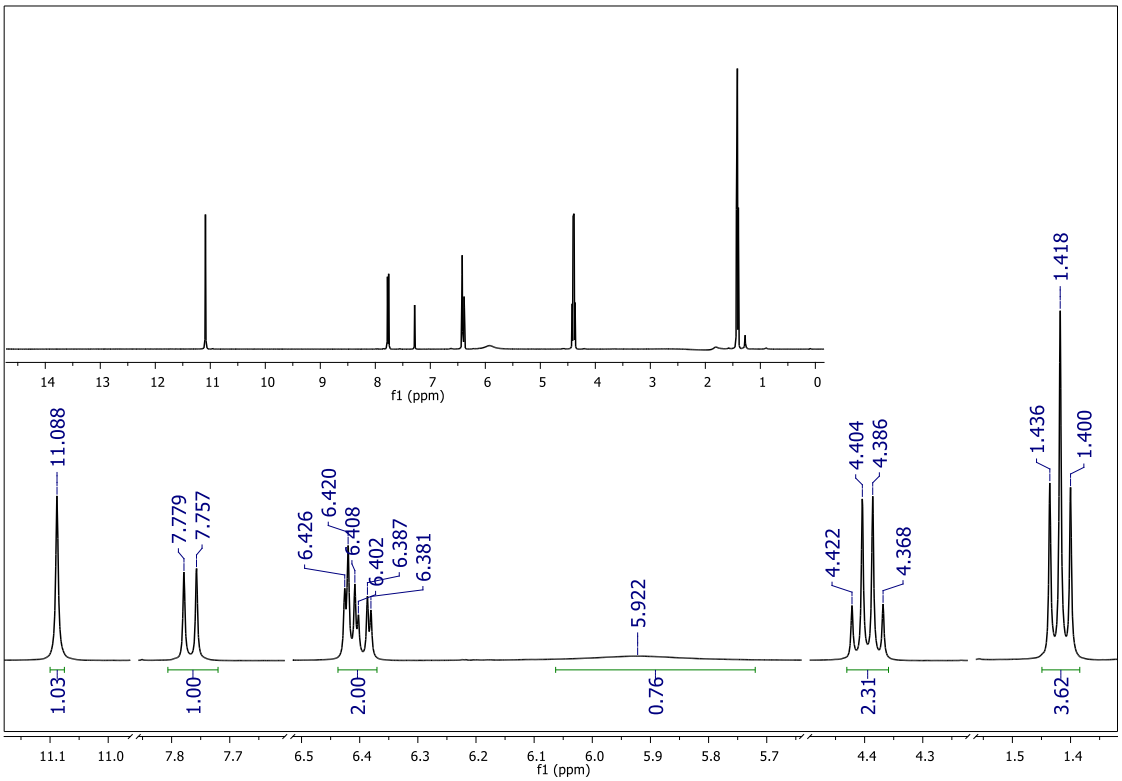

Figure S1. II) ^{13}C NMR spectrum of compound **1** (100 MHz – $CDCl_3$)

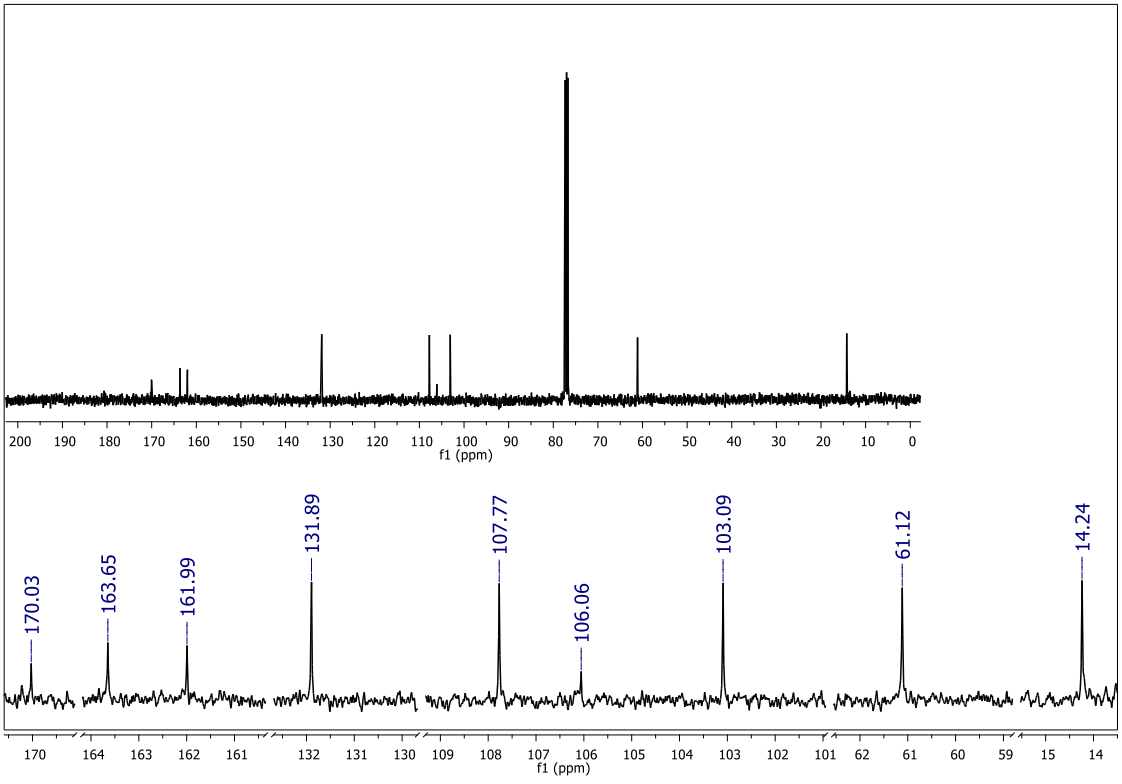

Figure S1. III) HPLC chromatogram of compound **1**

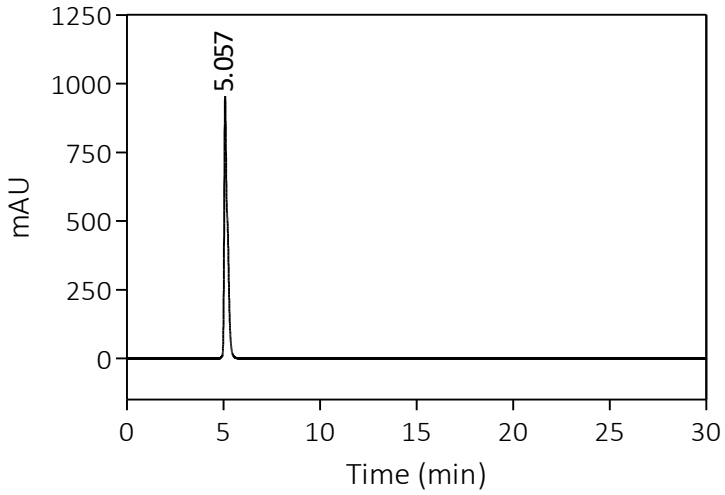

Figure S2. I) ^{1}H NMR spectrum of compound **2** (400 MHz – $CDCl_3$)

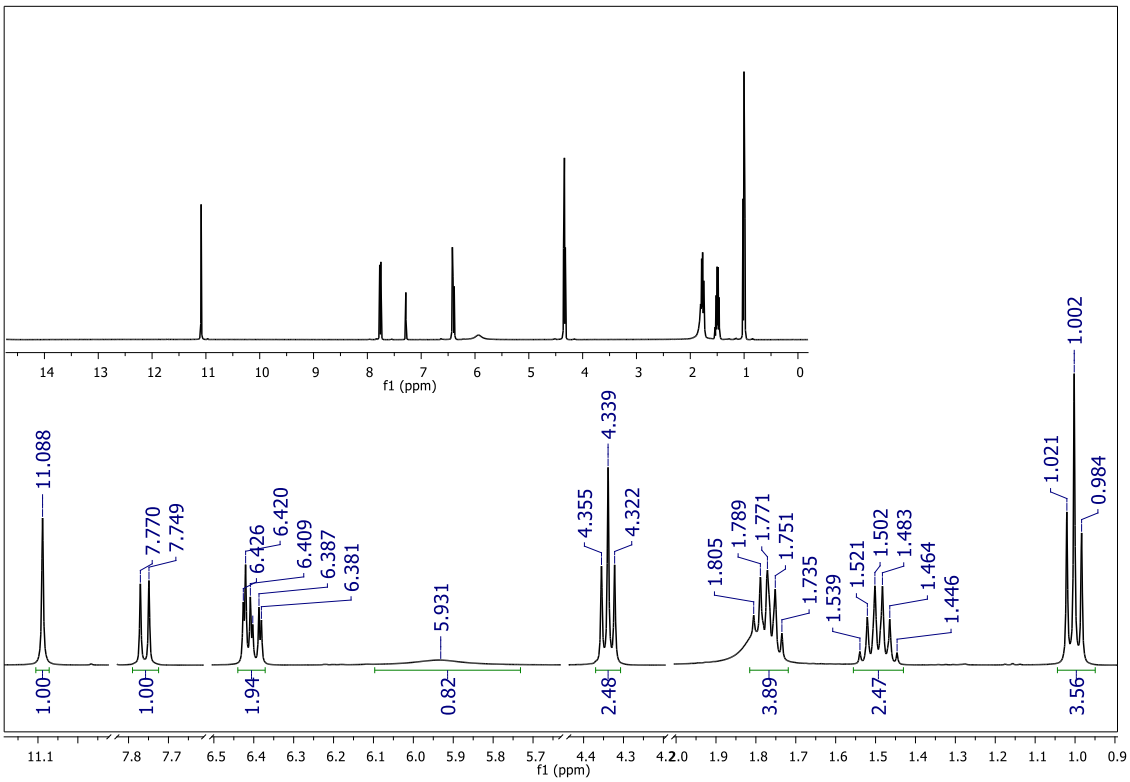

Figure S2. II) ^{13}C NMR spectrum of compound **2** (100 MHz – $CDCl_3$)

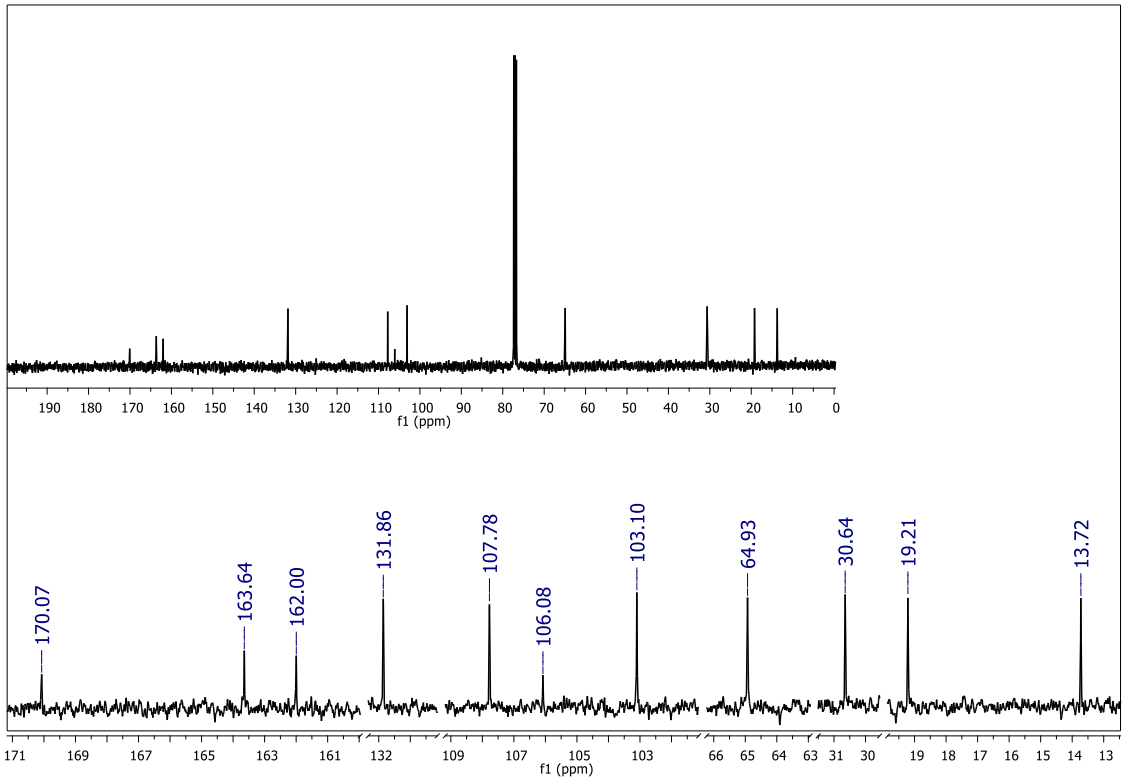

Figure S2. III) HPLC chromatogram of compound **2**

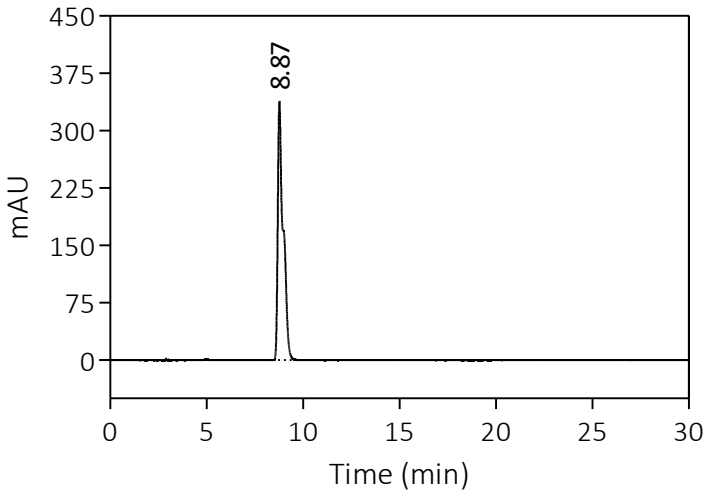

Figure S3. I) ^{1}H NMR spectrum of compound **3** (400 MHz – $CDCl_3$)

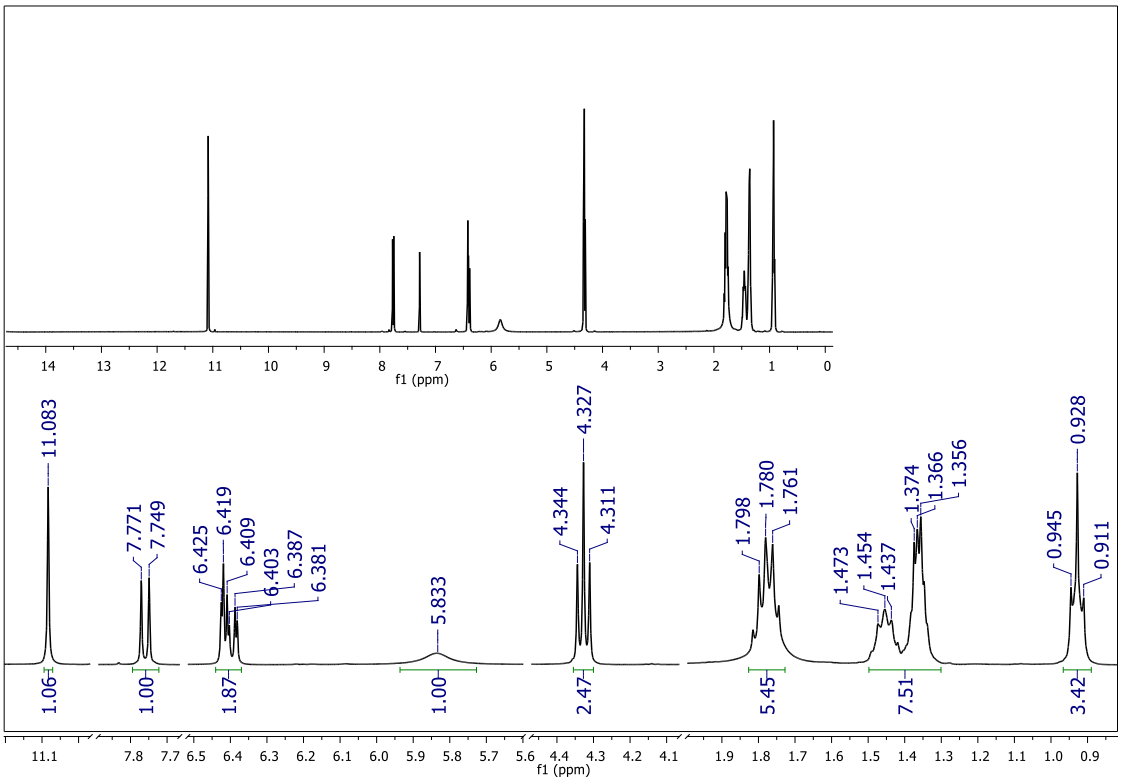

Figure S3. II) ^{13}C NMR spectrum of compound **3** (100 MHz – $CDCl_3$)

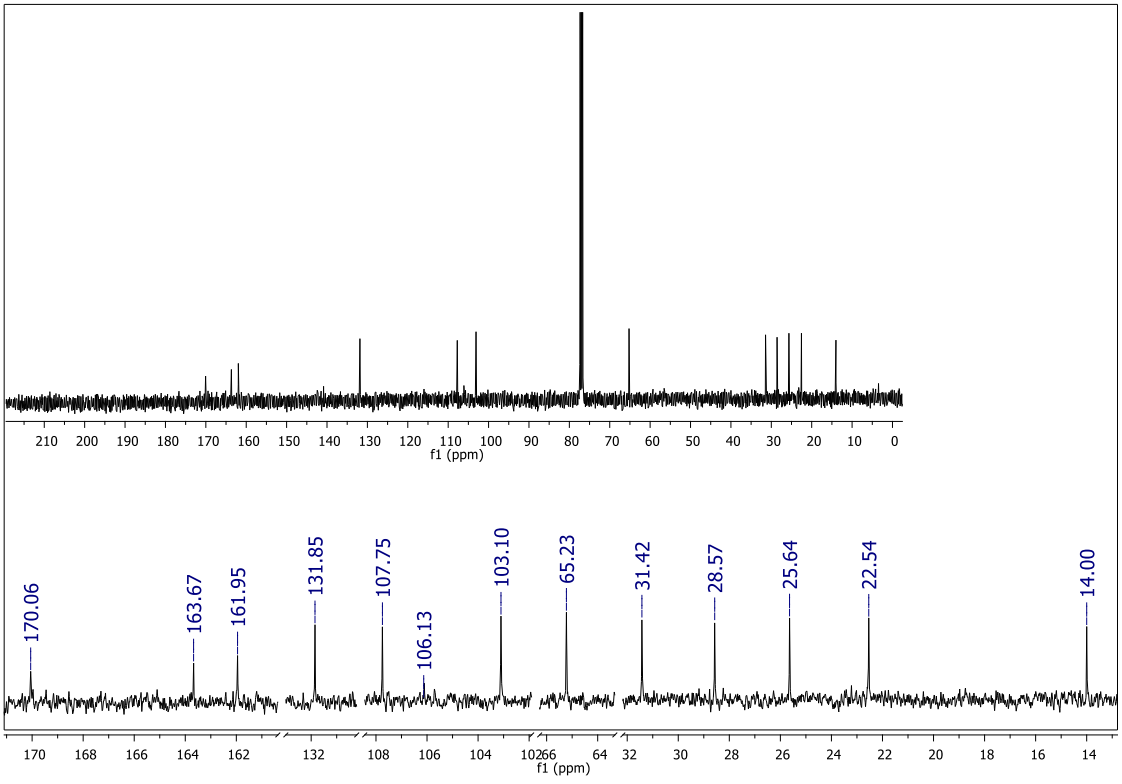

Figure S3. III) HPLC chromatogram of compound **3**

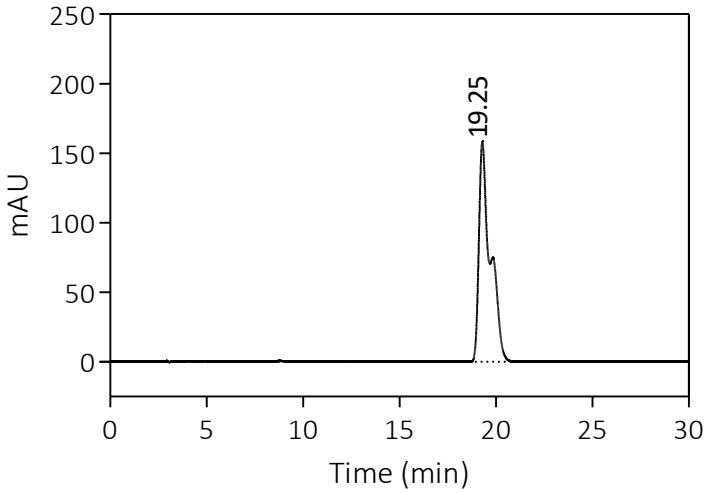

Figure S4. I) ^{1}H NMR spectrum of compound **4** (600 MHz – $CDCl_3$)

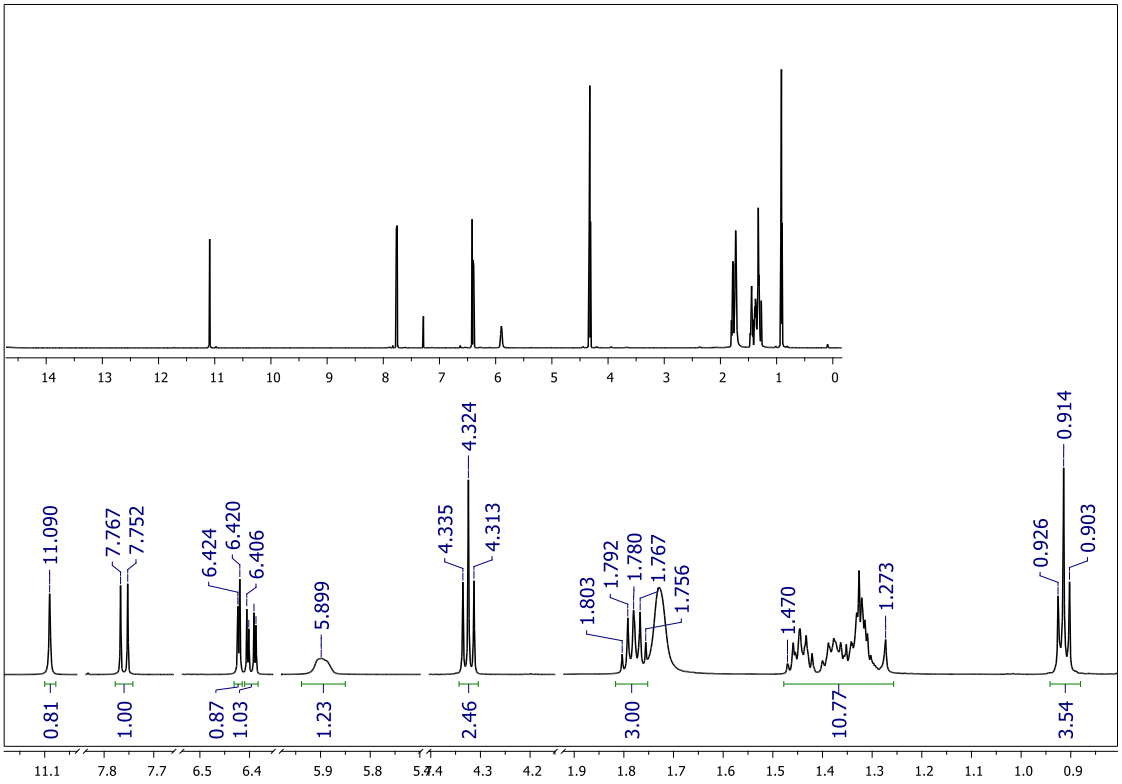

Figure S4. II) ^{13}C NMR spectrum of compound **4** (150 MHz – $CDCl_3$)

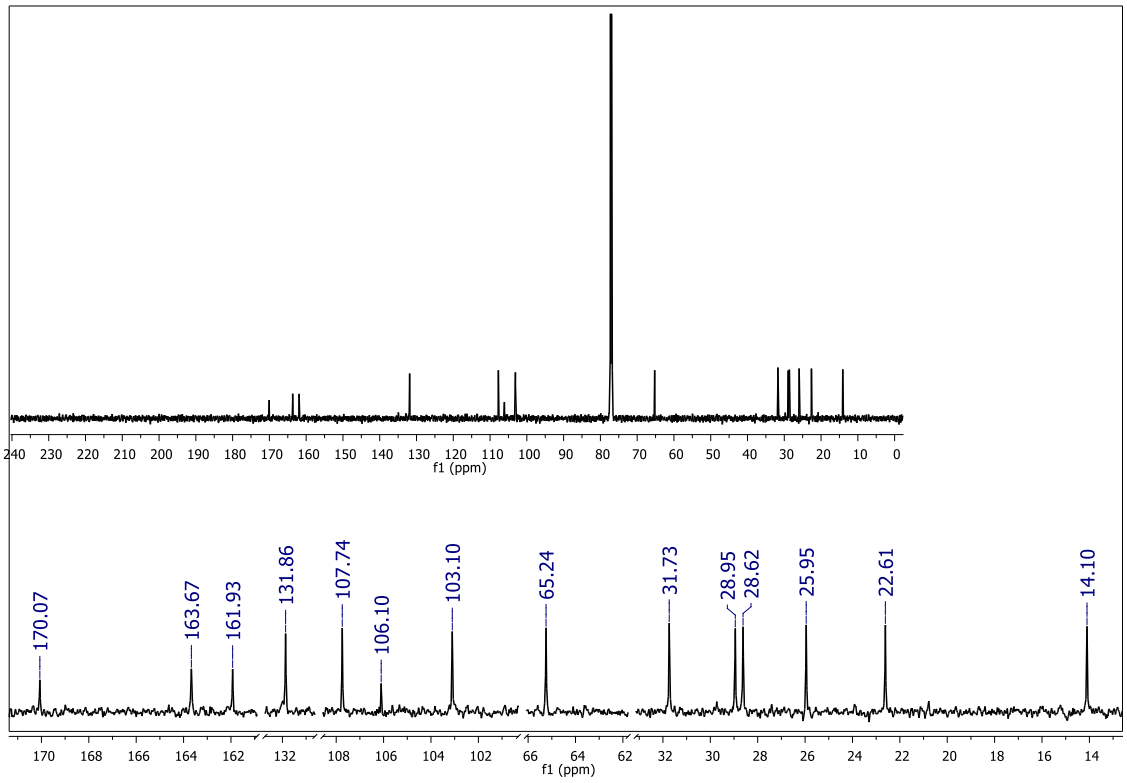

Figure S4. III) HPLC chromatogram of compound **4**

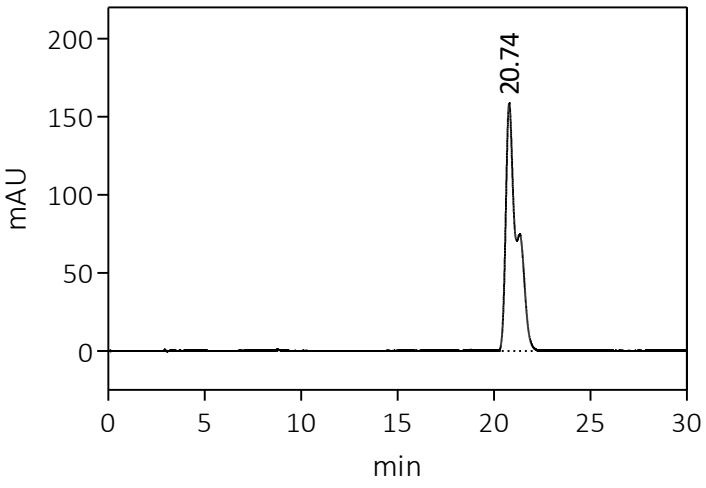

Figure S5. I) ^{1}H NMR spectrum of compound **5** (400 MHz – $CDCl_3$)

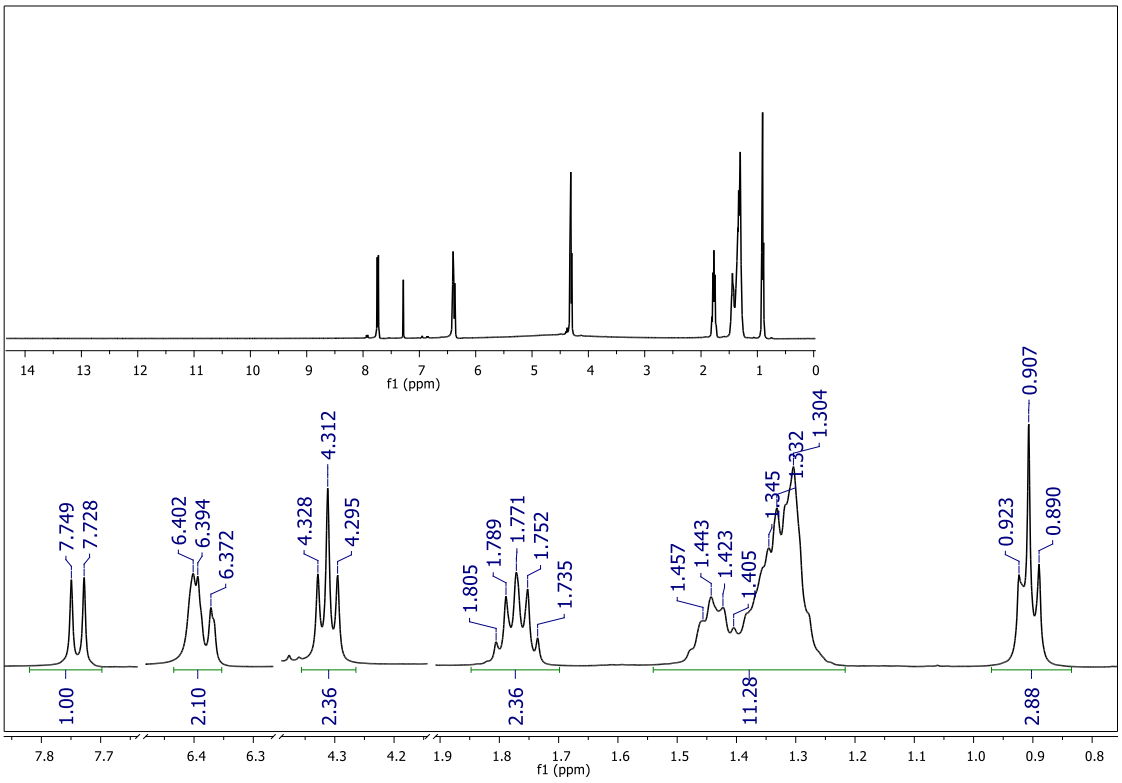

Figure S5. II) ^{13}C NMR spectrum of compound **5** (100 MHz – $CDCl_3$)

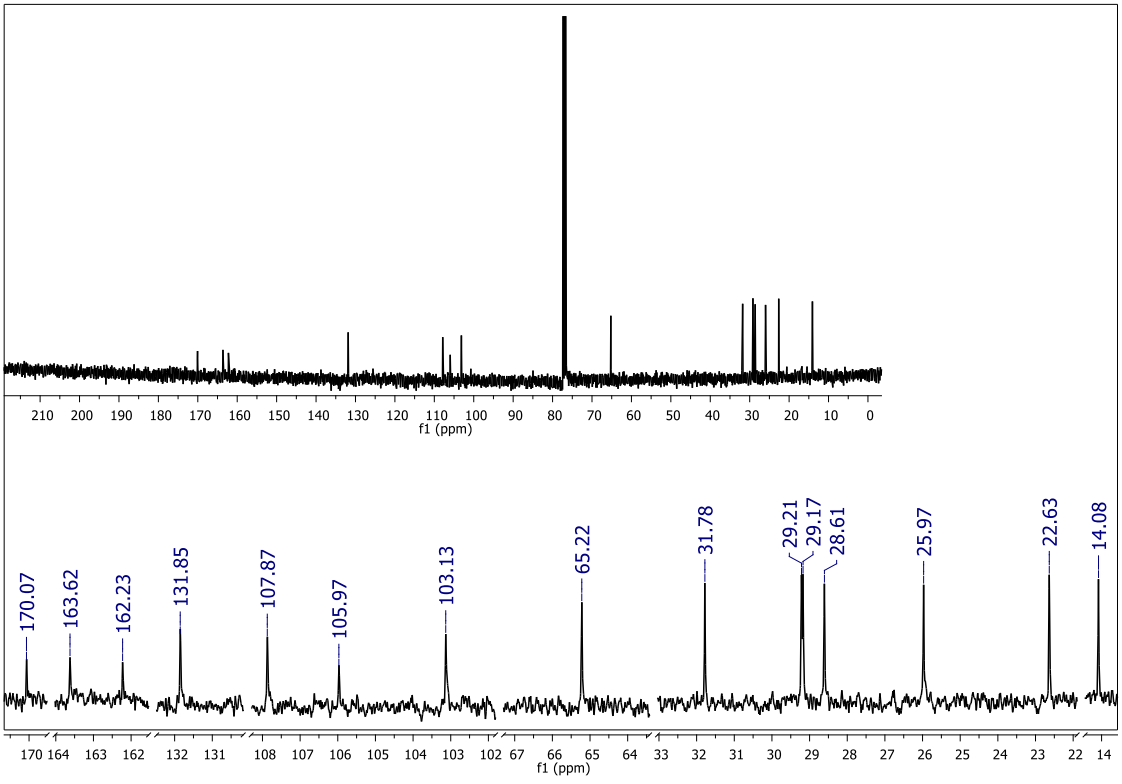

Figure S5. III) HPLC chromatogram of compound **5**

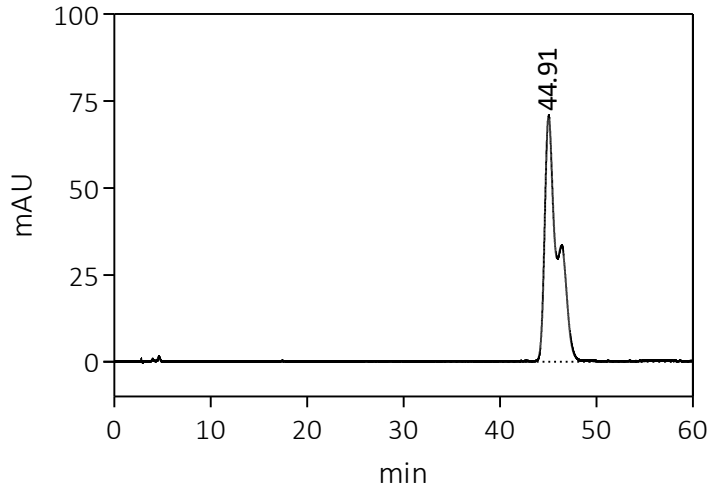

Figure S6. I) ^{1}H NMR spectrum of compound **6** (400 MHz – $CDCl_3$)

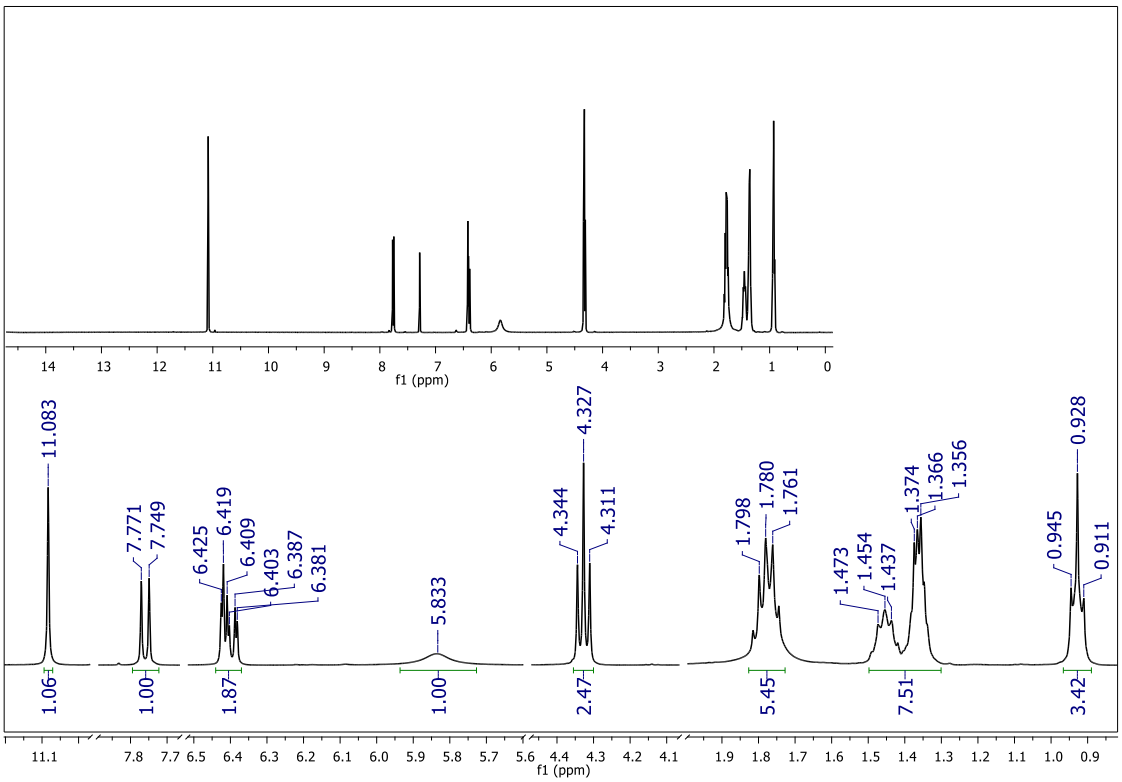

Figure S6. II) ^{13}C NMR spectrum of compound **6** (100 MHz – $CDCl_3$)

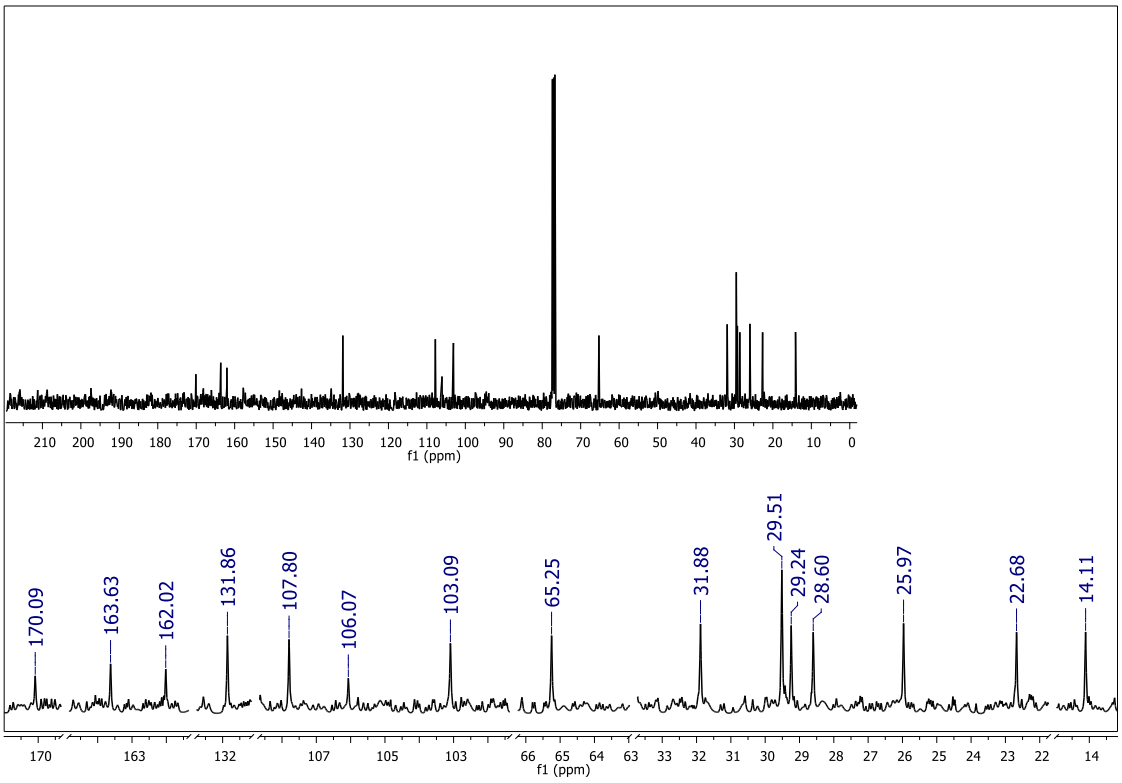

Figure S6. III) HPLC chromatogram of compound **6**

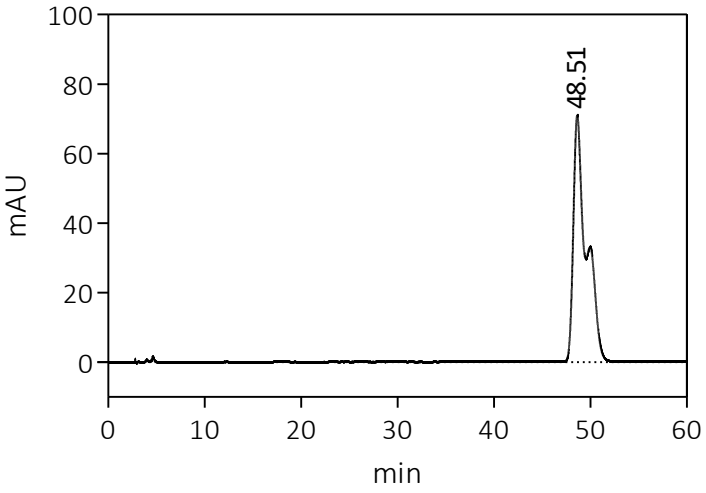

Figure S7. I) ^{1}H NMR spectrum of compound **7** (400 MHz – $CDCl_3$)

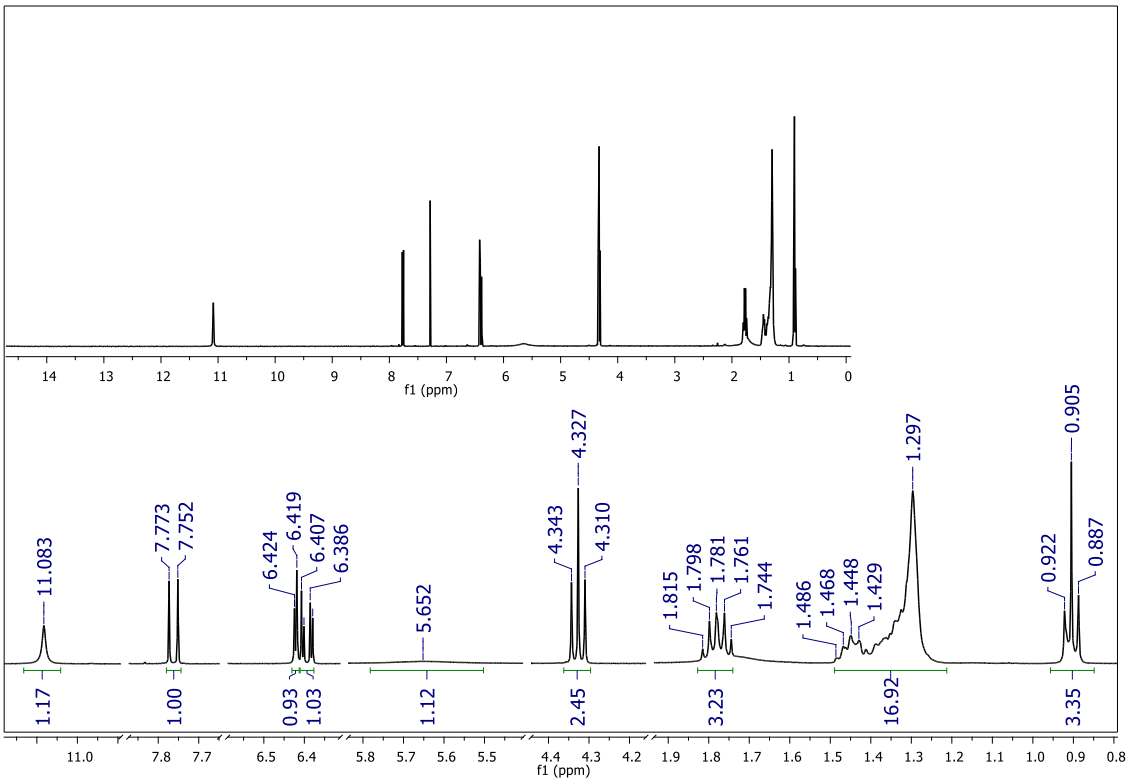

Figure S7. II) ^{13}C NMR spectrum of compound **7** (100 MHz – $CDCl_3$)

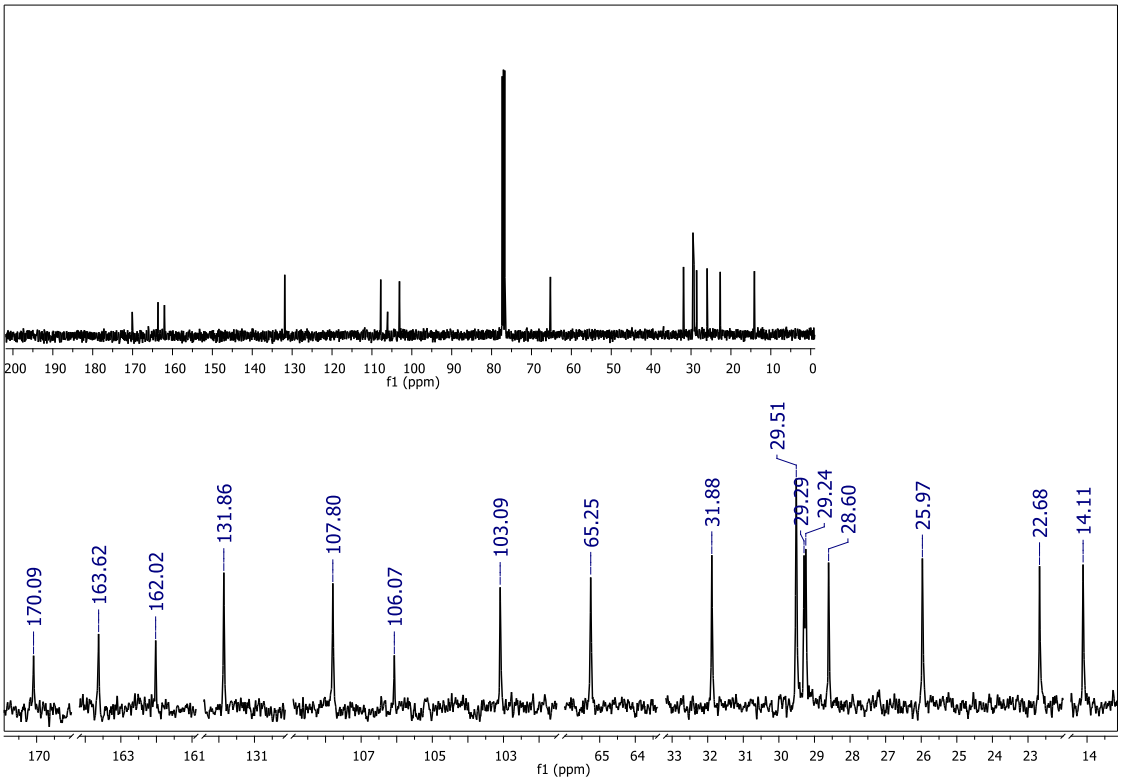

Figure S7. III) HPLC chromatogram of compound **7**

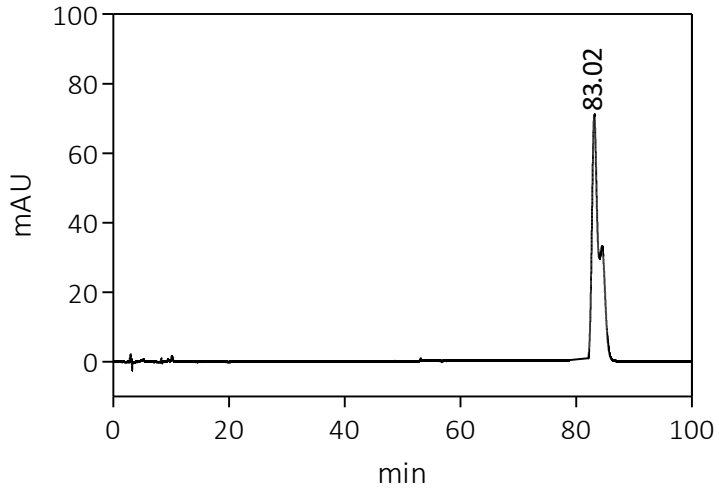

Figure S8. I) ^{1}H NMR spectrum of compound **8** (300 MHz – $CDCl_3$)

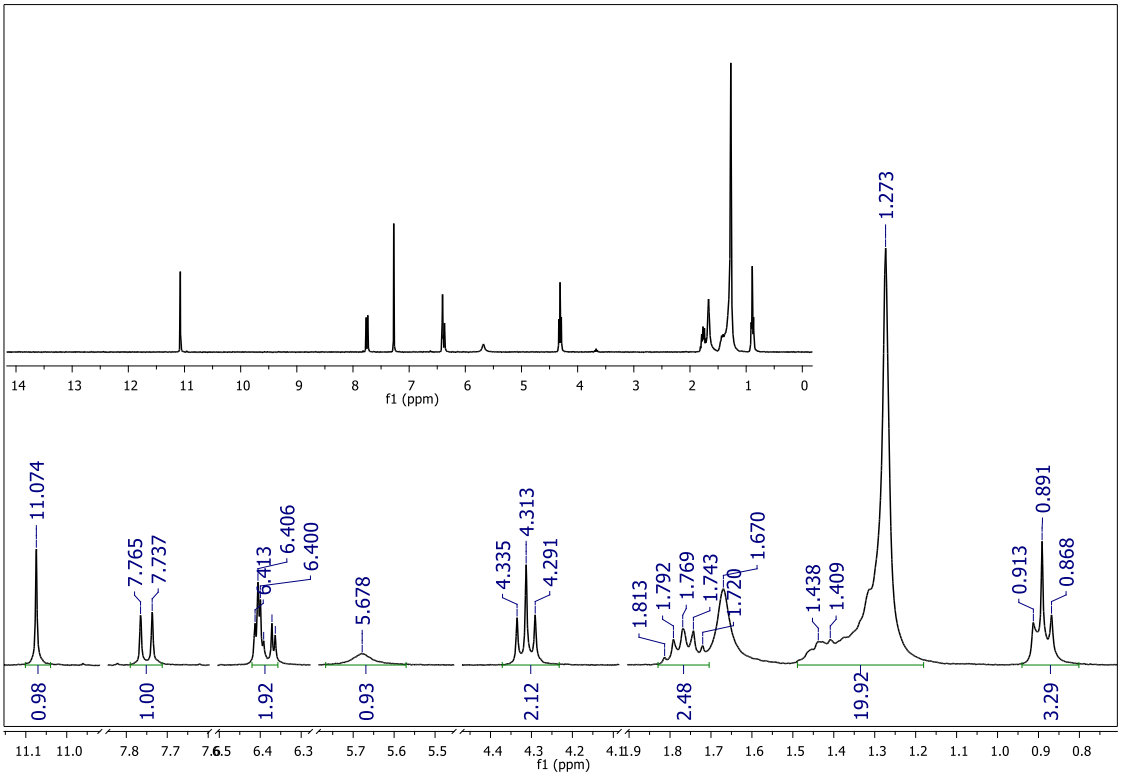

Figure S8. II) ^{13}C NMR spectrum of compound **8** (100 MHz – $CDCl_3$)

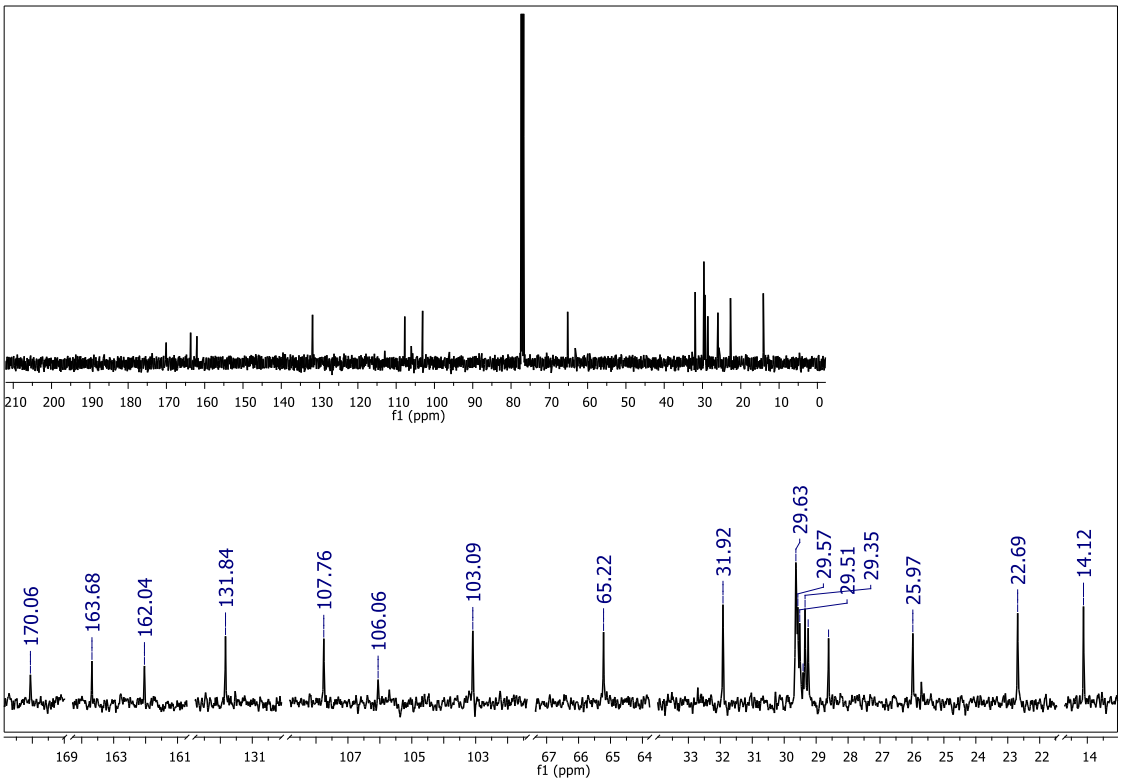

Figure S8. III) HPLC chromatogram of compound **8**

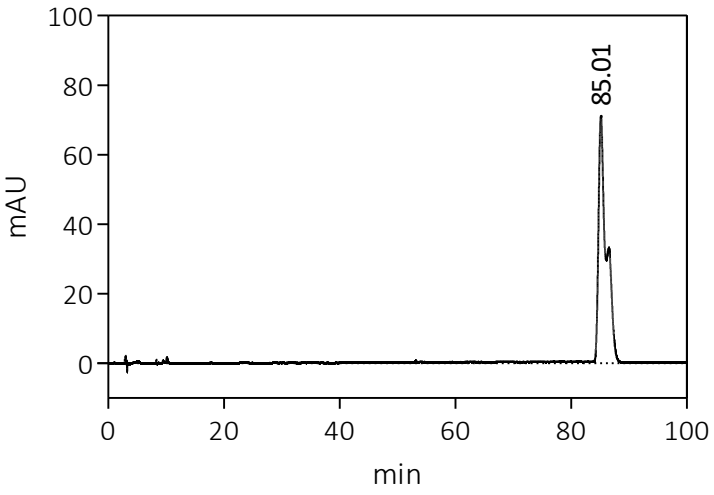

Figure S9. I) ^{1}H NMR spectrum of compound **9** (600 MHz – $CDCl_3$)

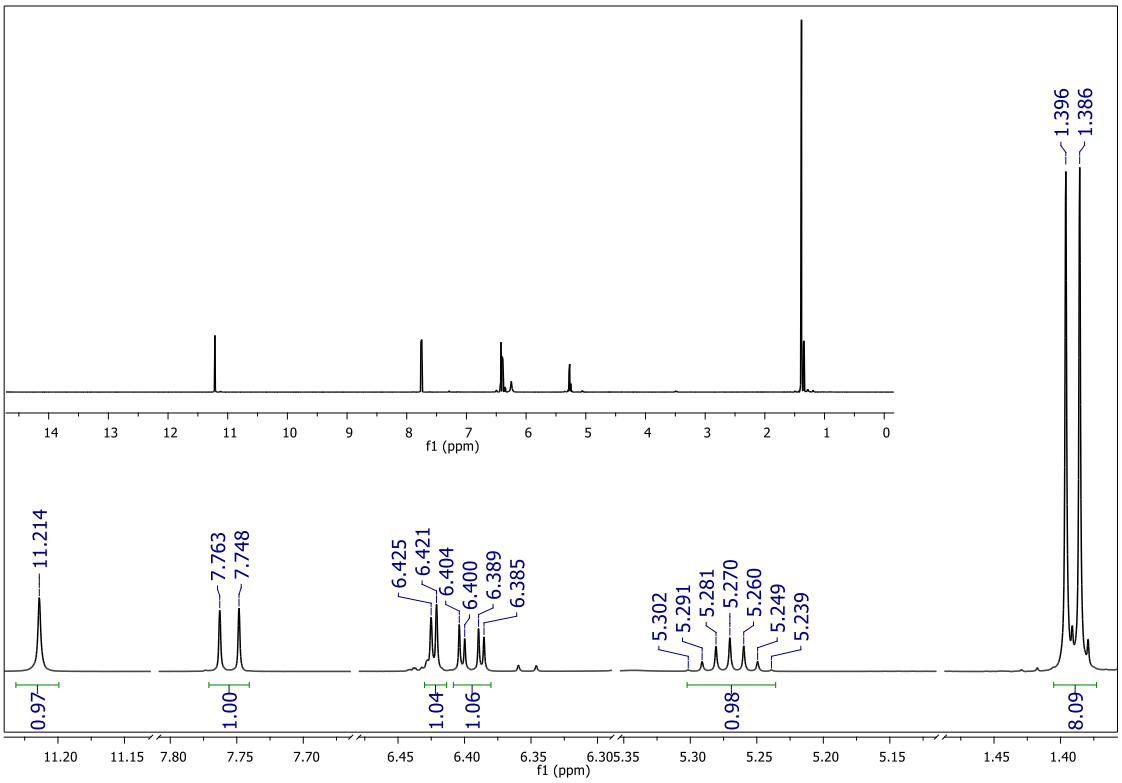

Figure S9. II) ^{13}C NMR spectrum of compound **9** (150 MHz – $CDCl_3$)

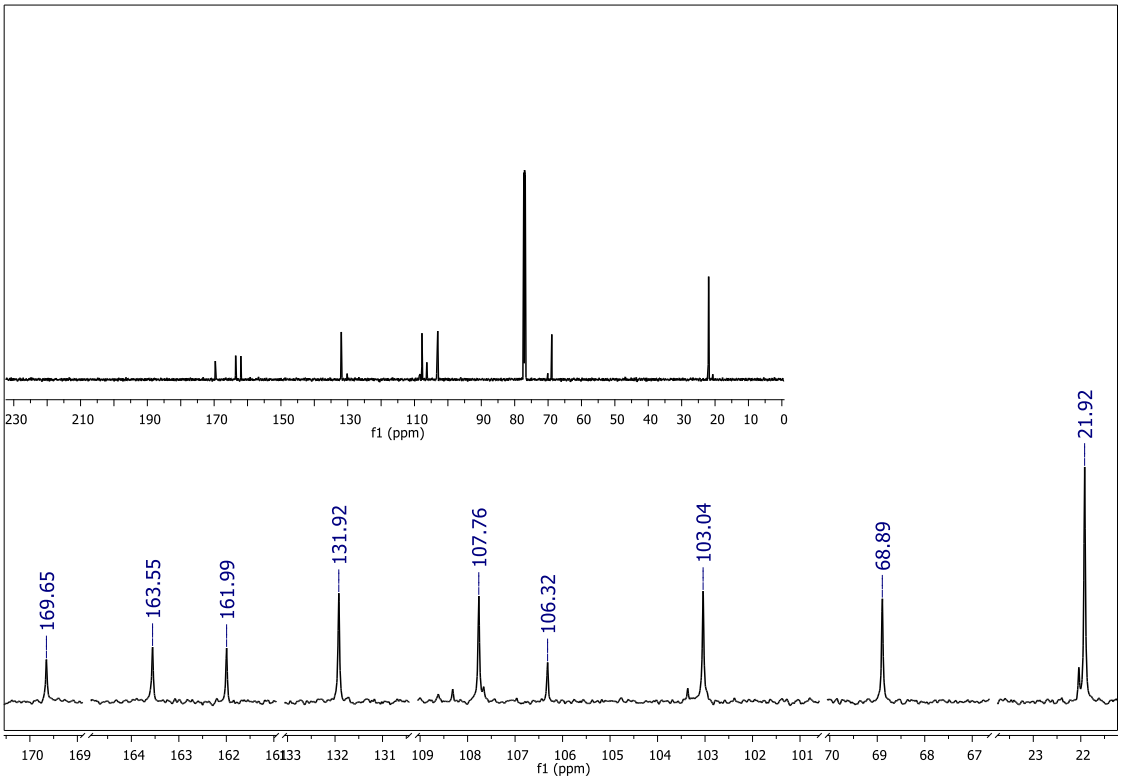

Figure S9. III) HPLC chromatogram of compound **9**

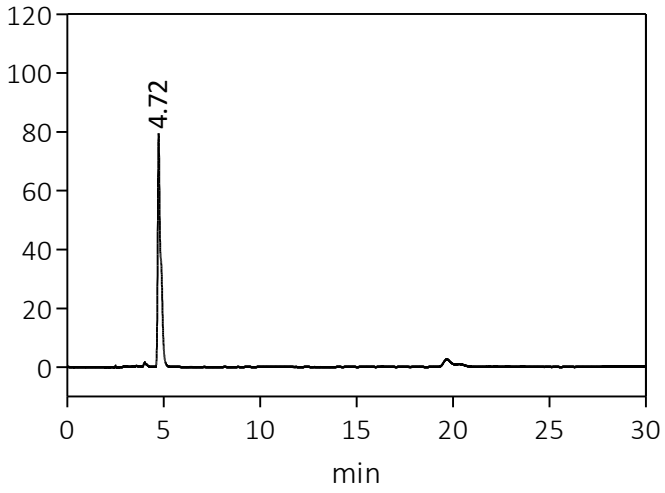

Figure S10. I) ^{1}H NMR spectrum of compound **10** (600 MHz – $CDCl_3$)

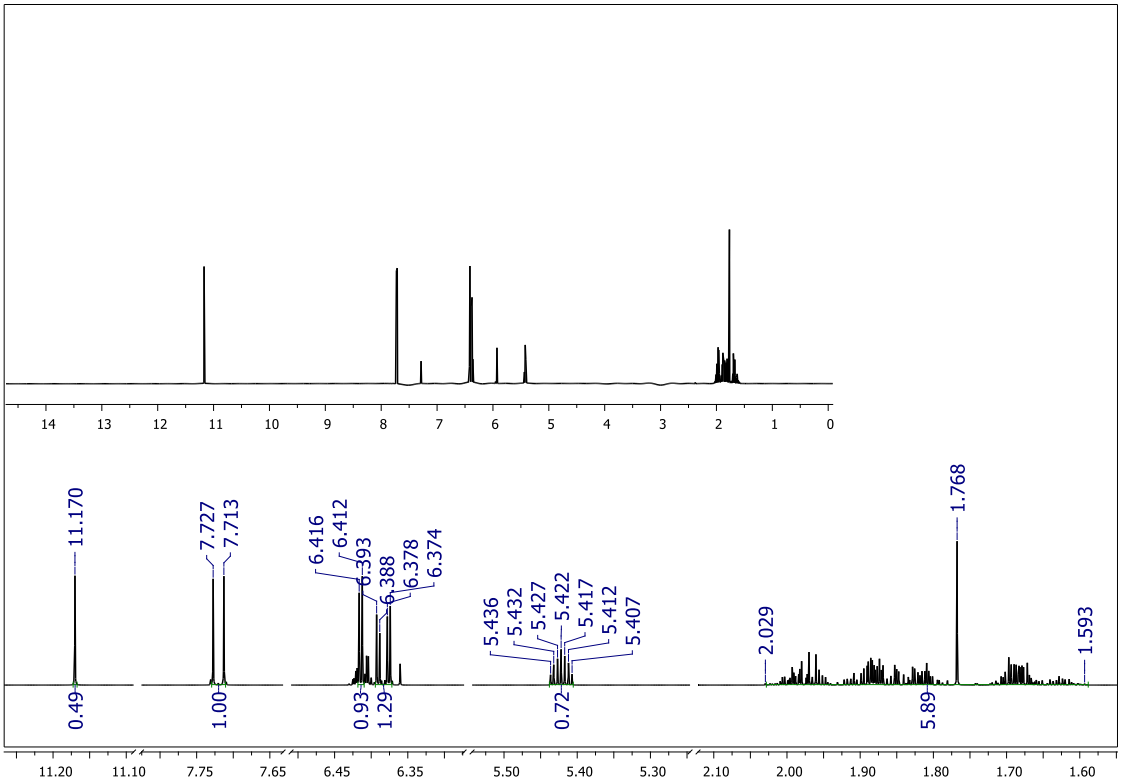

Figure S10. II) ^{13}C NMR spectrum of compound **10** (150 MHz – $CDCl_3$)

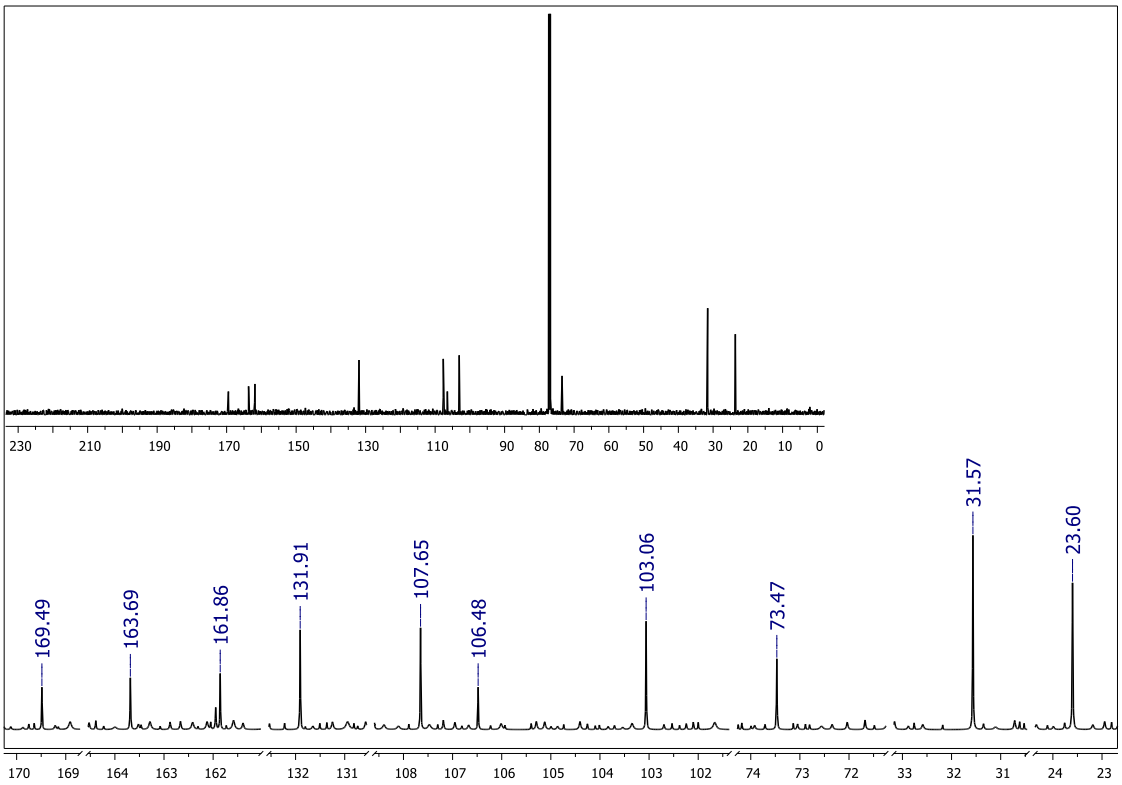

Figure S10. III) HPLC chromatogram of compound **10**

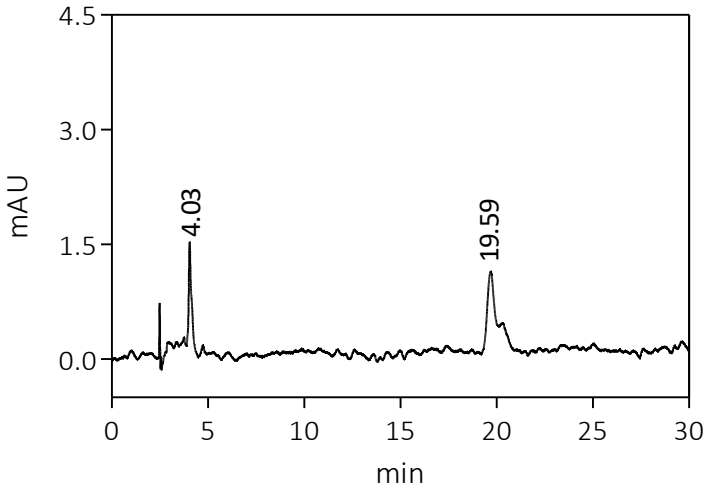

Figure S11. I) ^{1}H NMR spectrum of compound **11** (600 MHz – $CDCl_3$)

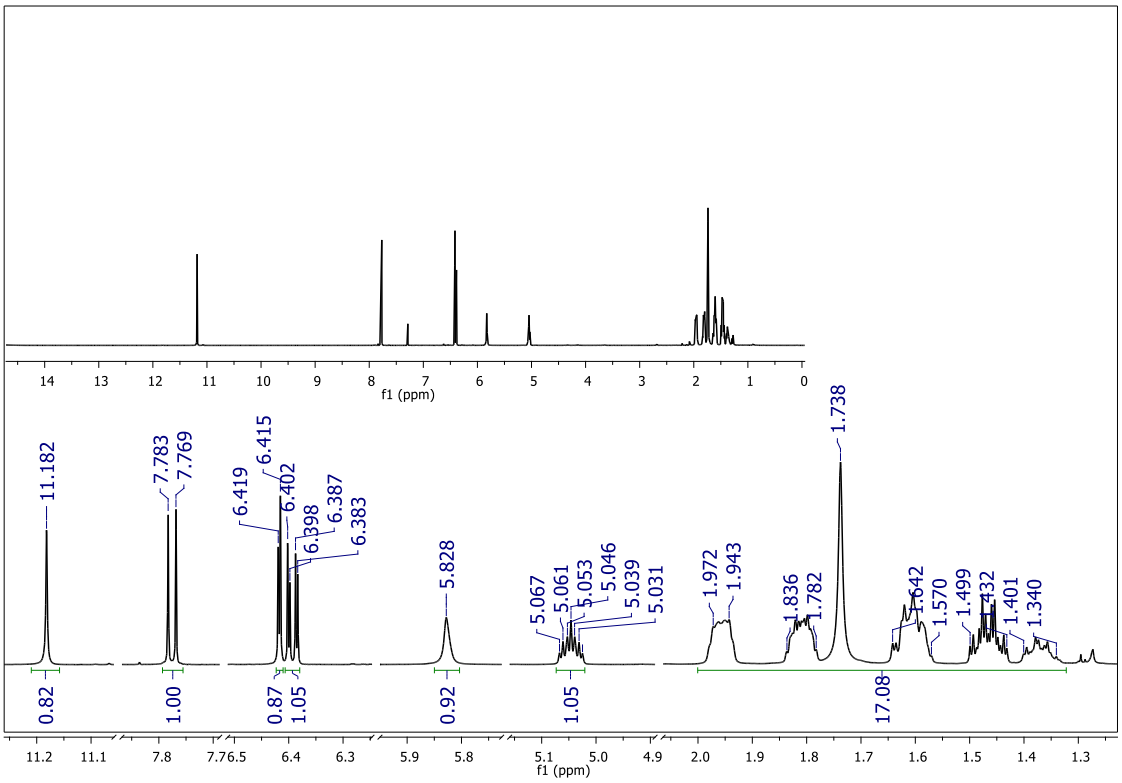

Figure S11. II) ^{13}C NMR spectrum of compound **11** (150 MHz – $CDCl_3$)

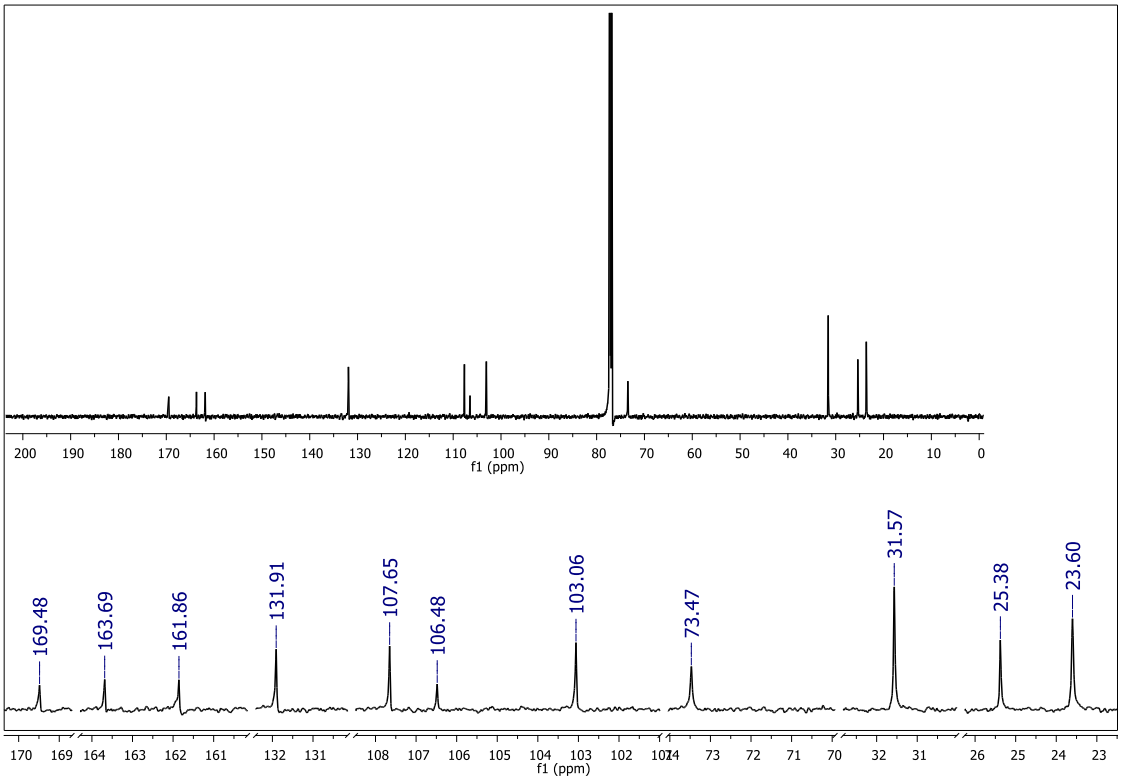

Figure S11. III) HPLC chromatogram of compound **11**

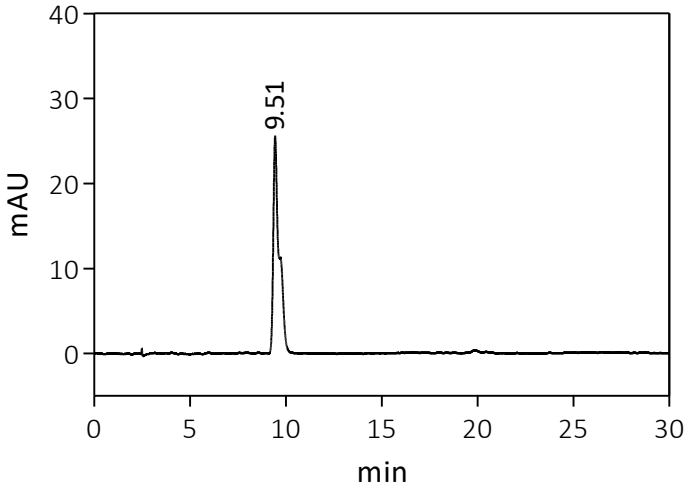

Figure S13. I) ^{1}H NMR spectrum of compound **13** (400 MHz – $CDCl_3$)

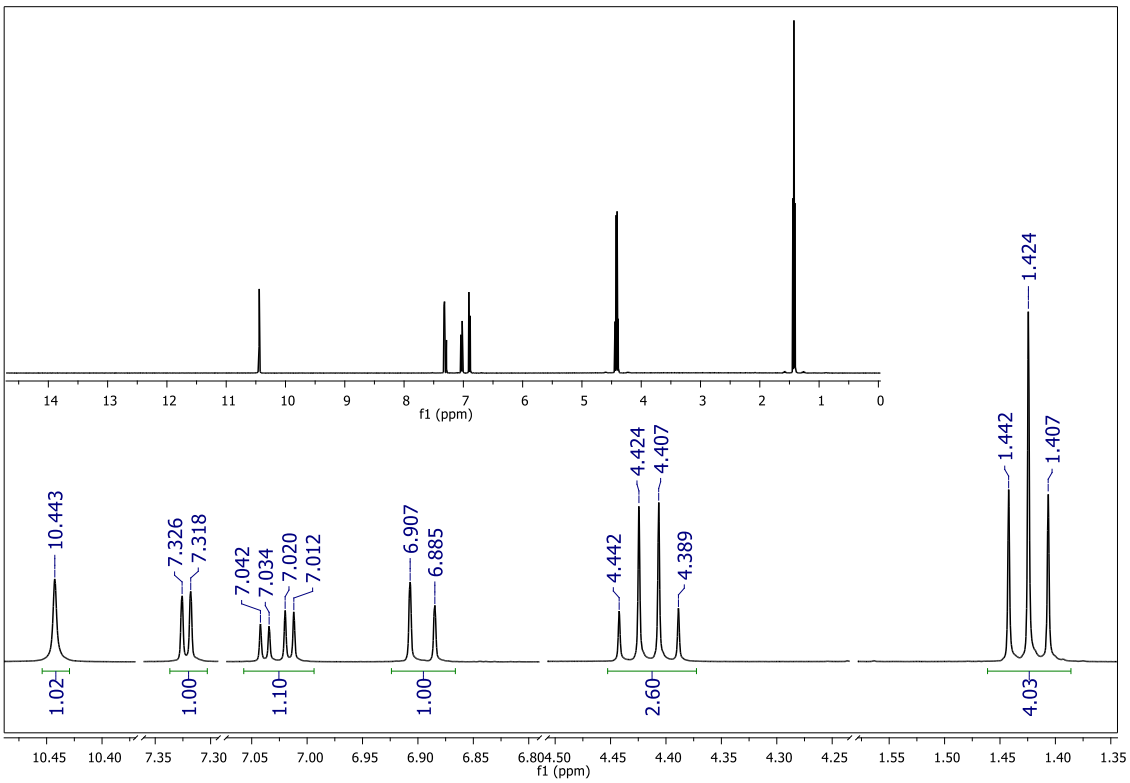

Figure S13. II) ^{13}C NMR spectrum of compound **13** (100 MHz – $CDCl_3$)

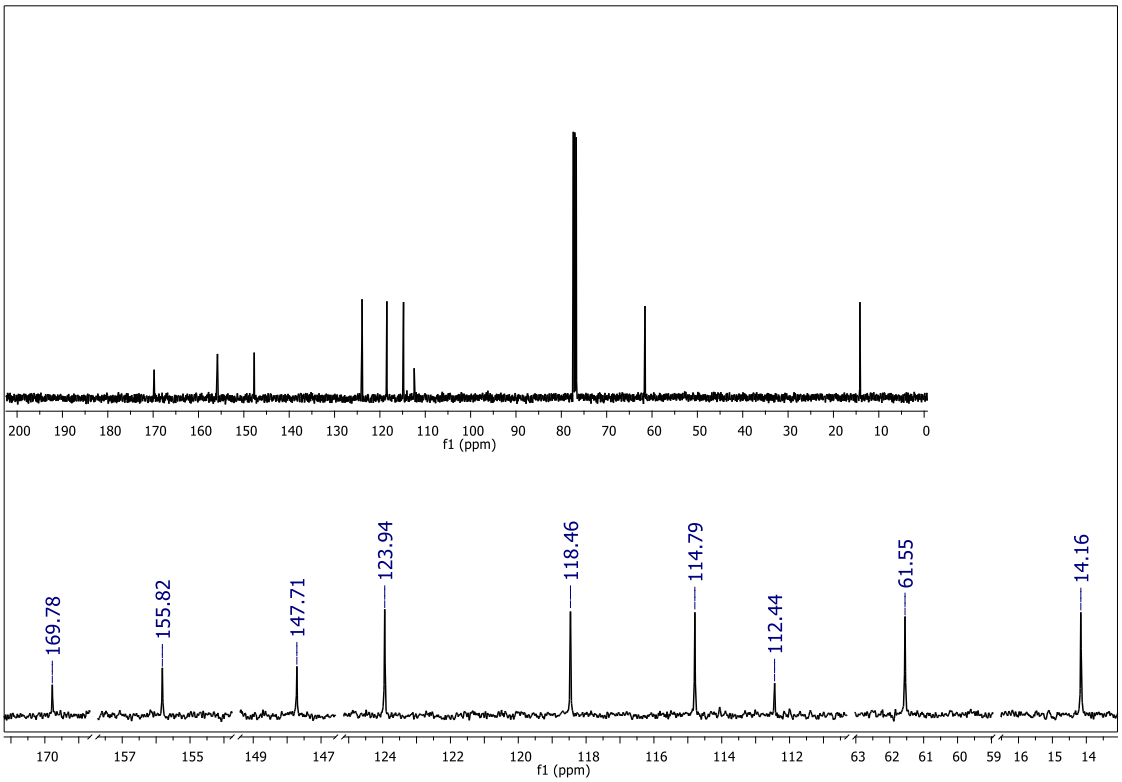

Figure S13. III) HPLC chromatogram of compound **13**

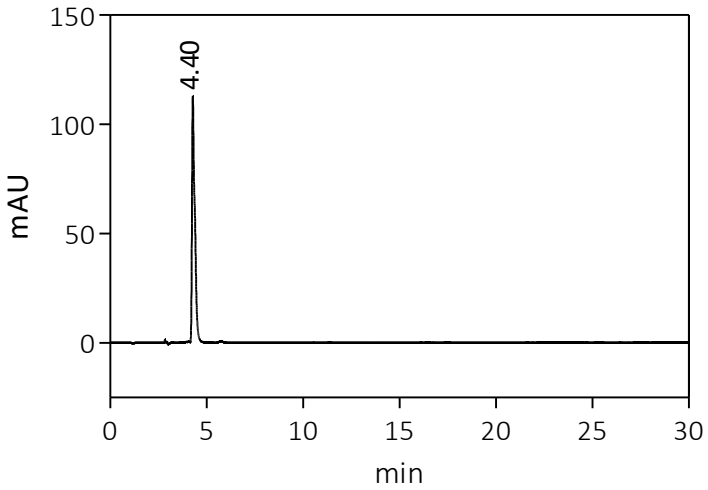

Figure S14. I) ^{1}H NMR spectrum of compound **14** (400 MHz – $CDCl_3$)

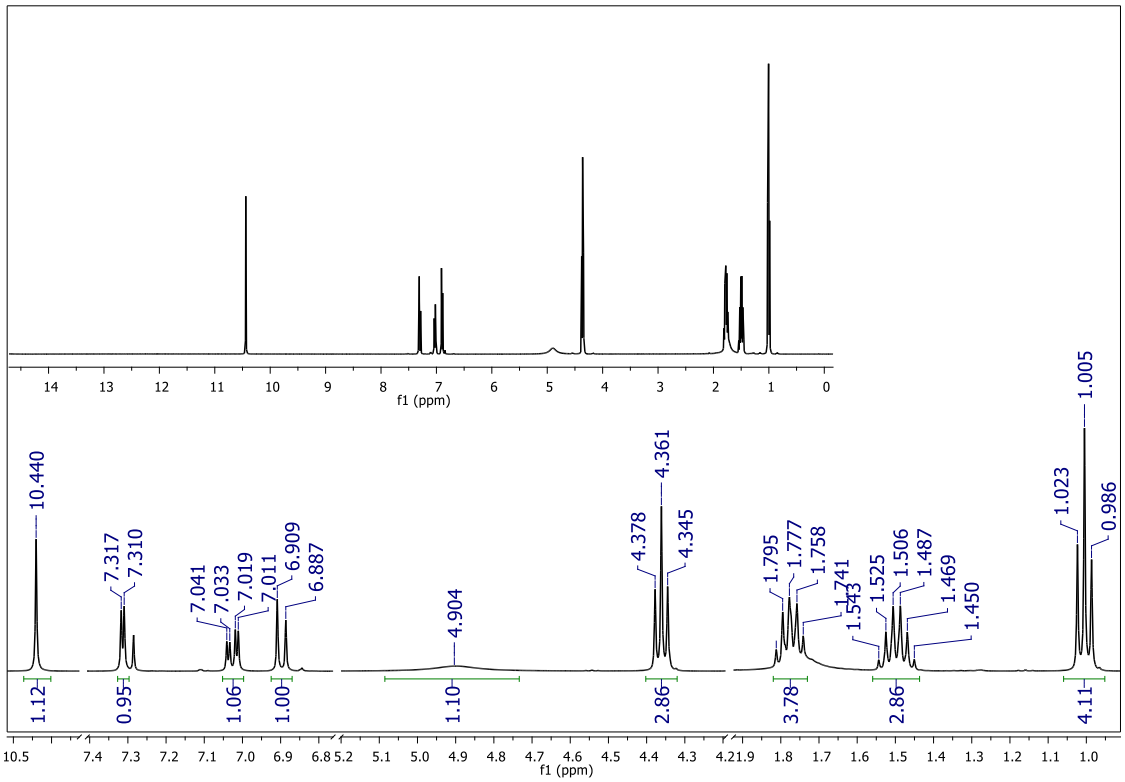

Figure S14. II) ^{13}C NMR spectrum of compound **14** (100 MHz – $CDCl_3$)

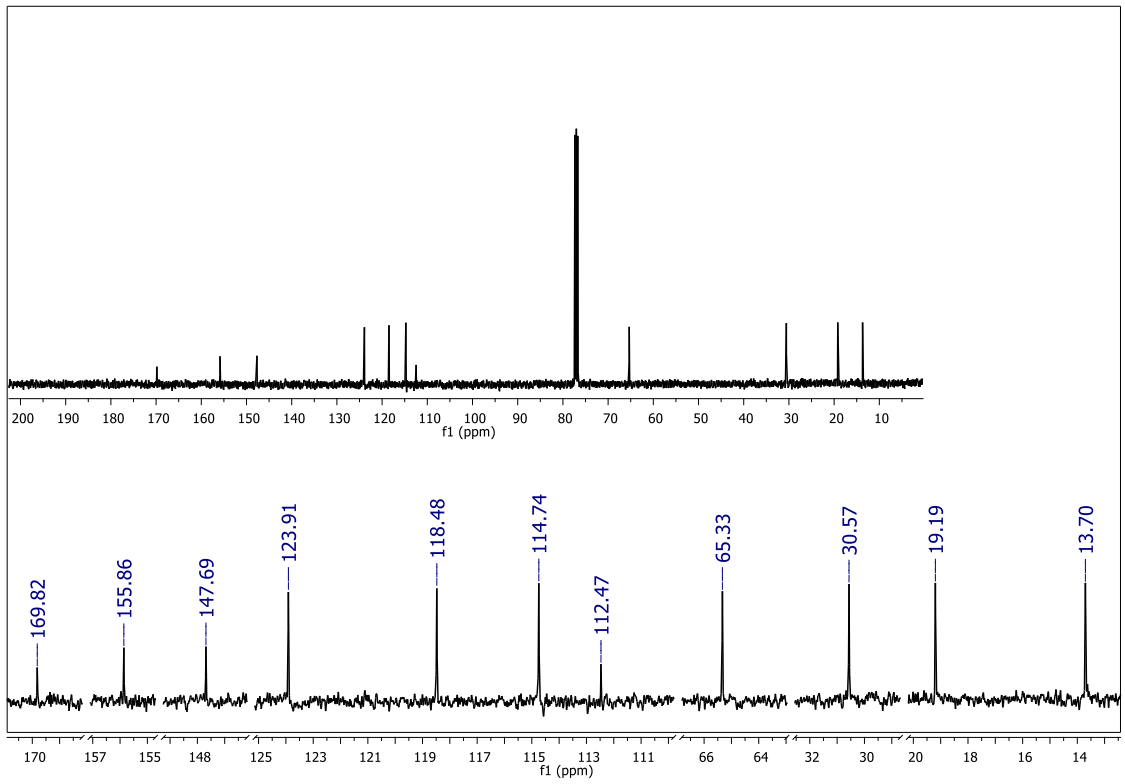

Figure S14. IIII) HPLC chromatogram of compound **14**

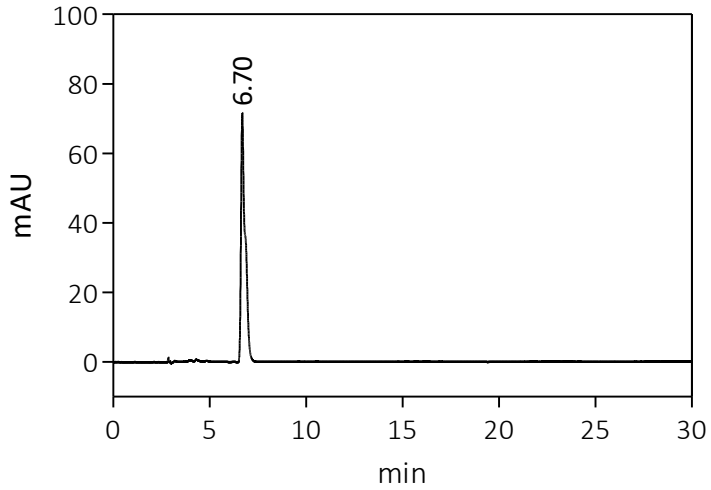

Figure S15. I) ^{1}H NMR spectrum of compound **15** (400 MHz – $CDCl_3$)

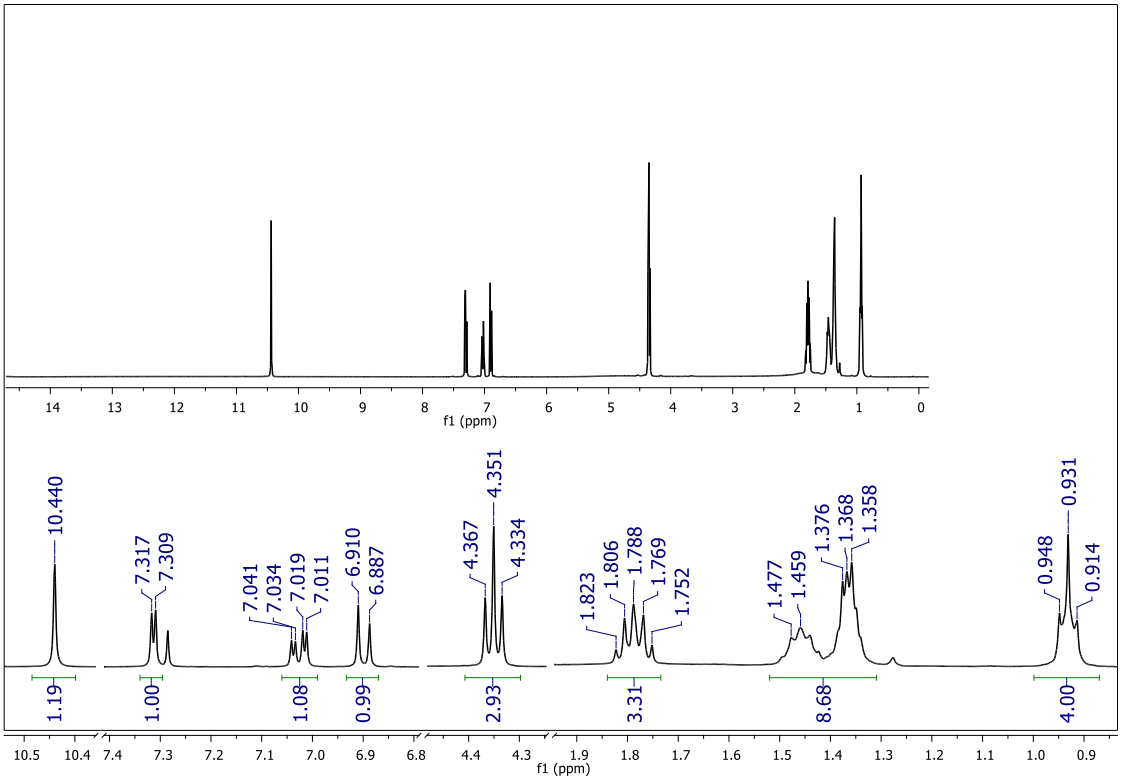

Figure S15. II) ^{13}C NMR spectrum of compound **15** (100 MHz – $CDCl_3$)

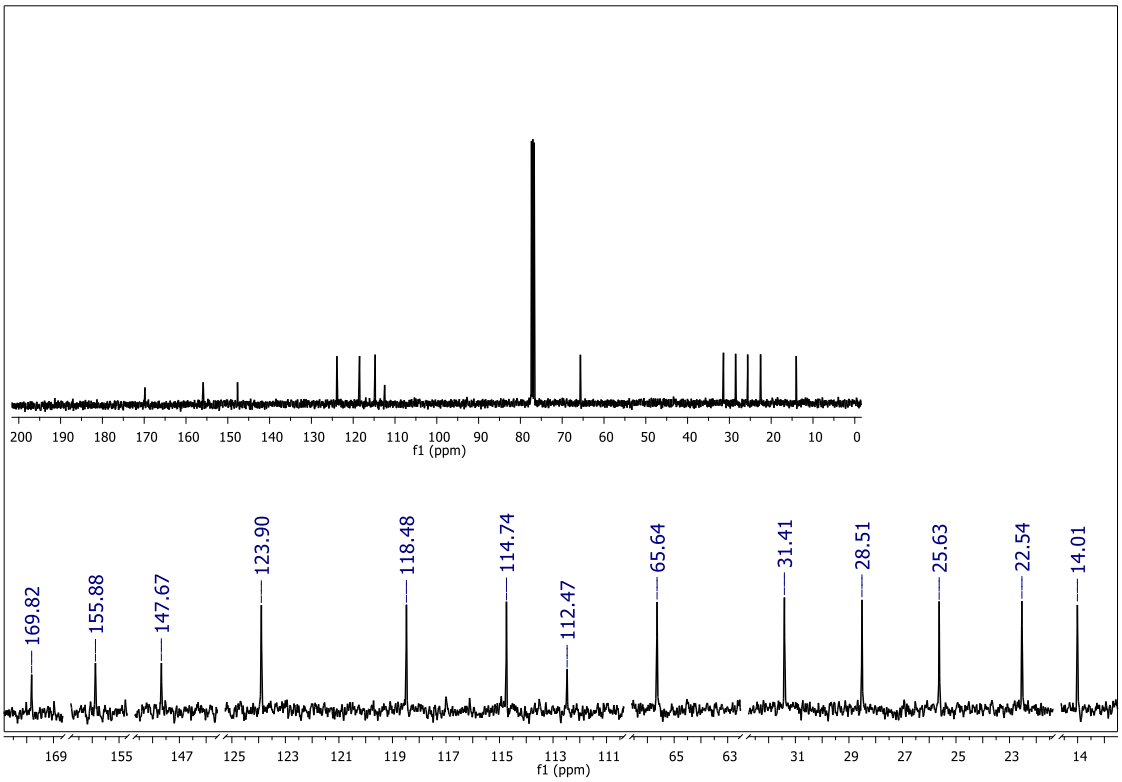

Figure S15. III) HPLC chromatogram of compound **15**

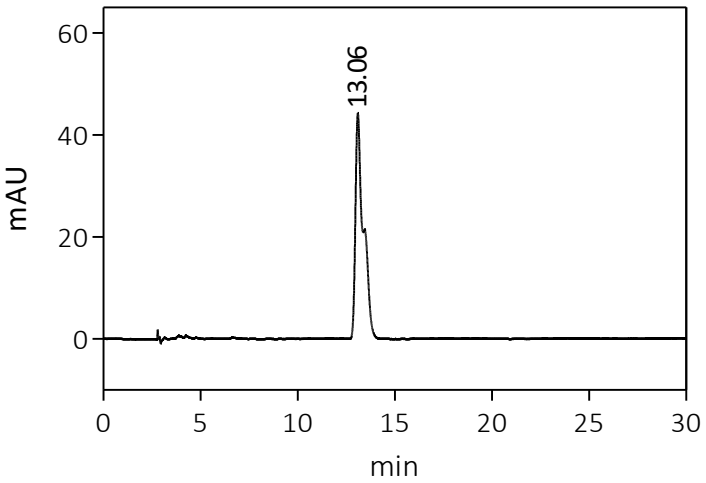

Figure S16. I) ^{1}H NMR spectrum of compound **16** (600 MHz – $CDCl_3$)

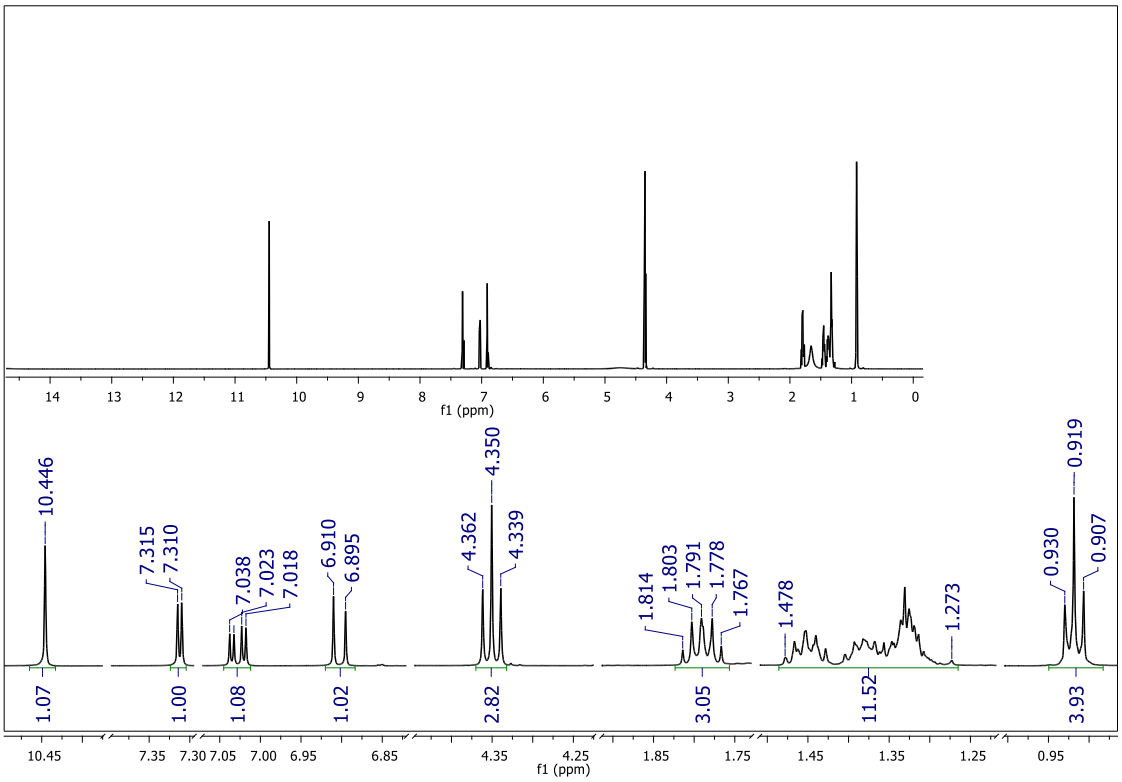

Figure S16. II) ^{13}C NMR spectrum of compound **16** (150 MHz – $CDCl_3$)

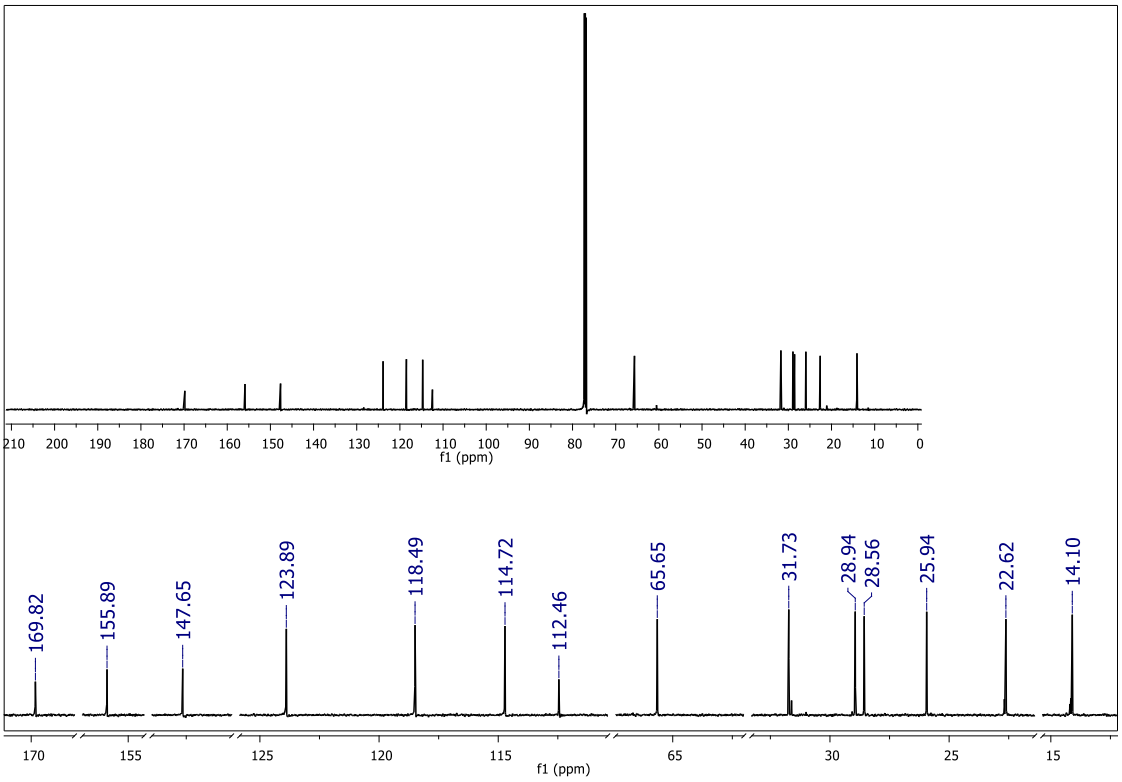

Figure S16. III) HPLC chromatogram of compound **16**

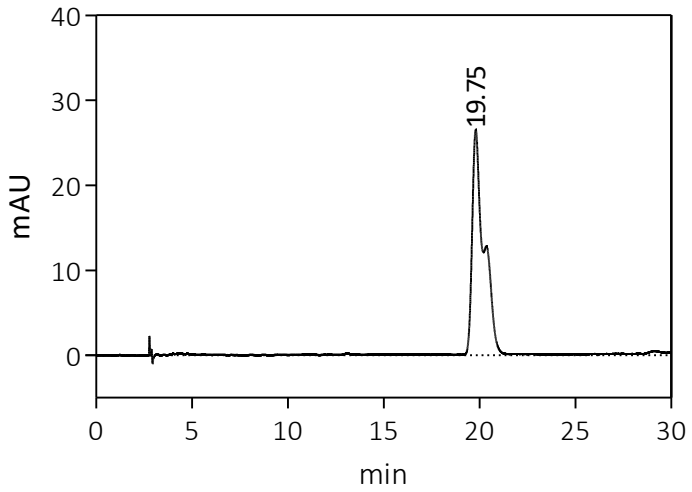

Figure S17. I) ^{1}H NMR spectrum of compound **17**(400 MHz – $CDCl_3$)

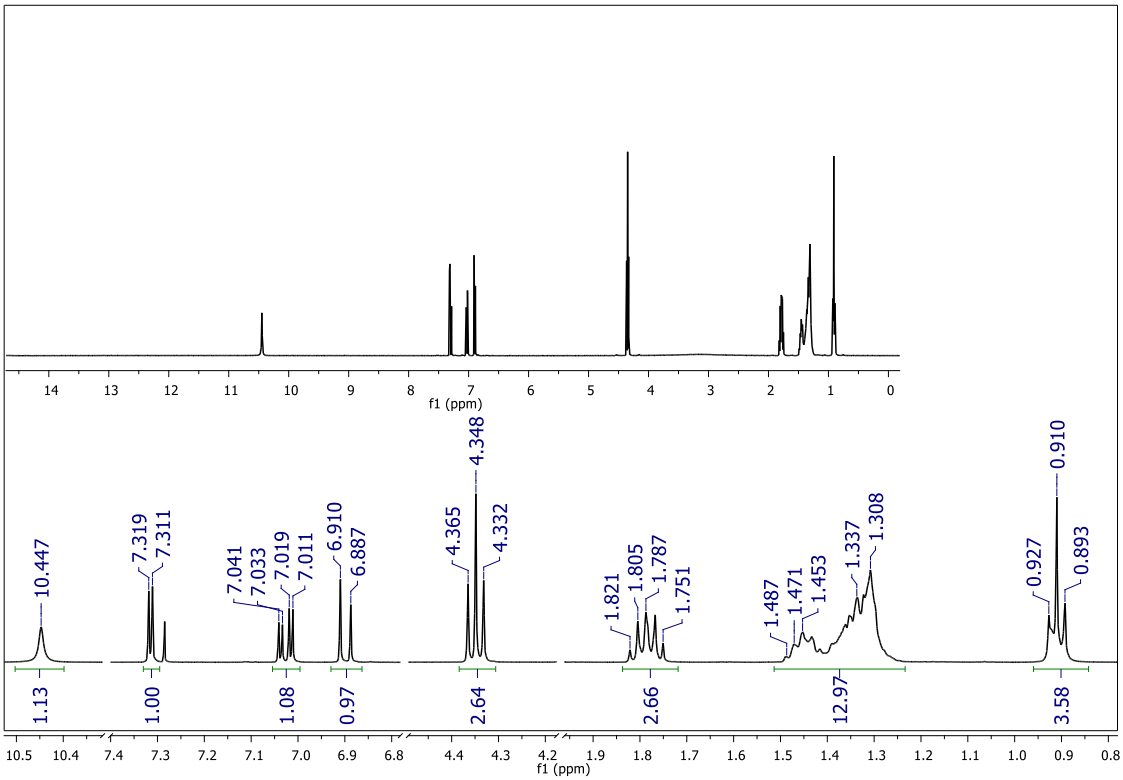

Figure S17. II) ^{13}C NMR spectrum of compound **17** (100 MHz – $CDCl_3$)

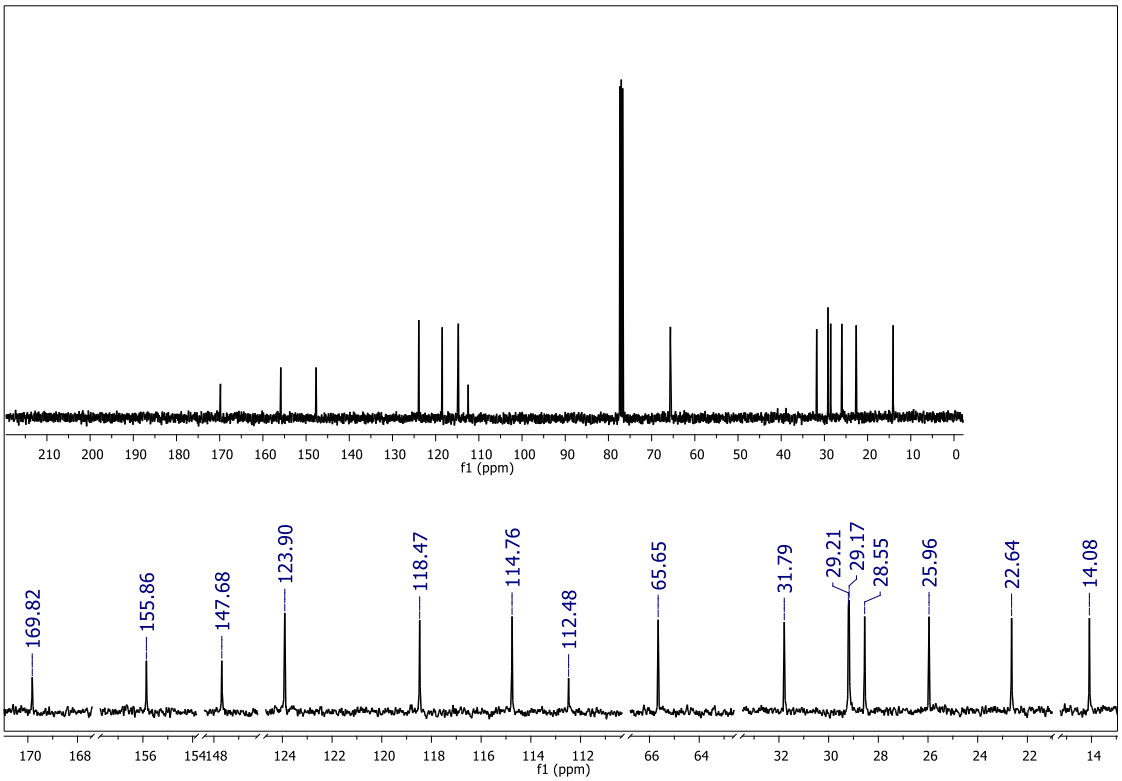

Figure S17. III) HPLC chromatogram of compound **17**

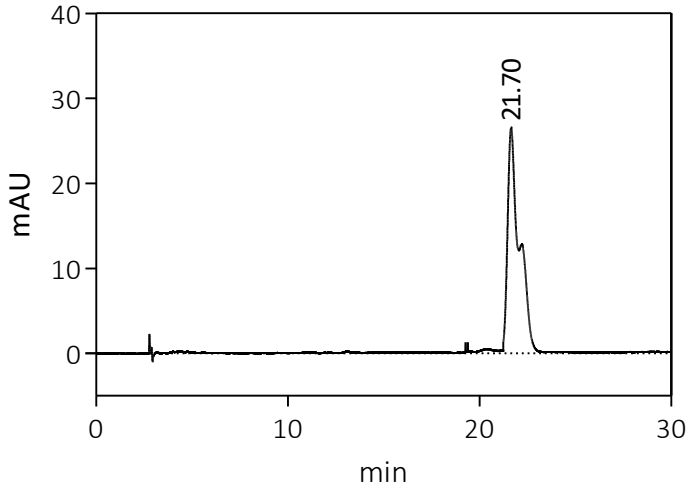

Figure S18. I) ^{1}H NMR spectrum of compound **18** (600 MHz – $CDCl_3$)

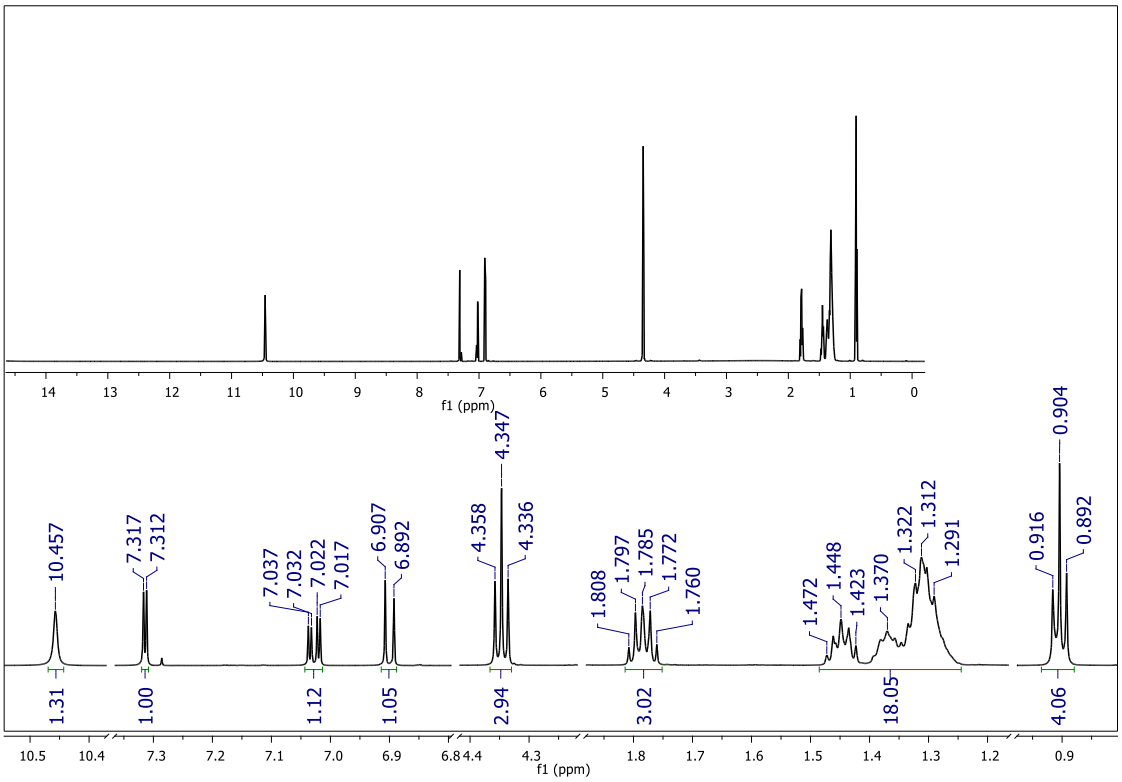

Figure S18. II) ^{13}C NMR spectrum of compound **18** (100 MHz – $CDCl_3$)

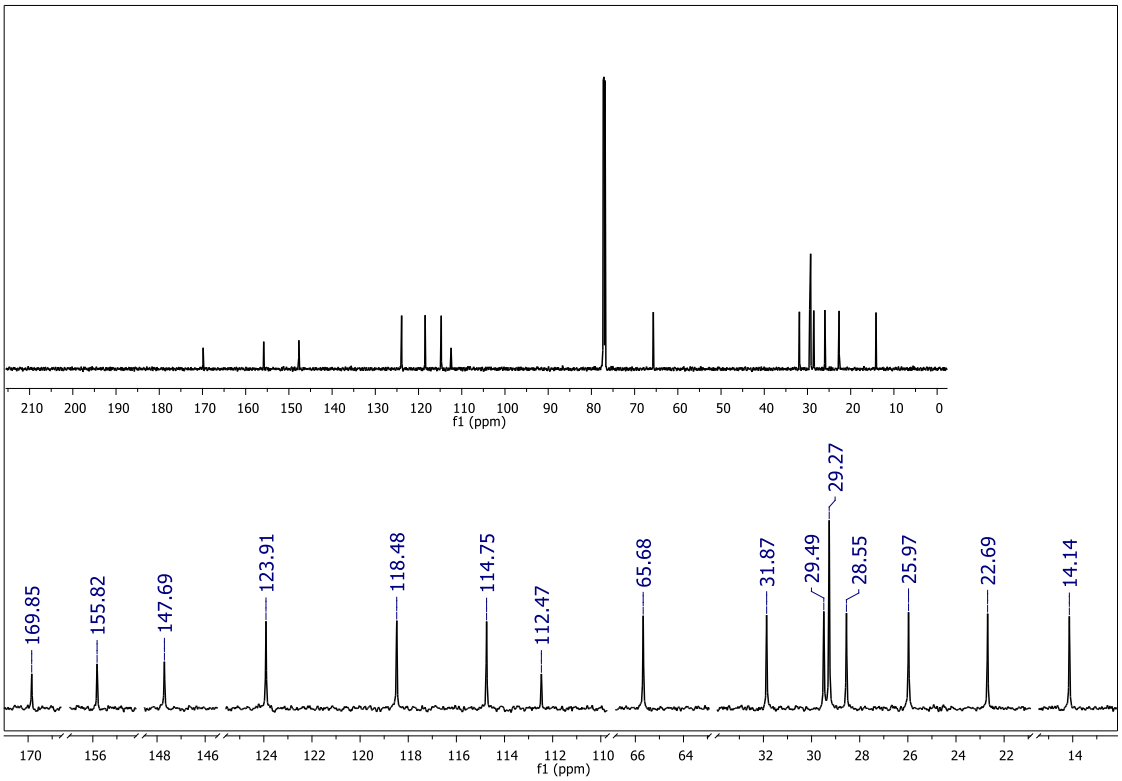

Figure S18. III) HPLC chromatogram of compound **18**

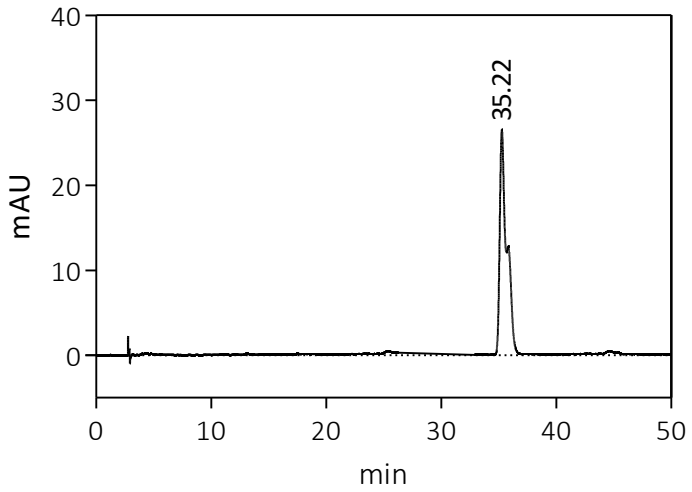

Figure S19. I) ^{1}H NMR spectrum of compound **19** (400 MHz – $CDCl_3$)

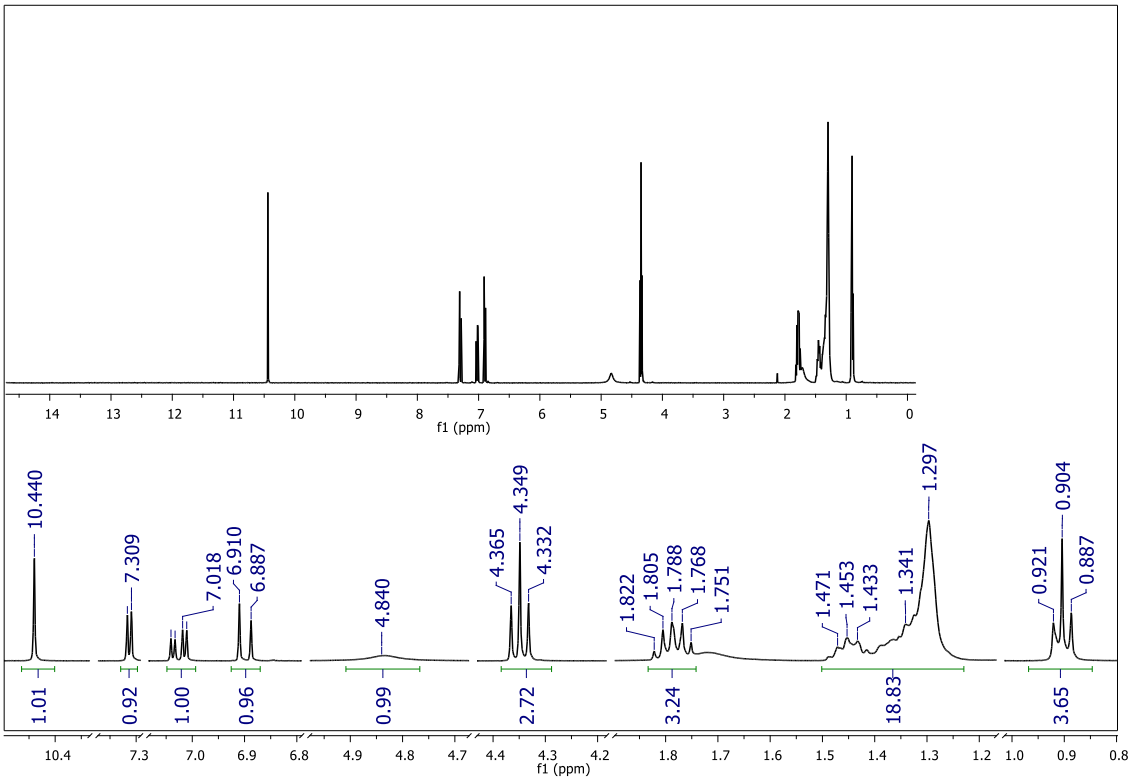

Figure S19. II) ^{13}C NMR spectrum of compound **19** (100 MHz – $CDCl_3$)

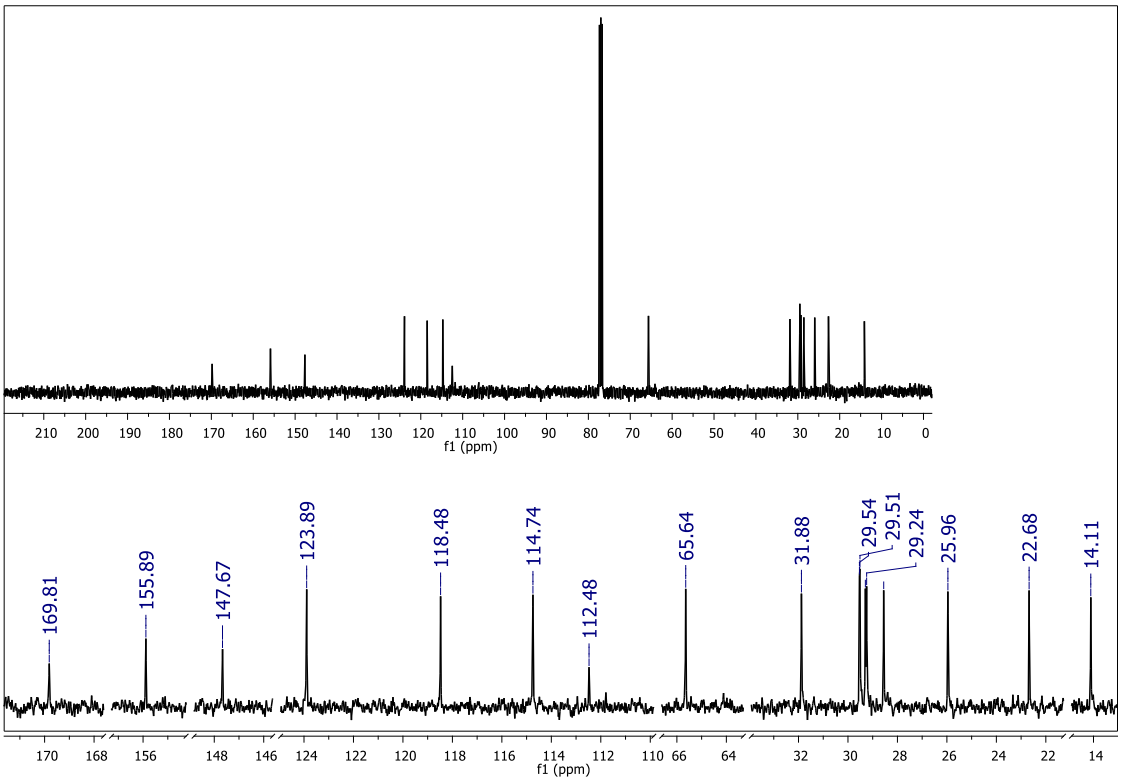

Figure S19. III) HPLC chromatogram of compound **19**

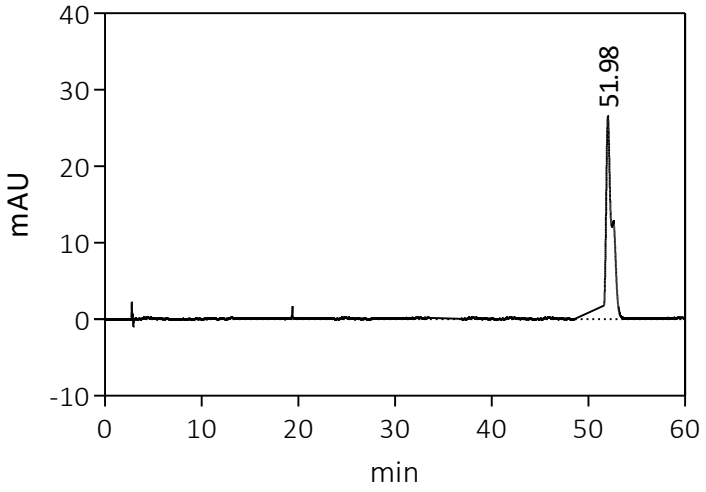

Figure S20. I) ^{1}H NMR spectrum of compound **20** (300 MHz – $CDCl_3$)

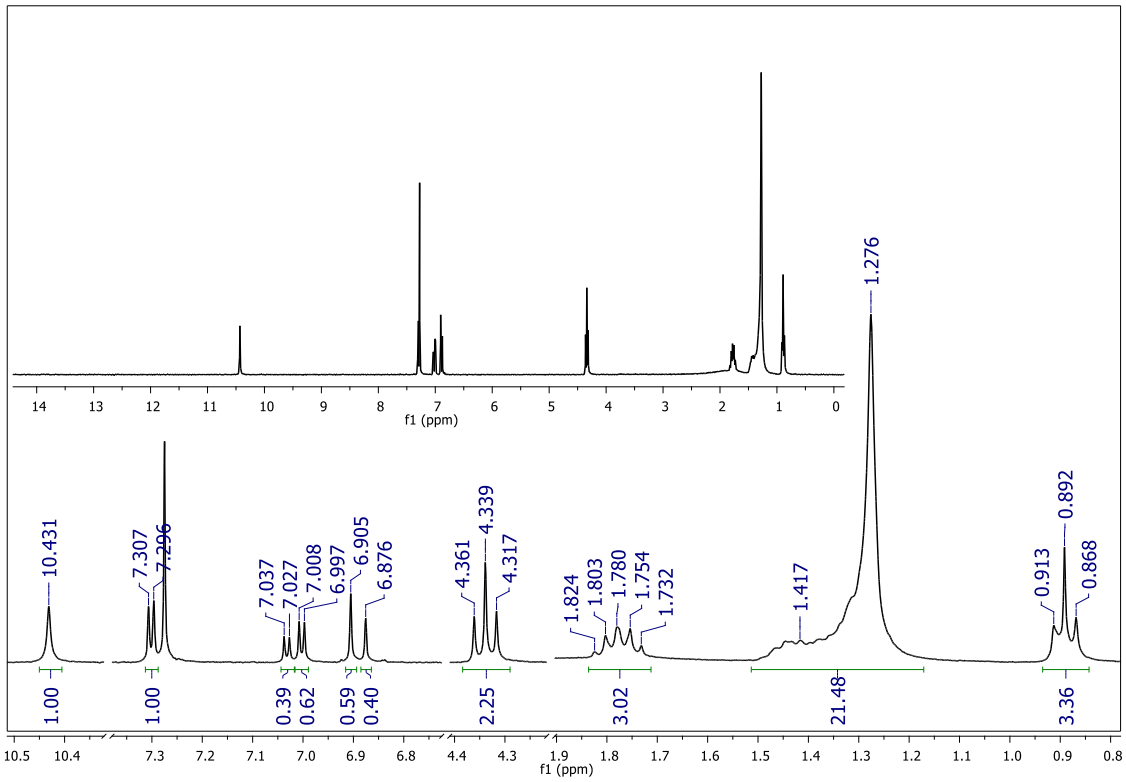

Figure S20. II) ^{13}C NMR spectrum of compound **20** (100 MHz – $CDCl_3$)

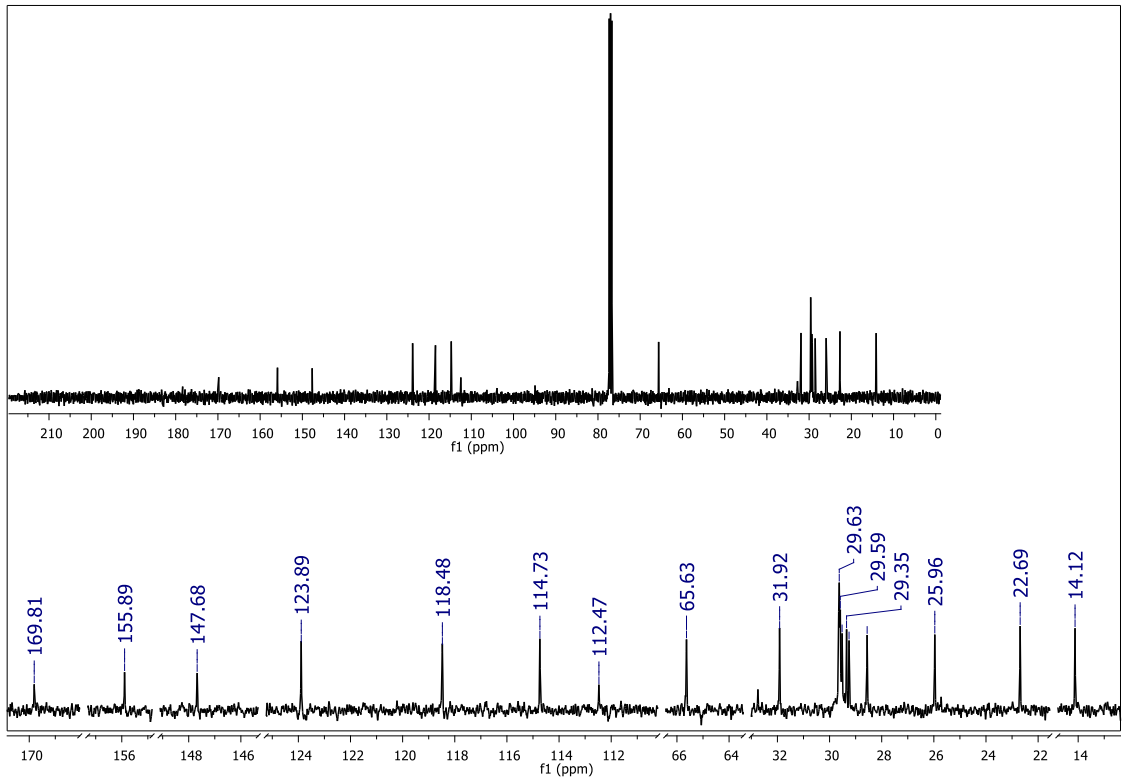

Figure S20. III) HPLC chromatogram of compound **20**

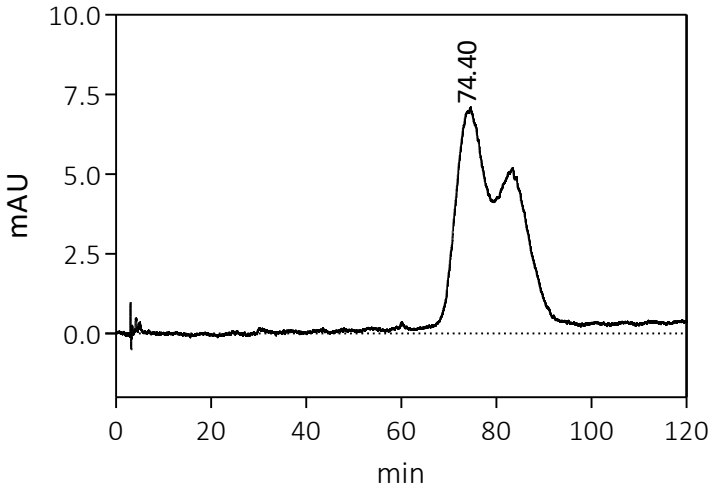

Figure S21. I) ^{1}H NMR spectrum of compound **21** (400 MHz – $CDCl_3$)

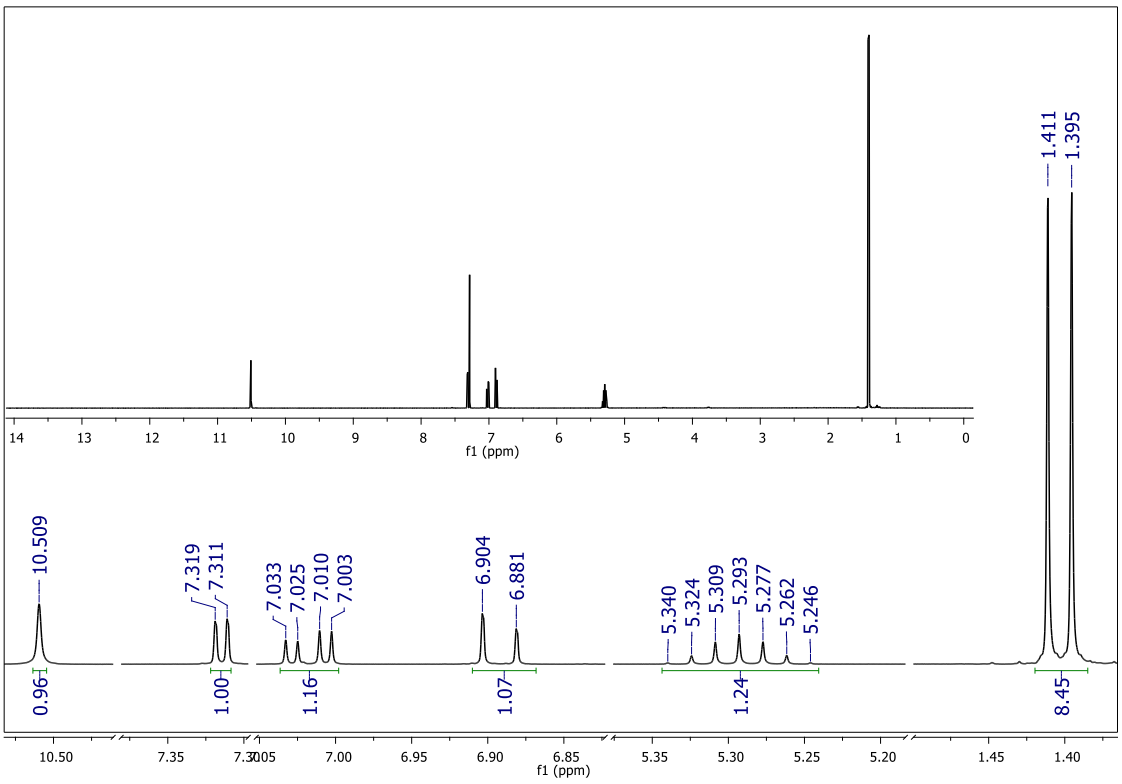

Figure S21. II) ^{13}C NMR spectrum of compound **21** (150 MHz – $CDCl_3$)

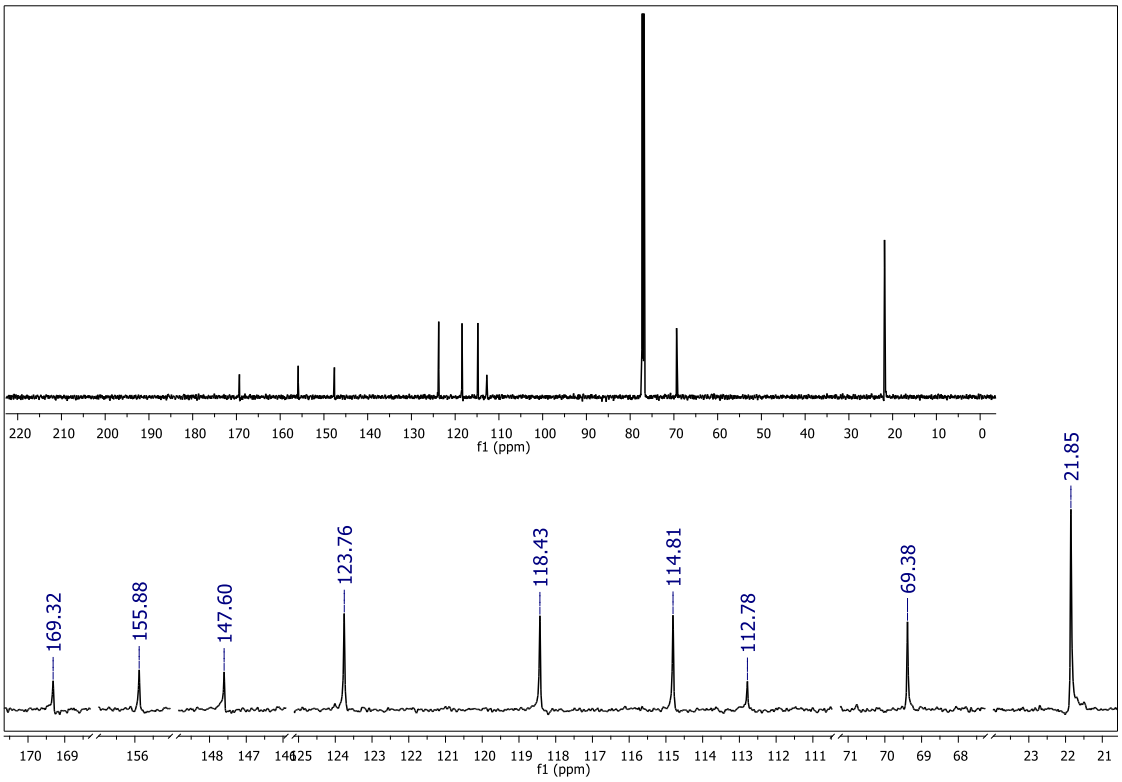

Figure S21. III) HPLC chromatogram of compound **21**

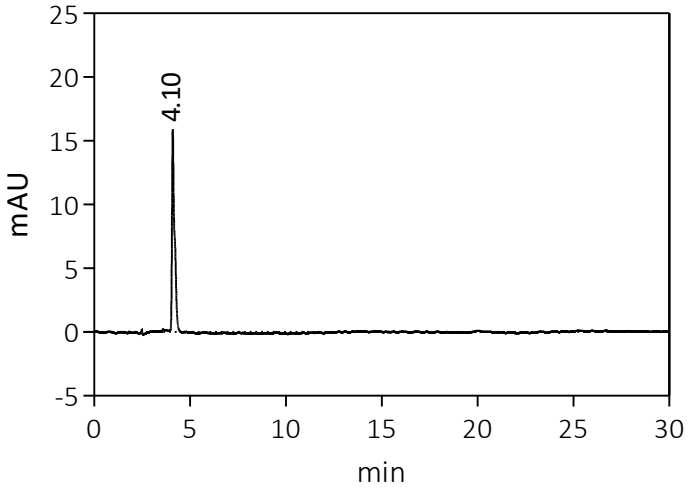

Figure S22. I) ^{1}H NMR spectrum of compound **22** (300 MHz – $CDCl_3$)

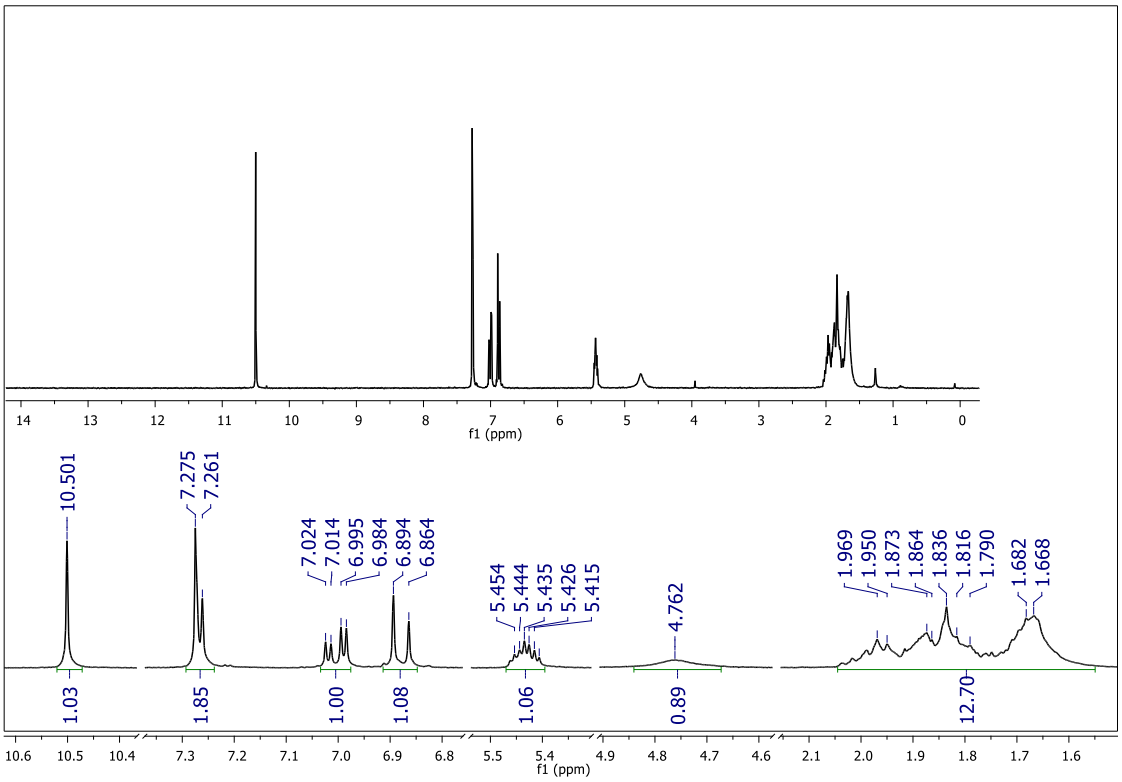

Figure S22. II) ^{13}C NMR spectrum of compound **22** (150 MHz – $CDCl_3$)

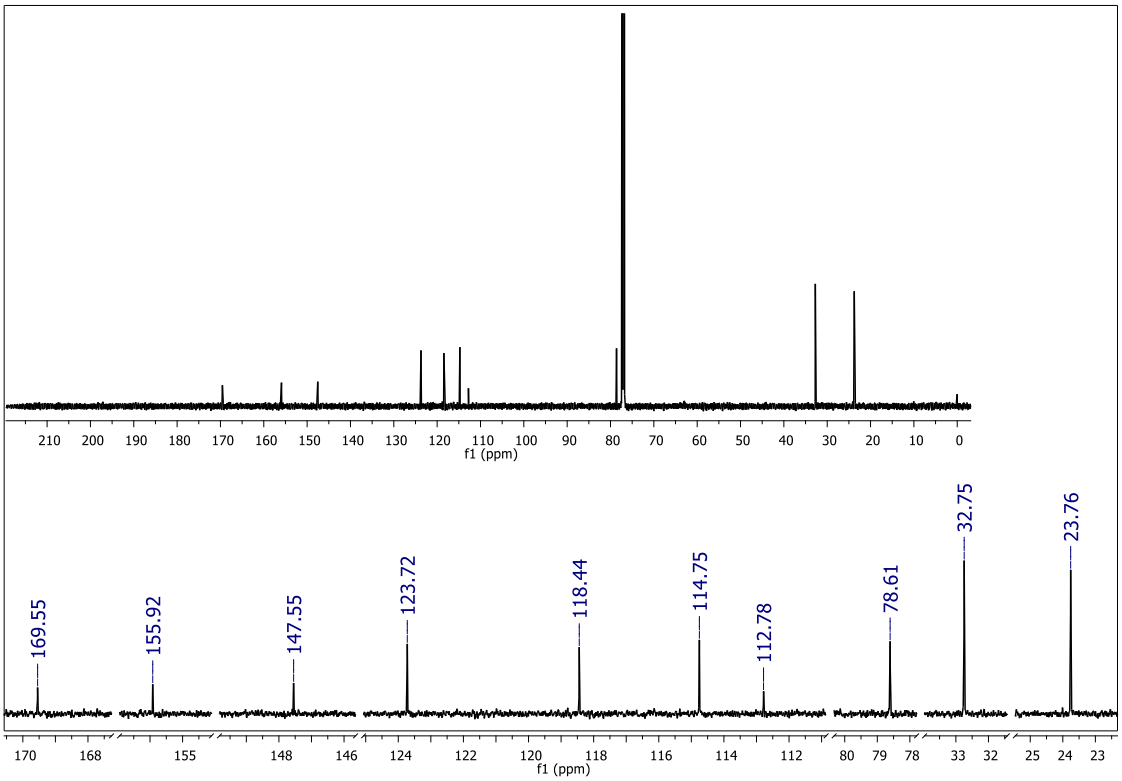

Figure S22. III) HPLC chromatogram of compound **22**

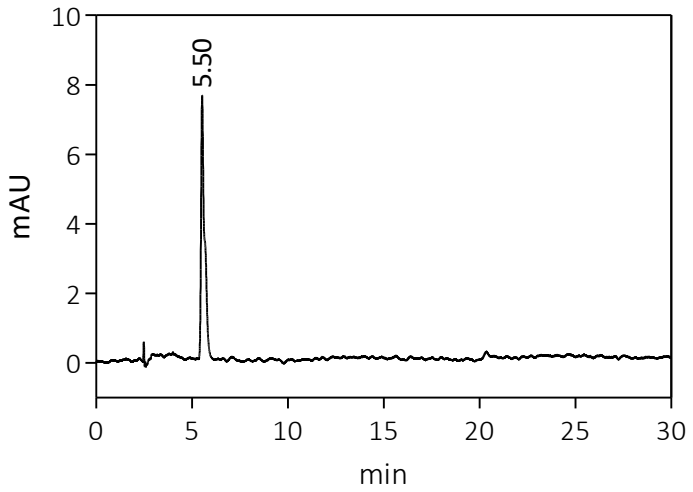

Figure S23. I) ^{1}H NMR spectrum of compound **23** (300 MHz – $CDCl_3$)

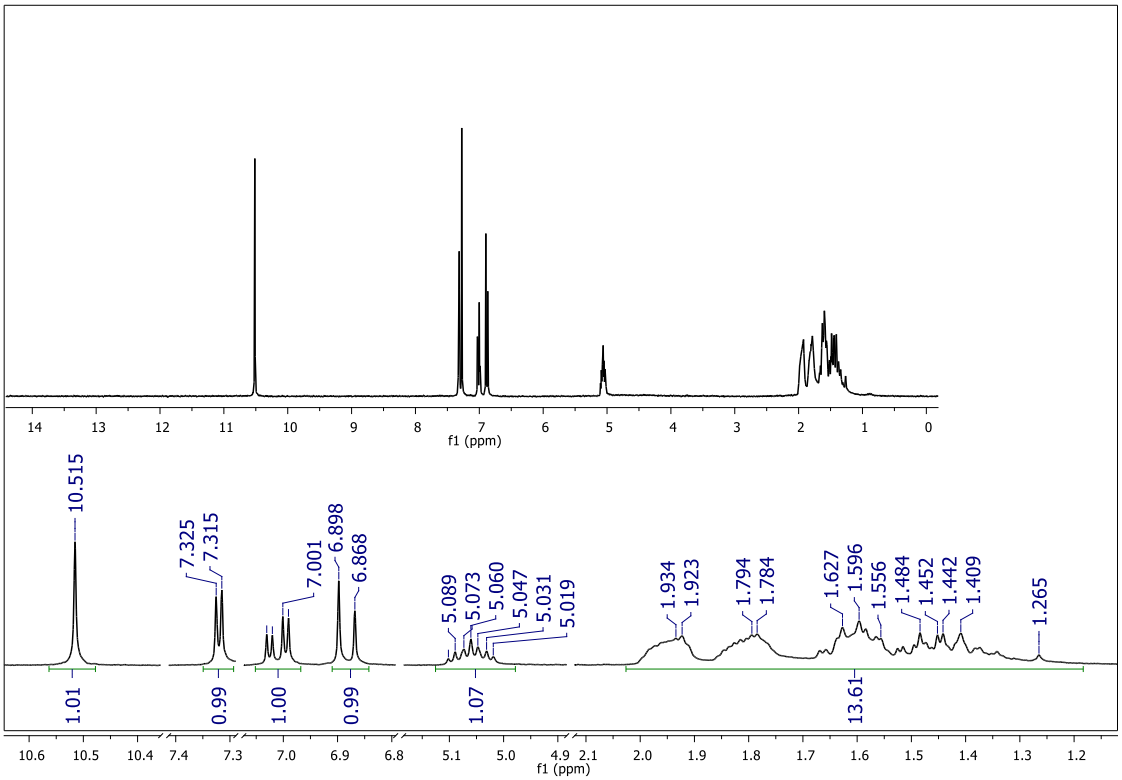

Figure S23. II) ^{13}C NMR spectrum of compound **23** (150 MHz – $CDCl_3$)

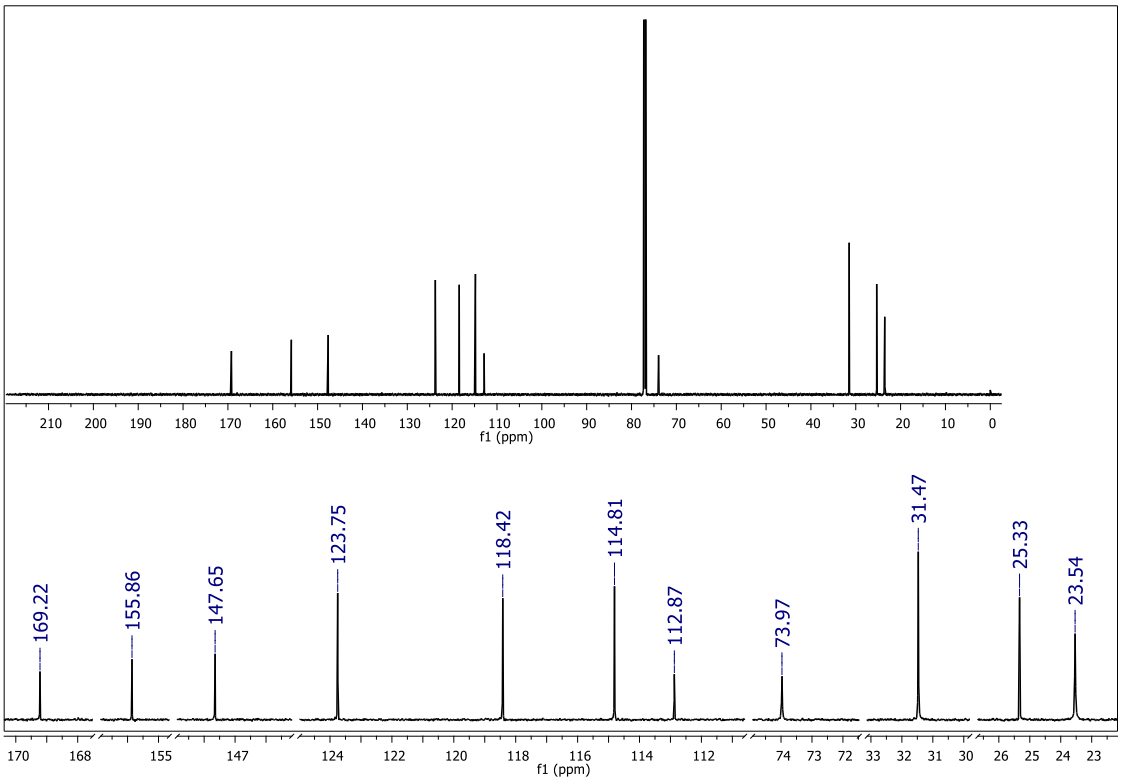

Figure S23. III) HPLC chromatogram of compound **23**

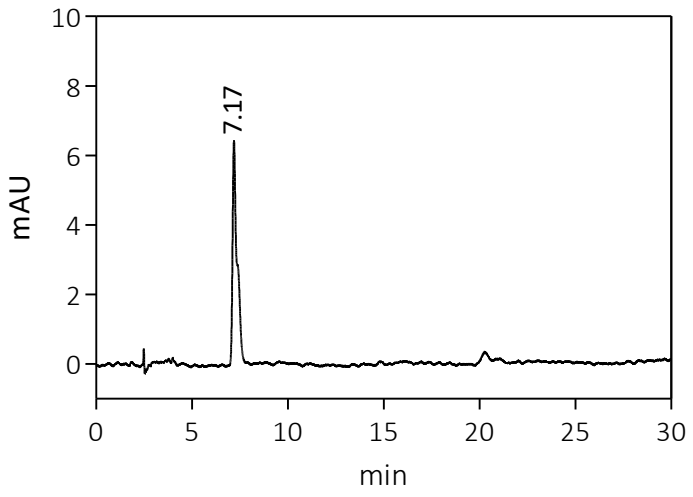

Figure S24. I) ^{1}H NMR spectrum of compound **24** (400 MHz – $CDCl_3$)

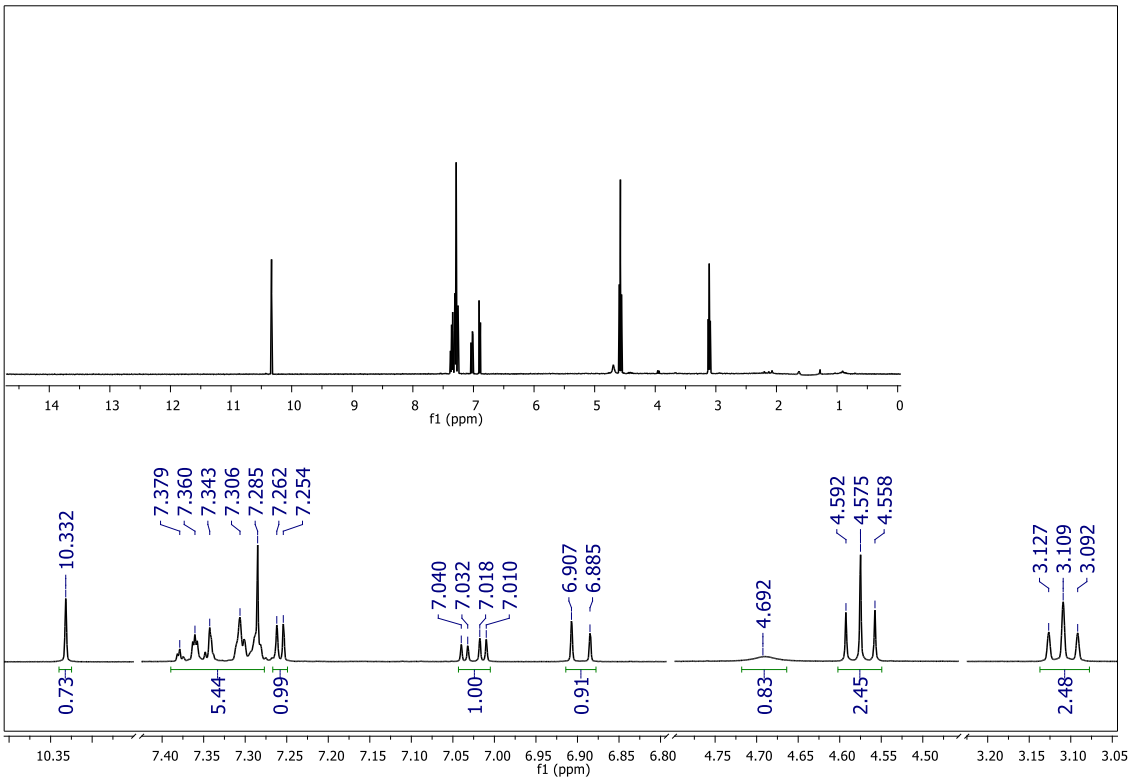

Figure S24. II) ^{13}C NMR spectrum of compound **24** (150 MHz – $CDCl_3$)

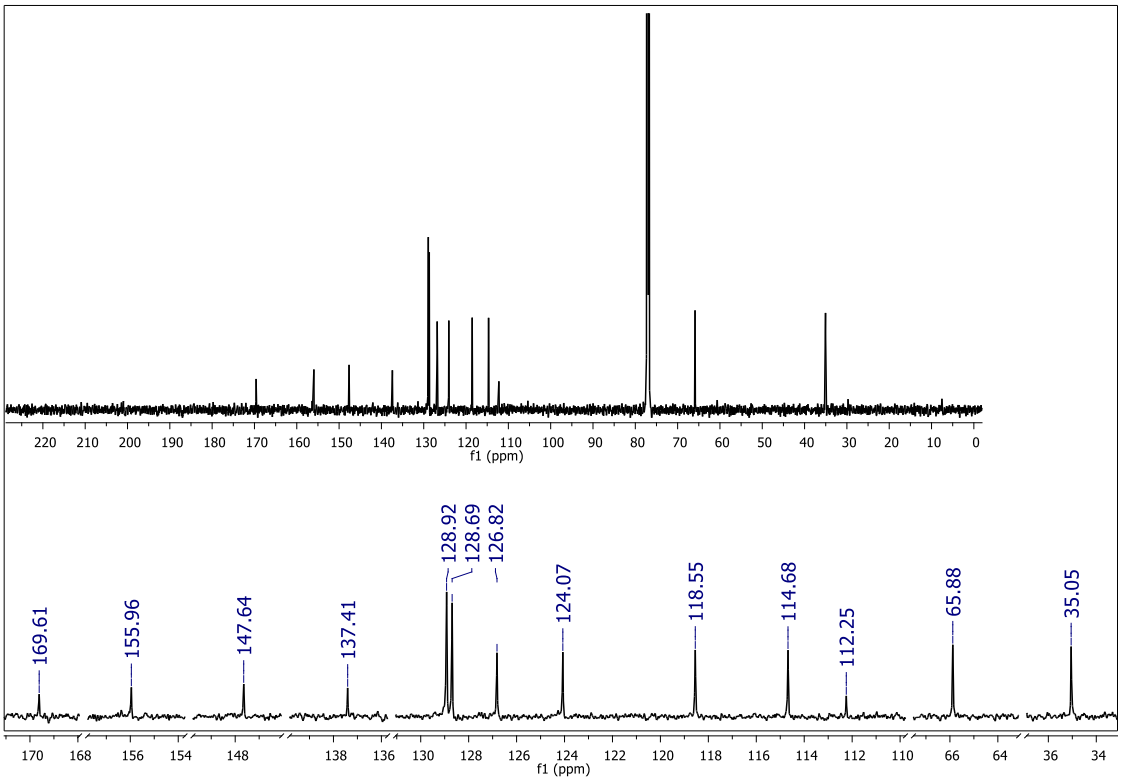

Figure S24. III) HPLC chromatogram of compound **24**

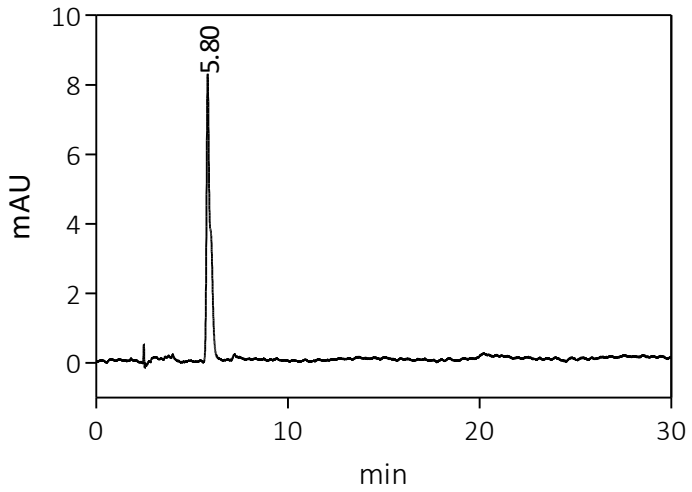

Figure S25. I) ^{1}H NMR spectrum of compound **25** (400 MHz – DMSO-d_6)

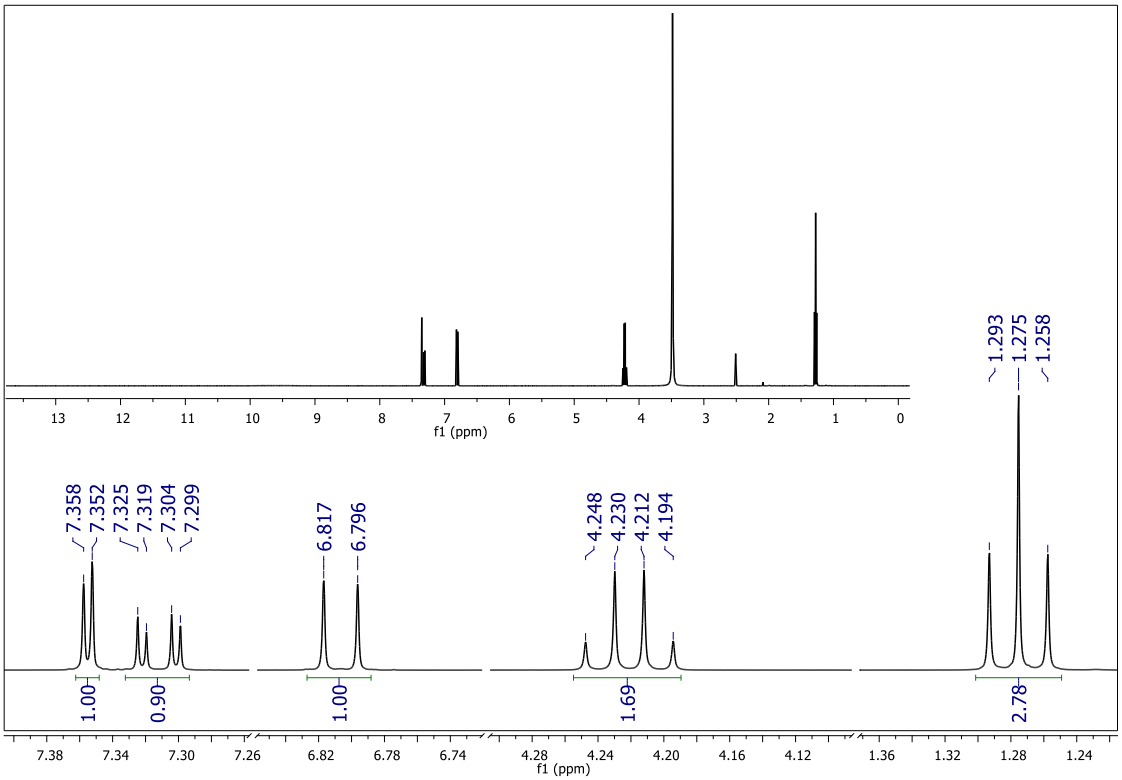

Figure S25. II) ^{13}C NMR spectrum of compound **25** (100 MHz – DMSO-d_6)

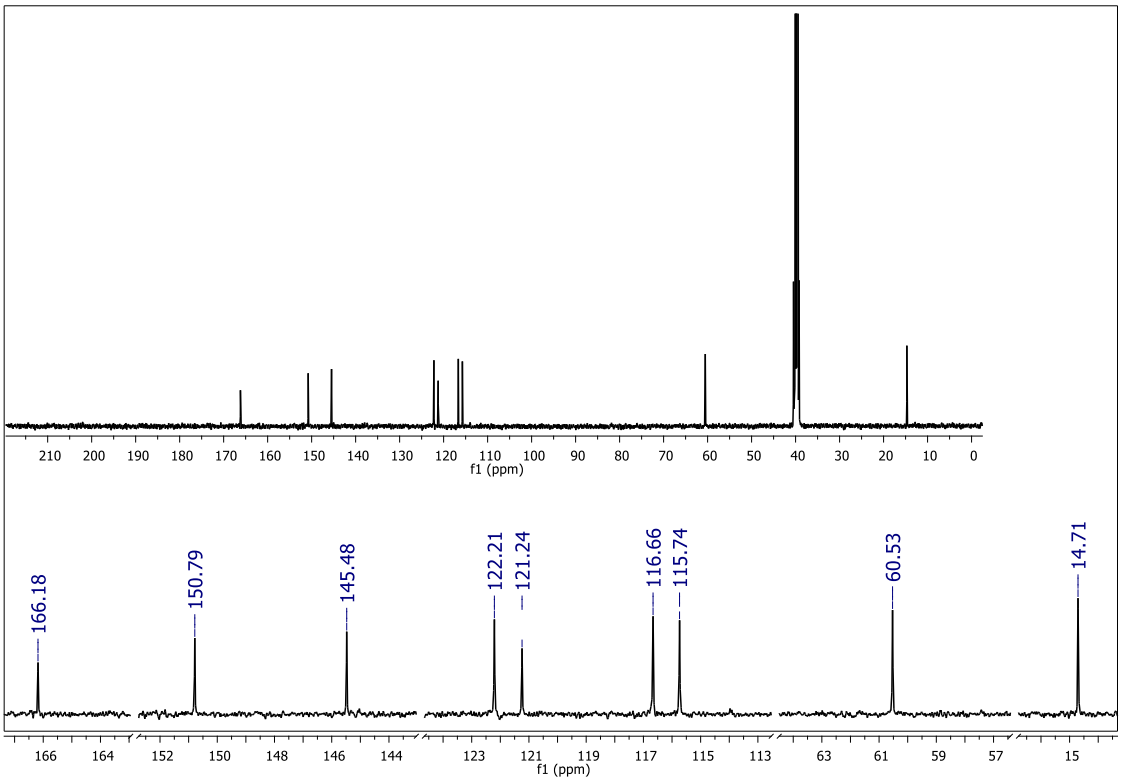

Figure S25. III) HPLC chromatogram of compound **25**

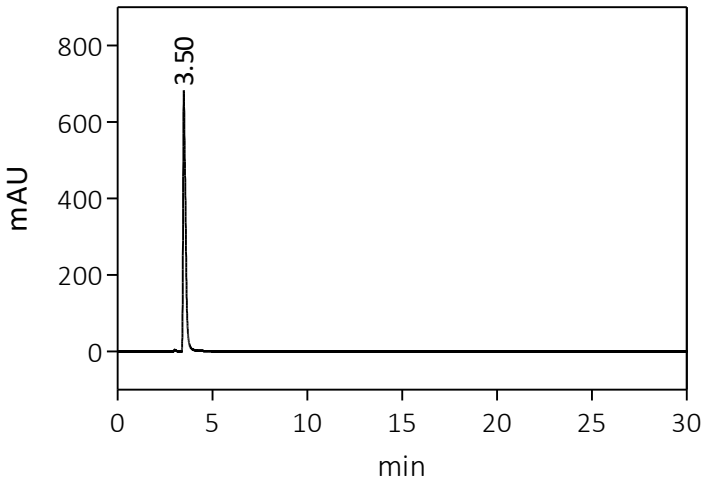

Figure S26. I) ^{1}H NMR spectrum of compound **26** (400 MHz – $CDCl_3$)

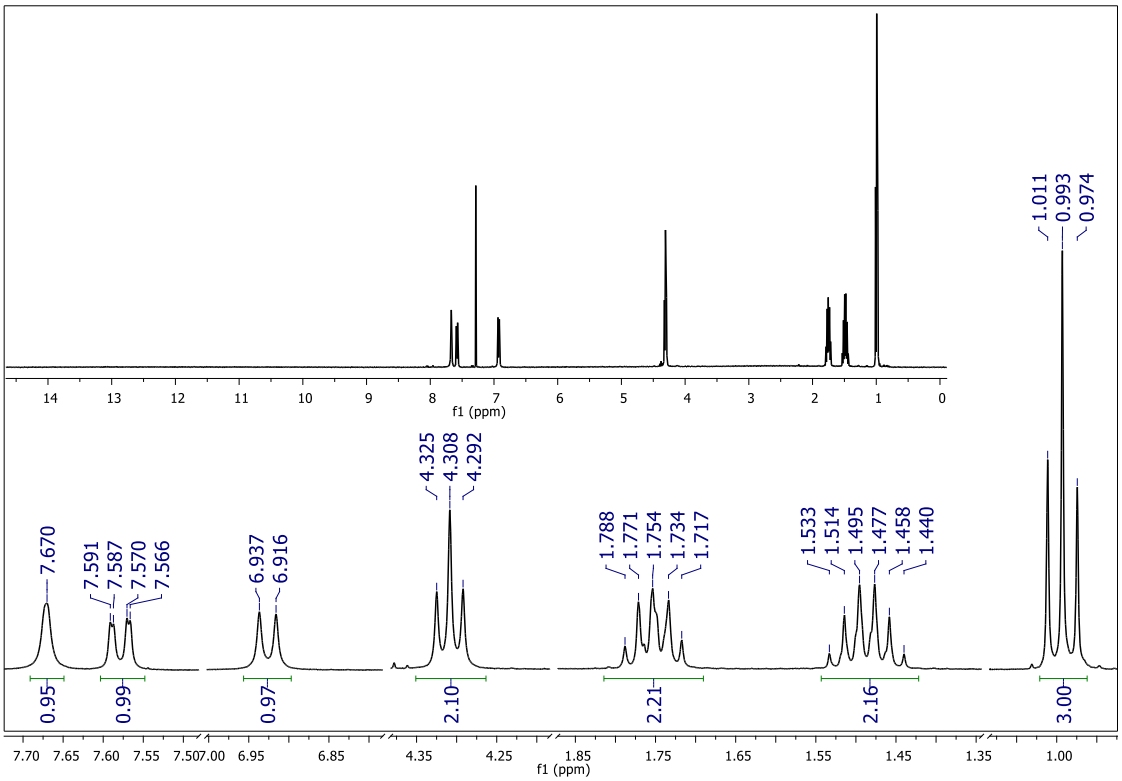

Figure S26. II) ^{13}C NMR spectrum of compound **26** (100 MHz – $CDCl_3$)

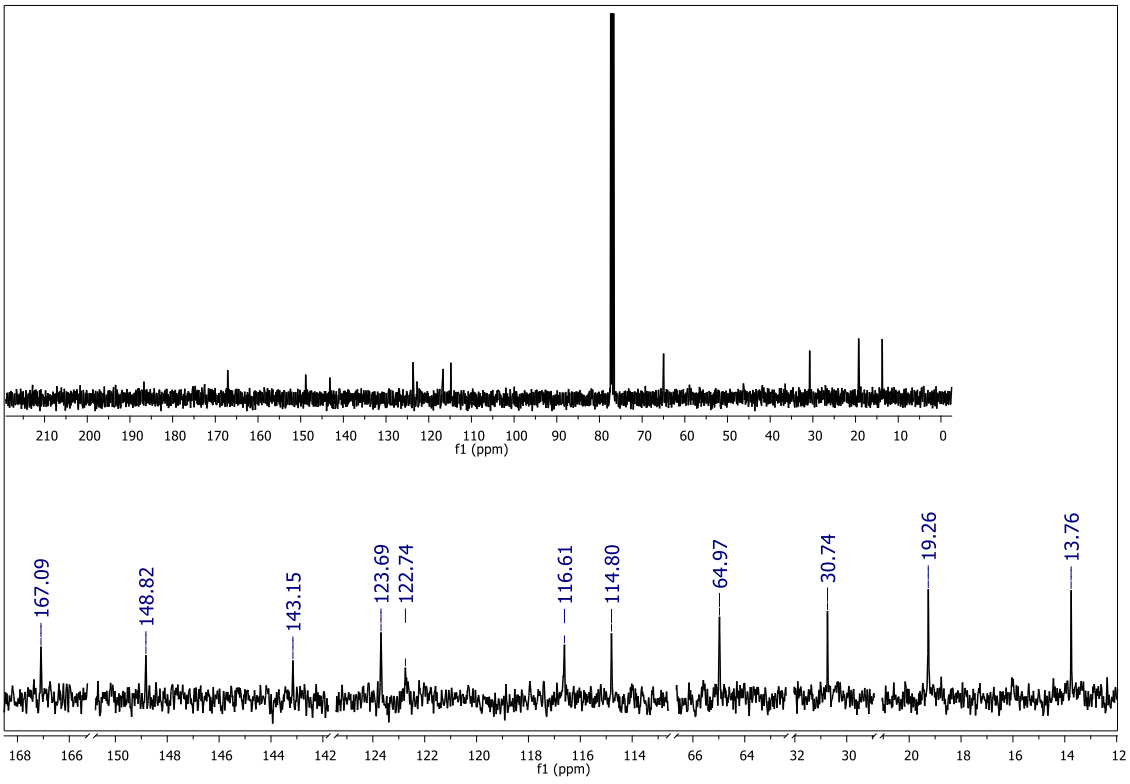

Figure S26. III) HPLC chromatogram of compound **26**

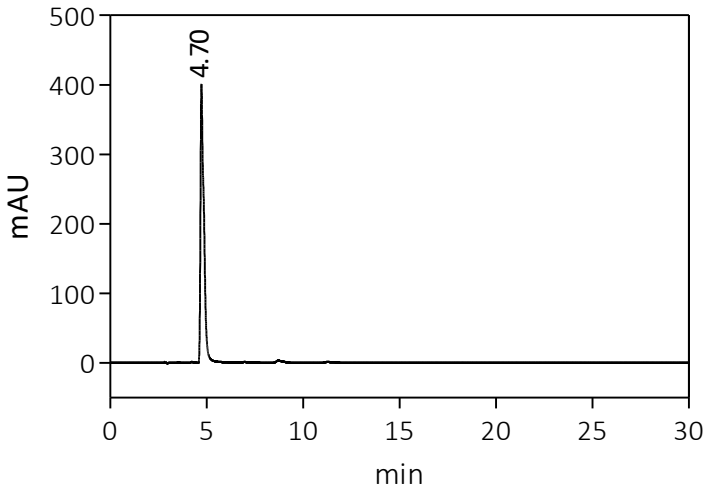

Figure S27. I) ^{1}H NMR spectrum of compound **27** (400 MHz – DMSO-d_6)

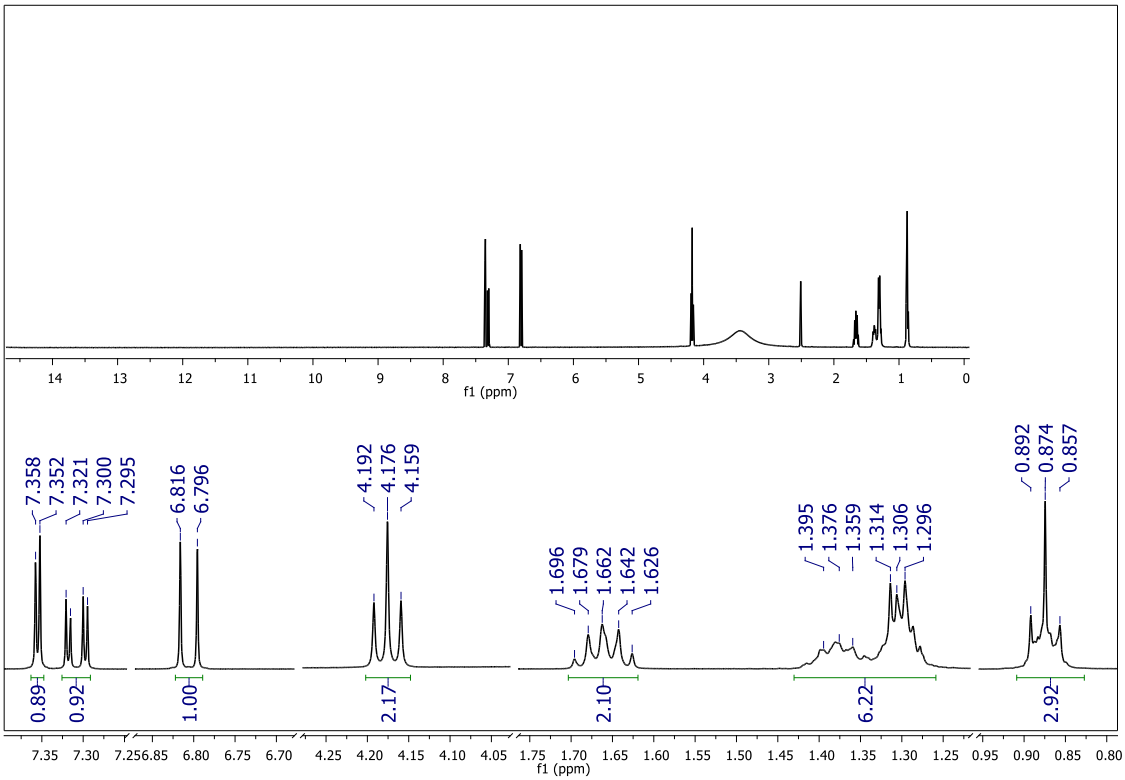

Figure S27. II) ^{13}C NMR spectrum of compound **27** (150 MHz – DMSO-d_6)

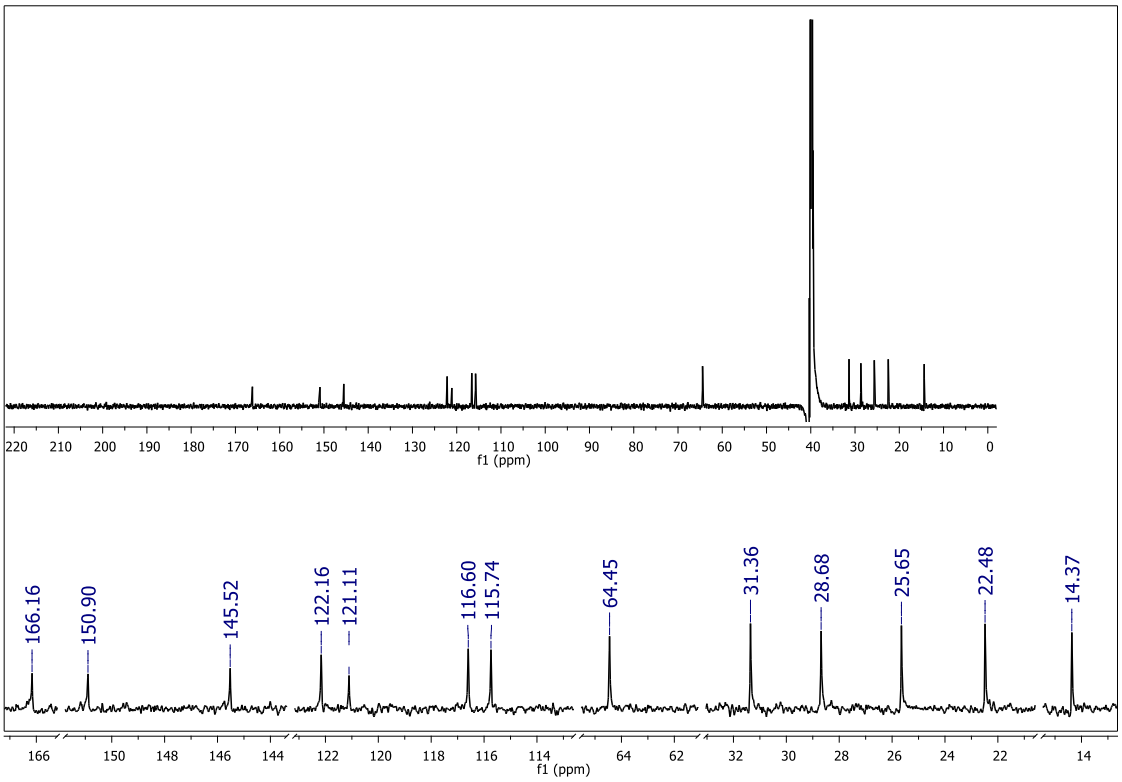

Figure S27. III) HPLC chromatogram of compound **27**

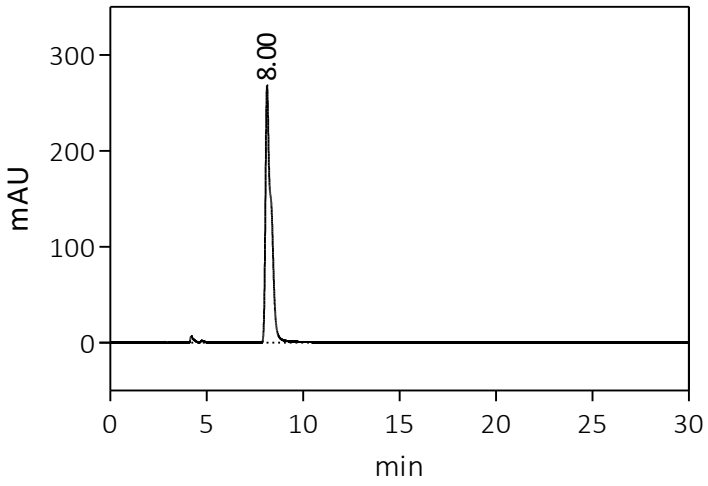

Figure S28. I) ^{1}H NMR spectrum of compound **28** (600 MHz – DMSO-d_6)

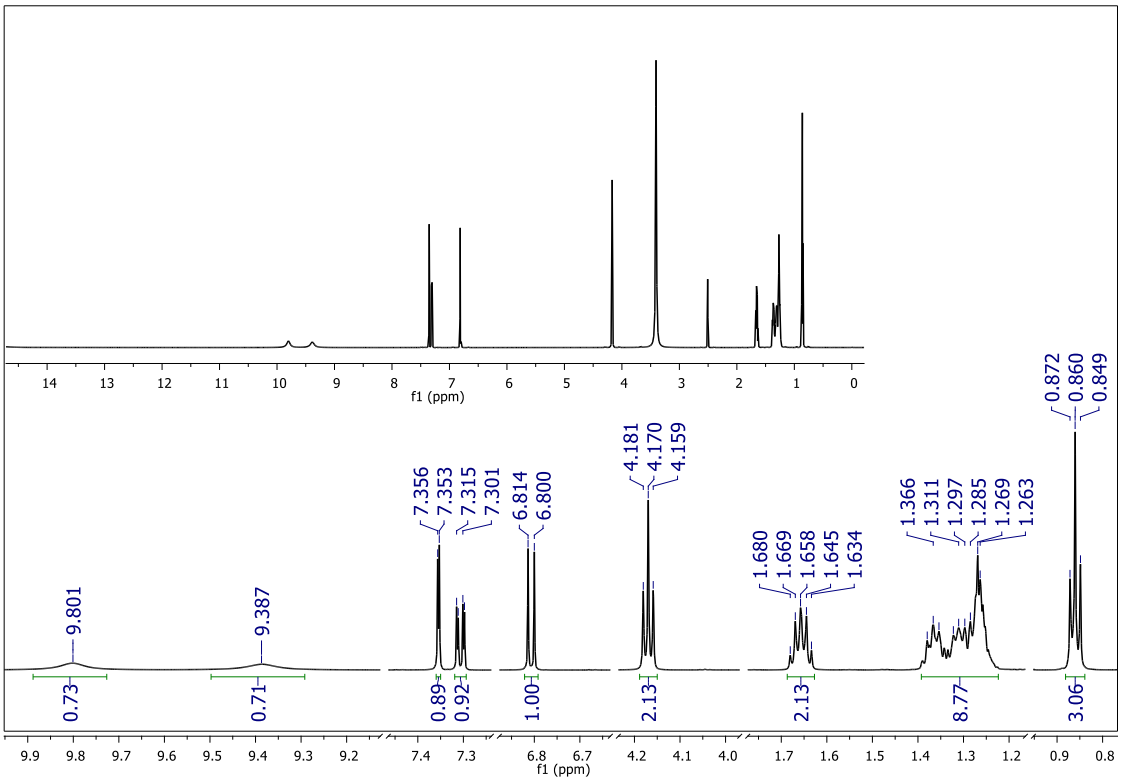

Figure S28. II) ^{13}C NMR spectrum of compound **28** (150 MHz – DMSO-d_6)

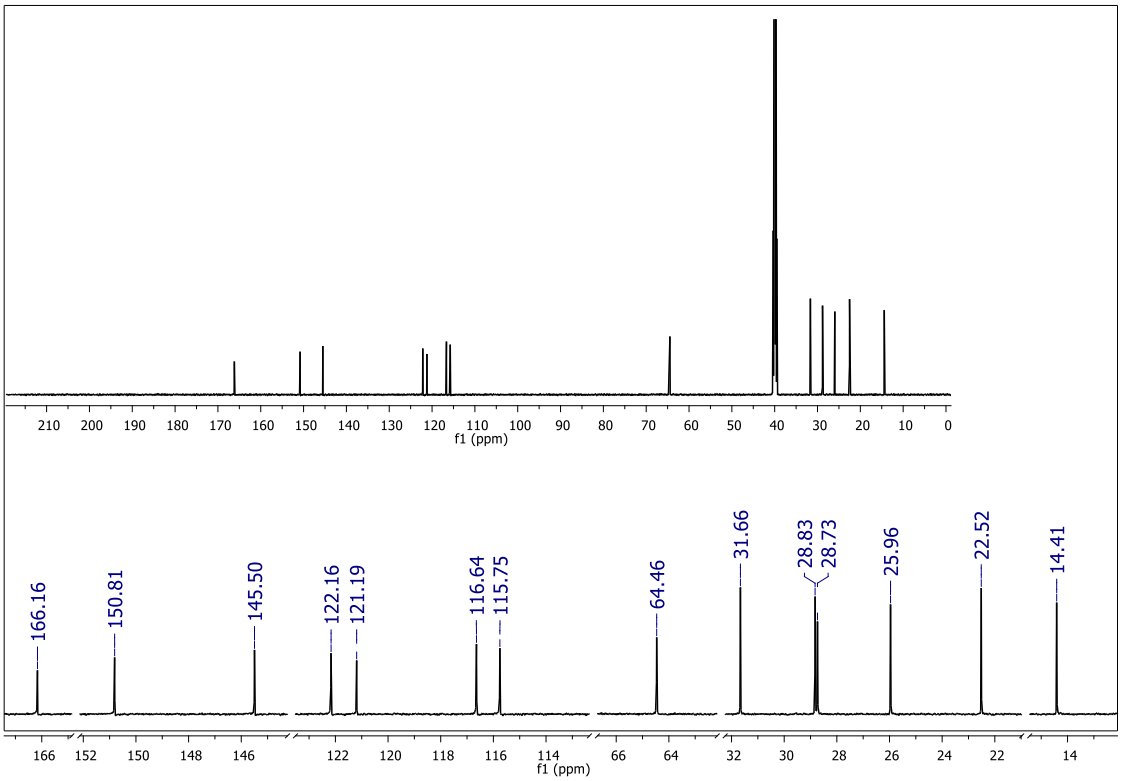

Figure S28. III) HPLC chromatogram of compound **28**

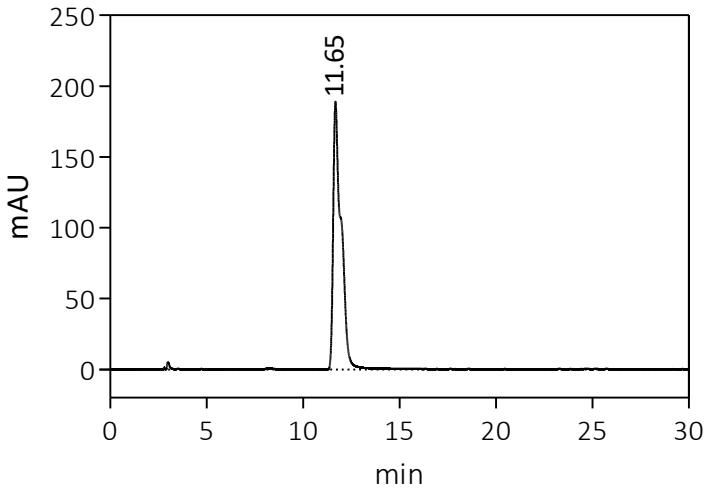

Figure S29. I) ^{1}H NMR spectrum of compound **29** (400 MHz – $CDCl_3$)

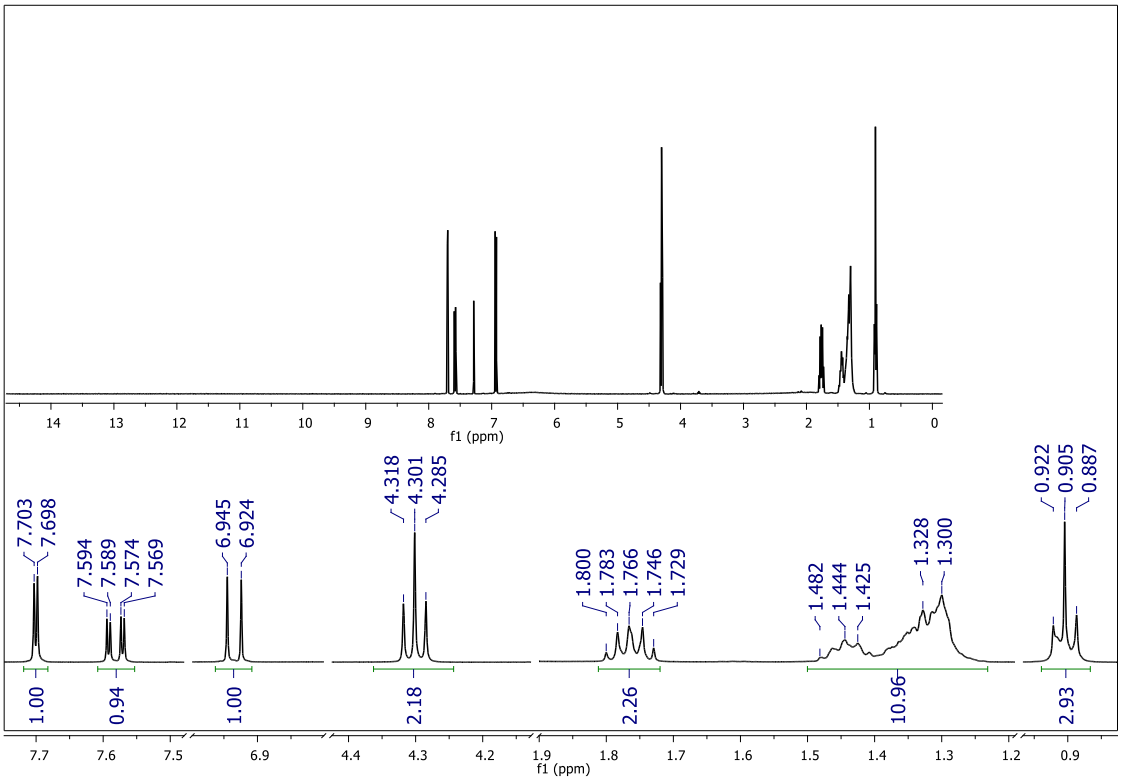

Figure S29. II) ^{13}C NMR spectrum of compound **29** (100 MHz – $CDCl_3$)

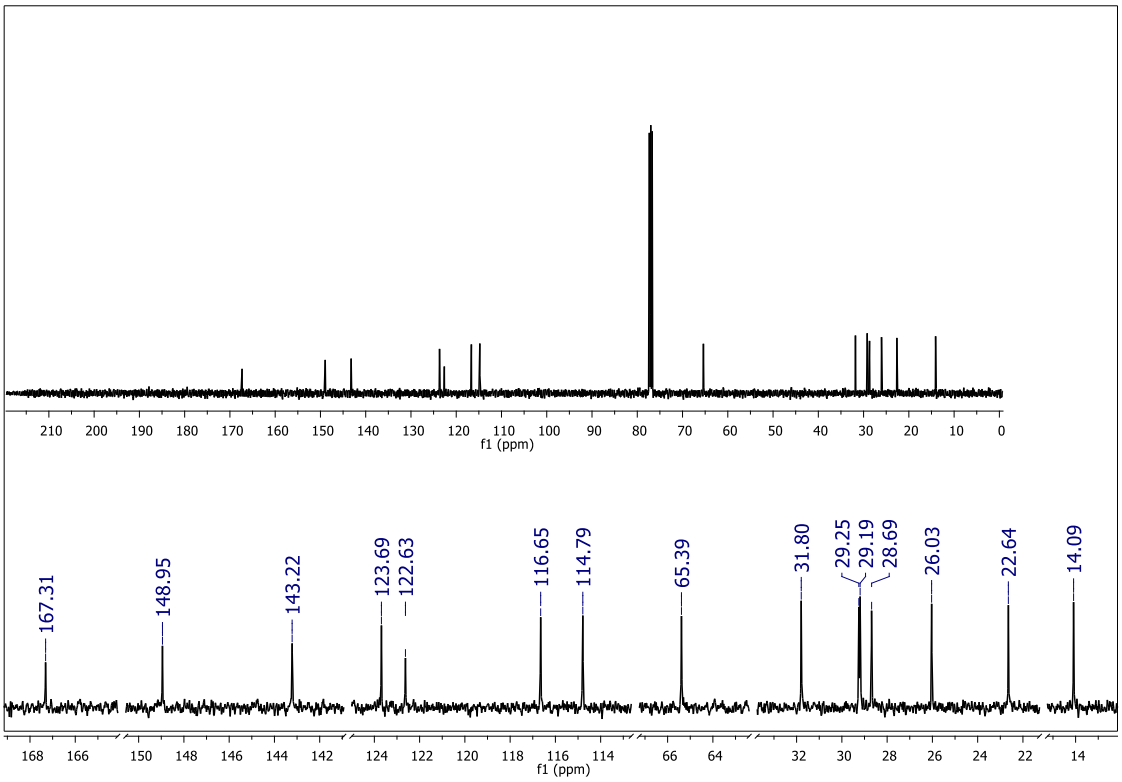

Figure S29. III) HPLC chromatogram of compound **29**

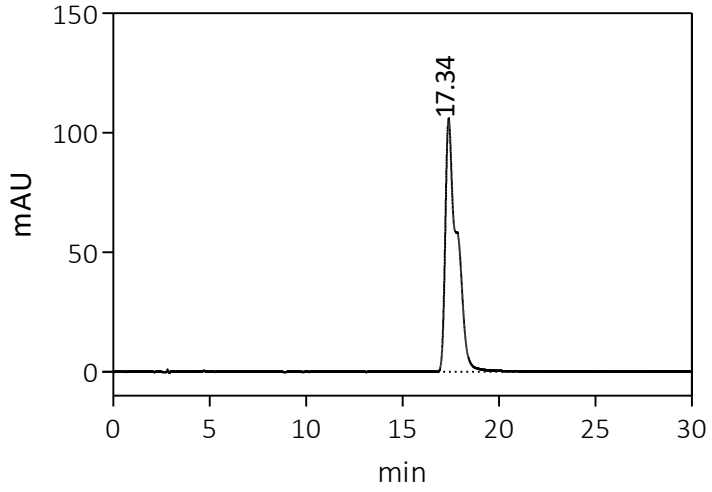

Figure S30. I) ^{1}H NMR spectrum of compound **30** (300 MHz – $CDCl_3$)

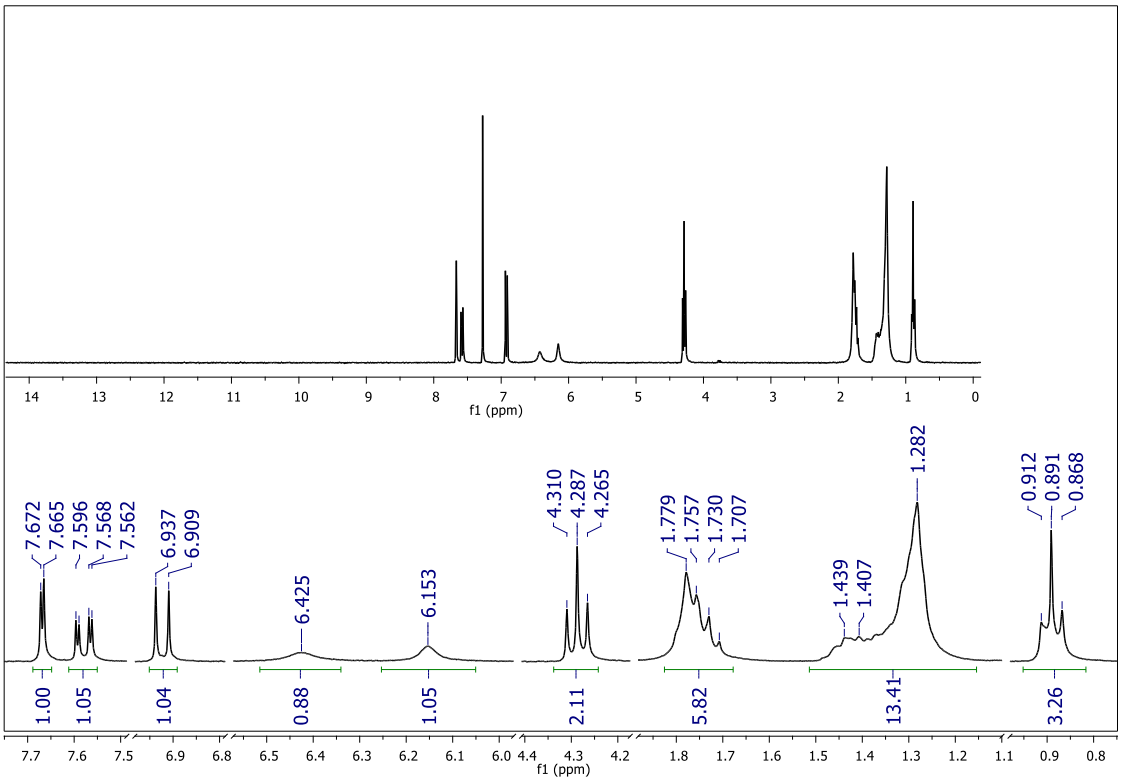

Figure S30. II) ^{13}C NMR spectrum of compound **30** (150 MHz – DMSO-d_6)

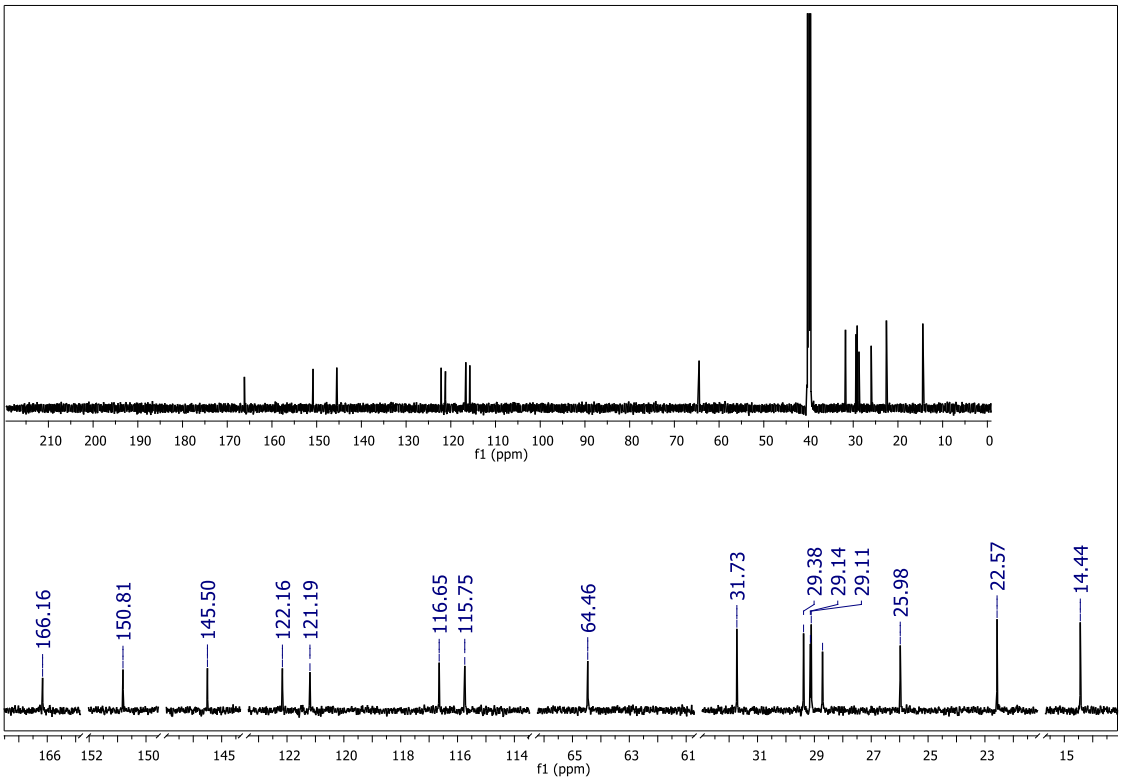

Figure S30. III) HPLC chromatogram of compound **30**

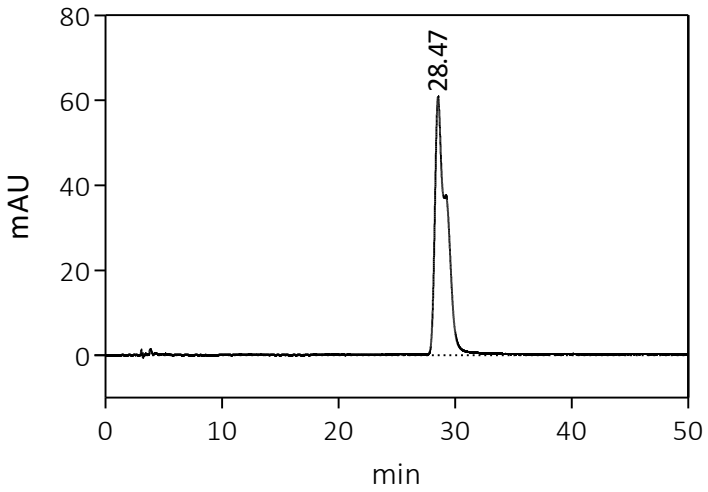

Figure S31. I) ^{1}H NMR spectrum of compound **31** (400 MHz – $CDCl_3$)

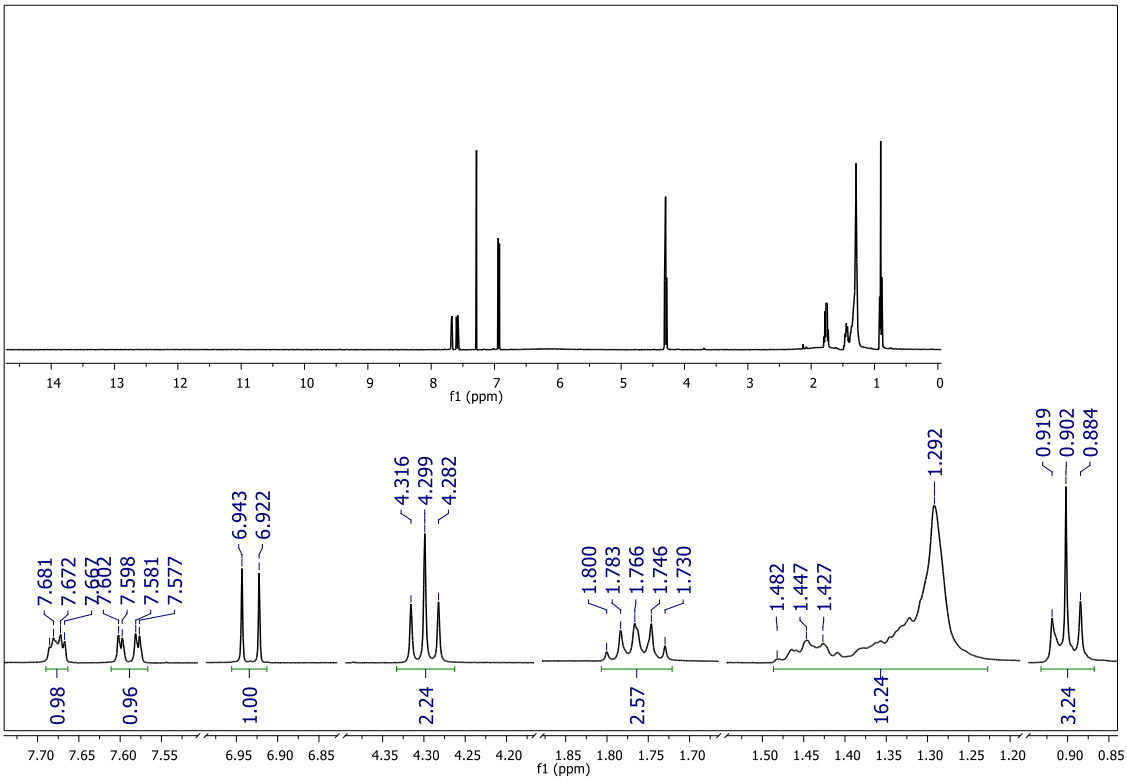

Figure S31. II) ^{13}C NMR spectrum of compound **31** (100 MHz – $CDCl_3$)

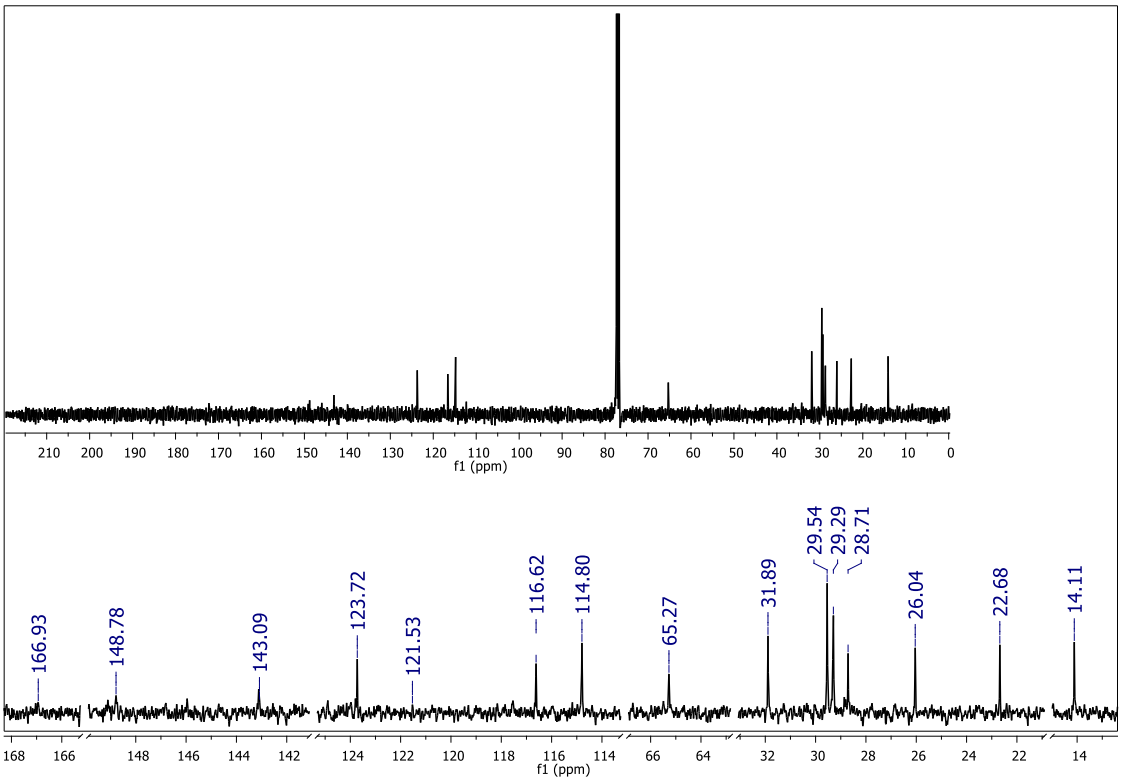

Figure S31. III) HPLC chromatogram of compound **31**

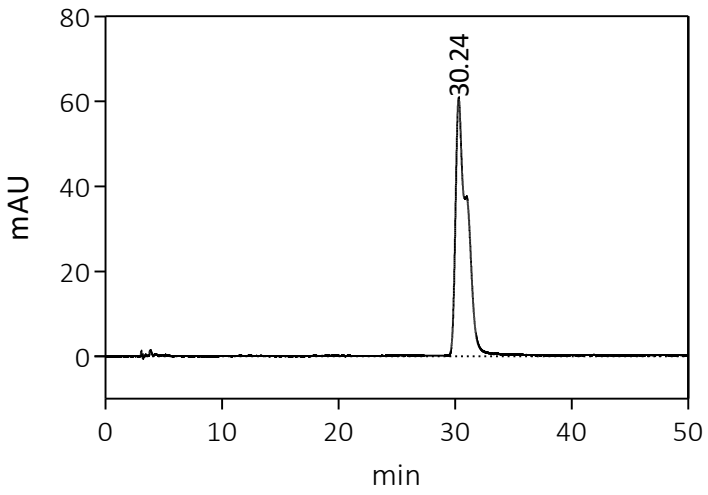

Figure S32. I) ^{1}H NMR spectrum of compound **32** (300 MHz – $CDCl_3$)

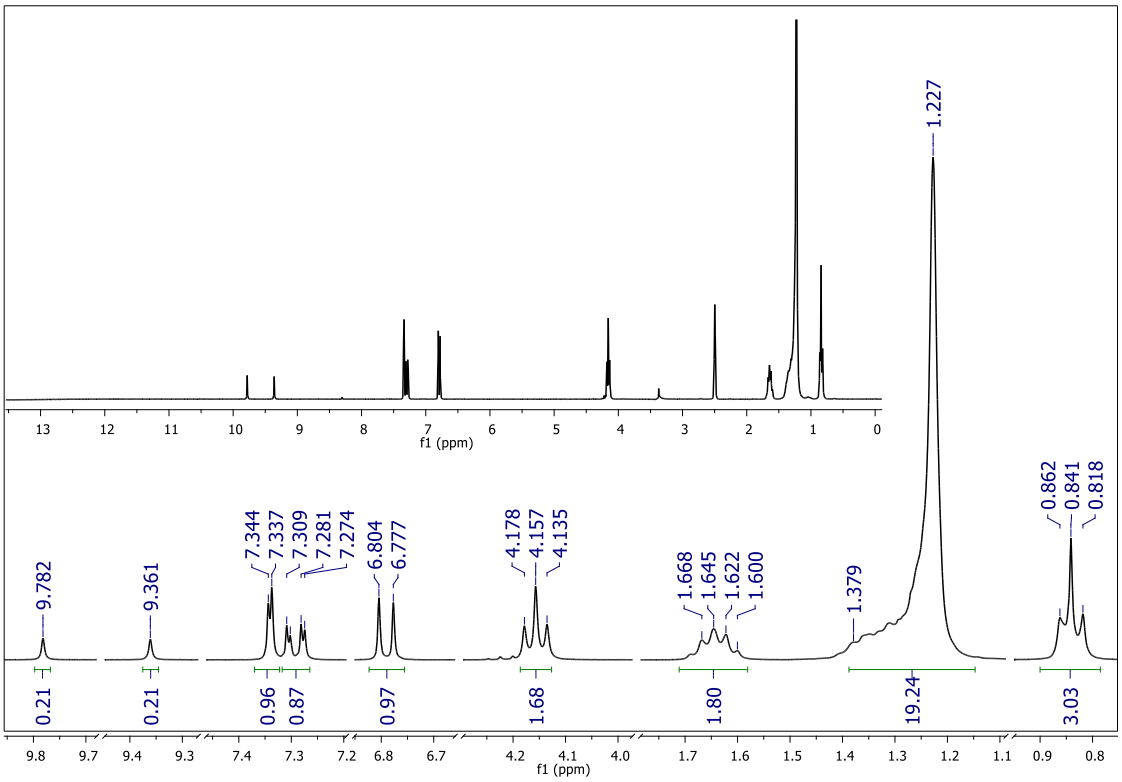

Figure S32. II) ^{13}C NMR spectrum of compound **32** (100 MHz – $CDCl_3$)

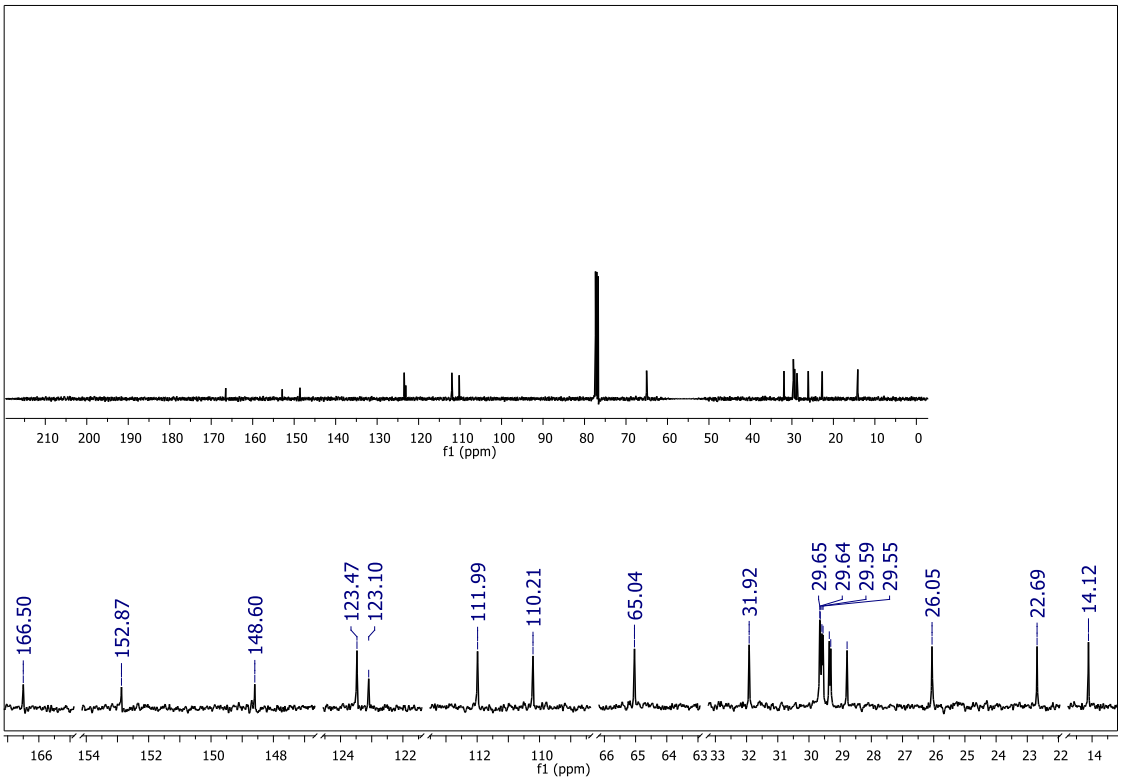

Figure S32. III) HPLC chromatogram of compound **32**

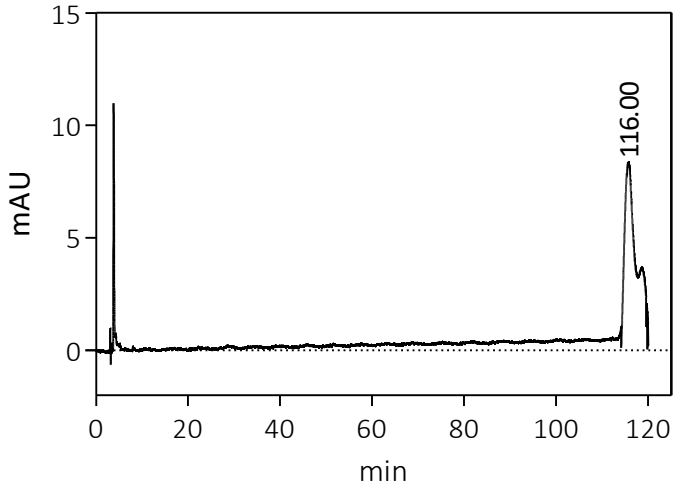

Figure S33. I) ^{1}H NMR spectrum of compound **33** (300 MHz – DMSO-d_6)

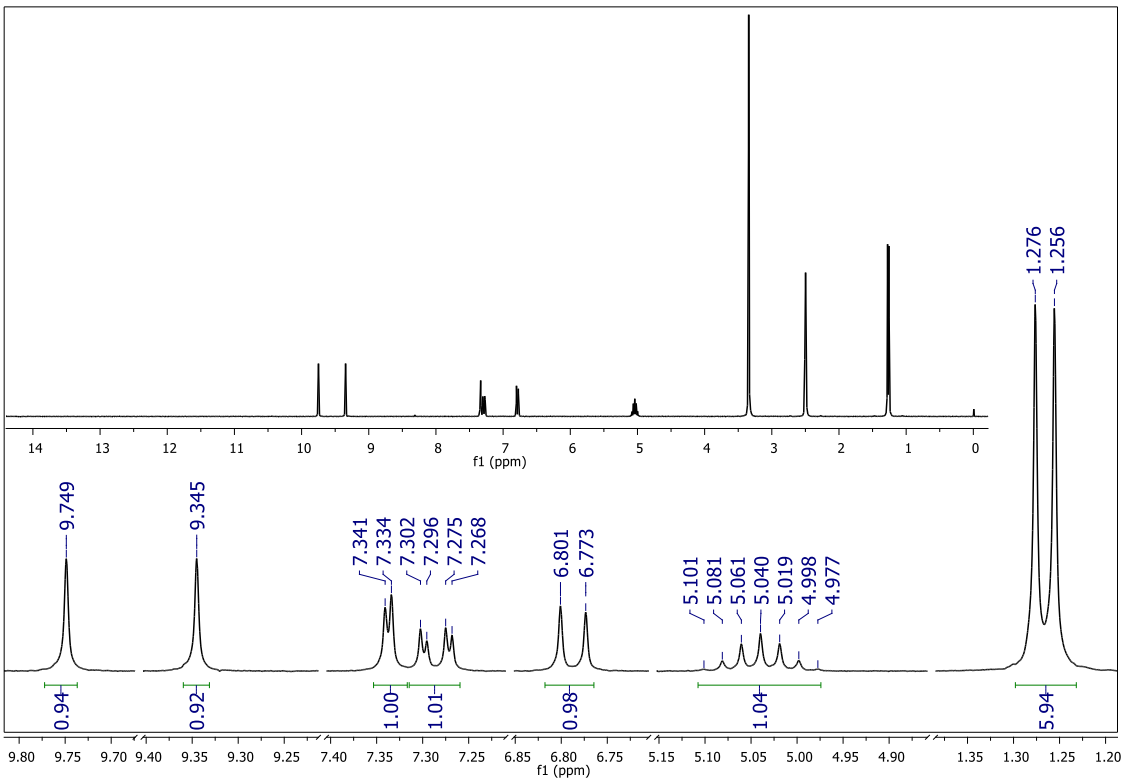

Figure S33. II) ^{13}C NMR spectrum of compound **33** (150 MHz – DMSO-d_6)

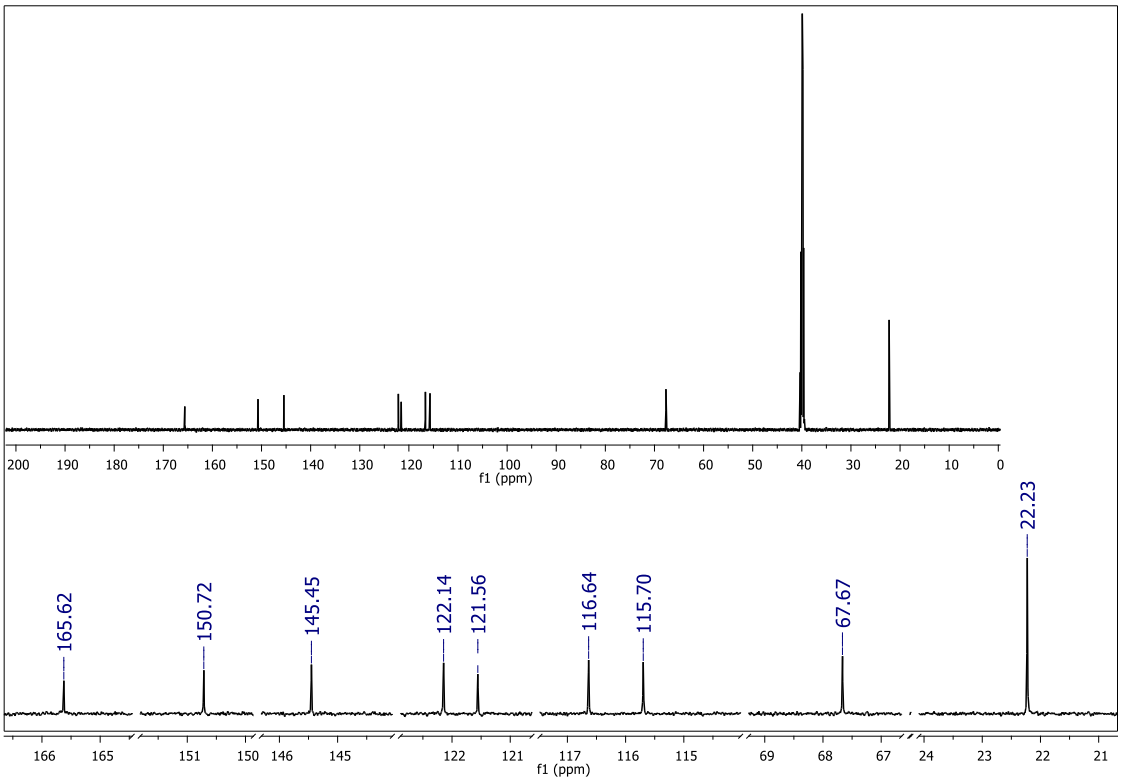

Figure S33. III) HPLC chromatogram of compound **33**

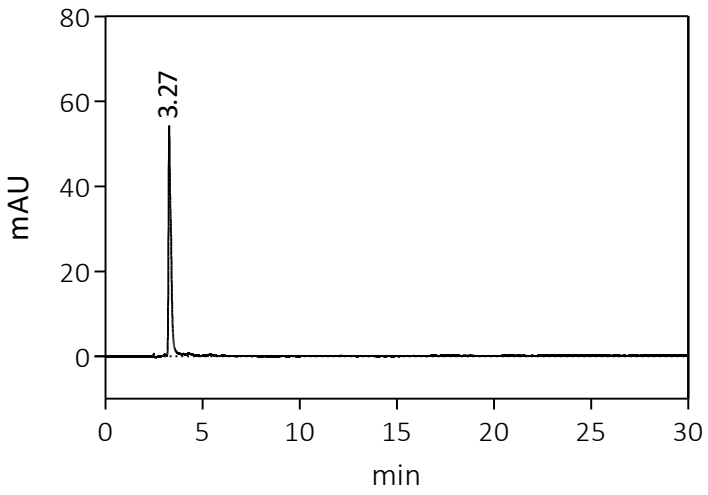

Figure S34. I) ^{1}H NMR spectrum of compound **34** (300 MHz – DMSO-d_6)

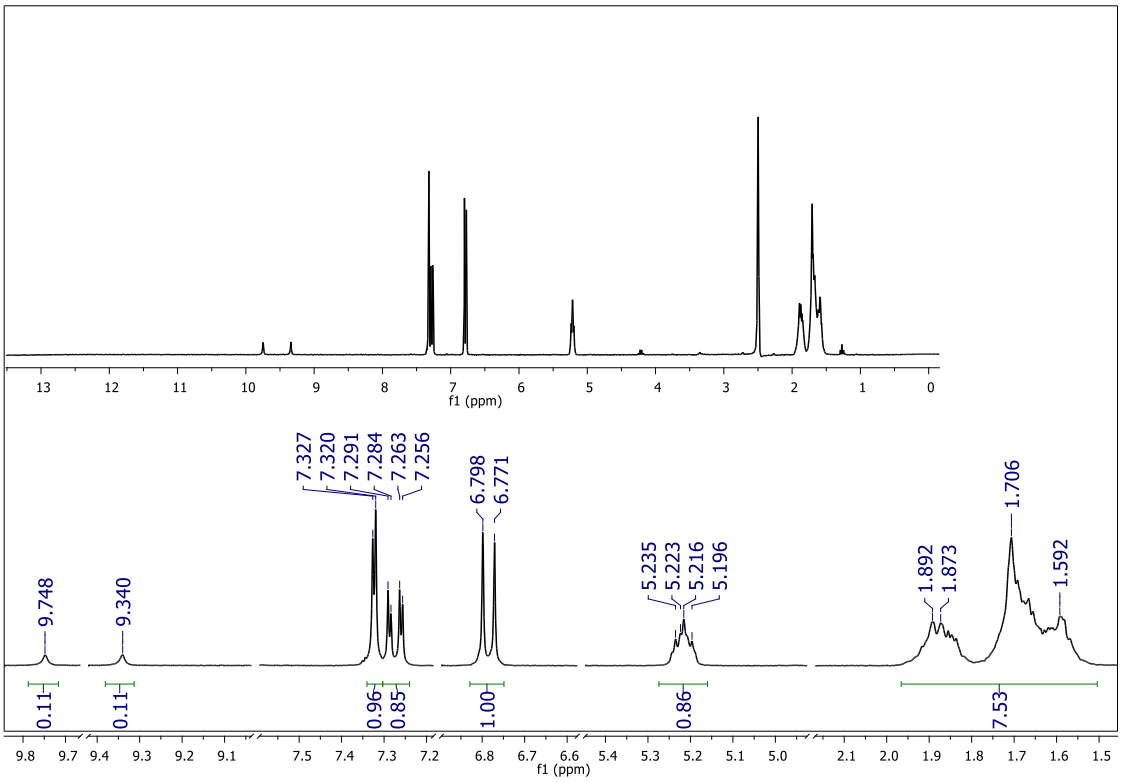

Figure S34. II) ^{13}C NMR spectrum of compound **34** (150 MHz – DMSO-d_6)

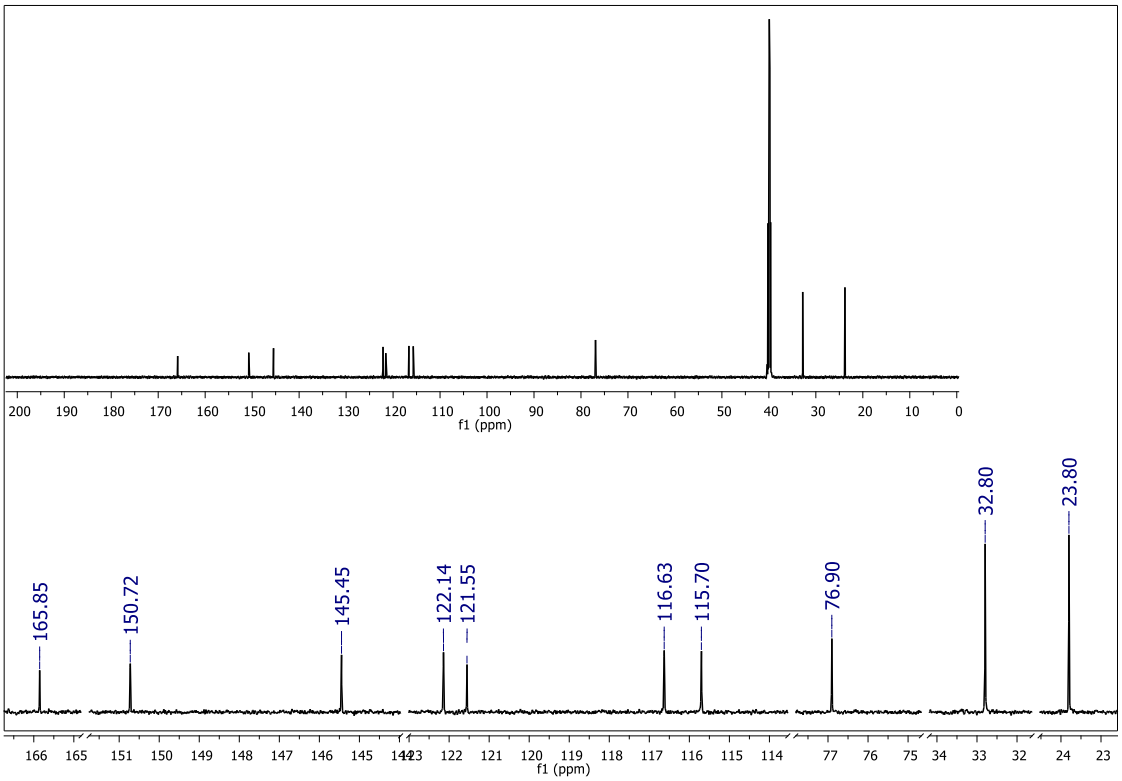

Figure S34. III) HPLC chromatogram of compound **34**

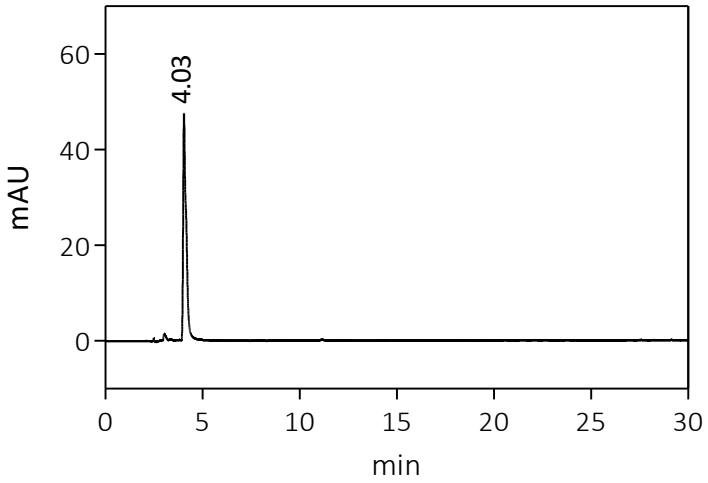

Figure S35. I) ^{1}H NMR spectrum of compound **35** (600 MHz – DMSO-d_6)

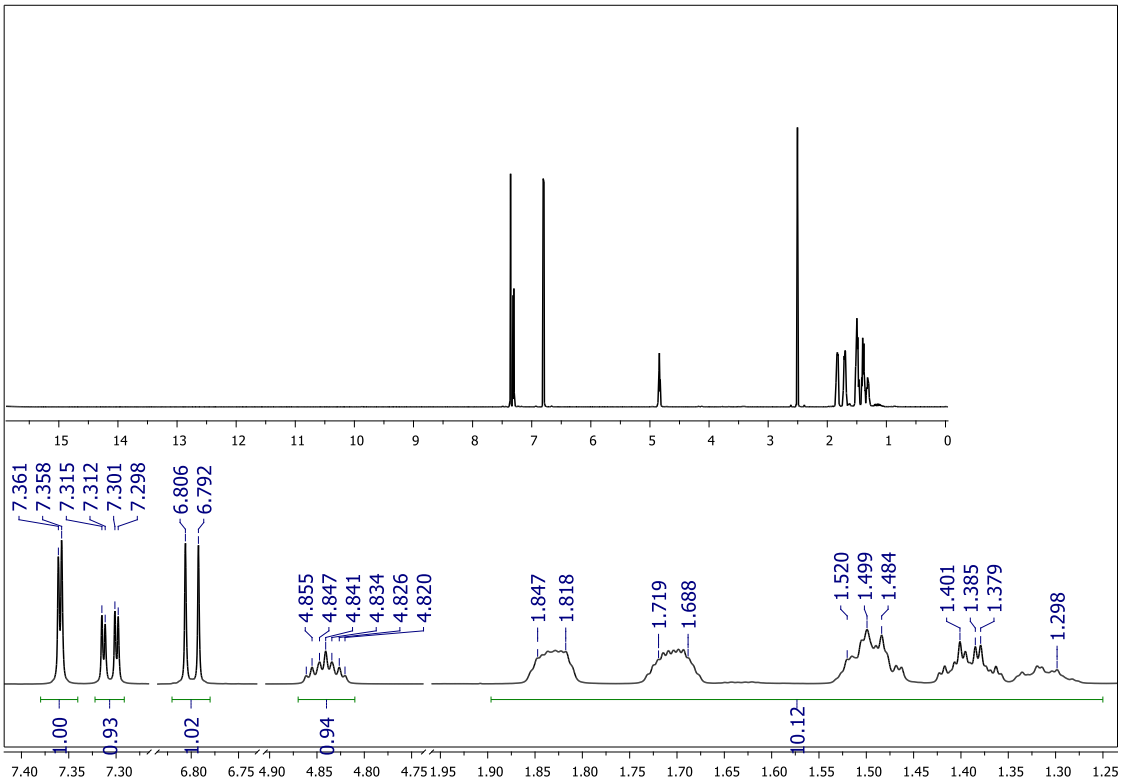

Figure S35. II) ^{13}C NMR spectrum of compound **35** (150 MHz – DMSO-d_6)

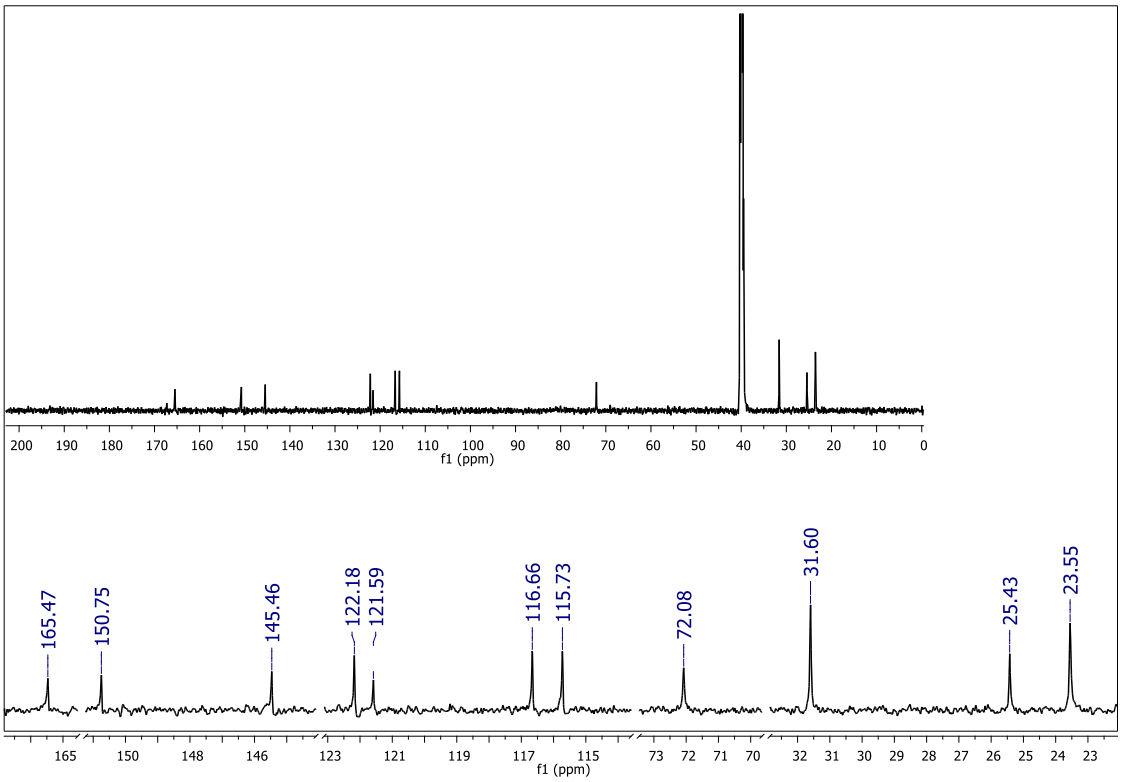

Figure S35. III) HPLC chromatogram of compound **35**

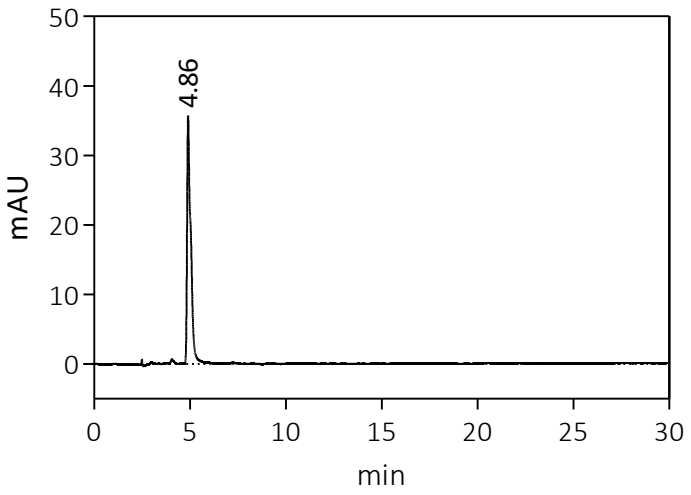

Figure S36. I) ^{1}H NMR spectrum of compound **36** (300 MHz – DMSO-d_6)

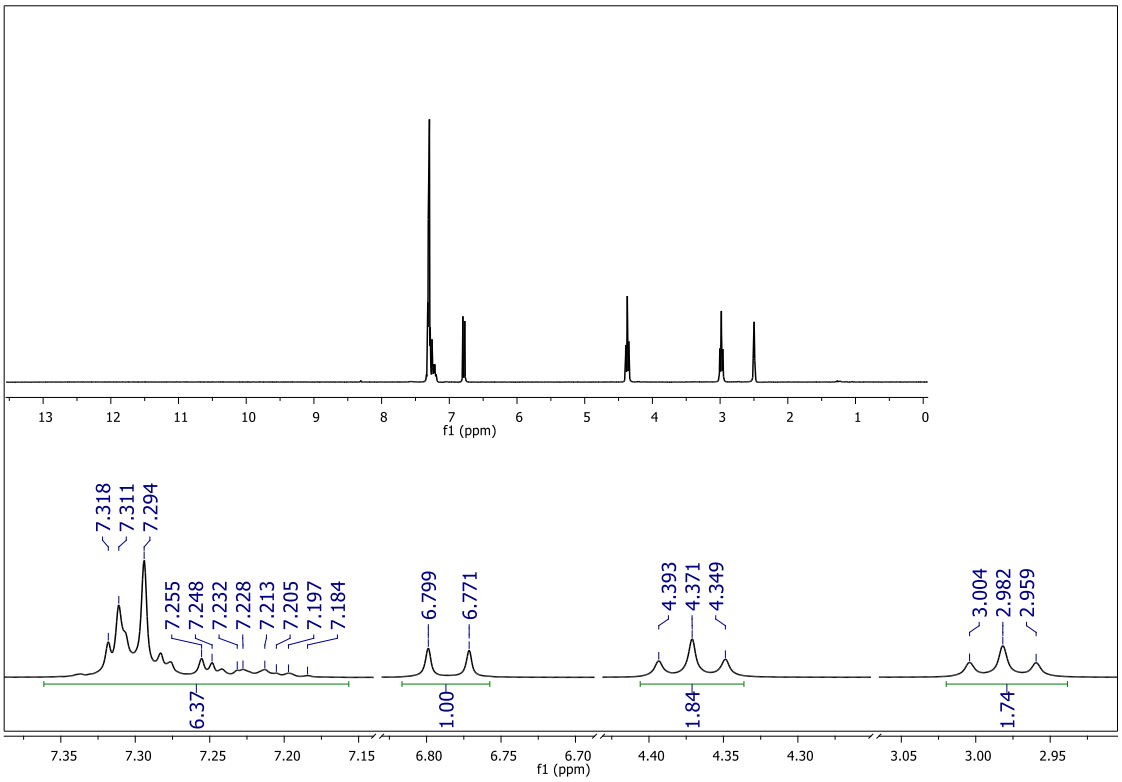

Figure S36. II) ^{13}C NMR spectrum of compound **36** (150 MHz – DMSO-d_6)

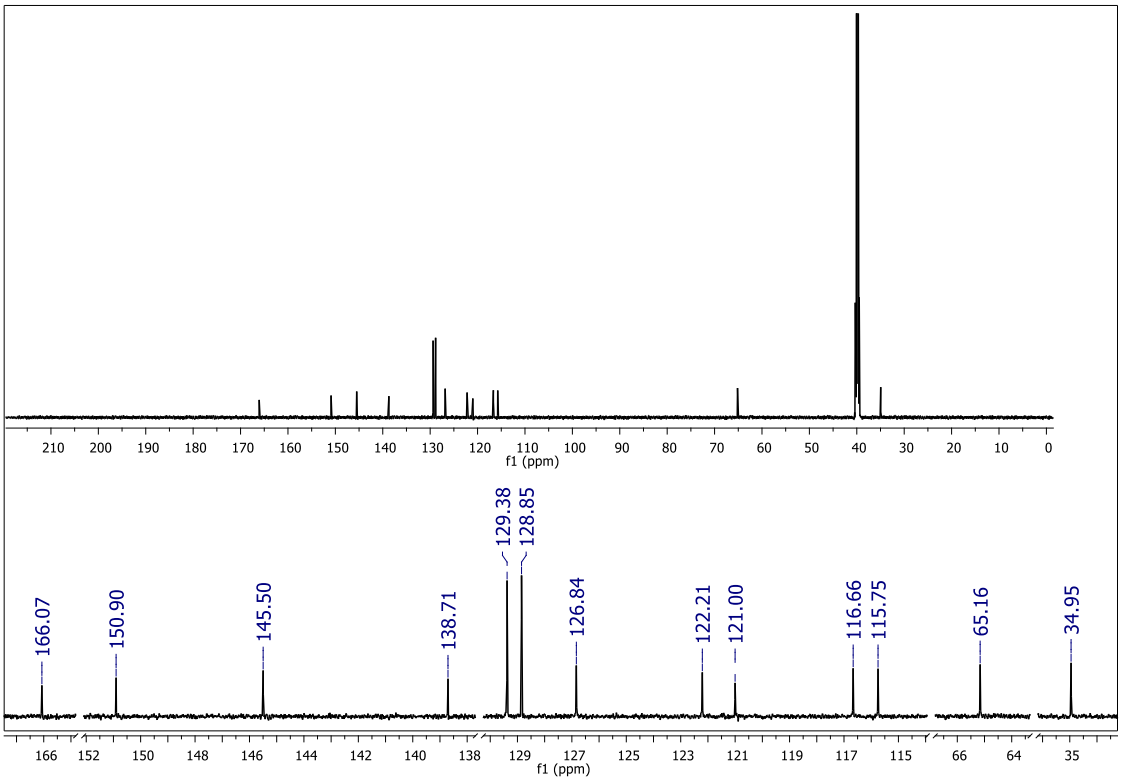

Figure S36. III) HPLC chromatogram of compound **36**

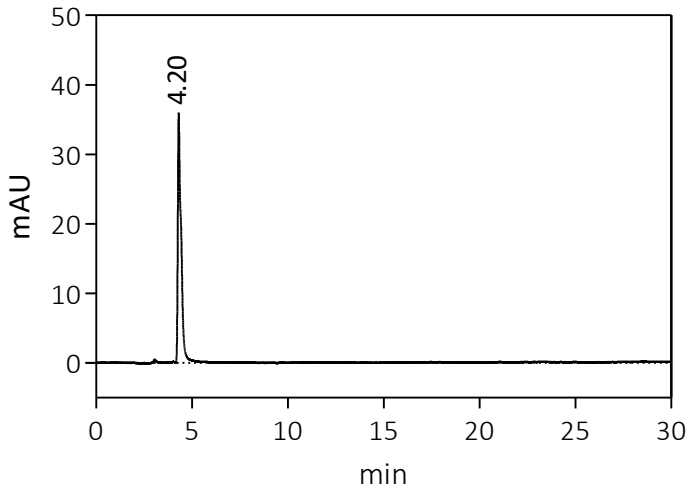

Capítulo 3

Heptyl Dihydroxybenzoates as an Alternative to Copper to Prevent Citrus Canker

Ana C. Nazaré[†]; Carlos R. Polaquini[†]; Lúcia B. Cavalca[§]; Graciele F. S. Pinto[⊥]; Adna S. Dorigo[¶], Annelise S. Rosa[¶], Rosana M. Kolb[⊥]; Osmar Malaspina[¶], Henrique Ferreira[§]* and Luis O. Regasini[†]*

[†]Department of Chemistry and Environmental Sciences, Institute of Biosciences, Humanities and Exact Sciences, São Paulo State University, São José do Rio Preto, SP 15054-000, Brazil;

[§]Department of Biochemistry and Microbiology, Biosciences Institute, São Paulo State University, Rio Claro, SP 13506-900, Brazil;

[⊥]Department of Biological Sciences, Faculty of Sciences and Languages, São Paulo State University, Assis, SP 19806-900, Brazil;

[¶]Center for the Study of Social Insects, Biosciences Institute, São Paulo State University, Rio Claro, SP 13506-900, Brazil;

*Corresponding authors: Tel.: +55-17-3221-2362. E-mail: regasini@ibilce.unesp.br and henrique.ferreira@linacre.oxon.org

ABSTRACT

Citrus canker is a devastating disease of several citrus species, which is caused by the Gram-negative bacterium *Xanthomonas citri* subsp. *citri* (Xcc). There are description of active compounds against Xcc by use *in vitro* assays, but few studies are focused on the combat of citrus canker carried out *in planta*. In our previous study, we described *in vitro* anti-Xcc activity of three alkyl dihydroxybenzoates: heptyl β-resorcylate (**4**), heptyl gentisate (**16**), heptyl protocathecuate (**28**). Here, we explored the ability of these esters to reduce the bacterial population of Xcc in plant and their phytotoxic and inseticidal effects. Heptyl dihydroxybenzoates were able to inhibit the onset of citrus canker symptoms. In the phytotoxicity tests with lettuce (*Lactuca sativa*), the compounds caused less growth inhibition than the cupric compound commonly used in citriculture, and they did not cause changes in the photosynthetic parameters in citrus seedlings. Finally, when evaluating toxicity in bees (*Scaptotrigona postica*), the esters effects were similar to the cupric compound. In this way we concluded the heptyl esters are efficient candidates against citrus canker, presenting potential to replace cupric compounds.

Keywords: *Xanthomonas citri* subsp. *citri*, plant disease, alkyl dihydroxibenzoates, bees.

1. INTRODUCTION

Brazil is the largest global producer and exporter of oranges, accounting for more than three-quarters of worldwide orange juice exports [1-3]. One of the diseases which cause significant damage to orange production is citrus canker, which is caused by *Xanthomonas citri* subsp. *citri* (Xcc) [4-6]. Citrus canker affects all types of citrus crops and its most common symptoms are necrotic lesions on fruits, leaves, and stems [7]. It is incident in the USA, South America (Brazil, Argentina, Bolivia, and Uruguay), and South-East Asian countries [8-10].

The main citrus canker chemical control is cupric compounds, which reduce inoculum build up on susceptible leaf tissues, preventing infection. On the other hand, successive applications and long-term use of cupric compounds may exert an enormous environmental impact due to their accumulation in the soil, which may impair the root growth of citrus trees and leach to aquatic bodies [11-15]. Furthermore, resistance to copper has also been reported for several species of *Xanthomonas* [16-21].

Although the search for new compounds which may control citrus canker is necessary, few studies in that regard can be found in the literature. Salicylic acid [22], D-Leucine, 3-indolylacetonitrile (IAN) [23], Nano-ZnO (Zinkicide) [24], ZnO-nCuSi [25, 26], TSOL [27] were able to reduce citrus canker lesions.

Recently, active compounds against Xcc have been described. Alkyl gallates highlighting nonyl, decyl, and dodecyl gallates (MIC 15.6 μg mL^{-1}) [28], D-Leucine, 3-indolylacetonitrile (IAN) [23] as potent biofilm inhibitors, bismerthiazol [29], and some antibiotics such as penicillin G (MIC 0.015 μg mL^{-1}), ampicillin (MIC 0.15 μg mL^{-1}), ciprofloxacin (MIC 0.15 μg mL^{-1}), streptomycin (MIC 16 μg mL^{-1}) showed activity against 107 Xcc isolates, considering that chloramphenicol (MIC 0.06 μg mL^{-1}) and tetracycline (MIC 0.06 μg mL^{-1}) were the most potent ones [30].

In the past years, our research group has been engaged in the study of phenolic compounds based on natural plant products against Xcc [6, 28, 31-34]. Among these, three series of alkyl dihydroxybenzoates were designed and synthesized with activity against Xcc. Alkyl dihydroxybenzoates (figure 1), including heptyl β-resorcylate (**4** - MIC 13.2 μg mL^{-1}), heptyl gentisate (**16** - MIC 20.2 μg mL^{-1}), and heptyl protocathecuate (**28** - MIC 22.2 μg mL^{-1}) showed potent anti-Xcc activity *in vitro*. In

addition, they have demonstrated low toxicity against eukaryotic cells, as well as the ability to act on Xcc membrane [6].

In this current study, we selected the heptyl dihydroxybenzoates **4**, **16,** and **28** and investigated their ability to reduce citrus canker symptoms through *in plant* assays. The phytotoxicity of heptyl esters in initial growth of lettuce (*Lactuca sativa*) and photosynthetic parameters of sweet orange (*C. sinensis*) seedlings were also carried out. Finally, we evaluated the toxicity against honeybees (*Scaptotrigona postica*), being the toxicity of the esters similar to the cupric compound commonly used in the crop.

2. MATERIALS AND METHODS

2.1. Compounds

The heptyl β-resorcylate (**4**), heptyl gentisate (**16**), and heptyl protocathecuate (**28**) were synthetized according to Fischer's Esterification [6].

2.2. Microorganisms

Xanthomonas citri subsp. *citri* strain 306 (IBSBF 1594) was kept in freezer at -80 °C in 40% glycerol. In order to perform the cellular rescue, an Eppendorf-type tube (cell stock) was removed to -80ºC freezer and placed in a thermal rack at -20 °C and immediately taken to the laminar flow. In the laminar flow, with the aid of a previously sterilized toothpick, an aliquot of cells was removed from the tube and then striated in solid Nitrogen Yeast Glycerol (NYG) medium; this plate with the solid NYG was incubated at 29ºC for 48h. After 48h the bacteria were pealed in a new plate. After a further 24h, the inoculum was prepared by scraping the cultured cells in solid medium and incubating in liquid medium for 12h at 29°C under rotation (180-200 rpm).

2.3. Xcc pathogenicity after treatment with heptyl dihydroxybenzoates on *Citrus sinensis* leaves

Citrus sinensis (L.) Osbeck was grown in greenhouse with temperature conditions between 25 and 35 ºC. For infiltration tests, Xcc cells were cultivated in NYG

to optical density (OD) at 600 nm and dispersed at 10^7 CFU mL^{-1} in NYG. Cells were exposed to compounds **4** (8.81 / 13.2), **16** (15.3 / 20.2), and **28** (17.3 / 22.2) (**Figure 1**, p. 163), copper oxychloride (38.3 / 43.1) and copper sulfate (19.3 / 24.1) at concentrations equivalent to their ½ MIC and MIC (µg mL^{-1}) for 12 h at 29 ºC [6] These concentrations were used to the assurance of 50% and 10% viable cells, respectively, which would be able to host colonization. Cell suspension (100 µL) was infiltrated into the abaxial surface of leaves by using hypodermic syringes. The following controls were used: (i) negative control (distilled water), (ii) vehicle control (cells treated with DMSO 1%), (iii) and positive control (untreated cells). The presence or absence of citrus canker symptoms was evaluated for three weeks every 7 days [28]. This experiment was performed in triplicates, for each test compound, three leaves of young *C. sinensis* plants were selected; the replicates were performed on different days.

2.4. Heptyl dihydroxybenzoates protective effect against citrus canker on *C. sinensis* leaves

Young *C. sinensis* individuals were kept under greenhouse conditions at temperatures ranging between 25 and 35 °C. The stage of vegetative development was V4-V5 leaves with 4 to 7 cm [31]; the branch to be studied was selected and marked with a string. The spray of compounds **4**, **16,** and **28** was 10×MIC and the solutions were sprayed to the run-off point (about 20 to 30 mL per plant). For the positive and solvent controls, copper oxychloride (600 µg mL^{-1} – this concentration is recommended by the manufacturer) and DMSO 1%, respectively, were used. After 24 h, a Xcc cell suspension was dispersed to 10^8 CFU mL^{-1} in saline solution (0.85% NaCl), and then sprayed onto the shoots and leaves. The development of canker symptoms was analyzed for one month, every 5 days. After this period, the leaves were collected and two parameters were evaluated: (i) the percentage of symptomatic leaves, which was related to the incidence of citrus canker, and (ii) the symptom severity rate, measuring the size and amount of lesion per leaf area. A total of 925 leaves (mean of 50 leaves per group) were analyzed. This experiment was performed in triplicates. The leaves were scanned with HP Scanjet 2400® equipment, then analyzed with ImageJ® software.

The data was analyzed through one-way analysis of variance (ANOVA) followed by Tukey's test (p<0.001). The data analyses were plotted with GraphPad Prism version 5.0 (GraphPad, San Diego, CA, USA).

2.5. Phytotoxicity of heptyl dihydroxybenzoates against *Lactuca sativa* initial growth

Compounds **4**, **16,** and **28** were solubilized in ethanol at 10×MIC value. Petri dishes used in the bioassays were sanitized with 2% sodium hypochlorite, rinsed with distilled water, then washed with 70% ethanol and dried at room temperature. A sheet of filter paper was added to each Petri dish and was moistened with 5 mL of each of the test solutions. The plates were dried in the dark at room temperature for 24 h. After evaporation, the filter papers were soaked with 5 mL of distilled water. The negative control was prepared, only with the addition of distilled water, and the positive control was prepared with copper oxychloride (600 µg mL^{-1}). Each treatment was performed with 50 seeds of Itapuã super ISLA lettuce, previously germinated (25 seeds per plate), with approximately 2 mm of radicular protrusion. Plates were kept in a B.O.D. incubator (Eletrolab, model 102 FC) at 25 °C (± 1 °C) with a photoperiod of 12 h. Bioassays totalized 72 h, and the analyzed parameters were the lengths of the main root and shoot.

The statistical analysis was performed using one-way analysis of variance (ANOVA) with Dunnett's post-test (p<0.0001). The data analyses were plotted with GraphPad Prism version 5.0 (GraphPad, San Diego, CA, USA).

2.6. Phytotoxicity assay against orange seedlings

The host citrus used was the cultivar lima of sweet orange (*Citrus sinensis*), which was grown in greenhouse between 25 and 35 ºC. The average height of the seedlings used in the assay was 27 cm. Compounds **4**, **16,** and **28** were solubilized in 0.05% ethanol at 10×MIC value and copper oxychloride (600 µg mL^{-1}). These solutions were sprayed onto the run-off point (about 5 mL per plant). Foliar physiological measurements of gas exchange and chlorophyll *a* fluorescence were performed on completely expanded young leaves in 3 individuals per treatment. Measurements were performed during the morning (between 8:30 AM and 11:00 AM) after 1 and 15 days in order to evaluate possible short and long term effects. Gaseous exchanges were measured through an open and portable infrared gas exchange system (LC pro-SD

ADC Bioscientific Ltd., UK) for determining maximum CO_2 assimilation (A_{max}) and stomatal conductance (g_s) values. These measurements were taken at a constant temperature of 26 °C and a constant saturating photon flux density of 1,400 μmol m^{-2} s^{-1}. The chlorophyll *a* fluorescence measurements were performed in leaves preadapted to the dark during 30 minutes, using a portable fluorometer [PAM Fluorometer - Junior (Walz)]. Different photochemical variables were obtained from chlorophyll *a* fluorescence parameters, namely: FM and F0, respectively maximum and minimum fluorescence of leaves adapted to the dark; and FM' and F0', maximum and minimum fluorescence of leaves adapted to light, respectively. We used the software WINCONTROL (V.3.18) (WALZ, Germany) [35] to obtain the maximum quantum yield values of photosystem II (Fv / Fm) and the maximum electron transport rate (ETR_{max} = ΔF / FM'× PAR × 0.5 × α). The mean value of 0.84 was used for leaf absorbance (α) [35, 36].

The statistical analyses were performed through One-way Anova with repeated measures followed by Tukey's test ($p<0.05$). The data analyses were plotted with GraphPad Prism version 5.0 (GraphPad, San Diego, CA, USA).

2.7. Toxicity evaluation against bees (*Scaptotrigona postica*)

The experimental group consisted of three replicates, composed of 10 worker bees (*Scaptotrigona postica*) from each of the 3 colonies, totaling 30 bees per experimental group. In the morning period, the bees were collected in plastic pots at the nests entrance. Individuals were maintained in 250 mL disposable plastic cages with a 2 mL Eppendorf type feeder with a central hole and two sides containing 50% sucrose solution, with or without addition of the compounds (**4**, **16,** and **28**). The cages were kept in B.O.D, with temperature set at 28 ºC ± 1 ºC and relative humidity at 70 ± 5%. During the intoxication, the treated groups received a feed containing heptyl dihydroxybenzoates (**4**, **16,** and **28**), which were diluted in DMSO 1%. Subsequently, serial dilutions were carried out and incorporated in sucrose solution at 1:1 proportion with distilled water in order to obtain the concentrations recommended by 0.1 MIC, MIC, and 10×MIC values. After 24 h, the number of dead bees was counted and the microtubes weighed indicating the amount of food consumed. This test was performed to protocols established by the Organization for Economic Cooperation and

Development (OECD). The data were analyzed using one-way analysis of variance (ANOVA) with Tukey's post-test (p<0.0001) and plotted with GraphPad Prism version 5.0 (GraphPad, San Diego, CA, USA).

3. RESULTS AND DISCUSSION

3.1. Xcc pathogenicity after treatment with heptyl dihydroxybenzoates on *Citrus sinensis* leaves

Formation of citrus canker lesions was observed in the positive control treatment (untreated cells), characterized by hyperplasia and hypertrophy in the region of infiltration, surrounded by a chlorotic halo (**Figure 2**, p. 165). In vehicle control experiments, DMSO 1% was not able to produce any lesions on the leaves. Heptyl esters demonstrated a similar activity, inhibiting lesion appearance. Compounds **4**, **16**, and **28** completely prevented the ability of Xcc to produce symptoms of citrus canker at ½ MIC and MIC (**Figure 2**, p. 165). Copper oxychloride (CO) and copper sulfate (CS) maintained the onset of symptoms similar to positive control (untreated cells) at ½ MIC value. Compounds **4**, **16**, **28**, CO, and CS were compared with positive control (PC), and the heptyl esters prevented the appearance of any lesions on the leaves. Copper compounds induced only a partial reduction of symptoms; such decrease was more apparent in the treatment with CS. This effect can be explained by the insolubility of CO in an aqueous medium. Behlau and co-authors (2017) reported that insoluble copper formulations are the most studied and also the most commonly used ones for the control of citrus canker [38-40], which justifies our choice of studying CO compared to heptyl esters.

Previously, our research group described the ability of alkyl gallates (3,4,5-trihydroxybenzoates) to prevent Xcc from producing citrus canker symptoms, thus inhibiting the appearance of lesions in sweet orange leaves [28]. Here, we show that alkyl heptyl dihydroxybenzoates were as effective as or more effective than gallates, assuming that the MIC concentration of gallates is about twice as high as that of alkyl dihydroxybenzoates [6]. Although the position of hydroxyls was relevant in Xcc cell assays [6], here the position of hydroxyl groups was irrelevant, since the heptyl dihydroxybenzoates (**4**, **16,** and **28**) had the same suppressing effect of citrus canker symptoms, thus demonstrating that these esters have equal protective potential against Xcc infection.

3.2. Heptyl dihydroxybenzoates had protective ability against citrus canker

In order to evaluate the protective ability of heptyl dihydroxybenzoates in sweet orange young plants, we performed a spray test which mimics natural Xcc infection by the action of the rain with wind. Xcc infection in healthy foliar tissues occurs through natural penetration in stomata and wounds [41-43]. The positive control (PC) was evaluated, in which only water and inoculum of Xcc were sprayed over sweet orange plants, and the incidence of symptomatic leaves was 80.1% (**Figure 3**, p. 166). Vehicle control (DMSO 1%) showed the percentage of symptoms of 80.3%.

Correlating the ester treatments with the PC, it was observed a 33.3% decrease in symptoms for compound **4**, 15.3% for compound **16,** and 28.6% for compound **28**. We also correlate the ability of heptyl esters to inhibit the onset of symptoms with the CO. The percentage of symptoms for the CO treatment was 58.7%, with a 26.7% decrease in symptoms in relation to the PC. Based on the statistical analysis (one-way ANOVA with Tukey's post-test), treatments with **4** and **28** heptyl esters and CO had no significant difference whereas the compound **16** showed lower protective capacity than the others.

In order to evaluate the second parameter of this assay, we used the diagrammatic scales described by Belasque Jr. and colleagues (2005). The symptom severity rate measured the leaf area affected by the lesions [44]. The sweet orange leaves were scanned and the images analyzed through software ImageJ. We measured total leaf area and area with citrus canker lesions by using color saturation differentiation (Black and White). We analyzed the difference between the areas taking the mean by treatment group. Results for severity rates were 1.3 (PC - water), 2.2 (VC – DMSO 1%), 0.6 (CO), 0.6 (**4**), 0.9 (**16**), and 0.6 (**28**); as a conclusion, the inhibitory capacity of the compounds was similar to the CO (**Figure 3**, p. 166).

3.3. Evaluation of phytotoxicity of heptyl dihydroxybenzoates against initial growth of *Lactuca sativa*

Phytotoxicity studies have increased in recent years as a means to ensure the safe use of compounds as agricultural defensives [45]. Inhibition of seedlings initial growth is a valid and sensitive indicator of environmental toxicity, since the initial growth phase is more sensitive than the germination one [46]. Several authors have shown that they have many advantages: simple, inexpensive, and require only a small

compound sample to be carried out [47-49]. The plant species commonly recommended by the US Environmental Protection Agency [50], the Food and Drug Administration [51], and the Organization for Economic Cooperation and Development [52] are cucumber (*Cucumis sativus*), lettuce (*Lactuca sativa*), radish (*Raphanus* spp.), red clover (*Trifolium pratense*), and wheat (*Triticuma estivum*) [45].

In the present study, we selected lettuce. We tested compounds at 10×MIC values, because these concentrations were able to inhibit citrus canker symptoms during spray tests. The negative control (NC) consisted of distilled water and seedlings presented mean root length of 2.4 cm and shoot of 0.5 cm in that treatment (**Figure 4**, p. 167). When evaluating the heptyl esters (**4**, **16,** and **28**), was observed that the root size was similar to that of the NC measurements, except for compound **4,** which had a root mean size 50% smaller than NC. Regarding the shoot, there was a decrease in all treatments (similar among **4**, **16,** and CO) and particularly lower to **28**. Finally, the CO was evaluated and we found a mean size 83% smaller than NC. Thus, the esters were less or similar phytotoxic against lettuce (*L. sativa*) than the CO.

3.4. Phytotoxicity of heptyl dihydroxybenzoates against young *C. sinensis*

Photosynthesis is a process of converting solar energy into chemical energy. The photosynthetic metabolism which consists of three phases: (i) diffusive phase (CO_2 flow internalized into leaf mesophyll through regulation of stomatal pores), (ii) photochemical phase (light uptake and production of ATP and NADPH), and (iii) biochemical phase (Calvin Cycle) [53]. Gaseous exchange parameters and photochemical parameters of the photosynthetic process were measured in *C. sinensis* in the presence and absence of the compounds. Measurements were performed after the first day of application of the negative control (NC - water), heptyl dihydroxybenzoates (**4**, **16,** and **28**) and CO, and after 15 days. The stomatal conductance (g_s) and maximum assimilation of CO_2 (A_{max}) are presented in figure 6, while effective quantum yield of photochemical conversion of PSII (photosystem II), photochemical and non-photochemical extinction coefficients of PSII, maximum photosystem II quantum yield (Fv/Fm), and maximum rate of electron transport (ETR_{max}) are shown in **Figure 5**, p. 168. The measurements were performed in the

morning at a controlled temperature of 26 °C and with the photon flux density of 1,400 μmol m^{-2} s^{-1}.

Chlorophyll *a* fluorescence data (**Figure 6**, p. 169) were analyzed to assess deleterious effects on chloroplasts. The application of the compounds on the leaves did not significantly alter the values of the parameters evaluated in relation to the control, showing absence of photoinhibitory damage, i.e., neither the esters nor the CO damaged the photosynthetic apparatus.

3.5. Toxicity of heptyl dihydroxybenzoates against *Scaptotrigona postica*

Seventy-five percent of crops depends on pollinators for their reproduction, and bees are the most important and efficient agents in that matter, both in natural and agricultural environments. However, pollinator populations have been drastically declining and the main mortality cause is the indiscriminate use of insecticides. Therefore, it is essential that all pesticides to be released into the environment be tested on bees. For the tests, the protocols established by the Organization for Economic Cooperation and Development 54] for the evaluation of pesticides on bees in laboratory were used and adapted for stingless bees (*Scaptotrigona postica*).

The average food intake per bee and the percentage of mortality of the bees was plotted in **Figure 7**, p. 170, being the negative control (NC) and the vehicle control (VC) constituted of sucrose 50% and DMSO 1%, respectively.

Firstly, the average food intake per bee (μg) was evaluated, and it can be noted that compounds **4** and **28** had their consumption rates very similar to the NC and VC, except for the lowest concentration of compound **4** (0.1 MIC) in that consumption was lower than the others. Compound **16** had low bee consumption at the three evaluated concentrations, which makes us infer that compound **16** possibly causes bee repellency, on average the behavior of heptyl ester **16** was similar to CO, which was evaluated only at application concentration in the crop (advised by the manufacturer). Bee mortality was also evaluated and it was observed that the higher the concentration, the higher the death rate, what would be expected. This dose-response behavior was curious for compound **16**, because was the least consumed by the bees, a fact that could be simply explained due to the starvation death of the bees, but the mortality increases with the concentration increase and beyond the repellency the compound **16** showed toxicity to the bees. When comparing the heptyl esters mortalities with the

CO, we had greater safety for the heptyl esters, because they showed lower mortality rates than the CO even at the highest concentrations. When assessing intermediate concentrations mortality is halved for compounds **4** and **28**.

In order to minimize potential effects from these compounds present in the crop on bees, it is recommended not to apply them during the blooming period, when the bees forage on flowers.

3.6. Conclusion

Dihydroxybenzoates **4**, **16**, and **28** interfered in Xcc pathogenicity and remained active during the citrus canker induction assay by inhibiting the onset of symptoms. The heptyl dihydroxybenzoates proved to be safe, having low toxicity in eukaryotic cells, in the germination of *L. sativa* seeds, and in young plants of *C. sinensis,* without altering their photosynthetic parameters, as for *S. postica* toxicity heptyl dihydroxybenzoates were similar to copper oxychloride. In conclusion, heptyl dihydroxybenzoates may be a viable alternative to copper, as a useful agent in the control of citrus canker.

3.7. Figures

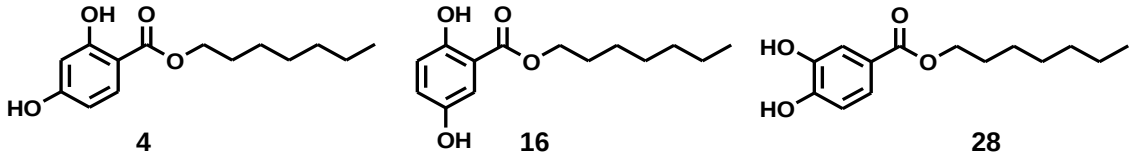

4 MIC 13.2 µg mL^{-1}

16 MIC 20.2 µg mL^{-1}

28 MIC 22.2 µg mL^{-1}

Figure 1. Heptyl dihydroxybenzoates and their Minimum Inhibitory Concentration (MIC) values against *Xanthomonas citri* subsp. *citri*

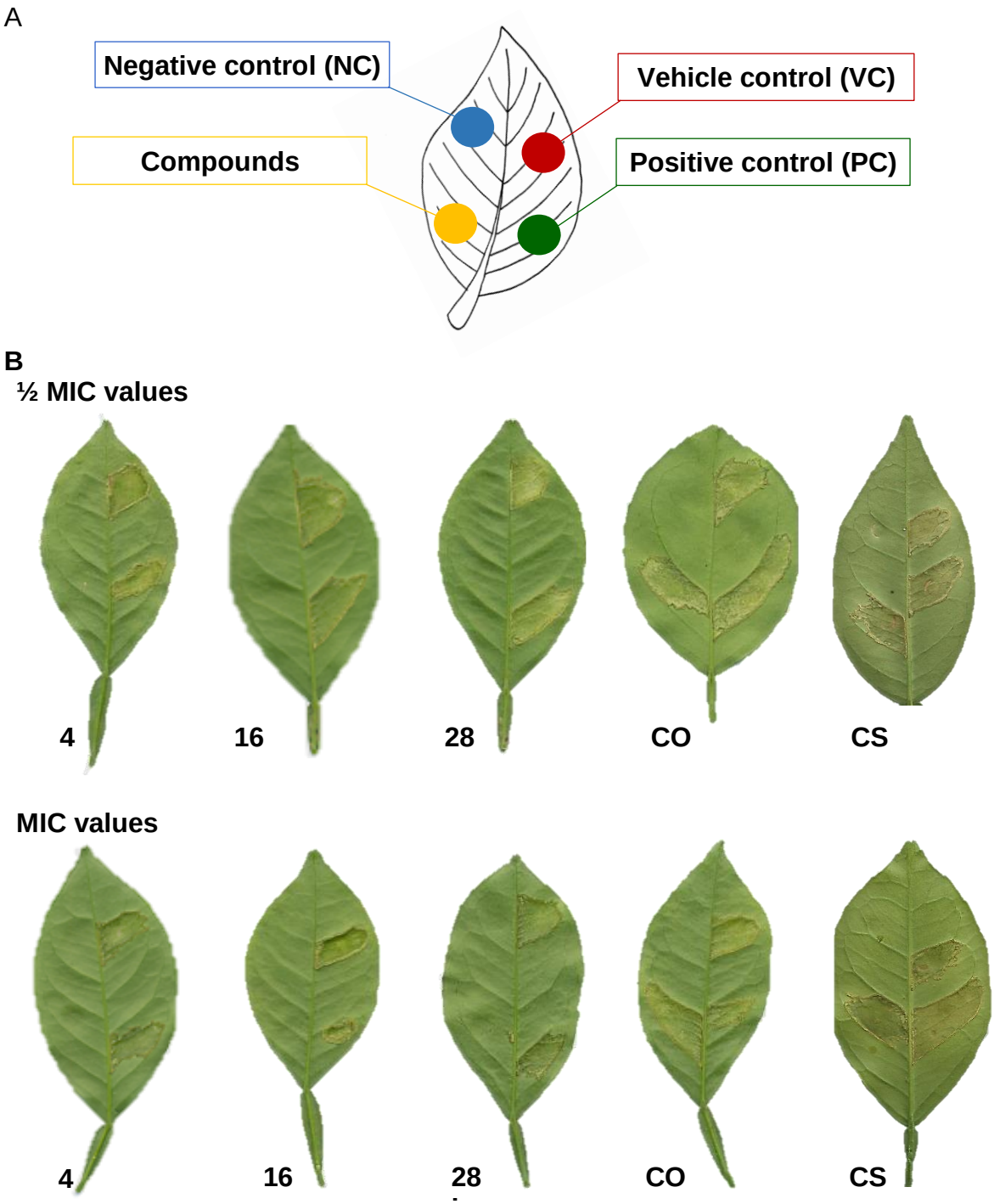

Figure 2. Infiltration points in abaxial face of the leaves, NC (distilled water); VC (cells treated with 1% DMSO); PC (untreated cells) (**A**); Citrus canker symptom in *C. sinensis* leaves after artificial inoculation of the treatement with heptyl dihydroxybenzoates and copper oxychloride (CO) and copper sulfate (CS) ½ MIC and MIC; representative images of triplicates after 3 weeks of infiltration (**B**).

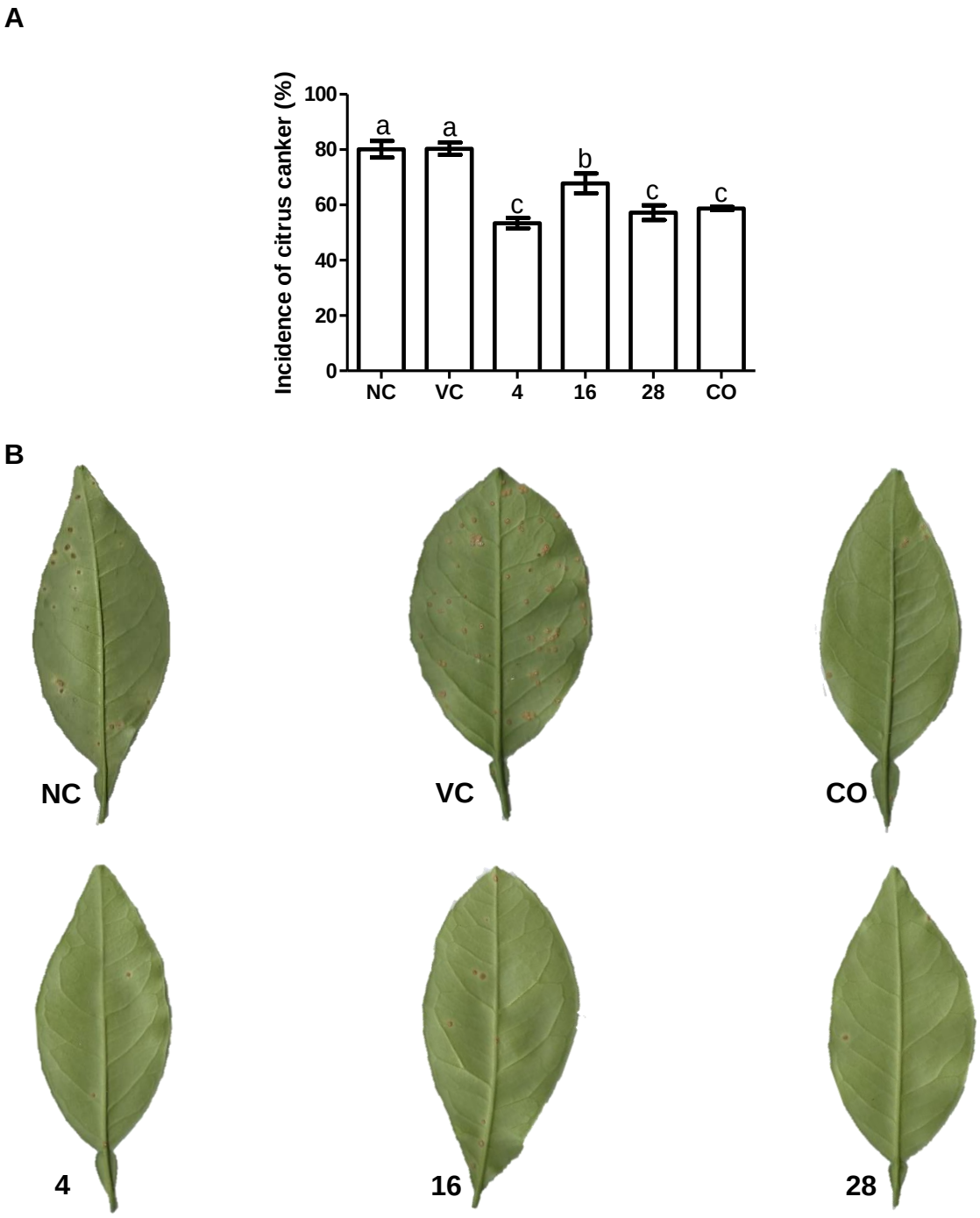

Figure 3. A) Percentage of citrus canker symptoms incidence in *Citrus sinensis* leaves. NC = negative control (distilled water), VC = vehicle control (DMSO 1%), heptyl dihydroxybenzoates (**4**, **16** and **28**) at 10×MIC values, or copper oxychloride (CO) at 600 µg mL^{-1}*. Data are means ± standard deviations. Significant differences among treatments were determined with ANOVA and Tukey's test; values followed by different letters are significantly different (p<0.001). *Concentration recommend by the manufacture. B) Representative symptom severity rate in *Citrus sinensis* leaves after spray test treatments.

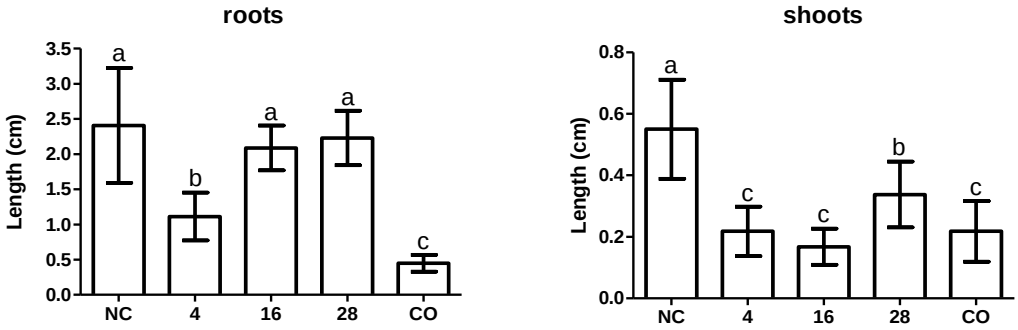

Figure 4. Initial growth roots and shoots of *L. sativa*. Negative control (NC), heptyl dihydroxybenzoates **4**, **16** and **28**, copper oxychloride (CO). Data presented with mean ± standard deviation (p<0.0001, ANOVA with Dunnett's post-test).

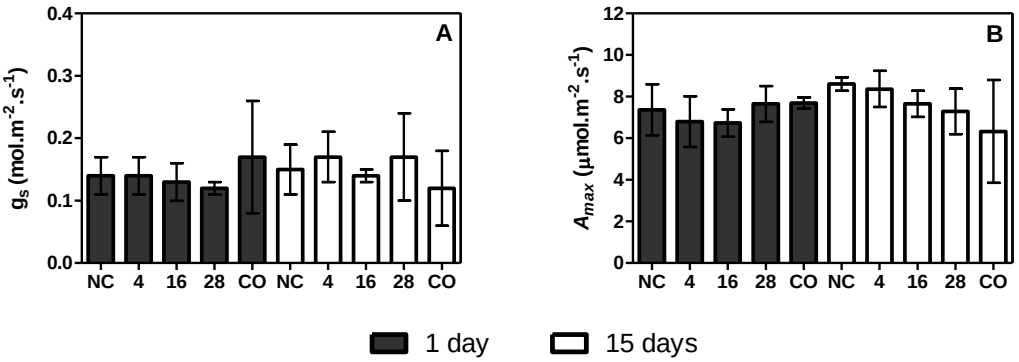

Figure 5. Leaves gas exchange after 1 and 15 days of treatment application in *C. sinensis*. Distilled water was applied as negative control (NC), other treatments were heptyl dihydroxybenzoates (**4**, **16** and **28**) and copper oxychloride (CO). (**A**) stomatal conductance - g_s, (**B**) maximum CO_2 assimilation - A_{max}. Data are means ± standard deviations; there were not significant differences among treatments with one-way ANOVA with repeated measures and Tukey's test (p>0.05).

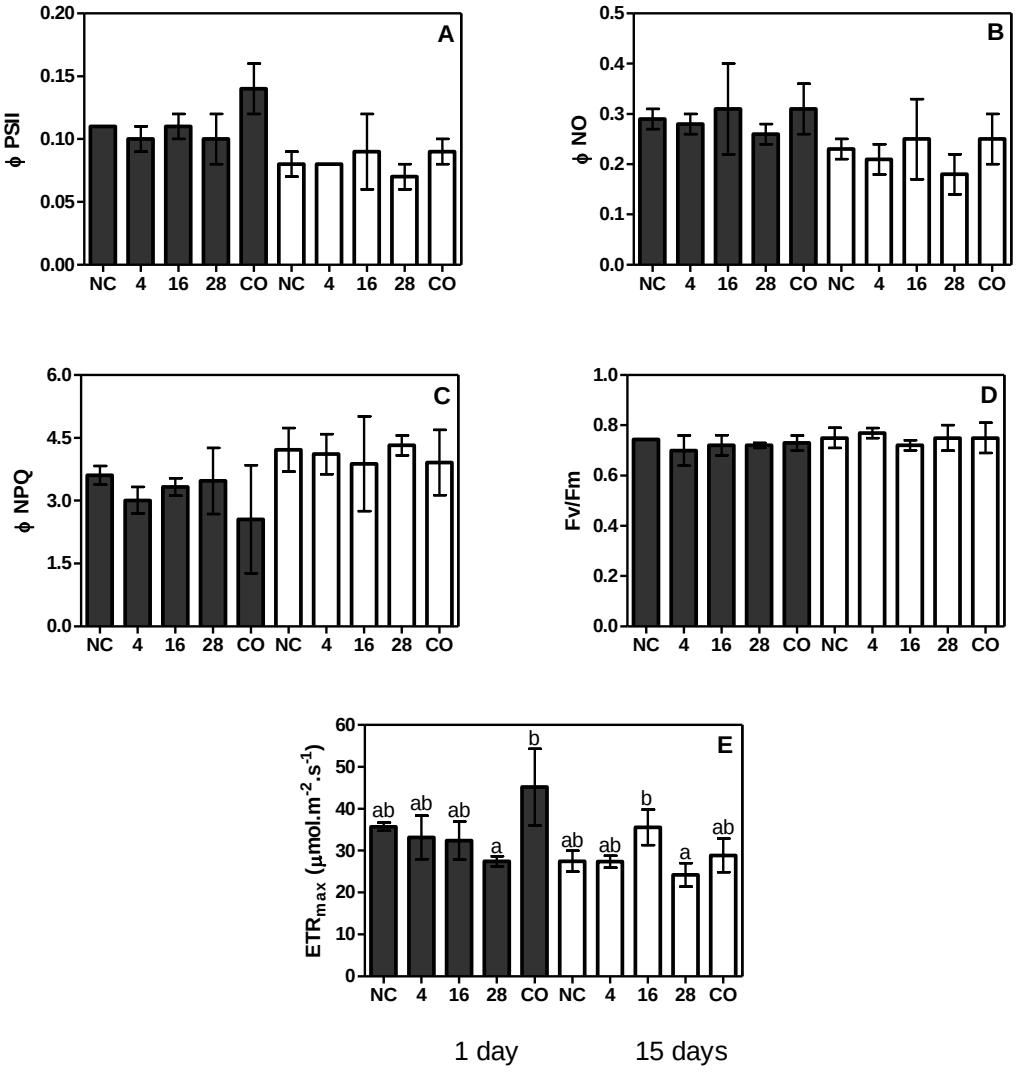

Figure 6. Chlorophyll *a* fluorescence measurements in leaves after 1 and 15 days of treatment application in *C. sinensis*. Distilled water was applied as negative control (NC), other treatments were heptyl dihydroxybenzoates (**4**, **16** and **28**) and copper oxychloride (CO). (**A**) effective quantum yield of photochemical conversion of PSII, (**B**) photochemical extinction coefficient of PSII (ϕNO), (**C**) non-photochemical extinction coefficient of PSII (ϕNPQ), (**D**) maximum photosystem II quantum yield (Fv/Fm), (**E**) maximum rate of electron transport (ETR_{max}). Data are means ± standard deviations. Significant differences among treatments were determined with one-way ANOVA with repeated measures and Tukey's test; values followed by different letters are significantly different (p<0.05). Data in figures **A**-**D** were not significantly different (p>0.05).

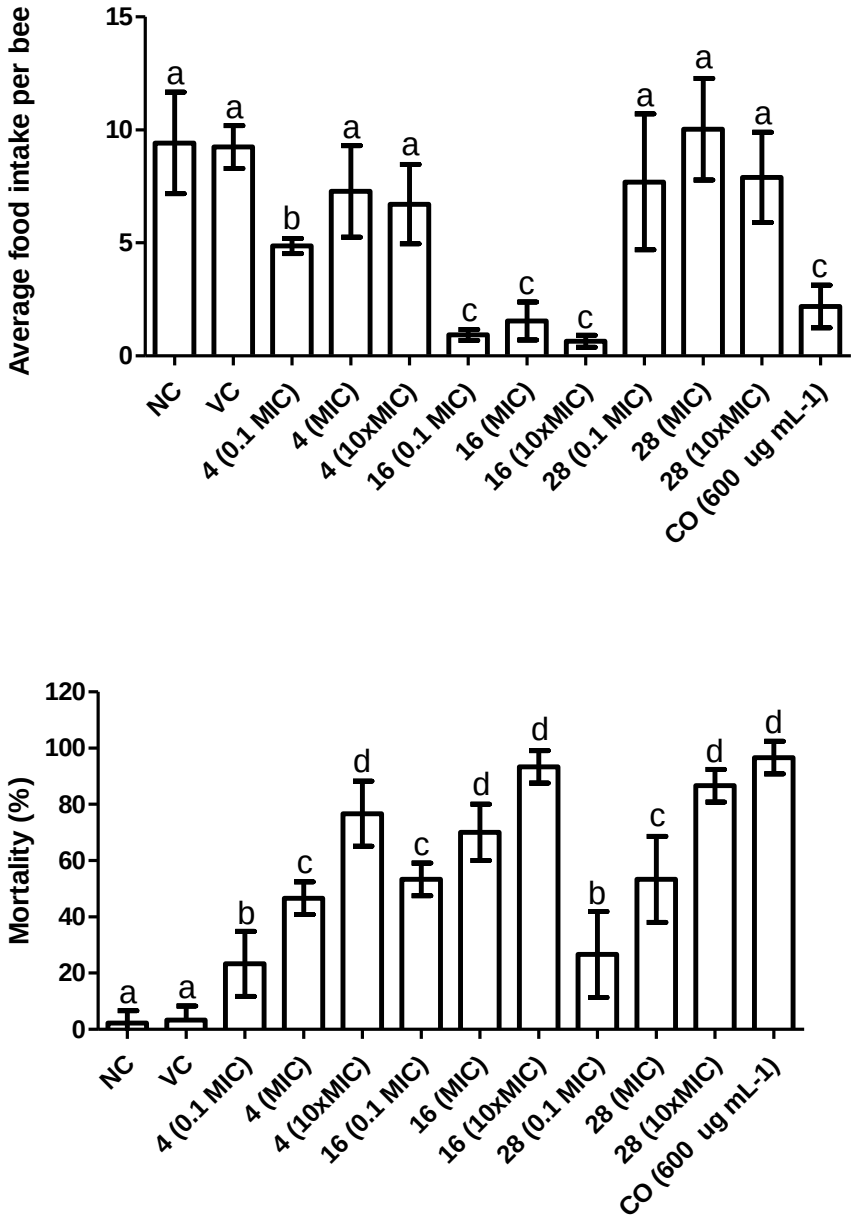

Figure 7. Average food intake per bee (µg) and Mortality rate of *Scaptotrigona postica*. NC = negative control (sucrose solution 50%), VC = vehicle control (DMSO 1%), heptyl dihydroxybenzoates (**4**, **16** and **28**) and copper oxychloride (CO). Data are means ± standard deviations. Significant differences among treatments were determined with one-way ANOVA with repeated measures and Tukey's test; values followed by different letters are significantly different (***p<0.0001).

ABBREVIATIONS

Xcc, *Xanthomonas citri* subsp. *citri*; NYG, Nitrogen Yeast Glicerol; OD, optical density; MIC, minimum inhibitory concentration; DMSO, dimethylsulfoxide; CO, copper oxychloride; CS, copper sulfate; PC, positive control; NC, negative control; VC, vehicle control.

ACKNOWLEDGMENTS

A.C.N. thanks FAPESP for a PhD scholarship (2015/08089-6), C.R.P. thanks the National Institute of Science and Genomics Technology for Citrus Improvement (Citrus-INCT) for the PhD scholarship (Grants FAPESP 2014/50880-0 and 465440/2014-2). The authors gratefully acknowledge the Center for Biomolecular Innovation (Grants FAPESP 2009/53989-4). This work was also supported by the thematic grant FAPESP 2015/50162-2 to H.F. and L.O.R.

FUNDING SOURCES

This research was funded by Coordination for the Improvement of Higher Education Personnel (CAPES), Brazilian Council for Scientific and Technological Development (CNPq) (Grants 471129/2013-5, 306251/2016-7 and 429322/2018-6), the São Paulo Research Foundation (FAPESP) (Grants 2013/50367-8, 2014/18330-0, 2015/50162-2, 2017/50216-0 and 2018/1508-2), “Biobased Economy” from the Netherlands Organisation for Scientific research (NWO, 729.004.005) and National Institute for Science and Technology - Biodiversity and Natural Products (INCT-BioNat).

4. REFERENCES

[1] Neves M. F.; Trombin, V. G.; Consoli, M. A.; Julca-Briceño, B. A.; Nogueira, J. G. Análisis del Sector Sucroenergético Brasileiro Bajo um Enfoque de Planificación Estratégica. *Agroalimentaria.* **2011**, 17, 29–45.

[2] Kalaki, R. B.; Neves, M. F. Plano estratégico para o sistema agroindustrial citrícola brasileiro. Gestão & Produção n. ahead, p. 0–0, 2017. (http://www.scielo.br/scielo.php?script=sci_arttext&pid=S0104-530X2017005001105&lng=pt&nrm=iso&tlng=en) on March 26, 2019.

[3] USDA, United States Department of Agriculture. Citrus: World Markets and Trade Foreign Agricultural Service/USDA Office of Global Analysis (https://apps.fas.usda.gov/psdonline/circulars/citrus.pdf) on August 1, 2018.

[4] Gottwald T. R.; Sun X.; Riley T.; Graham J. H.; Ferrandino F.; Taylor E. L. Geo-referenced spatiotemporal analysis of the urban citrus canker epidemic in Florida. *Phytopathology*. **2002**, 92, 361–377.

[5] Lanza, F. E.; Marti W.; Silva Jr., G. J.; Behlau, F. Characteristics of citrus canker lesions associated with premature drop of sweet orange fruit. *Phytopathology*. **2018**, 109, 44–51.

[6] Nazaré, A. C.; Polaquini, C. R.; Cavalca, L. B.; Anselmo, D. B.; Saiki, M. F. C.; Monteiro, D. A.; Zielinska, A.; Rahal, P.; Gomes, E.; Scheffers, D. J.; Ferreira, H.; Regasini, L. O. . Design of antibacterial agents: alkyl dihydroxybenzoates against *Xanthomonas citri* subsp. *citri*. *Int J Mol Sci*. **2018**, 19(10), 3050.

[7] Duan, S.; Jia, H.; Pang, Z.; Teper, D.; White, F.; Jones, J.; Zhou, C.; Wang, N. Functional characterization of the citrus canker susceptibility gene CsLOB1. *Mol Plant Pathol.* **2018**, 19, 1908−1916.

[8] Das, A. K. Citrus canker – A review. *J. Appl. Hort.*, **2003**, 5, 52-60.

[9] Ference, C. M.; Gochez, A. M.; Behlau, F; Wang, N.; Graham, J. H.; Jones, J. B. Recent advances in the understanding of *Xanthomonas citri* ssp. *citri* pathogenesis and citrus canker disease management. *Mol Plant Pathol.* **2018**, 19, 1302–1318.

[10] Vos, S.; Camilleri, M.; Diakaki, M. Pest survey card on *Xanthomonas citri* pv. *citri* and pv. *aurantifolii*. *European Food Safety Authority (EFSA)*, **2019**.

[11] Kandeler, F.; Kampichler, C.; Horak, O. Influence of heavy metals on the functional diversity of soil microbial communities. *Biol. Fertil. Soils*. **1996**, 23, 299-306.

[12] Crémazy, A.; Wood, C. M.; Smith, D. S.; Ferreira, M. S.; Johannsson O. E.; Giacomin, M.; Val, A. L. Investigating copper toxicity in the tropical fish cardinal tetra (*Paracheirodon axelrodi*) in natural Amazonian waters: Measurements, modeling, and reality. *Aquat.Toxicol*. **2016**, 180, 353-363.

[13] Graham, J. H.; Timmer, L. W.; Fardelmann, D. Toxicity of fungicidal copper in soil to citrus seedlings and vesicular–arbuscular mycorrhizal fungi. *Phytopathology*. **1986**, 76, 66–70.

[14] Alva, A. K.; Graham, J. H.; Anderson, C. A. Soil-pH and copper effects on young Hamlin orange trees. *Soil. Sci. Soc. Am. J.* **1995**, 59, 481–487.

[15] Fan, J. H.; He, Z. L.; Ma, L. N. Q.; Stoffella, P. J. Accumulation and availability of copper in citrus grove soils as affected by fungicide application. *J. Soil Sediment.* **2011**, 11, 639–648.

[16] Canteros, B. I. Copper resistance in Xanthomonas campestris pv. citri. In Proceedings of the 9th International Conference Centre for Advanced Study in Botany Plant Pathogenic Bacteria, Chennai, India, 21–23 December **1999**; 455–459.

[17] Albrigo, L. G.; Timmer, L. W.; Townsend, K.; Beck, H. W. Copper fungicides-residues for disease control and potential for spray burn. *Proc. Florida State Hortic. Soc.* **1997**,110, 67–70.

[18] Canteros, B. I.; Gochez, A. M.; Rybak, M. A.; Minsavage, G. V.; Jones, J. B.; Stall, R. E. Management and characterization of plasmid-encoded copper resistance in *Xanthomonas axonopodis* pv. *citri.* **2010** p. 145. International Conference on Plant Pathogenic Bacteria. 12. ICPPB. 2010 06 07–11, June 7–11, 2010. Saint-Denis, France. FR.

[19] Graham, J. H.; Leite, R. P.; Yonce, H. D. Streptomycin controls citrus canker in Brazil and Florida and reduces risk of copper phytotoxicity on grapefruit. *Phytopathology*. **2007**, 97, S42.

[20] Behlau, F.; Canteros, B. I.; Minsavage, G. V.; Jones, J. B.; Graham, J. H. Molecular characterization of copper resistance genes from *Xanthomonas citri* subsp *citri* and *Xanthomonas alfalfae* subsp *citrumelonis*. *Appl. Environ. Microb.* **2011**, 77, 4089–4096.

[21] Behlau, F.; Hong, J. C.; Jones, J. B.; Graham, J. H. Evidence for acquisition of copper reistance genes from different sources in citrus-associated xanthomonads. *Phytopathology*, **2013**, 103, 409–418.

[22] Wang, Y.; Liu, J. H. Exogenous treatment with salicylic acid attenuates occurrence of citrus canker in susceptible navel orange (*Citrus sinensis* Osbeck). *J. Plant Physiol*. **2012**, 169, 1143–1149.

[23] Li, J.; Wang, N. Foliar application of biofilm formation–inhibiting compounds enhances control of citrus canker caused by *Xanthomonas citri* subsp. *citri*. *Phytopathology*. **2014**, 104(2), 134−142.

[24] Santra, S.; Huang, Z.; Rajasekaran, P.; Das, S.; Prajapati, R.; Ternary agrichemical compositions and related methods. *Google Patents*; **2018**.

[25] Young, M.; Ozcan, A.; Myers, M. E.; Johnson, E. G.; Graham, J. H.; Santra, S. Multimodal generally recognized as safe ZnO/Nanocopper composite: A novel antimicrobial material for the management of Citrus phytopathogens. *J. Agr. Food Chem.* **2018**, 66, 6604-6608.

[26] Fu, L.; Wang, Z.; Dhankher, O. P.; Xing, B. Nanotechnology as a New Sustainable Approach for Controlling Crop Diseases and Increasing Agricultural Production. *Oxford University Press*, **2019**.

[27] Mendis, H. C.; Ozcan, A.; Santra, S.; De La Fuente, L. A novel Zn chelate (TSOL) that moves systemically in citrus plants inhibits growth and biofilm formation of bacterial pathogens. *PLoS ONE*, **2019**, 14, e0218900.

[28] Silva I. C.; Regasini, L. O.; Petrônio, M. S.; Silva, D. H. S.; Bolzani, V. S.; Belasque Jr., J.; Sacramento, L. V. S.; Ferreira, H. Antibacterial Activity of Alkyl Gallates against *Xanthomonas citri* subsp. *citri*. *J. Bacteriol*. **2013**, 195, 85.

[29] Yu, X.; Armstrong, C.M.; Zhou, M.; Duan, Y. Bismerthiazol Inhibits *Xanthomonas citri* subsp. *citri* Growth and Induces Differential Expression of Citrus Defense-Related Genes. *Phytopathology*. **2016**, 7, 693–701.

[30] Gholami, D.; Aminzadeh, S.; Alavi, S.M.; Kazemipour, N.; Ghoroghi, A.; Emruzi, Z. Comparison of antibiotics and bacteriocins antibacterial activity on *Xanthomonas citri* subsp. *citri. Iran J Fish Sci.* **2018**, 17(1), 162−178.

[31] Fundecitrus, Fundo de Defesa da Citricultura. Guia de fases de desenvolvimento vegetativo da planta de citros. (http://www.fundecitrus.com.br/comunicacao/download_manual/25) on February 15, 2019.

[32] Król, E.; Borges, A. S.; Silva, I. C.; Polaquini, C. R.; Regasini, L. O.; Ferreira, H.; Scheffers, D. J. Antibacterial activity of alkyl gallates is a combination of direct targeting of FtsZ and permeabilization of bacterial membranes. *Front in Microbiol*. **2015**, 6, 1-12.

[33] Kopacz, M. M.; Lorenzoni, A. S. G.; Polaquini, C. R.; Regasini, L. O.; Scheffers, D. J. Purification and characterization of FtsZ from the citrus canker pathogen *Xanthomonas citri* subsp*. citri. MicrobiologyOpen*. **2018**, e00706.

[34] Savietto, A.; Polaquini, C. R.; Kopacz, M.; Scheffers, D. J.; Marques, B. C.; Regasini, L. O.; Ferreira, H. Antibacterial activity of monoacetylated alkyl gallates against *Xanthomonas citri* subsp*. citri. Archives of Microbiology*. **2018**, 200(6), 929−937.

[35] Genty, B.; Briantais, J. M.; Baker, N. R. The relationship between quantum yield of photosynthetic electron transport and quenching of chlorophyll fluorescence. *Biochimica et Biophysica Acta*. **1989**, 990 (1), 87–92.

[36] Baker, N. R. Chlorophyll fluorescence: a probe of photosynthesis in vivo. *Ann. Rev. of Plant Biology*. **2008**, 59, 89–113.

[37] Maxwell, K.; Johnson, G. N. Chlorophyll fluorescence a practical guide. *J of Exp Botany*. **2000**, 51, 659–668.

[38] Behlau, F.; Belasque Jr., J.; Graham, J. H.; Leite Jr., R. P. Effect of frequency of copper applications on control of citrus canker and the yield of young bearing sweet orange trees. *Crop Prot.* **2010**, 29, 300–305.

[39] Graham, J. H.; Dewdney, M. M.; Myers, M. E. Streptomycin and copper formulations for control of citrus canker on grapefruit. *Proc. Fla. State Hort. Soc*. **2010**, 123, 92–98.

[40] Behlau, F.; Scandelai, L. H. M.; Silva Jr., G. J.; Lanza, F. E. Soluble and insoluble copper formulations and metallic copper rate for control of citrus canker on sweet orange trees. *Crop Prot.* **2017**, 94, 185-191.

[41] Bock, C. H.; Poole, G. H.; Parker, P. E.; Gottwald, T. R. Plant Disease Severity Estimated Visually, by Digital Photography and Image Analysis, and by Hyperspectral Imaging. *CRC Crit Rev Plant Sci.* **2010**, 29, 59-107.

[42] Schubert, T.; Friedmann, F.; Regenbrecht, H. The experience of presence: factor analytic insights. *Presence (Camb)*. **2001**, 10, 266–281.

[43] Gottwald, T. R.; Graham, J. H. A device for precise and nondisruptive stomatal inoculation of leaf tissue with bacterial pathogens. *Phytopathology*. **1992**, 82, 930-935.

[44] Belasque Jr., J.; Bassanezi, R. B.; Spósito, M. B.; Ribeiro, L. M.; Jesus Jr., W. C.; Amorim, L. Escalas diagramáticas para avaliação da severidade do cancro cítrico. *Fitopatol. Bras*. **2005**, 30, 387-393.

[45] Priac, A.; Badot, P. M.; Crini G. Treated wastewater phytotoxicity assessment using *Lactuca sativa*: Focus on germination and root elongation test parameters. *Comptes Rendus Biologies*. **2017**, 340, 188-194.

[46] Pinto, G. F. S.; Kolb, R. M. Seasonality affects phytotoxic potential of five native species of Neotropical savana. *Botany*. **2016**, 94, 81–89.

[47] Mayer, A. M.; Polijakoff-Mayber, A. In The germination of seeds. 4.ed. Great Britan: Pergamon Press, 1989. 270 p.

[48] Banks, M. K.; Schultz K. E. Comparison of Plants for Germination Toxicity Tests in Petroleum-Contaminated. *Soils*. *Water, Air, and Soil Pollution*. **2005**, 167, 211–219.

[49] Salvatore, M. D.; Carafa, A. M.; Carratù, G. Assessment of heavy metals phytotoxicity using seed germination and root elongation tests: A comparison of two growth substrates. *Chemosphere*. **2008**, 73, 1461-1464.

[50] USEPA - United States Environmental Protection Agency. 1996. Ecological Effects Test Guidelines. Seed Germination/ Root Elongation Toxicity Test.

[51] Food and Drug Administration: 1987, Seed germination and root elongation. Environmental Assessment Technical Assistance Document 4.06, the Center for Food Safety and Applied Nutrition and the Center for Veterinary Medicine, U.S. Department of Health and Human Services, Washington, D.C.

[52] OECD, 2003. Organisation for Economic Cooperation and Development: OECD guideline 208. Terrestrial plant test: 208; Seedling emergence and seedling growth test.

[53] Machado, E. C.; Schmidt, P. T.; Medina, C. L.; Ribeiro, R. V. Respostas da fotossíntese de três espécies de citros a fatores ambientais. *Pesquisa Agropecuária Brasileira*. **2005**, 40(12), 1161–1170.

[54] OECD, 1998a. Agricultural Policy Reform and the Rural Economy in OECD Countries, OECD, Paris.

[55] OECD, 1998b. “Agriculture in a Changing World: Which Policies for Tomorrow?”, Press Communiqué, Meeting of the OECD Committee for Agriculture at Ministerial level, OECD, Paris.

Capítulo 4

1. CONSIDERAÇÕES FINAIS

O gênero *Xanthomonas* compõe um grupo de bactérias que atinge culturas agrícolas economicamente importantes, como arroz, feijão, tomate, laranja, pimentão, maracujá, uva e outros (Graham et al., 2004).

O enfoque deste trabalho foi a *Xanthomonas citri* subsp. *citri*, o agente etiológico do cancro cítrico, que acomete os pomares de citrus. O controle químico deste patógeno no campo consiste na aplicação de substâncias cúpricas, largamente utilizadas no controle de fitobacterioses, pois protegem o tecido vegetal da infecção e reduzem a população bacteriana na superfície foliar, devido a formação temporária de uma película protetora (Behlau et al., 2010). Com isso, são necessárias novas aplicações de cobre, o que pode causar a resistência bacteriana. Com o surgimento de cepas resistentes ao cobre tem se realizado pesquisas de novas substâncias antibacterianas (Behlau et al., 2013; Scapin et al., 2015; Graham et al., 2016; Canteros et al., 2017; Richard et al., 2017; Martins et al., 2018; Gochez et al., 2018).

No **Capítulo 2** foram avaliadas a atividade anti-Xcc dos ácidos β-resorcílico, gentísico e protocatecuico demonstrando-se inativos (MIC> 100 μg mL^{-1}). Avaliou-se o potencial anti-Xcc de três séries de ésteres alquílicos, constituída por diidroxibenzoatos de etila, *n*-butila, *n*-hexila, *n*-octila, *n*-decila e *n*-dodecila, sendo estes ativos contra Xcc, destacando os ésteres hexílicos e octílicos. Posteriormente, foram preparados e testados os ésteres de heptila e nonila. Os menores valores de CIM foram obtidos para os ésteres heptílicos (**4**, **16** e **28**). Estudamos diidroxibenzoatos de alquila ramificados, cíclicos e aromáticos para analisar os efeitos estereoeletrônicos na atividade anti-Xcc, no entanto, não obtivemos conclusões claras sobre a relação estrutura e atividade antibacteriana destas substâncias (**Tabela 1 Capítulo 2**, p. 60).

Silva e colaboradores descreveram a atividade anti-Xcc de galatos de alquila. Visando investigar a relevância do número de grupos hidroxila na atividade anti-Xcc, comparando-os aos diidroxibenzoatos de alquila. Os diidroxibenzoatos heptílicos exibiram valores de CIM de 52 μM (**4**), 80 μM (**16**) e 88 μM (**28**) contra Xcc, sendo assim mais ativos que o galato de heptila (CIM = 116 μM) (Silva et al., 2013). Este conjunto de dados indicou que a redução no número de hidroxilas aumentou a

atividade anti-Xcc. Comparações entre os valores de CIM dos ésteres **4**, **16** e **28** sugerem que as hidroxilas nas posições 2 e 4 (DHB **4**) aumentaram a atividade anti-Xcc quando comparadas às posições 2 e 5 (DHB **16**), bem como 3 e 4 (DHB **28**).

Isso foi corroborado por outros dados referentes aos ácidos diidroxibenzóicos (DA) e seus ésteres que tiveram atividade antimicrobiana descrita contra bactérias Gram-positivas e Gram-negativas (Liu, Hsu & Yin, 2008; Kuet et al., 2009; Chao & Yin, 2009; Mandalari et al., 2010; Bisignano et al., 2013). Alguns DAs, como ácido *o*-pirocatecuico, β-resorcílico, gentísico, ϒ-resorcílico e protocatecuico mostram atividade contra *Campylobacter jejuni*, *Escherichia coli*, *Listeria monocytogenes* e *Salmonella enterica* (Friedman, Henika & Mandrel, 2003).

Merkl e colaboradores analisaram a atividade antimicrobiana dos ácidos protocatecuíco, gentísico, ferúlico, cafeíco, vanílico e *p*-hidroxibenzóico e os seus ésteres de metila, etila, *n*-propila, *n*-butila e *n*-hexila, contra *E. coli*, *Bacillus cereus*, *L. monocytogenes*, *Saccharomyces cerevisiae* e *Fusarium culmorum* e relatou diferenças significativas entre os valores de CIM dos ácidos e seus ésteres. Em geral, os ésteres butílicos foram duas vezes mais ativos que os ácidos de origem. Além disso, os autores associaram o aumento da atividade antibacteriana com o tamanho da cadeia alquílica lateral (Merkl et al., 2010).

O aumento da cadeia alquílica promove uma diminuição na solubilidade em água, favorecendo a formação de micelas, as quais são incapazes de atravessar a membrana de células bacterianas. O caráter anfifílico dos diidroxibenzoatos de alquila permite a formação de micelas, devido à hidrofilicidade dos grupos hidroxila e a longa cadeia carbônica hidrofóbica (Wermuth, 2008; Merkl et al., 2010).

A substância com maior lipofilicidade foi o β-resorcilato de dodecila (2,4 diidroxibenzoato de dodecila - **8**) e a substância com menor lipofilicidade foi o ácido protocatecúico (**ácido 3,4-DHB**). O aumento do tamanho da cadeia lateral alquílica, aumenta a lipofilicidade dos ésteres, promovendo maior permeação na fase estacionária formada por ODS (octadecilsilano), culminando em tempos de retenção maiores. O DHB **4** tem duas hidroxilas nas posições 2,4 (*meta*-posicionadas), o **16** tem duas hidroxilas em 2,5 (*para*-posicionadas) e o **28** tem duas hidroxilas nas posições 3,4 (*orto*-posicionadas). Os valores de log$P_{o/a}$ de 5,1 (**4**), 5,0 (**16**) e 4,3 (**28**) são próximos, sendo a substância **4** a mais lipofílica.

Neste trabalho, demonstramos que os diidroxibenzoatos de heptila não apresentavam citotoxicidade (**Tabela 2, Capítulo 2**, p. 61) dentro da faixa de concentração testada (12,5 a 200 µM). Nossos resultados corroboram os estudos de Medina-Alarcón e colaboradores, que relataram que os protocatecuatos de alquila não mostraram toxicidade contra as linhagens celulares MRC-5 e HepG2 (Medina-Alarcón et al., 2017).

Ao observamos as curvas de crescimento de Xcc (**Figura 1, Capítulo 2**, p. 62) durante o tratamento com as substâncias, notou-se um atraso na fase exponencial, que prolongou o tempo para que a colônia bacteriana atingisse a fase estacionária. Este atraso foi mais evidente quando se aumentou a concentração das substâncias. As interações dos ésteres com as células de Xcc apresentaram curvas diferentes, o que é um fato interessante, uma vez que os ésteres possuem o mesmo tamanho de cadeia carbônica. Portanto, isso nos fez considerar a relevância das hidroxilas no crescimento de Xcc. Comparando os DHB ao controle positivo e ao controle veículo no **item 2.8** do **Capítulo 2**, p. 60, o crescimento bacteriano sofreu um atraso de aproximadamente 18 h até atingir a fase estacionária. No entanto, ao avaliar o comportamento do DHB **16** observamos uma maior inibição do crescimento bacteriano, diminuindo significativamente a altura da curva (menor densidade óptica). Portanto, pode-se inferir que a ação do DHB **16** sobre Xcc é maior que a ação do DHB **4**. O perfil do DHB **28** apresentou aumento do crescimento bacteriano de 20 a 30 h, posteriormente a este tempo a inibição do crescimento de Xcc continuou mais eficaz do que aquela apresentada por DHB **4**, mas com menor capacidade de inibição em relação ao DHB **16** (**Figura 1, Capítulo 2**, p. 62).

Ao avaliamos o oxicloreto de cobre, encontramos um valor de CIM de 43,1 µg mL^{-1} contra Xcc e contra as células eucarióticas não demonstrou toxicidade. Nas curvas de crescimento das colônias tratadas com o oxicloreto de cobre, notamos que o padrão de curva não se alterou e o oxicloreto de cobre mostrou-se inativo nas condições testadas. Behlau e colaboradores descreveram o oxicloreto de cobre como uma formulação de cobre insolúvel (ICuF) (syn. Copper fixo), sendo a forma mais estudada e comumente utilizada de cobre para o controle do cancro cítrico (Behlau et al., 2010; Behlau et al., 2017). A insolubilidade pode estar relacionada a baixa atividade do oxicloreto de cobre.

A concentração bactericida mínima foi determinada pela observação do crescimento bacteriano em placas de Petri transferidas das placas do ensaio de microdiluição em caldo. Obtivemos ação bactericida para os ésteres **11**, **22**–**24**, **31** e **36** a 100 μg mL^{-1}, para os ésteres **2**, **3**, **15**, **27**–**30** a 50 μg mL^{-1} e para os ésteres **4** e **16** a 25 μg mL^{-1}.

Investigamos os diidroxibenzoatos de alquila quanto a interferência na divisão celular de Xcc mediada por FtsZ (Lutkenhaus & Addinall, 1997). A proteína FtsZ está relacionada à tubulinas eucarióticas (Lowe & Amos, 1998), por possuir atividade GTPásica (de Boer, 1992; Ray Chaudhuri & Park, 1992) e capacidade de se polimerizar de modo dependente de GTP (Erckson & Stoffer, 1996). O ensaio de regeneração contínua do substrato foi realizado para caracterizar a atividade GTPásica (Margalit et al., 2004). Os ésteres **4**, **16** e **28** apresentaram inibição da atividade GTPásica de FtsZ (**Figura 4, Capítulo 2**, p. 65). Esses dados sugerem que os três compostos promoveram alterações nos protofilamentos, levando à despolimerização, e impedindo a divisão celular bacteriana.

Os ésteres heptílicos **4**, **16** e **28** afetaram a integridade da membrana (**Figura 2, Capítulo 2**, p. 63), mas apenas **28** mostrou alta permeabilidade similar à nisina. Portanto, similarmente aos galatos de alquila (Król et al., 2015), as substâncias **4**, **16** e **28** exibem atividade antibacteriana pela combinação da inibição de FtsZ e de permeabilização da membrana.

No **Capítulo 3**, dando sequência aos experimentos, avaliamos a capacidade dos ésteres heptílicos **4**, **16** e **28** sobre a patogenicidade de Xcc. Nas folhas de *C. sinensis* foram infiltradas suspensões de células de Xcc tratadas previamente com os diidroxibenzoatos (**4**, **16** e **28**) a ½ MIC e MIC. Em ambas as concentrações, a Xcc perdeu sua capacidade de colonização, não observando a formação de lesões características do cancro cítrico (**Figura 2, Capítulo 3**, p. 162).

Comparando os ésteres aos compostos de cobre observamos a inibição parcial dos sintomas, sendo essa redução mais aparente no tratamento com sulfato de cobre. Este efeito pode ser explicado pela insolubilidade do oxicloreto de cobre em meio aquoso. Behlau e pesquisadores relataram que as formulações insolúveis de cobre são as mais estudadas e utilizadas para o controle do cancro cítrico (Behlau et al., 2010; Graham et al., 2010), o que justificou nossa seleção para o estudo comparativo com os ésteres heptílicos.

A inibição da capacidade patogênica de Xcc por DHB corrobora com dados anteriormente descritos para os galatos de alquila, os quais inibiram completamente o aparecimento de lesões em folhas de *Citrus limonia* (Silva et al., 2013). Os diidroxibenzoatos heptílicos demonstraram eficácia similar aos galatos (Nazaré et al., 2018). Para este ensaio, o número e a posição das hidroxilas não foi relevante, obtendo o mesmo efeito supressor nos sintomas do cancro cítrico, evidenciando que os ésteres (**4**, **16** e **28**) têm atividade protetora contra a infecção Xcc.

Para confirmar a capacidade protetora dos diidroxibenzoatos heptílicos **4**, **16** e **28** em plantas jovens de *C. sinensis*, seguimos a metodologia do teste de pulverização, que simula a infecção natural em condições de campo pela ação da chuva e vento. A infecção de Xcc em tecidos foliares saudáveis ocorre através dos estômatos e ferimentos (Gottwald e Graham, 1992; Schubert et al., 2001; Bock et al., 2010). Inicialmente, foram avaliadas a incidência de sintomas por grupo (tratamento) das folhas coletadas. Obtendo-se 80,1% de folhas sintomáticas no controle positivo (folhas não-tratadas), 80,3% no controle de veículo (DMSO 1%), 53,4% (**4**), 67,8% (**16**) e 57,2% (**28**) nos tratamentos com os diidroxibenzoatos de heptila (**Figura 3, Capítulo 3**, p. 163). Correlacionando os tratamentos com os ésteres e controle positivo observou-se a diminuição de 33,3% nos sintomas para o DHB **4**, 15,3% para o DHB **16** e 28,6% para o DHB **28**. Correlacionamos a capacidade dos ésteres heptílicos inibirem o início dos sintomas com o oxicloreto de cobre. Os sintomas para o tratamento com oxicloreto de cobre foi de 58,7%, com uma redução de 26,7% nos sintomas em relação ao controle positivo. Com base na análise estatística (one-way ANOVA com pós-teste de Tukey) os tratamentos com ésteres heptílicos e oxicloreto de cobre não apresentaram diferença significativa.

Utilizamos as escalas diagramáticas descritas por Belasque Jr. e colaboradores (2005) para avaliar a severidade dos sintomas. Obtivemos as taxas de severidade de 1,3 no controle positivo (água), 2,2 no controle veículo (DMSO 1%), 0,6 para o oxicloreto de cobre, 0,6 (**4**), 0,9 (**16**) e 0,6 (**28**), verificando que a capacidade inibitória das substâncias foi semelhante ao oxicloreto de cobre (**Figura 3, Capítulo 3**, p. 163). Portanto, os diidroxibenzoatos heptílicos são alternativas para o cobre.

Foram realizados estudos de fitotoxicidade para avaliar a segurança dos ésteres (Priac, Badot e Crini, 2017). A inibição do crescimento inicial de plântulas é um indicador válido e sensível de toxicidade ambiental, sendo a fase inicial de

crescimento mais sensível que a germinação (Pinto e Kolb, 2016). Vários autores mostraram que os testes de fitotoxicidade têm muitas vantagens: são simples, economicamente viáveis e requerem uma pequena quantidade de amostra (Mayer e Poljakoff-Mayber, 1989, Banks & Schultz, 2005; Salvatore, Carafa e Caratù, 2008). As plantas geralmente recomendadas pela Agência de Proteção Ambiental dos EUA (EPA, 1996), pela Food and Drug Administration (FDA, 1987) e pela Organização para Cooperação e Desenvolvimento Econômico (OECD, 2003) são pepino (*Cucumis sativus*), alface (*Lactuca sativa*), rabanete (*Raphanus* spp.), trevo vermelho (*Trifolium pratense*) e trigo (*Triticuma estivum*) (Priac, Bandot e Crini, 2017).

No presente trabalho, optamos por trabalhar com alface. A concentração usada para os testes foi 10 × CIM, porque foi a concentração capaz de inibir o aparecimento de sintomas no teste de pulverização **item 2.2, Capítulo 3**, pg. 152. Na avaliação dos ésteres heptílicos (**4**, **16** e **28**), os comprimentos médios das raízes foram semelhantes ao das medidas do controle negativo (**Figura 4, Capítulo 3**, p. 164), com exceção do DHB **4**, sendo o comprimento médio das raízes 50% menor que a do controle negativo. Nos caules, todos causaram redução igual a **4**, **16** e CO, sendo menor para **28**. Finalmente, o oxicloreto de cobre foi avaliado e encontramos um comprimento médio de raiz de 0,4 cm (83% menor que o controle negativo). Assim, os ésteres heptílicos foram menos fitotóxicos ou similares ao oxicloreto de cobre.

Avaliamos os parâmetros de trocas gasosas e fotoquímicos do processo fotossintético em folhas de *C. sinensis*. Os ésteres e o oxicloreto de cobre mostraram ausência de dano fotoinibitório, ou seja, não danificaram o aparato fotossintético, sendo assim considerados seguros para plantas jovens de *C. sinensis*.

Setenta e cinco por cento das lavouras dependem de polinizadores para a sua reprodução e as abelhas são os agentes mais importantes e eficientes tanto em ambientes naturais como agrícolas. Para o Brasil, o valor econômico estimado pela polinização é estimado em R$ 43 bilhões por ano (BPBES, 2018). Entretanto, o declínio populacional de polinizadores tem sido observado drasticamente e entre as causas atribuídas a eventos de mortalidade, o principal é o uso indiscriminado de agrotóxicos. Portanto, torna-se essencial que todos os pesticidas lançados no meio ambiente sejam testados em abelhas. A toxicidade dos ésteres heptílicos foi testada contra as abelhas sem ferrão (*Scaptotrigona postica*). Para os testes, os protocolos estabelecidos pela Organização para Cooperação e Desenvolvimento Econômico

(OECD, 1998a, 1998b) para a avaliação de pesticidas em abelhas em laboratório foram utilizados e adaptados para abelhas sem ferrão (*Scaptotrigona postica*).

Foram avaliadas as médias do consumo de alimento por abelha (µg) e a porcentagem de morte das abelhas, sendo o controle negativo e o controle de veículo constituídos por sacarose 50% e DMSO 1%, respectivamente.

Inicialmente avaliou-se a ingestão de alimento por abelha, e pode-se observar que os ésteres heptílicos **4** e **28** tiveram suas taxas de consumo semelhantes às dos controles, exceto a menor concentração da substância **4** (0,1 MIC) em que o consumo foi mais baixo do que as demais. O éster **16** apresentou baixa ingestão das abelhas para as três concentrações avaliadas, o que nos fez inferir que a substância **16** pode causar efeito repelente às abelhas. Avaliando o comportamento da média das concentrações do éster **16** observou-se efeito similar ao composto cúprico (CO) avaliado somente na concentração de aplicação na lavoura recomendada pelo fabricante. Em relação a taxa de mortalidade das abelhas observou-se que quanto maior a concentração, maior o número de abelhas mortas. Porém, este comportamento dose-resposta foi curioso para o éster **16**, pois foi o menos consumido pelas abelhas, fato que poderia ser simplesmente explicado devido à morte das abelhas por inanição, mas a mortalidade aumenta dependentemente da concentração, sendo assim, além da repelência a substância **16** foi tóxica para as abelhas. Ao compararmos as mortalidades dos ésteres heptílicos com o oxicloreto de cobre (CO), notou-se que os ésteres foram mais seguros, pois apresentaram menores taxas de mortalidade que o CO, mesmo nas maiores concentrações. Ao avaliar as concentrações intermediárias, a mortalidade foi reduzida pela metade para os compostos **4** e **28**.

De qualquer forma, para minimizar os efeitos dos ésteres heptílicos nas abelhas, recomenda-se aplicá-los fora do período de floração, quando as abelhas forrageiam nas flores.

2. CONCLUSÕES GERAIS

Os 36 diidroxibenzoatos propostos foram obtidos, purificados e tiveram sua hidrofobicidade determinada. Os diidroxibenzoatos de alquila demonstraram atividade contra Xcc no ensaio de microdiluição em caldo, sendo os diidroxibenzoatos heptílicos (**4**, **16**, e **28**) selecionandos devido a seus menores valores de CIM. Os

diidroxibenzoatos hepitílicos exibiram atraso na fase exponencial de Xcc, afetaram a integridade da membrana de Xcc, inibiram a atividade GTPásica da proteína FtsZ, sugerindo a inibição da divisão celular bacteriana. Os diidroxibenzoatos **4**, **16**, e **28** interferiram na patogenicidade de Xcc, e se mantiveram ativos no ensaio de indução de cancro cítrico inibindo o aparecimento de sintomas. Os diidroxibenzoatos heptílicos demonstraram ser seguros, exibindo baixa toxicidade em células eucarióticas, no desenvolvimento inicial de *L. sativa* e em plantas jovens de *C. sinensis*, não alterando seus parâmentos fotossintéticos. Quanto a toxicidade em *S. postica* os diidroxibenzoatos heptílicos foram menos tóxicos ou com toxicidade similar ao oxicloreto de cobre.

Com isso, pode-se concluir que os diidroxibenzoatos heptílicos podem ser uma alternativa viável ao cobre, sendo agentes úteis no controle do cancro cítrico. As perspectivas deste trabalho seriam ensaios em maior escala (campo), ensaios de sinergismo com substâncias cúpricas, ensaios de estabilidade dos diidroxibenzoatos heptílicos e desenvolvimento de formulações agroquímicas.

3. REFERÊNCIAS

ALVES, M. J. et al. Antimicrobial activity of phenolic compounds identified in wild mushroons, SAR analysis and docking studies. **Journal of Applied Microbiology**, v. 115, n. 2, p. 346–357, 2013.

BANKS, M. K.; SCHULTZ K. E. Comparison of Plants for Germination Toxicity Tests in Petroleum-Contaminated. **Soils. Water, Air, and Soil Pollution**. v. 167, p. 211–219, 2005.

BEHLAU, F. et al. Effect of frequency of copper applications on control of citrus canker and the yield of young bearing sweet orange trees. **Crop Protection**, v. 29, n. 3, p. 300–305, 2010.

BEHLAU, F. et al. Evidence for acquisition of copper resistance genes from different sources in citrus-associated xanthomonads. **Phytopathology**, v. 103, n. 5, p. 409–418, 2013.

BEHLAU, F. et al. Soluble and insoluble copper formulations and metallic copper rate for control of citrus canker on sweet orange trees. **Crop Protection**, v. 94, p. 185-191, 2017.

BISIGNANO, C.et al. Antibacterial activities of almond skins on *cagA*-positive and-negative clinical isolates of *Helicobacter pylori.* **BMC Microbiol**. v. 13, p. 103, 2013.

BOCK, C. H.; PARKER, P. E.; GOTTWALD, T. R. Effect of simulated wind-driven rain on duration and distance of dispersal of *Xanthomonas axonopodis* pv. *citri* from canker-infected citrus trees. **Plant Disease**, v. 89, n. 1, p. 71–80, 2005.

BPBES disponível em: https://www.bpbes.net.br/, Acesso: novembro, 2018.

CANTEROS, B. I., GOCHEZ, A. M., MOSCHINI, R. C. Management of citrus canker in Argentina, a success story. **Plant Pathology**, v. 33, n. 5, p. 441–449, 2017.

CHAO, C.Y.; YIN, M.C. Antibacterial effects of roselle calyx extracts and protocatechuic acid in ground beef and apple juice. **Foodborne Pathog. Dis.**, v. 6, p. 201–206, 2009.

DE BOER, P.A. et al. Roles of MinC and MinD in the Site-Specific Septation Block Mediated by The MinCDE System of *Escherichia coli*. **J. Bacteriol**., v. 174, p. 63–70, 1992.

ERICKSON, H.P.; STOFFLER, D. Protofilaments and rings, two conformations of the tubulin family conserved from bacterial FtsZ to alpha/beta and gamma tubulin. **J. Cell Biol.**, v. 135, p. 5–8, 1996.

FRIEDMAN, M.; HENIKA, P.R.; MANDRELL, R.E. Antibacterial Activities of Phenolic Benzaldehydes and Benzoic Acids against Campylobacter jejuni, Escherichia coli, Listeria monocytogenes, and *Salmonella enterica*. **J. Food Prot**., v. 10, p. 1811–1821, 2003.

GHOLAMI, D. et al. Comparison of antibiotics and bacteriocins antibacterial activity on *Xanthomonas citri* subsp. *citri*. **Iranian Journal of Fisheries Sciences**, v. 17, n. 1, p. 162-178, 2018.

GOCHEZ, A. M. et al. Pacbio sequencing of copper-tolerant *Xanthomonas citri* reveals presence of a chimeric plasmid structure and provides insights into reassortment and shuffling of transcription activator-like effectors among, *X*. *citri* strains. **BMC Genom**., v. 19, p. 16, 2018.

GOTTWALD, T. R.; GRAHAM, J. H. A device for precise and nondisruptive stomatal inoculation of leaf tissue with bacterial pathogens. **Phytopathology**, v. 82, p. 930-935, 1992.

GRAHAM, J. H., BROOKS, C., YONCE, H. D. Importance of early season copper sprays for protection of Hamlin orange fruit against citrus canker infection and premature fruit drop. **Proceedings Florida State Horticultural Society**, v. 129, p. 74–78, 2016.

GRAHAM, J. H.; DEWDNEY, M. M.; MYERS, M. E. Streptomycin and copper formulations for control of citrus canker on grapefruit. **Proceedings of the Florida State Horticultural Society**, v. 123, p. 92–98, 2010.

KRÓL, E. et al. Antibacterial activity of alkyl gallates is a combination of direct targeting of FtsZ and permeabilization of bacterial membranes. **Frontiers in Microbiology**, v. 6, p. 1-12, 2015.

KUETE, V. et al. Antimicrobial activity of the crude extract, fractions and compounds from stem bark of *Ficus ovate* (Moraceae). **J. Ethnopharmacol**., v. 124, p. 556–561, 2009.

LI, J.; WANG, N. Foliar application of biofilm formation-inhibiting compounds enhances control of citrus canker caused by *Xanthomonas citri* subsp. *citri*. **Phytopatology**, v. 104, n. 2, p. 134–42, 2014.

LIU, W.; HSU, C.; YIN, M. In Vitro Anti-*Helicobacter pylori* Activity of Diallyl Sulphides and Protocatechuic Acid. **Phytother. Res**., v. 22, p. 53–57, 2008.

LÖWE, J.; AMOS, L.A. Crystal structure of the bacterial cell-division protein FtsZ. **Nature**, v. *8*, p. 391, **1998**.

LUTKENHAUS, J. Assembly Dynamics of the Bacterial MinCDE System and Spatial Regulation of the Z Ring. **Annual Reviews Biochemistry**, v. 76, p. 539–562, 2007.

MANDALARI, G.; et al. Antimicrobial potential of polyphenols extracted from almond skins. **Lett. Appl. Microbiol.**, v. 51, p. 83–89, 2010.

MARGALIT, D. N. et al. Targeting Cell Division: Small-Molecule Inhibitors of FtsZ GTPase Perturb Cytokinetic Ring Assembly and Induce Bacterial Lethality. **Proc. Natl. Acad. Sci. USA**, v. 101, p. 11821–11826, 2004.

MARTINS, P. M. M. et al. Persistence in Phytogenic Bacteria: Do Know Enough? **Front. Microniol**., v. 9, p. 1–14, 2018.

MAYER, A. M.; POLIJAKOFF-MAYBER, A. In The germination of seeds. 4.ed. Great Britan: Pergamon Press, 1989. 270 p.

MEDINA-ALARCÓN, K. P. et al. Alkyl Protocatechuate Loaded Nanostructured Lipid Systems as a Treatment Strategy for *Paracoccidioides brasiliensis* and *Paracoccidioides litizii In Vitro.* **Frontiers in Microbiology** v.12, n. 8, p. 1048, 2017.

MERKL, R. et al. Antimicrobial and Antioxidant Properties of Phenolic Acids Alkyl Esters, **Czech Journal of Food Sciences**., v. 28, n. 4, p. 275-279, 2010.

NIHEI, K., NIHEI A. & KUBO I. Rational Design of Antimicrobial Agents: Antifungal Activity of Alk(en)yl Dihydroxybenzoates and Dihydroxyphenyl Alkanoates. **Bioorganic & Medicinal Chemistry Letters**, v. 13, n. 22, p. 3993–3996, 2003.

OECD, 1998a. Agricultural Policy Reform and the Rural Economy in OECD Countries, OECD, Paris.

OECD, 1998b. “Agriculture in a Changing World: Which Policies for Tomorrow?”, Press Communiqué, Meeting of the OECD Committee for Agriculture at Ministerial level, OECD, Paris.

PINTO, G. F. S.; KOLB, R. M. Seasonality affects phytotoxic potential of five native species of Neotropical savana. **Botany.**, v. 94, p. 81–89, 2016.

PRIAC, A.; BADOT, P. M.; CRINI G. Treated wastewater phytotoxicity assessment using *Lactuca sativa*: Focus on germination and root elongation test parameters. **Comptes Rendus Biologies**., v. 340, p. 188-194, 2017.

RAYCHAUDHURI, D.; PARK, J.T. Escherichia coli cell-division gene ftsZ encodes a novel GTP-binding protein. **Nature**, v. 17, p. 359–392, 1992.

RICHARD, D. et al. Complete Genome Sequences of Six Copper-Resistant *Xanthomonas citri* pv. *citri* Strains Causing Asiatic Citrus Canker, Obtained Using Long-Read Technology. **Genome Announcements**, v. 5, n. 12, p. e00010-17, 2017.

SALVATORE, M. D.; CARAFA, A. M.; CARRATÙ, G. Assessment of heavy metals phytotoxicity using seed germination and root elongation tests: A comparison of two growth substrates. **Chemosphere**., v. 73, p. 1461-1464, 2008.

SCAPIN, M. S. et al. Tree-row-volume-based sprays of copper bactericide for control of citrus canker. **Crop Protection**, v. 77, p. 119–126, 2015.

SCHUBERT, T. S. et al. Meeting the challenge of Eradicating Citrus Canker in Florida-Again. **Plant Disease**, v. 85, n. 4, p. 340–356, 2001.

SILVA, I. C. et al. Antibacterial Activity of Alkyl Gallates against *Xanthomonas citri* subsp. *citri*. **Journal Bacteriolology**, v. 195, n. 1, p. 85, 2013.

SOARES, L. A. et al. Anti-*Trichophyton* Activity of Protocatechuates and Their Synergism with Fluconazol. **Evidence-Based Complementary and Alternative Medicine**, 2014.

WERMUTH, C.G. *The Pratice of Medicinal Chemistry*; London Academic Press: London, UK, 2008; Volume 3, pp. 273–287.